AGES 881–974

ISSN 0003–2654

The Analyst

A monthly international journal dealing with all branches of the theory and practice of analytical chemistry, including instrumentation and sensors, and physical, biochemical, clinical, pharmaceutical, biological, environmental, automatic and computer-based methods

Vol.116 No.9 September 1991

The Analyst

The Analytical Journal of The Royal Society of Chemistry

Editorial Manager, Analytical Journals: Judith Egan

Editor, *The Analyst*
Harpal S. Minhas
The Royal Society of Chemistry,
Thomas Graham House, Science Park,
Milton Road, Cambridge CB4 4WF, **UK**
Telephone 0223 420066.
Fax 0223 423623. Telex No. 818293 ROYAL.

US Associate Editor, *The Analyst*
Dr J. F. Tyson
Department of Chemistry,
University of Massachusetts,
Amherst MA 01003, USA
Telephone 413 545 0195
Fax 413 545 4490

Senior Assistant Editor
Paul Delaney

Assistant Editors
Brenda Holliday, Paula O'Riordan, Sheryl Whitewood

Editorial Secretary: Claire Harris

Advertisements: Advertisement Department, The Royal Society of Chemistry, Burlington House, Piccadilly, London, W1V 0BN. Telephone 071-437 8656. Telex No. 268001. Fax 071-437 8883.

The Analyst (ISSN 0003–2654) is published monthly by The Royal Society of Chemistry, Thomas Graham House, Science Park, Milton Road, Cambridge CB4 4WF, UK. All orders, accompanied with payment by cheque in sterling, payable on a UK clearing bank or in US dollars payable on a US clearing bank, should be sent directly to The Royal Society of Chemistry, Turpin Transactions Ltd., Blackhorse Road, Letchworth, Herts SG6 1HN, United Kingdom. Turpin Transactions Ltd., distributors, is wholly owned by the Royal Society of Chemistry. 1991 Annual subscription rate EC £246.00, USA $580, Rest of World £283.00. Purchased with *Analytical Abstracts* EC £551.00, USA $1299.00, Rest of World £634.00. Purchased with *Analytical Abstracts* plus *Analytical Proceedings* EC £648.00, USA $1527.00, Rest of World £745.00. Purchased with *Analytical Proceedings* EC £313.00, USA $738.00, Rest of World £360.00. Air freight and mailing in the USA by Publications Expediting Inc., 200 Meacham Avenue, Elmont, NY 11003.

USA Postmaster: Send address changes to: *The Analyst,* Publications Expediting Inc., 200 Meacham Avenue, Elmont, NY 11003. Second class postage paid at Jamaica, NY 11431. All other despatches outside the UK by Bulk Airmail within Europe, Accelerated Surface Post outside Europe. PRINTED IN THE UK.

Information for Authors

Full details of how to submit material for publication in *The Analyst* are given in the Instructions to Authors in the January issue. Separate copies are available on request.

The Analyst publishes papers on all aspects of the theory and practice of analytical chemistry, fundamental and applied, inorganic and organic, including chemical, physical, biochemical, clinical, pharmaceutical, biological, environmental, automatic and computer-based methods. Papers on new approaches to existing methods, new techniques and instrumentation, detectors and sensors, and new areas of application with due attention to overcoming limitations and to underlying principles are all equally welcome. There is no page charge.

The following types of papers will be considered:

Full research papers.

Communications, which must be on an urgent matter and be of obvious scientific importance. Rapidity of publication is enhanced if diagrams are omitted, but tables and formulae can be included. Communications receive priority and are usually published within 5–8 weeks of receipt. They are intended for brief descriptions of work that has progressed to a stage at which it is likely to be valuable to workers faced with similar problems. A fuller paper may be offered subsequently, if justified by later work. Although publication is at the discretion of the Editor, communications will be examined by at least one referee.

Reviews, which must be a critical evaluation of the existing state of knowledge on a particular facet of analytical chemistry.

Every paper (except Communications) will be submitted to at least two referees, by whose advice the Editorial Board of *The Analyst* will be guided as to its acceptance or rejection. Papers that are accepted must not be published elsewhere except by permission. Submission of a manuscript will be regarded as an undertaking that the same material is not being considered for publication by another journal.

Regional Advisory Editors. For the benefit of potential contributors outside the United Kingdom and North America, a Group of Regional Advisory Editors exists. Requests for help or advice on any matter related to the preparation of papers and their submission for publication in *The Analyst* can be sent to the nearest member of the Group. Currently serving Regional Advisory Editors are listed in each issue of *The Analyst.*

Manuscripts (four copies typed in double spacing) should be addressed to:

Harpal S. Minhas, Editor, *The Analyst,*
Royal Society of Chemistry,
Thomas Graham House,
Science Park, Milton Road,
CAMBRIDGE CB4 4WF, UK *or*:

Dr. J. F. Tyson
US Associate Editor, *The Analyst*
Department of Chemistry
University of Massachusetts
Amherst MA 01003, USA

Particular attention should be paid to the use of standard methods of literature citation, including the journal abbreviations defined in Chemical Abstracts Service Source Index. Wherever possible, the nomenclature employed should follow IUPAC recommendations, and units and symbols should be those associated with SI.

All queries relating to the presentation and submission of papers, and any correspondence regarding accepted papers and proofs, should be directed either to the Editor, or Associate Editor, *The Analyst* (addresses as above). Members of the Analytical Editorial Board (who may be contacted directly or via the Editorial Office) would welcome comments, suggestions and advice on general policy matters concerning *The Analyst.*

Fifty reprints are supplied free of charge.

Thickness-shear-mode Acoustic Wave Sensors in the Liquid Phase
A Review

Michael Thompson,* Arlin L. Kipling† and Wendy C. Duncan-Hewitt‡
Department of Chemistry, University of Toronto, 80 St. George Street, Toronto, Ontario M5S 1A1, Canada

Ljubinka V. Rajaković and Biljana A. Čavić-Vlasak
Faculty of Technology and Metallurgy, University of Belgrade, Carnegie Street 4, 11000 Belgrade, Yugoslavia

Summary of Contents

Introduction

The use of piezoelectric acoustic wave devices as chemical sensors has its origins in the work of Sauerbrey[1] and King[2] who carried out microgravimetric measurements in the gas phase. In their work, they assumed that a thin film applied to a thickness-shear-mode (TSM) device could be treated in sensor measurements as an equivalent mass change of the quartz crystal itself. Accordingly, a shift in the resonance frequency of an oscillating AT-cut crystal could be correlated quantitatively with a change in mass added to or removed from the surface of the device. This concept has been exploited extensively in the fabrication of chemically selective sensors for the gas phase, where a binding agent is incorporated into a film which is then deposited onto the TSM device.

In recent times, there has been an increasing amount of attention paid to the operation and applications of the TSM sensor when it is exposed to the liquid phase.[3–29] Studies have been made of: *in situ* deposition of films on the sensor surface, interfacial chemistry and bulk liquid phase properties such as density, viscosity and conductivity. Where deposition or removal of surface species has been involved, frequency shifts have invariably been interpreted in terms of Sauerbrey-like alteration of acoustic wavelength as postulated for the gas phase. In contrast, Thompson *et al.*[17] proposed that the possibility of changes of interfacial properties such as free energy and slippage were related to the behaviour of the liquid-phase TSM sensor.

In this present paper the theoretical aspects are reviewed and measurement methods and applications are suggested for the TSM device operated in the liquid phase. Particular emphasis is placed on the role of interfacial parameters, a number of which are depicted in Fig. 1, in determining the response of the device. It is recognized that other acoustic wave structures, such as plate-mode and surface acoustic wave sensors, have been employed in the liquid phase. However, in order to be concise the present review deals for the most part only with thickness-shear-mode devices.

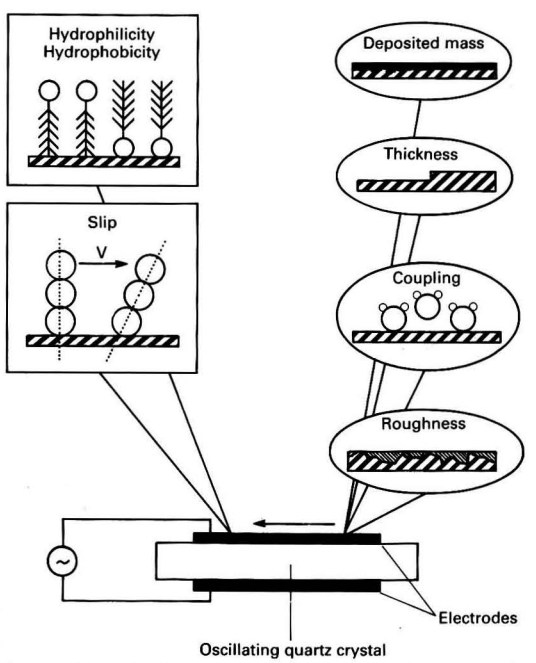

Fig. 1 Schematic diagram of interfacial factors that govern the behaviour of the oscillating TSM sensor in the liquid phase

* To whom correspondence should be addressed.

† Permanent address: Department of Physics, Concordia University, 1455 de Maisonneuve Boulevard, Montreal, Quebec H3G 1M8, Canada.

‡ Permanent address: Faculty of Pharmacy, University of Toronto, 19 Russell Street, Toronto, Ontario M5S 1A1, Canada.

Theoretical Aspects

The TSM Sensor in the Gas Phase

In order to consider carefully the behaviour of the TSM structure in the liquid phase, it is necessary to review briefly the physical aspects of the operation of the sensor in the gas phase.

For AT-cut piezoelectric crystals, the resonant condition corresponds to a thickness shear oscillation in which the shear wave propagates through the bulk of the material, perpendicular to the faces of the crystal. The atomic displacements corresponding to this shear motion are thus parallel to the crystal surface. If material is deposited on either one or both faces of the crystal, the resonant frequency decreases. The first quantitative investigation of this effect was made by Sauerbrey[1] who derived the relationship for the change in frequency ΔF (in Hz) caused by the added mass ΔM (in g):

$$\Delta F = -\frac{2F_q^2}{\sqrt{\mu_q \rho_q}} \times \frac{\Delta M}{A} \quad (1)$$

where F_q is the fundamental resonant frequency of unloaded quartz, μ_q is the shear modulus of AT-cut quartz (2.947×10^{11} g cm^{-1} s^{-2}), ρ_q is the density of quartz (2.648 g cm^{-3}) and A is the surface area in cm^2. Note that ΔM is the total mass added to both faces of the crystal but A is the area of only one face. Collecting constants and letting $\Delta m = \Delta M/A$ gives

$$\Delta F = -C_1 \Delta m \quad (2)$$

where $C_1 = 2.26 \times 10^{-6} F_q^2$ Hz cm^2 g^{-1} and Δm is added mass per unit area in g cm^{-2}. Hence ΔF is linearly related to Δm and this simple relationship is the basis for the application of piezoelectric crystals with a detection limit that has been estimated to be of the order of 10^{-12} g.[2] For a 5 MHz crystal, according to eqn. (2) a decrease in frequency of 1 Hz is caused by an added mass of 18 ng cm^{-2}. For a 9 MHz crystal $\Delta m = 5.5$ ng cm^{-2} when $\Delta F = -1$ Hz, or $\Delta F/\Delta m = -0.18$ Hz cm^2 ng^{-1}. The sensitivity of a particular crystal can be defined as $\Delta F/\Delta M$ and, for example, for a 9 MHz crystal with an electrode diameter of 0.5 cm ($A = 0.20$ cm^2), $\Delta F/\Delta M = 0.9$ Hz ng^{-1}, ignoring the minus sign.

Sauerbrey's theory has been verified for the application of 'rigid' overlayers up to a mass load of $\Delta m/m = 2\%$[30] where m is mass per unit area of the unloaded quartz. Several attempts have been made to expand Sauerbrey's theory by including a number of other parameters associated with deposited thin films. These are collected together in Table 1 for reference.

Stockbridge[31] applied a perturbation analysis to the loaded crystal. His mathematically rigorous approach was not, however, of immediate practical utility. Miller and Bolef[32,33] applied a continuous acoustic wave analysis to a resonator formed by the quartz crystal and a deposited film. Provided that the acoustic losses in the quartz and thin film are small, it can be shown that the frequency is dependent on the shear wave velocity and density of both the film and quartz. Behrndt[34] pointed out that the multiple oscillation period measurement technique is superior to the frequency measurement. Lu and Lewis[35] and Lu[36] have shown that for a metal film the acoustic impedance of the film is an important factor in determining the frequency response. Glassford[37,38] made the first attempt to analyse the frequency response associated with an imposed liquid film and droplet deposit. By using the Navier–Stokes equation and a Rayleigh perturbation analysis Glassford was able to derive a relationship which included liquid viscosity, droplet size, velocity distribution and mass loading. Mecea and Bucur[39] developed an energy transfer model which constitutes the most complex theory describing the functioning of the TSM acoustic wave device in the gas phase. They considered the mechanism of thin film interaction with the elastic properties of the resonating quartz crystal. The analogy of electrical reactance in series for two components has been applied to a coated piezoelectric crystal by Crane and Fischer.[40]

The TSM Sensor in the Liquid Phase

In 1984, the view was expressed that liquid phase operation of the TSM device would not be possible because of oscillation

Table 1 Gas phase theories of TSM acoustic wave quartz sensors*

Equation	Authors[Ref]	Mathematical model	Comments
(1)	Sauerbrey[1]	$\Delta F = -2.26 \times 10^{-6} F_q^2 \frac{\Delta M}{A}$	Only the effect of added mass is considered
(2)	Miller and Bolef[32,33]	$\Delta F = \frac{-2F_q^2 m_f}{\rho_q V_q A}$	Propagation of the acoustic wave from the quartz into the deposited film is considered
(3)	Behrndt[34]	$\Delta\tau = \frac{1}{N\rho_q A} m_f$	The change of period is considered
(4)	Lu and Lewis[35] and Lu[36]	$\tan\left(\frac{\pi F_c}{F_q}\right) = -\frac{Z_f}{Z_q}\tan\left(\frac{\pi F_c}{F_f}\right)$	The acoustic impedance of the film is considered
(5)	Glassford[37,38]	$\Delta F_l = \frac{\Delta F_s}{b}\int_0^b (D\cos\phi)^2 dz$	Mass loading by a liquid film is considered
(6)	Mecea and Bucur[39]	$\frac{F_q^2}{F_c^2} = 1 + \frac{2\rho_f l_f\{1-\exp[-r_o/r_e]^2\}}{\rho_q l_q\{1-\exp[-r/r_e]^2\}}$	Effects of electrode, film and quartz diameters on the sensitivity of a crystal coated with a thin or non-dissipating film are considered
(7)	Crane and Fischer[40]	$\frac{\Delta F}{F_q} = -\frac{\alpha\tan lb(1-\tan h^2 kb) + \beta\tan h\, kb\,(1+\tan^2 lb)}{\pi\rho_q V_q (1+\tan h^2 kb\tan^2 lb)}$	Bulk modulus, viscosity, density, and film thickness are considered

* A glossary of the symbols used is given in the Appendix.

suppression caused by viscous damping effects,[41] despite an earlier study which demonstrated that a coated TSM device could be employed as a detector for liquid chromatography. The subsequent successful measurements in the liquid phase that involved new experimental techniques, spawned attempts to provide theories for coupling of the oscillating surface to a liquid medium. In this area attempts have continued to the present time; the various theories are summarized in Table 2.

The first argument, based upon an empirical formulation was presented by Nomura and Minemura.[5] The change in the resonant frequency that occurs on coupling one face of a piezoelectric crystal to an aqueous solution is ascribed to the density, ρ (g cm^{-3}), and specific conductivity, κ (Ω^{-1} cm^{-1}) of the solution. For organic liquids the resulting change in frequency for total immersion of the device arises from the density (ρ) and viscosity [$\eta(cP)$] of the liquid.[7] Although good agreement with experimental results was obtained, the disadvantages of these relationships are obvious; the numerical constants are characteristic of each particular crystal and the relationships are not based on a physical model.

In 1985 two simple physical models were developed by Bruckenstein and Shay[13] and Kanazawa and Gordon[14] which predict the change of frequency of a sensor immersed in a liquid medium. The latter theory treats the quartz as a lossless elastic solid, and the liquid as a purely viscous fluid. The frequency shift arises from coupling the oscillation of the crystal, involving a standing shear wave, with a damped propagation shear wave in the liquid. A simple relationship was derived which expresses the change in resonant frequency of a piezoelectric crystal, due to the total contact of one face of the crystal with liquid, in terms of parameters that are characteristic of the crystal and the liquid phase [eqn. (10), Table 2]. The relationship for the change in frequency, ΔF, is derived with the assumption that the transverse velocity of the quartz surface is identical with that of the adjacent fluid layer. This simple shear wave model also provides a physical explanation of the fact that the velocity is important for TSM acoustic wave devices operating in the liquid phase. According to this theory the crystal does not drive the entire bulk of the liquid as the transverse displacement decays exponentially in the liquid with a characteristic decay length (Fig. 2). This distance (δ) varies with $(\eta_L)^{\frac{1}{2}}$ and is the effective thickness of the liquid when it is treated as a rigid sheet. Accordingly, the added mass of liquid can be derived as $\delta\rho_L = (2\rho_L\eta_L/\omega)^{\frac{1}{2}}$. Physically this model predicts that only a thin layer of liquid will undergo displacement at the surface of the bulk wave device, and the device response will be a function of the mass of this layer. By using dimensional analysis Bruckenstein and Shay[13] derived a similar although not identical relationship which can be applied to the bulk acoustic wave devices with one or two faces in contact with the liquid. In eqn. (11) (Table 2) ΔF is the difference between the frequency in air and the frequency in liquid when the liquid is in contact with one or both electrodes of the crystal (ΔF for two electrodes in the liquid is twice as large as for one electrode). For a 9 MHz crystal with one electrode ($n = 1$) in contact with water ($\rho_L = 1$ g cm^{-3}, $\eta_L = 10^{-2}$ g cm^{-1} s^{-1}), the theory predicts that $\Delta F = -6100$ Hz.

It appears that both theories introduced new parameters for

Table 2 Liquid phase theories of TSM acoustic wave quartz sensors*

Equation	Authors[Ref]	Mathematical model	Comments
(8)	Nomura and Minemura[5]	$\Delta F = A_1\kappa_L^{0.611} - B_1(d_L - 1)^{1.02}$	Empirical formulation for aqueous solution. Conductivity and specific gravity are considered
(9)	Nomura and Okuhara[7]	$\Delta F = A_2\eta_L^{0.5} + B_2\rho_L^{0.5} - C$	Empirical formulation. Viscosity and density are considered
(10)	Kanazawa and Gordon[14]	$\Delta F = -F_q^{1.5}\left[\frac{\eta_L\rho_L}{\pi\mu_q\rho_q}\right]^{0.5}$	Viscosity and density are considered. Interfacial effects are disregarded
(11)	Bruckenstein and Shay[13]	$\Delta F = -2.26\times10^{-6}nF_q^{1.5}(\eta_L\rho_L)^{0.5}$	Viscosity and density are considered. Interfacial effects are disregarded
(12)	Schumacher and co-workers[25,29]	$\Delta F = -\frac{2F_q^2\Delta m_L}{(\mu_q\rho_q)^{0.5}}$	Surface roughness is considered
(13)	Schumacher and co-workers[25,29]	$\Delta m_L = \frac{\rho_L\varepsilon}{2}$	
(14)	Heusler *et al.*[42]	$F_q - F_{qm} = A_3(p - p_m)^2$	Surface stress is considered
(15)	Hager[44]	$\Delta F = -k_1\Delta(\rho_L\eta_L)^{0.5} + f(\Delta\varepsilon_L)$	Hydrodynamic coupling analysis. Liquid dielectric constant is considered
(16)	Muramatsu *et al.*[22]	$R_1 = \frac{A}{k_2^2}(2\pi F_q\rho_L\eta_L)^{0.5}$	Resistance of equivalent circuit is considered
(17)	Yao and Zhou[45]	$\Delta F = C_0 + C_1\rho_L^{0.5} + C_2\eta_L^{0.5} - C_3\varepsilon_L$	Similar to Nomura and Okuhara model[7] but liquid dielectric constant is considered
(18)	Shana *et al.*[46]	$\frac{\Delta F}{F_q} = -\left(\frac{F_q\rho_L\eta_L}{\pi\rho_q\bar{C}_{66}}\right)^{0.5}\lvert\tanh(k_3h)\rvert$	Piezoelectric effects are considered

* A glossary of all the symbols used is given in the Appendix.

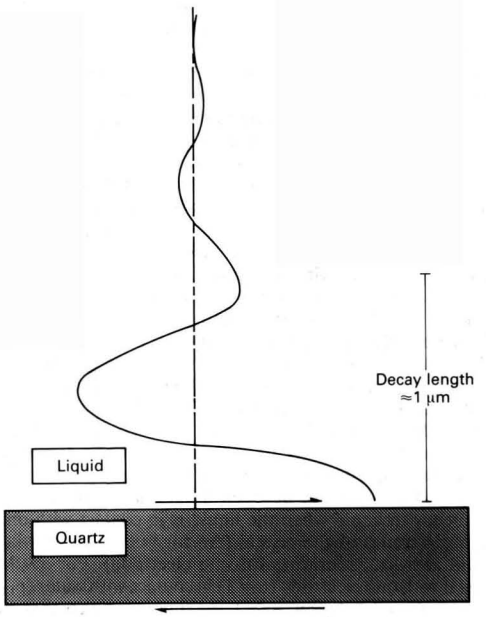

Fig. 2 Propagation of the transverse shear wave from the TSM sensor into a liquid

the mass of a thin boundary film, in this instance a liquid film. Apparently, η_L and ρ_L are the parameters which are relevant to the operation and characterization of these devices in the liquid phase. Although experimental verification has been claimed for both theories, these approaches lack consideration of the microscopic boundary conditions between the crystal surface and liquid. Specifically, in order to understand the behaviour of acoustic wave sensors operating in the liquid phase, it is important to consider the effect of chemical reactions and processes that change in addition to mass, structure, surface free energy, interfacial viscosity and, possibly, diffusion on the crystal surface.

More recent theories have examined some interfacial phenomena. Schumacher and co-workers[25,29] showed that surface roughness can also drastically affect the resonant frequency. They considered a roughened surface made up from hemicylinders with liquid entrapments which can be equivalently represented by a rigidly attached liquid layer. Under these conditions the frequency shift should contain the parameter $\Delta m_L = \rho_L \varepsilon/2$, where Δm_L is the mass per unit area of the liquid confined in the cavities of the roughened surface and ε is the mean diameter of the hemicylinders.

Heusler *et al.*[42] promoted the theory of surface stress influence on the resonant frequency. The internal strains of quartz crystals immersed in a liquid arise as a result of hydrostatic pressure. Parabolic dependence of the resonant frequency, F_q, on the pressure, p, at the oscillator face [eqn. (14), Table 2] could be related to the elastic energy stored in the quartz. Hager and Verge[43] and Hager[44] derived a model using hydrodynamic coupling analysis to determine fluid properties. In their work , viscous energy losses, fluid velocity at the crystal surface and the dielectric effect of the liquid were considered. The frequency shift is described by an empirical equation with constants depending on the crystal equivalent circuit and the working conditions. Considering an electromechanical coupling analysis for the computation of equivalent circuit parameters of piezoelectric devices in contact with a liquid, Muramatsu *et al.*[22] developed a linear relationship between ΔF and $(\eta_L \rho_L)^{\frac{1}{2}}$ for alcohol–water solutions. Shifts from linearity were observed for high-viscosity liquids and when both faces of the crystals were in contact with water. According to Yao and Zhou[45] the frequency response of an acoustic wave sensor in the liquid phase depends on the dielectric and conductance effects of the liquid. Based on their experimental measurements an empirical relationship resembling the expression of Nomura and Okuhara[7] [eqn. (9), Table 2] was derived [eqn. (17), Table 2]. As shown by Shana *et al.*[46] a comprehensive analysis including piezoelectric effects could also be used to study a thin film of viscous liquid [eqn. (18), Table 2]. When the piezoelectric effect is neglected this theory is similar to that derived by Kanazawa and Gordon.[14]

Thompson and co-workers[17,18] have shown that the response of the sensor can be associated with changes in interfacial surface structure, surface free energy and/or interfacial viscosity. From a qualitative analysis of the operation of TSM acoustic wave devices in a liquid, two aspects were introduced. First, chemistry at the interface can lead to a perturbation of acoustic wave transmission caused by alteration of the partial-slip boundary condition at the interface. Secondly, as discussed by many of the workers mentioned above, the continuum viscosity and density of the bulk liquid will be important in determining the frequency response. Using the Navier–Stokes equation for Newtonian fluids and an expression describing transverse damped wave propagation, it was shown that the penetration depth of the wave is about 1 μm. The influence of the interfacial free energy and viscosity within this range of the penetration depth was considered. These effects could be associated with either new material deposited on the interface or by the time required for molecular re-orientation in the interfacial boundary layer. As an efficient acoustic bond demands continuity of stress and displacement across the interface, wave propagation could be altered by out-of-equilibrium interfacial effects. For such an example, it was suggested that the frequency of a crystal exposed to water may increase despite an apparent increase in deposited material. Clearly, in order to accept this argument it is necessary to invoke the controversial slip boundary condition for a solid–liquid interface in which either the solid or the liquid is in motion.

Solving the differential equations of motion for the oscillatory system, consisting of the TSM device and the liquid with which it is in contact, requires that mathematical continuity be invoked at the interface. In order to accommodate the possibility of interfacial slip at the sensor–liquid interface,[47] Duncan-Hewitt and Thompson[48] have introduced the concept of additional interfacial regions of finite thickness in the liquid. These layers are endowed with mechanical properties that can be used to explain the experimental finding that coupling with the liquid phase appears to decrease with decreasing surface wettability. The existence of these proposed additional fluid layers has been verified by a wealth of experimental and theoretical work.[49]

In particular, thermodynamic analyses of adsorption isotherms indicate that at vapour saturation the bulk liquid must be at equilibrium with a surface adjacent film. Between this denser and more viscous layer and the bulk is a thin, monomolecular transitional region which is rarified relative to the bulk under incomplete wetting conditions, as in Fig. 3. Under completely non-wetting conditions, it is expected that this region would be indistinguishable from the vapour; acoustic waves would be reflected from this interface and the TSM sensor should behave as though no bulk liquid were present.

Using the molecular theory of viscosity proposed by Krausz and Eyring,[50] Duncan-Hewitt and Thompson[48] have provided a link between measurable bulk liquid properties such as density, viscosity, surface tension and contact angle, and the TSM sensor response. The model has provided results that are in agreement with the experimental results obtained to date and obeys the boundary conditions described above.

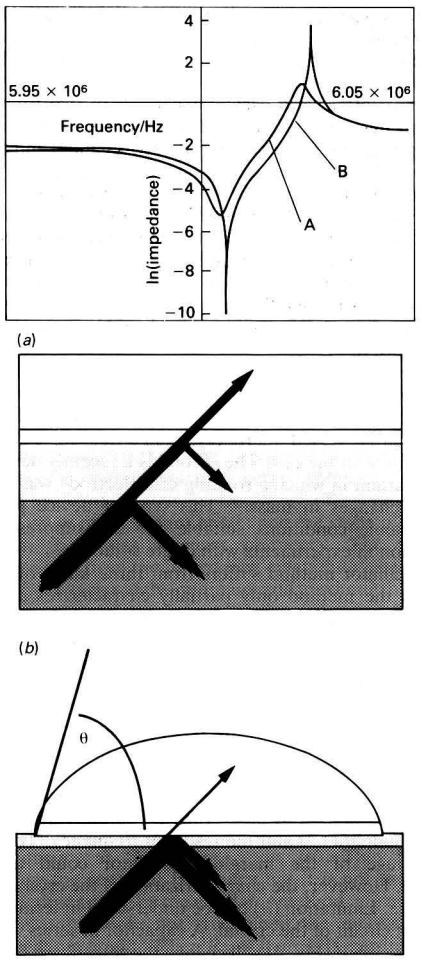

Fig. 3 Four-layer model of the TSM sensor in liquid with predicted impedance–frequency plots for (*a*) complete wetting and (*b*) incomplete wetting. Layers depicted from bottom to top are: solid piezoelectric material, interfacial liquid structure, rarified layer and bulk liquid

Measurement Methods

There are two types of methods used to characterize a quartz crystal sensor electrically, which may be called the active and passive methods. The active method is more commonly known as the oscillator method. In this method the quartz crystal is part of an oscillator circuit. It is connected between the output and input of the oscillator amplifier and provides positive feedback that causes oscillation of the circuit. The resonant frequency of the quartz crystal is measured by an electronic counter. The quartz crystal is active in the sense that it is continuously oscillating at a frequency controlled by the quartz crystal itself.

In the passive method the quartz crystal is connected externally to an instrument which applies a sinusoidal voltage at various frequencies across the terminals of the crystal. Voltages are measured and then the electrical characteristics of the crystal, the impedance for example, can be found from the voltages. The crystal does not determine the frequencies at which the measurements are made and in this sense it is passive.

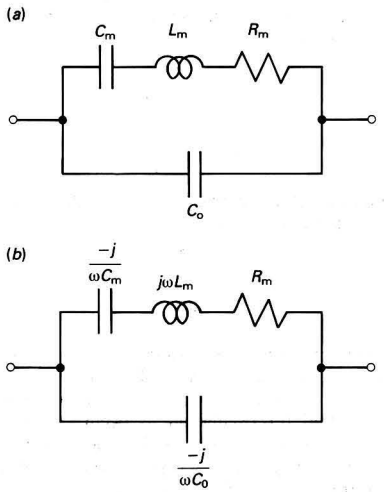

Fig. 4 Equivalent circuit of the TSM sensor with (*a*) parameters and (*b*) impedances of the circuit elements

Cady[51] was a pioneer in the development of the piezoelectric quartz crystal for frequency control in the communications field. His treatment is advanced and difficult to understand, but is one of the milestones in the literature. Bottom[52] has presented the fundamentals of the theory of the quartz crystal simply and clearly. This work is recommended for beginners in the subject. Both Bottom[52] and Cady[51] have derived the equivalent circuit of the quartz crystal (Fig. 4). This circuit is the electrical model of the crystal in a gas, but it is not a good representation of the crystal in a liquid. When the crystal is immersed in a liquid, energy flows out of the quartz into the liquid in the form of acoustic waves and this is dependent on the properties of the sensor–liquid interface which are not included in the circuit model. However, the equivalent circuit does illustrate the main features of the behaviour of the quartz crystal in liquids of low viscosity. Hence the measurement methods will be described with reference to the impedance of the equivalent circuit in Fig. 4. Most quartz crystals are discs of AT-cut quartz which are TSM devices, that is, the atoms of the quartz oscillate in the plane of the disc. The resonant frequency of the sensors is in the range from 2 to 20 MHz.

The impedance, Z, of the quartz crystal is complex: $Z = R + jX$, where R is the real part of Z, the resistive part, and X is the imaginary part of Z, the reactance. For the equivalent circuit (Fig. 4) the expression for the admittance, Y, is simpler than the expression for Z. By definition, Y is the reciprocal of Z (*i.e.*, $Y = 1/Z$) therefore if Z is complex, so is Y: $Y = G + jB$; where the conductance, G, is the real part of Y and the susceptance, B, is the imaginary part of Y. For the circuit shown in Fig. 4,

$$G = \frac{R_m}{R_m^2 + \left(\omega L_m - \frac{1}{\omega C_m}\right)^2} \quad (3)$$

and

$$B = \frac{-\left(\omega L_m - \frac{1}{\omega C_m}\right)}{R_m^2 + \left(\omega L_m - \frac{1}{\omega C_m}\right)^2} + \omega C_o \quad (4)$$

The quantity, ω, is the angular frequency (in rad s^{-1}) and is defined by $\omega = 2\pi f$ where f is the frequency in Hz. For brevity the angular frequency will be called simply the frequency.

From $Z = 1/Y$, the real and imaginary parts of Z in terms of G and B can be written as

$$R = \frac{G}{G^2 + B^2} \quad (5)$$

$$X = \frac{-B}{G^2 + B^2} \quad (6)$$

The magnitude of impedance, $|Z|$, and the phase of impedance, θ_z, are defined as

$$|Z| = \sqrt{R^2 + X^2} \quad (7)$$

$$\theta_z = \tan^{-1}\frac{X}{R} \quad (8)$$

The oscillator method measures the lower of the two frequencies of the quartz crystal for which $\theta_z = 0$. The explanation for this is as follows. There are two conditions that must be satisfied for oscillation to occur: the phase shift around the loop should be zero and the loop gain should be unity, the loop being the closed path from the input of the amplifier through the amplifier to its output, and back to the input through the feedback circuit element. The amplifiers used in the oscillator method have a zero phase shift and therefore the crystal must also have a phase shift of zero in order to satisfy the first oscillation condition. When the crystal is connected between the input and output of the amplifier, the loop gain is larger at the low frequency of zero phase and, hence, the second condition of oscillation is satisfied at this frequency. From eqn. (8), $X/R = 0$ when $\theta_z = 0$ and from eqns. (5) and (6), $-B/G = X/R$. Equation (4) divided by eqn. (3), with B/G set equal to zero, is a quadratic equation in ω and its solution gives the two frequencies of zero phase: ω_s, called the series resonant frequency, the low frequency of zero phase and therefore the frequency measured by the oscillator method; and ω_p, called the parallel resonant frequency. If $R_m = 0$,

$$\omega_{s0} = \sqrt{\frac{1}{L_m C_m}} \quad (9)$$

$$\omega_{p0} = \sqrt{\frac{1}{L_m C_m} + \frac{1}{L_m C_o}} \quad (10)$$

where ω_{s0} is ω_s when $R_m = 0$ and similarly for ω_{p0}. However, in a liquid, assuming that the equivalent circuit is an adequate representation of the crystal, R_m is of the order of magnitude of $10^3\ \Omega$ hence eqn. (9) is not the frequency measured by the oscillator method.

The most often used oscillator consists of two transistor-transistor-logic inverters connected in series to give a non-inverting amplifier (zero phase shift between input and output voltage) with the quartz sensor connected from the output to the input of the amplifier.[10,13,15,20] Oscillators with single transistors have also been used.[7] A marginal oscillator has been used;[17,18] this is an oscillator with additional feedback applied internally which changes the gain of the oscillator amplifier in response to a change of energy dissipation in the quartz crystal, such that the amplitude of the output voltage of the amplifier remains constant. A wideband marginal amplifier is shown in Fig. 5.

In order to carry out concurrent electrochemical measurements, two different experimental arrangements have been employed. The first is based on a stationary configuration[24–27] in which an immersed quartz crystal in a housing is kept at a fixed position in the cell. The second is a recently developed elegant variant in which a rotating disc electrode was used to measure changes in mass.[53] This type of device provides hydrodynamic conditions suitable for the suppression of polarization in experiments with dilute solutions.

The oscillator method suffers from three kinds of limitations: (*a*) the method only partially characterizes a quartz crystal sensor because only one quantity, the series resonant frequency, is measured; (*b*) the resonant frequency depends on the capacitance in series with the crystal[20] and in some instances on the type of oscillator used;[29] and (*c*) the crystal does not oscillate when it is in solutions of high viscosity and if the crystal oscillates when the liquid is in contact with one electrode, it will often not oscillate if both electrodes are exposed to the liquid.

Regarding limitation (*a*), more information can be extracted from this method by measuring the output voltage of the oscillator amplifier,[54] and the resonant frequency. The feedback voltage of the marginal oscillator could also be measured. However, the characterization of the crystal is still incomplete. Limitation (*b*) can be understood in terms of the equivalent circuit of the crystal. A capacitor in series with the equivalent circuit (Fig. 4) will change the zero-phase frequencies. Different oscillators may have amplifiers with phase shifts that are not exactly zero and the oscillator circuit may have a capacitance which appears in series or in parallel with

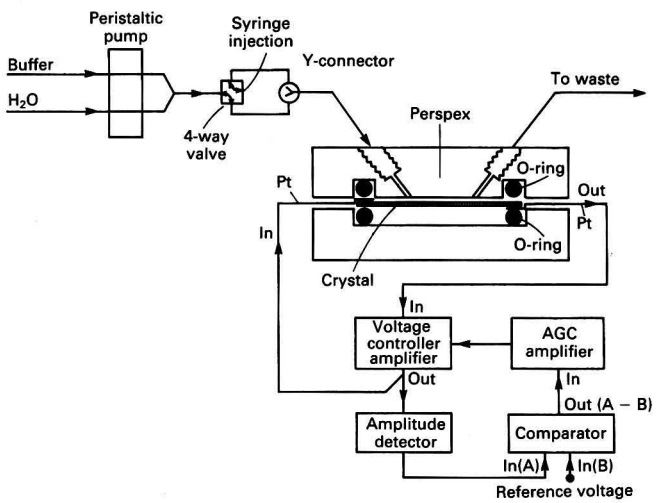

Fig. 5 Cell design for TSM sensor operation in liquid with wideband marginal oscillator and automatic gain control system. Also shown is the sensor incorporated into a liquid flow-through arrangement (reprinted by kind permission of the Institute of Electrical and Electronics Engineers)

the quartz crystal. Finally, the last limitation (*c*) is a fundamental deficiency of the oscillator method due to the fact that at high viscosities both resonant frequencies cease to exist because the phase shift of the crystal is always less than zero.[55] Therefore, one of the conditions for oscillation (for an amplifier of zero phase shift) cannot be satisfied and, in principle, the circuit will not oscillate.

The network analysis method is a passive method that has been recently developed by Kipling and Thompson[55] that completely characterizes a quartz crystal sensor. This method can be used when a liquid of any viscosity is in contact with one or both electrodes of the sensor. Sinusoidal voltages incident on and reflected from the quartz crystal are measured repeatedly for a large number of frequencies in the resonant frequency range, that is, in the range that includes ω_s and ω_p. (For sensors with f_s and f_p of the order of 10^7 Hz, $f_s - f_p$ is of the order 10^4 Hz, where $f = \omega/2\pi$.) The experimental values of magnitude and phase of impedance, for example, can be calculated at each frequency from the measured voltages and then characteristic quantities can be found from the impedance–frequency curves. Some characteristic quantities from the phase measurements are: series resonant frequency; parallel resonant frequency; frequency of maximum phase and the value of maximum phase; and the slope of the phase curve at the series resonant frequency. The prominent characteristics from the impedance magnitude measurements are the frequencies at the minimum and maximum magnitudes of impedance and the corresponding values of impedance magnitudes. The theoretical values of $|Z|$ and θ_z for the equivalent circuit are found by substituting eqns. (3) to (6) into eqns. (7) and (8).

Muramatsu and co-workers[22,23] used an impedance analyser to partially characterize a quartz crystal. This is a passive method in which, essentially, measurements are made of a voltage applied across the crystal and the current flowing through the crystal. They measured the maximum value of G and the frequency at which G is maximum. From inspection of eqn. (3), the maximum value of G, G_{max}, is $G_{max} = 1/R_m$ and the frequency at G_{max} is ω_{s0}, eqn. (9). They called this frequency the resonant frequency but it is not the resonant frequency measured by the oscillator method, ω_s, unless $R_m = 0$ which is certainly not true when the quartz crystal is immersed in a liquid. When $R_m \neq 0$, ω_s is larger than ω_{s0} and ω_p is smaller than ω_{p0}. Both $\omega_s - \omega_{s0}$ and $\omega_{p0} - \omega_p$ are proportional to R_m^2.[52]

Applications

Detectors for Liquid Chromatography

Use of the acoustic wave device as a universal mass detector for liquid chromatography was first suggested by Shulz and King.[56] In reality these workers did not employ the sensor in an *in situ* configuration. Liquid samples from the eluent were simply sprayed onto a crystal surface. The first genuine flow-through design was published by Konash and Bastiaans.[4] In this work a coated sensor was employed of which only one face was exposed to the liquid eluent. Although stable and mass sensitive detection was achieved, the system exhibited poor reproducibility. Oda and Sawada[57] incorporated a piezoelectric device in a flow cell as a photoacoustic detector in order to monitor chromatographic eluents, but the effects employed were associated with electroacoustic properties rather than piezoelectric operation. Finally, poly(ethylenimine)-coated crystals have been used for detecting various species in hydrocarbon solution,[58] but in this study it was concluded that response time must be improved in order to cope with the short residence times involved in chromatographic detector cells.

For the interest of the reader, we should note at this point that acoustic wave devices have been employed successfully as gas chromatographic detectors in a number of areas.[59–62]

Determination of Inorganic Species

Over the last several years, a single group, that of Nomura and co-workers,[6,8–10,12,15,63–69] has contributed significantly to the detection of a variety of inorganic species in the liquid phase using a TSM quartz crystal sensor. Generally these moieties were imposed at the sensor–liquid interface by the processes of electrodeposition or adsorption from aqueous solution. A summary of this work is presented in Table 3. Frequency dependence on liquid properties, such as specific conductance of electrolytes in solution[70,71] has also been considered. Examples are the determination of micromolar concentrations of Hg^{II} in waste water and microgram amounts of drugs containing iodine in biological material.

Finally, Martin *et al.*[72] studied the mass sensitivity of plate mode devices, modified with ethylenediamine ligands, for low concentrations of Cu^{II} ions in solution.

Development of Biosensors

It has been stressed a number of times in the recent literature that direct detection, possibly in an *in situ* manner, of analytical pairs such as antibody–antigen complexes and DNA hybrids could offer an attractive alternative to existing procedures. Not surprisingly, the appropriate possibilities for acoustic wave sensors in this area have been explored.

Roederer and Bastiaans[11] were the first to employ an acoustic wave device in an immunoassay procedure. A surface acoustic wave (SAW) sensor was immersed in an aqueous medium for the detection of an antibody by reaction with an antigen immobilized on the surface of the quartz. Although

Table 3 Detection of inorganic species in aqueous solution using a quartz crystal sensor, from the work by Nomura and co-workers

Analyte	Coating on Au electrode	Procedure	Concentration range/μmol dm^{-3}	Reference
CN^-	Ag	Dissolution of Ag, measurement in air	0.1–10	63
CN^-	None	Dissolution of Au	100–1000	64
Ag^+	Pt	Electrodeposition	0.005–0.05	6
Ag^+	Pt	Internal electrodeposition	1–10	10
Ag^+	Pt	Electrodeposition	0.2–30	12
I^-	Ag on Pt	Electrodeposition	0.3–10	8
I^-	Ag on Pt	Electrodeposition	0.5–7	15
Pb^{2+}	Pt	Adsorption	3–50	65
Pb^{2+}	Copper(II) oleate	Absorption	3–40	66
Fe^{3+}	Pt	Adsorption	10–100	9
Fe^{3+}, Al^{3+}	Silicone oil on Pt	Absorption	5–100	67
Hg^{2+}	None	Electrodeposition	2–30	68
Cu^{2+}	Poly(vinylpyridine)	Adsorption	5–35	69

the specific binding of the complementary antigen was demonstrated, non-specific adsorption had taken place to a significant extent. Thompson *et al.*[17] were first to study interfacial immunochemistry by means of a TSM device in the liquid phase. An antigenic component was immobilized on an auxiliary thin film of polyacrylamide gel or directly on the crystal surface. However, the response of the device to the antibody was tentatively ascribed to interfacial perturbation of acoustic energy transmission rather than to a classical mass signal. In subsequent work the same group reviewed, on a qualitative basis, the diffusion-to-capture of interfacial immunochemical reactions, acoustic wave propagation through the liquid–solid interface and the characterization of piezoelectric crystal operation in water.[18] It was postulated that shear wave devices are capable of generating two distinct types of analytical signals. Firstly, thin films characterized by a shear modulus of elasticity would provide a Sauerbrey-type mass measurement. Secondly, capture at a liquid–solid shearing surface could lead to a differential signal associated with the introduction of new material at the interface. The main idea is that acoustic wave devices operating in the liquid phase respond to a change in interfacial conditions, not to the absolute amount of added mass.

A piezoelectric immunosensor for the detection of *Candida albicans* microbes was developed by Muramatsu *et al.*[21] Anti-*Candida* antibody was covalently bonded on the plated platinum electrodes. The frequency of the crystal was recorded before and after dipping into a suspension of *Candida*. The frequency change was observed and correlated with a concentration of *Candida* in the range 1×10^6–5×10^8 cells cm^{-3}. Muramatsu *et al.*[21] also measured the response of AT-cut 9 MHz piezoelectric crystals to samples of human IgG under various operational conditions.[22] Crystals were modified by immobilizing Protein A on the oxidized palladium layer on the electrode surface with (3-aminopropyl)triethoxysilane. Shifts in frequency were ascribed to the affinity reaction of Protein A and human IgG.

Davis and Leary[73] claimed to be able to continuously monitor the reaction of immunoglobulins with Protein A at the sensor surface. A frequency change of approximately 1 Hz for each 10 ng of added immunoglobulin was observed. They pointed out that because frequency decreases were demonstrated for added material at the sensor surface, the Sauerbrey mechanism must be correct. This was postulated despite the fact that no experiments confirming added material at the interface were mentioned. An indirect immunoassay involving polymer particles was developed by Kurosawa *et al.*[74] In their work the antibody–antigen reaction was carried out on latex and the frequency changes were regarded as being due to viscosity or density changes of bulk solution associated with aggregation of the latex particles.

In addition to the TSM-device work outlined above, research has continued on the performance of immunoassays using the SAW device,[75] in which the quartz surface of the sensor was etched and treated with (3-glycidyloxypropyl)-trimethoxysilane prior to immobilization of an antibody against influenza virus A. Frequency shifts were observed on exposure of the sensor to the virus.

Richards and Bach[76] have worked with DNA hybridization systems. In an ingenious experiment a DNA probe-type experiment was performed in which amplification of mass was obtained using iron oxide microparticles. These entities, bearing one of the reacting pairs, were attracted to the sensor surface by a magnetic field.

Finally in this section, we should note that a number of studies have been performed in which the final bioanalytical signal has been obtained from the sensor in the gas phase, subsequent to reactions in solution.[77–82] In view of the central theme of this review details of this work will not be outlined.

Properties of Thin Films

As has been the situation for the gas phase, a number of studies have been concerned with the *in situ* liquid behaviour of organic multilayers in the TSM sensor, both with respect to selective adsorption into such films and to their physical properties. Okahata *et al.*[83] argued from studies involving adsorption of hydrophobic alcohols or cholesterol into various synthetic multilayer matrices, that the frequency response could not be correlated with density or viscosity changes of the film. The direct detection of the selective interaction between phospholipid or cholesterol multibilayer films cast on a piezoelectric crystal with cyclodextrins has been reported.[84] Depending on their cavity sizes, cyclodextrins form soluble molecular-selective inclusion complexes through interaction with lipidic species. The cast films on crystal surfaces were stable and did not peel off the plate, even under harsh conditions in aqueous solution, which were confirmed by frequency observations of the crystal. Calibration showed that a decrease in frequency of 1 Hz corresponded to an increase in mass of 1.27 ng. Thickness-shear-mode acoustic wave devices have been used successfully to follow phase transitions in liquid crystals and lipid multilayers.[85]

Rajakovic *et al.*[86] examined the role of the device-to-water acoustic interaction and, accordingly, the part played by interfacial viscosity in determining the frequency response. Frequency measurements in water for TSM sensors with gold, aluminium and silanized aluminium electrodes were obtained by the oscillator method. In that paper a number of aluminium electrode-based sensors were silanized using aminopropyltriethoxysilane and dichlorodimethylsilane and then exposed to water or aqueous solutions. The results showed that physical conditions at the polymeric silane–water interface can radiate the flow of acoustic energy into the surrounding medium as indicated earlier in this review.

Conclusions

It is evident from the progress reviewed in this article that the frequency response of the TSM device in liquids is governed by a number of factors. (Indeed the measurement of series resonant frequency produces a less than complete picture of the system.) Among these parameters, significant but hitherto unrecognized for the TSM sensor, is the role played by molecular slip and viscosity at the sensor–liquid interface. This observation opens up a number of new possibilities for application of the technique including, for example, the study of the physics of fluids at interfaces, surface structure of polymer films, extrusion phenomena, flow in porous media, lubrication and the development of a new type of signal for biosensor design. There is evidence in the literature that the above is now being recognized, at least with respect to the physical chemistry of liquids.[87–90]

Finally, we would like to emphasize that several of the interfacial arguments presented in this review have been discussed by other authors with respect to the different types of acoustic wave devices. In particular, readers are advised to consult the work of Ricco and Martin[91] on plate devices and Diller and Frederick[92] on torsional structures.

The authors are grateful to the Natural Sciences and Engineering Research Council of Canada for support of our work. Additionally, we appreciate the Fellowships provided to two of us, Lj. V. R. and B. A. C-V., by the Serbian Research Council of Yugoslavia.

APPENDIX

Glossary of symbols used:

A	Area of the quartz plate
A_1	Numerical constant
A_2	Numerical constant
A_3	Numerical constant
b	Liquid film thickness
B_1	Numerical constant
B_2	Numerical constant
C_0	Numerical constant
C_1	Numerical constant
C_2	Numerical constant
C_3	Numerical constant
$\bar{C}_{66}$	Stiffened elastic constant due to intrinsic viscosity of the quartz crystal
d_L	Specific gravity of liquid
D	Ratio of velocity amplitude at z and velocity amplitude at crystal surface, $z = 0$
f	Numerical constant
ΔF	Frequency change due to film
ΔF_l	Frequency change due to a liquid film
ΔF_s	Frequency change due to a solid film
F_c	Resonant frequency of the quartz crystal with the film
F_f	Resonant frequency of the film
F_q	Resonant frequency of the quartz crystal without the film
$F_q - F_{qm}$	Change of resonant frequency of the quartz crystal due to $p - p_m$
h	Height of liquid layer
k	Real part of the propagation coefficient of the film
k_1	Numerical constant
k_2	Electromechanical coupling constant
l	Imaginary part of the propagation coefficient of the film
l_f	Film thickness
l_q	Quartz crystal thickness
Δm_L	Mass per unit area of equivalent liquid layer
m_q	Mass of the quartz crystal
m_f	Mass of the film
ΔM	Change in mass due to solid film
n	Number of sides of crystal in contact with liquid (n = 1 or 2)
N	Frequency constant of the specific crystal cut
$p - p_m$	Pressure difference between the two sides of the quartz crystal
r_o	Radius of the film
r_e	Radius of the electrode
r	Radius of the quartz crystal
R_1	Resistance of equivalent circuit of quartz crystal
V_q	Phase velocity of a shear wave in quartz
z	One direction in a rectangular coordinate system
Z_f	Acoustic impedance of the film
Z_q	Acoustic impedance of the quartz
α	Real part of the characteristic impedance of the film
β	Imaginary part of the characteristic impedance of the film
ε	Mean diameter of hemicylinders
ε_L	Dielectric constant of a liquid
η_L	Dynamic viscosity of a liquid
κ_L	Specific conductivity of a liquid
μ_q	Shear modulus of quartz
ρ_f	Density of the film
ρ_L	Density of liquid
ρ_q	Density of quartz
$\Delta\tau$	Period change due to a solid film
ϕ	Phase angle by which the acoustic wave at z lags that at the crystal surface, $z = 0$

References

1 Sauerbrey, G., *Z. Phys.*, 1959, **155**, 206.
2 King, W. H., Jr., *Anal. Chem.*, 1964, **36**, 1735.
3 Mieure, J. P., and Jones, J. L., *Talanta*, 1969, **16**, 149.
4 Konash, P. L., and Bastiaans, G. J., *Anal. Chem.*, 1980, **52**, 1929.
5 Nomura, R., and Minemura, A., *Nippon Kagaku Kaishi*, 1980, **1980**, 1621.
6 Nomura, T., and Iijima, M., *Anal. Chim. Acta*, 1981, **131**, 97.
7 Nomura, R., and Okuhara, M., *Anal. Chim. Acta*, 1982, **142**, 281.
8 Nomura, T., and Mimatsu, T., *Anal. Chim. Acta*, 1982, **143**, 237.
9 Nomura, T., and Maruyama, M., *Anal. Chim. Acta*, 1983, **147**, 365.
10 Nomura, T., and Nagamune, T., *Anal. Chim. Acta*, 1983, **155**, 231.
11 Roederer, J. E., Bastiaans, G. J., *Anal. Chem.*, 1983, **55**, 2333.
12 Nomura, T., and Tsuge, K., *Anal. Chim. Acta*, 1985, **169**, 257.
13 Bruckenstein, S., and Shay, M., *Electrochim. Acta*, 1985, **30**, 1295.
14 Kanazawa, K. K., and Gordon, J. G., *Anal. Chim. Acta*, 1985, **175**, 99.
15 Nomura, T., Watanabe, M., and West, T. S., *Anal. Chim. Acta*, 1985, **175**, 107.
16 Muramatsu, H., Kajiwara, K., Tamiya, E., and Karube, I., *Anal. Chim. Acta*, 1986, **188**, 257.
17 Thompson, M., Dhaliwal, G. K., and Arthur, C. L., *Anal. Chem.*, 1986, **58**, 1206.
18 Thompson, M., Dhaliwal, G. K., Arthur, C. L., and Calabrese, G. S., *IEEE Trans. Ultranson. Ferroelec. Freq. Contr.*, 1987, **UFFC-34**, 128.
19 Calabrese, G. S., Wohltjen, H., and Roy, M. K., *Anal. Chem.*, 1987, **59**, 833.
20 Yao, S-Z., and Mo, Z-H., *Anal. Chim. Acta*, 1987, **193**, 97.
21 Muramatsu, H., Dicks, J. M., Tamiya, E., and Karube, I., *Anal. Chem.*, 1987, **59**, 2760.
22 Muramatsu, H., Tamiya, E., and Karube, I., *Anal. Chem.*, 1988, **60**, 2142.
23 Muramatsu, H., Tamiya, E., Suzuki, M., and Karube, I., *Anal. Chim. Acta*, 1988, **215**, 91.
24 Schumacher, R., Pesek, J., and Melroy, O., *J. Phys. Chem.*, 1985, **89**, 4338.
25 Schumacher, R., Borges, G., and Kanazawa, K. K., *Surf. Sci.*, 1985, **163**, L621.
26 Bruckenstein, S., and Swathirajan, S., *Electrochim. Acta*, 1985, **30**, 851.
27 Stöckel, R., and Schumacher, R., *Be·. Bunsenges. Phys. Chem.*, 1987, **91**, 345.
28 Beck, R., Pittermann, U., and Weil, K. G., *Ber. Bunsenges. Phys. Chem.*, 1988, **92**, 1363.
29 Schumacher, R., *Angew. Chem. Int. Ed. Engl.*, 1990, **29**, 329.
30 *Applications of Piezoelectric Quartz Crystal Microbalances*, eds. Lu, C-S., and Czanderna, A. W., Elsevier, Amsterdam, 1984.
31 Stockbridge, C. D., in *Vacuum Microbalance Techniques*, ed. Behrndt, K. H., Plenum, New York, vol. 5, 1966, p. 193.
32 Miller, J. G., and Bolef, D. I., *J. Appl. Phys.*, 1968, **39**, 4589.
33 Miller, J. G., and Bolef, D. I., *J. Appl. Phys.*, 1968, **39**, 5815.
34 Behrndt, K. H., *J. Vac. Sci. Technol.*, 1971, **8**, 622.
35 Lu, C-S., and Lewis, O., *J. Appl. Phys.*, 1972, **43**, 4385.
36 Lu, C-S., *J. Vac. Sci. Tech.*, 1975, **12**, 578.
37 Glassford, A. P. M., in *Progress in Astronautics and Aeronautics*, ed. Smith, A. M., American Institute of Aeronautics and Astronautics, New York, 1977, vol. 56, p. 175.
38 Glassford, A. P. M., *J. Vac. Sci. Technol.*, 1978, **15**, 1836.
39 Mecea, V., and Bucur, R. V., *Thin Solid Films*, 1979, **60**, 73.
40 Crane, R. A., and Fischer, G., *J. Phys. D.*, 1979, **12**, 2019.
41 Guilbault, G. G., in *Applications of Piezoelectric Quartz Crystal Microbalances*, eds. Lu, C-S., and Czanderna, A. W., Elsevier, New York, 1984, vol. 7, p. 251.

42 Heusler, K. E., Grzegorzewski, A., Jäckel, L., and Pietrucha, J., *Ber. Bunsenges. Phys. Chem.*, 1988, **92**, 1218.
43 Hager, H. E., and Verge, P. D., *Sens. Actuators*, 1985, **7**, 271.
44 Hager, H. E., *Chem. Eng. Commun.*, 1986, **43**, 25.
45 Yao, S-Z., and Zhou, T-A., *Anal. Chim. Acta*, 1988, **212**, 61.
46 Shana, Z. A., Radtke, D. E., Kelkar, U. R., Josse, F., and Haworth, D. T., *Anal. Chim. Acta*, 1990, **231**, 317.
47 Blake, T. D., *Coll. Surf.*, 1990, **47**, 135.
48 Duncan-Hewitt, W. C., and Thompson, M., *Anal. Chem.*, submitted for publication.
49 Wiggins, P. M., *Progr. Polym. Sci.*, 1988, **13**, 1.
50 Krausz, A. S., and Eyring, H., *Deformation Kinetics*, Wiley, New York, 1974.
51 Cady, W. G., *Piezoelectricity*, Dover, New York, 1964.
52 Bottom, V. E., *Introduction to Quartz Crystal Unit Design*, Van Nostrand Reinhold, New York, 1982.
53 Grzegorzewski, A., and Heusler, K., *J. Electroanal. Chem. Interfacial Electrochem.*, 1987, **228**, 455.
54 Mecea, V., and Bucur, R. V., *J. Phys. E.*, 1974, **7**, 348.
55 Kipling, A. L., and Thompson, M., *Anal. Chem.*, 1990, **62**, 1514.
56 Schulz, W. W., and King, W. H., *J. Chromatog. Sci.*, 1973, **11**, 343.
57 Oda, S., and Sawada, T., *Anal. Chem.*, 1981, **53**, 471.
58 Charlesworth, J. M., *Anal. Chem.*, 1990, **62**, 76.
59 Wohltjen, H., and Dessy, R., *Anal. Chem.*, 1979, **51**, 1465.
60 Heckl, W. M., Marassi, F. M., Kallury, K. M. R., Stone, D. C., and Thompson, M., *Anal. Chem.*, 1990, **62**, 32.
61 Thompson, M., and Stone, D. C., *Anal. Chem.*, 1990, **62**, 1897.
62 Grate, J. W., Snow, A., Ballantine, D. S. Jr., Wohltjen, H., Abraham, M. H., McGill, R. A., and Sasson, P., *Anal. Chem.*, 1988, **60**, 869.
63 Nomura, T., and Hattori, O., *Anal. Chim. Acta*, 1980, **115**, 323.
64 Nomura, T., *Anal. Chim. Acta*, 1981, **124**, 81.
65 Nomura, T., Yamashita, T., and West, T. S., *Anal. Chim. Acta*, 1982, **143**, 243.
66 Nomura, T., Okuhara, M., and Hasegawa, T., *Anal. Chim. Acta*, 1986, **182**, 261.
67 Nomura, T., and Ando, M., *Anal. Chim. Acta*, 1985, **172**, 353.
68 Nomura, T., and Fujisawa, M., *Anal. Chim. Acta*, 1986, **182**, 267.
69 Nomura, T., and Sakai, M., *Anal. Chim. Acta*, 1986, **183**, 301.
70 Shouzhuo, Y., and Zhihong, M., *Anal. Chim. Acta*, 1987, **193**, 97.
71 Shouzhuo, Y., and Lihua, N., *Anal. Proc.*, 1987, **24**, 336.
72 Martin, S. J., Ricco, A. J., Niemczyk, T. M., and Frye, G. C., *Sens. Actuators*, 1989, **20**, 253.
73 Davis, K. A., and Leary, T. R., *Anal. Chem.*, 1989, **61**, 1227.
74 Kurosawa, S., Tawara, E., Kamo, N., Ohta, F., and Hosokawa, T., *Chem. Pharm. Bull.*, 1990, **38**, 1117.
75 Bastiaans, G. J., US Patent 4735906 A, 1988, April 5th; *Chem. Abstr.*, 1988, **109**, 69931r.
76 Richards, J. C., and Bach, D. T., Eur. Pat. Appl., EP 295965 A2, 1988, December 21st; *Chem. Abstr.*, 1988, **111**, 150067b.
77 Ebersole, R., and Ward, M. D., *J. Am. Chem. Soc.*, 1988, **110**, 8623.
78 Grande, L. H., Green, C. R., and Paul, D. W., *Sens. Actuators*, 1988, **14**, 387.
79 Prusak-Sochaczewski, E., and Luong, J. H. T., *Anal. Lett.*, 1990, **23**, 183.
80 Shous, A., Dorman, F., and Najarian, J., *J. Biomed. Mater. Res.*, 1972, **6**, 565.
81 Oliveria, R. J., and Silver, S. F., US Patent, 4242096, 1980, December 2nd.
82 Fawcett, N. C., Evans, J. A., Chien, L-C., and Flowers, N., *Anal. Lett.*, 1988, **21**, 1099.
83 Okahata, Y., Ebato, H., and Ye, X., *J. Chem. Soc., Chem. Commun.*, 1988, 1037.
84 Okahata, Y., and Ye, X., *J. Chem. Soc., Chem. Commun.*, 1988, 1147.
85 Okahata, Y., and Ebato, H., *Anal. Chem.*, 1989, **61**, 2185.
86 Rajaković, Lj. V., Čavić-Vlasak, B. A., Ghaemmaghami, V., Kallury, K. M. R., Kipling, A. L., and Thompson, M., *Anal. Chem.*, 1991, **63**, 615.
87 Orata, D. O., and Buttry, D. A., *J. Electroanal. Chem. Interfacial Chem.*, 1988, **257**, 71.
88 Lee, P. C. Y., Guo, X., and Tang, M. S. H., *J. Appl. Phys.*, 1988, **63**, 1850.
89 Furukawa, S., Nomura, T., and Yasuda, T., *J. Phys. D*, 1989, **22**, 1785.
90 Lasky, S. J., and Buttry, D. A., *J. Am. Chem. Soc.*, 1988, **110**, 6258.
91 Ricco, A. J., and Martin, S. J., *App. Phys. Lett.*, 1987, **21**, 1474.
92 Diller, D., and Frederick, N. V., *Int. J. Thermophys.*, 1989, **10**, 145.

Paper 1/01556G
Received April 3rd, 1991
Accepted May 7th, 1991

On-line Immunoaffinity Sample Pre-treatment for Column Liquid Chromatography: Evaluation of Desorption Techniques and Operating Conditions Using an Anti-estrogen Immuno-precolumn as a Model System

Aria Farjam, Anita E. Brugman, Henk Lingeman* and Udo A. Th. Brinkman
Department of Analytical Chemistry, Free University, De Boelelaan 1083, 1081 HV Amsterdam, The Netherlands

An immunoaffinity precolumn (immuno-precolumn) containing an immobilized antibody directed against estrogen steroids, was used as a model system for the evaluation of different desorbing techniques, suitable for on-line coupling to column liquid chromatography (LC). Desorption of estrogen analytes from the immuno-precolumn proved to be impossible with the buffers and chaotropic solutions frequently used in affinity desorption. Micellar solutions are effective in obstructing the antibody–antigen reaction, but their use as desorbing solutions was not found to be practical because of the large interferences introduced into the chromatograms. Desorption with aqueous solutions at elevated temperature, created by microwave action or conventional heating, although effective is not practical in this instance, because the agarose used in this study as the stationary phase for the immuno-precolumn is prone to heat decomposition. The most effective and practical approach is desorption with a methanol–water mixture (95 + 5 v/v). On-line dilution of the eluate allows the concentration of the desorbed analytes using a reversed-phase LC system with subsequent separation and ultraviolet detection. The performance of the system with spiked urine and plasma samples, which were introduced directly into the system, was evaluated and the results were compared with immunoselective desorption.

Keywords: *Immunoaffinity precolumn; column switching; column liquid chromatography; estrogen; urine and plasma samples*

For the determination of trace levels of analytes in complex samples, a highly selective sample pre-treatment is necessary. In this field immunoaffinity chromatography is a powerful technique. Antibodies raised against the target analytes when immobilized on a solid support and packed into a precolumn, can be used for the selective solid-phase extraction of the analytes. If this technique is combined with chromatographic separation and subsequent detection, a powerful analytical system is obtained, which combines the positive features of both techniques. The good group selectivity of the antibody is combined with the efficiency of chromatography in order to discriminate and quantify several analytes in a single run.

Full automation of such analytical systems can be achieved by coupling the immuno-precolumn to column liquid chromatography (LC) with a column switching system.[1–10] The critical point in such an immunoaffinity LC system is the on-line desorption of the analytes from these precolumns. As immunosorbents often have a relatively low capacity for the analytes of interest, in most instances large volume immuno-precolumns (up to 1 ml) have to be used for effective clean-up and preconcentration of the samples. Quantitative desorption of the analytes from the large volume immuno-precolumn must be combined with an efficient refocusing of the analytes on the reversed-phase LC system. Moreover, desorption should neither de-activate the immunosorbent irreversibly nor introduce impurities into the system. Also, it would be of great benefit, if the desorbing technique were not just suitable for a single antibody, but applicable to a wide range of different antibody–analyte systems.

In previous studies an immunoselective desorbing technique has been employed,[7–9] in which the desorbing solution contains one or more cross-reacting compounds. Because of their affinity for the antibody, these compounds are able to displace trapped analytes from the immuno-precolumn. Using this technique almost totally aqueous solutions could be used for desorption, the eluate could be used directly for preconcentration of the analytes on a reversed-phase precolumn. Another on-line desorbing technique was employed with an anti-aflatoxin immuno-precolumn.[10] A methanol–water mixture (70 + 30 v/v) was used to desorb the immuno-precolumn. After desorption the eluate was diluted on-line with water in order to allow concentration of the analytes of interest using a reversed-phase LC column.

In this study the performance of several desorbing techniques for on-line immunoaffinity sample pre-treatment coupled to LC are evaluated. An anti-estrogen immuno-precolumn is used as a model system. Immunoselective desorption,[7–9] non-selective desorption with methanol,[10] desorption with so-called chaotropic solutions (solutions containing compounds that disrupt the water structure), with anionic and cationic micellar solutions and at elevated temperature are compared. The practicability of the on-line methanol desorption is finally demonstrated with spiked urine and plasma samples. The possibility of using this technique with other antibody–analyte systems is also discussed.

Experimental

Reagents

The anti-estrogen antiserum was a gift from Organon (Oss, The Netherlands). Cyanogen bromide (CNBr) activated Sepharose 4B was obtained from Pharmacia (Woerden, The Netherlands). Liquid chromatography grade acetonitrile and methanol were obtained from Baker (Deventer, The Netherlands) and Merck (Darmstadt, Germany), respectively. Liquid chromatography grade water was prepared from demineralized water using a Milli-Q (Millipore, Bedford, MA, USA) water purification system, with subsequent filtration over an LC column filled with 40 μm Baker C_{18} bonded phase material. The eluents were de-gassed under vacuum in an ultrasonic bath. The steroids estrone (E1), β-estradiol (E2), β-estriol (E3), ethynylestradiol (EE) and

* To whom correspondence should be addressed.

17-β-estradiol-17-acetate (E2Ac) were obtained from Sigma (St. Louis, MO, USA). Stock solutions of the steroids were prepared in ethanol (1 mg ml^{-1}) and stored at 4 °C until they were used.

The E3 stock solution was purified by preparative LC. One milligram was dissolved in 1 ml of an acetonitrile–water mixture (40 + 60 v/v) and injected onto a 250 × 10 mm i.d. Baker C_{18} bonded phase column for preparative LC (40 μm particles). Tetrahydrofuran–acetonitrile–water (5 + 20 + 75 v/v) was used as the eluent. All of the other chemicals were from various sources, and of analytical-reagent grade.

Apparatus

The set-up of the LC system used for the non-selective desorption is schematically shown in Fig. 1. It consisted of a Kratos (Ramsey, NJ, USA) Model 400 pump (pump 1); two Kontron (Zürich, Switzerland) Model 410 pumps (pumps 2 and 3) equipped with laboratory-built membrane pulse dampers; a Kontron MCS 670 tracer valve switching unit; and a Kontron Model Anacomp 200 programmer, which controlled the high-pressure switching valves (V1–V3), the solvent selection valve and the flow of pump 1. A Kratos Model 757 Spectroflow ultraviolet (UV) detector set at 280 nm was used together with a Kipp & Zonen (Delft, The Netherlands) BD 40 recorder for peak area measurements. A coiled $\frac{1}{16}$ in stainless-steel capillary with a 0.5 mm i.d., an internal volume of 1 ml, and a helix of 5 cm was used as the mixing coil. The analytical column was a 100 × 3.0 mm i.d. stainless-steel column packed in-house with 5 μm LiChrosorb RP-18 from Merck. This column was protected with a 10 × 2.0 mm i.d. stainless-steel guard column packed with the same material. The 20 × 3.0 mm i.d. C_{18} precolumn was packed with 40 μm Baker C_{18} bonded phase material.

The immuno-precolumns were laboratory-built 10 × 10 mm i.d. or 10 × 4.0 mm i.d. stainless-steel columns equipped with 5 μm stainless-steel screens, and with polytetrafluoroethylene (PTFE) rings as column inlets and outlets. The packing procedure of the immuno precolumns is described elsewhere.[7]

The mobile phase for the LC was an acetonitrile–water mixture (65 + 35 v/v) with 10% v/v tetrahydrofuran at a flow rate of 0.5 ml min^{-1}.

Non-selective Desorption With Aqueous Methanol

The final procedure developed in this study was comprised of the following steps (see also Fig. 1): 1, flushing the immuno-precolumn with 15 ml of water; 2, loading the sample on the immuno-precolumn; 3, flushing the immuno-precolumn with 15 ml of water; 4, flushing the C_{18} precolumn with 6 ml of water; 5, desorbing the immuno-precolumn with 3.7 ml of methanol–water (95 + 5 v/v). (The eluate is diluted on-line *via* the T-piece with a 16-fold excess of water and the analytes are subsequently concentrated on the C_{18} precolumn and, then, separated on the C_{18} separation column); and 6, flushing the immuno-precolumn with 5 ml of methanol–water (95 + 5 v/v). The flushing volumes indicated for steps 1, 3, 5 and 6 were used with a 10 × 10 mm i.d. immuno-precolumn. If immuno-precolumns of a different size were used, the flushing volumes were adapted correspondingly.

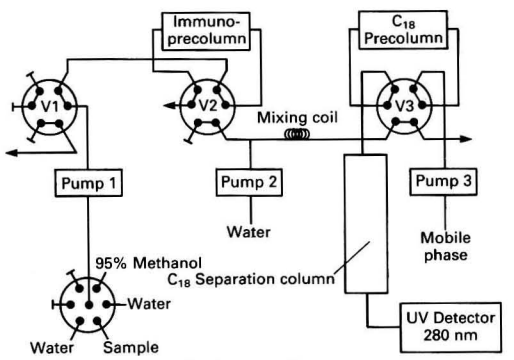

Fig. 1 Set-up of the on-line immunoaffinity liquid chromatographic system used for non-selective desorption. The system is described under Apparatus

Immunoselective Desorption

For immunoselective desorption the set-up in Fig. 1 was changed by removing pump 2, the T-piece and the mixing coil that connects V2 to V3, such that the C_{18} precolumn could be reconditioned with water by pump 1 (*cf.* Fig. 1 in reference 9). The analytical procedure is essentially the same as that with the non-selective methanol desorption, except that desorption (step 5) is performed with 60 ml of acetonitrile–water (5 + 95 v/v) containing 260 μg l^{-1} of each of E2 and E2Ac as displacers. The immuno-precolumn and the C_{18} precolumn are switched in series during this step. Flushing of the immuno-precolumn was performed with 20 ml of methanol–water (70 + 30 v/v).

The flushing volumes indicated were used with a 10 × 10 mm i.d. immuno-precolumn. For immuno-precolumns of a different size the flushing volumes were adapted correspondingly.

Microwave Desorption

The immunosorbent was packed into a 40 × 5.2 mm i.d. glass column and placed in a 200 ml water-bath inside a microwave oven, Model H 2500 (Bio-Rad, Richmond, CA, USA). The temperature sensor of the microwave oven was put in the water-bath. The immuno-precolumn was connected to the column switching system *via* two 0.5 mm i.d. PTFE capillaries. The PTFE outlet capillary was coiled over a length of 50 cm and inserted into a 20 °C water-bath, which was outside the microwave oven, in order to cool the eluate to room temperature after desorption. Analysis was performed according to the immunoselective procedure, except that no displacer was present in the desorbing solution. The microwave oven was programmed to raise the temperature to the pre-set value at the start of the desorption (step 5). Usually this was achieved within 20 s. After desorption, the immuno-precolumn was immediately placed into the 20 °C water-bath outside the oven.

Immunosorbent

The preparation of the anti-estrogen immunosorbent on the CNBr-activated Sepharose 4B has been reported in a previous study.[3] If not indicated otherwise, all of the quantitative measurements were performed with immuno-precolumns that had already been used for at least ten runs so as to obtain a constant capacity.

The capacity of the 10 × 10 mm i.d. immuno-precolumn was determined by overloading it with 30 ml of a standard solution containing 66 μg l^{-1} of each of EE, E1 and E2. The analysis was performed according to the non-selective desorption procedure.

Urine and Plasma Samples

Urine samples

Samples were collected from three healthy male volunteers, they were then pooled, divided into 100 ml fractions and stored at −20 °C. The samples were thawed 1 h before use.

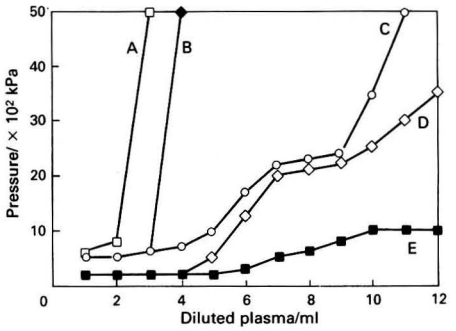

Fig. 2 Pressure as a function of the amount of plasma pumped over different types of screens. Unfiltered plasma, which had been diluted 4-fold with water, was pumped over different types of screens that had been inserted into a $\frac{1}{16}$ in Valco female–female connector: flow rate, 2 ml min^{-1}. A, a polyester screen with 20 μm pores; B, a stainless-steel screen with 7 μm pores; C, a nylon screen with 20 μm pores; D, a stainless-steel screen with 13 μm pores; and E, a stainless-steel screen with 36 μm pores were compared

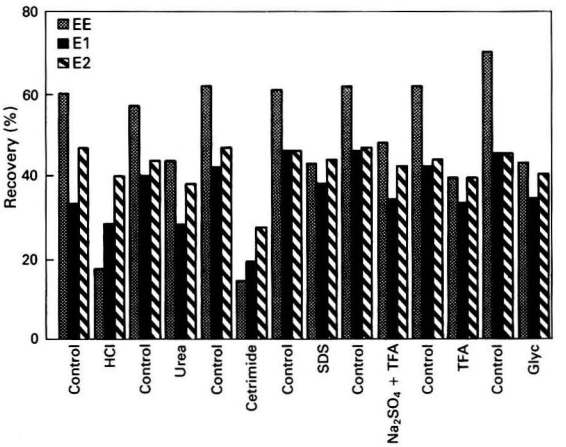

Fig. 3 Recovery of the estrogens EE, E1 and E2, if loaded from solutions containing the indicated desorbing agents. In all instances 4.8 ml of a solution containing 10.5 μg l^{-1} of each estrogen dissolved in the desorber-containing solutions or in water (control), were loaded on to a 10 × 4 mm i.d. immuno-precolumn. The desorber solutions were 0.1 mol dm^{-3} glycine–HCl buffer, pH 2 (Glyc); 0.2% (m/m) trifluoroacetic acid (TFA); 0.2% (m/m) sodium sulphate plus 0.2% (m/m) TFA, pH 2 (Na_2SO_4 + TFA); 3.4 mol dm^{-3} sodium dodecylsulphate (SDS); 3.1 mol dm^{-3} hexadecyltrimethylammonium chloride (cetrimide); 4 mol dm^{-3} urea (urea) and 0.5% (m/m) HCl (HCl). Analysis was performed by means of immunoselective desorption

Analysis of plasma samples

The plasma samples from healthy volunteers were a gift from the State University of Utrecht (Utrecht, The Netherlands). The samples were divided into 10 ml fractions and stored at −20 °C. The samples were thawed 1 h before use.

The set-up for the automated analysis contains a stainless-steel screen (pore size, 7 μm), which is incorporated into a Valco female–female union positioned directly after the pump used for loading the samples. This screen has a filter function and is replaced if the pressure in the system becomes too high; usually once a week. The screen also helps to prevent blocking of the switching valves and the expensive immuno-precolumn. However, with plasma analyses, this screen tends to block after the passage of only small volumes of diluted plasma (see Fig. 2). In order to eliminate this problem, various types of screen were tested. As can be seen in Fig. 2, the 36 μm stainless-steel screen gave the best results. Therefore, this screen was used in the systems if plasma samples were to be analysed.

Results and Discussion

Desorption with Aqueous Solutions

In classical immunoaffinity chromatography, buffers of either high or low pH or aqueous solutions containing chaotropic compounds are used for breaking antibody–antigen interactions, *i.e.*, for desorption. Desorption of protein antigens from immunoaffinity columns using these techniques has frequently been reported.[11] In principle, such solutions are a good choice for on-line desorption coupled to reversed-phase LC, as concentration of the analytes can be performed efficiently on a reversed-phase column from the purely aqueous eluate. By using the anti-estrogen immuno-precolumn as a test system, a number of conventional desorbing solutions were investigated.

An aqueous solution containing the desorbing agent to be tested was used to preconcentrate the analytes of interest on to an immuno-precolumn. Desorption and determination of the trapped analytes were performed by means of immunoselective desorption (see Experimental). In order to define a good desorber, the amount of analyte trapped on the immuno-precolumn should be close to zero. The amount of the analytes EE, E1 and E2, trapped on the immuno-precolumn, if loaded from different desorber-containing solutions is shown in Fig. 3. After each measurement, as a control, the analytes were also loaded from a purely aqueous solution, in order to monitor a decrease of immuno-precolumn capacity. With most of the desorbing solutions tested the recoveries were rather close to the recoveries of the control experiments, especially with E1 and E2. The 'best' deactivation of the antibody–estrogen interaction was obtained using hexadecyltrimethylammonium chloride (cetrimide) with recoveries (n = 3) for EE, E1 and E2 of 14, 19 and 27%, respectively. Obviously, none of the solutions tested efficiently prevents the binding of the analytes to the immobilized antibodies or, alternatively, in the proposed LC system, disrupt these bonds.

The buffer and chaotropic solutions, which work well for the desorption of proteins in conventional immunoaffinity chromatography, are obviously not generally suitable for the desorption of small molecules (see also references 7 and 12). The most probable explanation is, that in conventional immunoaffinity chromatography these desorbing solutions interact with the sorbed protein, *i.e.*, change its structure, much more than with the immobilized antibody, which, owing to its multipoint attachment to the stationary phase, is more resistant to structural changes than the free protein. As small molecules are mostly not prone to structural changes as a result of the action of the buffer or chaotropic solutions, their desorption from the immobilized antibody is difficult. If, however, the structure of a small molecule can be changed by a buffer or chaotropic agent, desorption will occur. Such a situation is typically encountered when the small analyte possesses an acidic or basic group. Desorption can then be achieved with a buffer that changes the analyte structure by either protonation or deprotonation.[13–15]

Desorption with Micellar Solutions

The experiments described above included the use of an anionic sodium dodecyl sulphate (SDS) and a cationic (cetrimide) surfactant. It is known that the physico-chemical properties of surfactants can differ significantly below and above their critical micellization concentration (c.m.c.) In order to determine the influence of the surfactants on the antibody–antigen interaction as a function of their concentration, the estrogens were loaded onto the immuno-precolumn

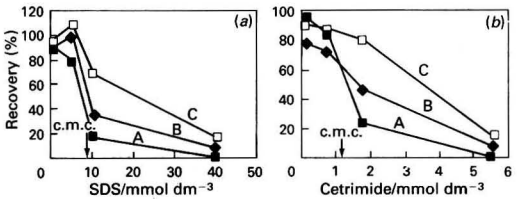

Fig. 4 Recovery as a function of the amount of surfactant added to the sample solution. Standard solutions (30 ml) containing 2.5 μg l^{-1} of each estrogen: A, EE; B, E1; and C, E2 and various amounts of the surfactants (*a*) sodium dodecylsulphate (SDS) and (*b*) hexadecyltrimethylammonium chloride (cetrimide) were loaded on a 10 × 10 mm i.d. immuno-precolumn. Analysis was performed according to the non-selective desorption technique. Where c.m.c. = critical micellization concentration

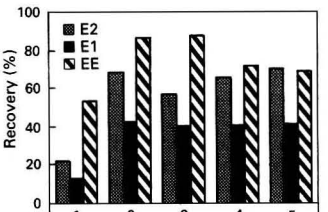

Temperature/°C		20	55	55	55	55
Type of heat action	(*i*) Microwave		✓	✓	✓	
	(*ii*) Water-bath	✓				✓
Acetonitrile (% v/v)		5	5	5	12	12
Volume of desorber/ml		60	60	30	30	30

Fig. 5 Recovery as a function of thermodesorption conditions. A standard sample (15 ml) containing 5 μg l^{-1} of each of the three estrogens EE, E1 and E2 was loaded onto a 40 × 5.2 mm i.d. immuno-precolumn (column volume, 850 μl). Analysis was performed according to the immunoselective desorption technique, but no displacer was present in the desorbing solutions

from solutions containing different concentrations of surfactant. In contrast with the earlier experiments, methanol–water (95 + 5 v/v) was now employed for desorption (non-selective). This was to prevent secondary effects caused by the cross-reacting steroids present in the immunoselective desorbing solution.

As can be seen in Fig. 4, estrogen recoveries ($n = 2$) close to 100% were achieved, if the surfactants were present in the sample solutions at concentrations below their c.m.c. At their c.m.c. about 8 mmol dm^{-3} for SDS and 1 mmol dm^{-3} for cetrimide, a sharp decrease of analyte recovery was observed. At concentrations of about five times the c.m.c. the recovery ($n = 2$) of all of the steroids was less than 20%. Obviously the presence of either cationic or anionic micellar species prevents binding of the analytes on to the immobilized antibody. The decrease in the recovery was significantly more rapid with SDS than with cetrimide.

Micellar solutions, therefore, seem to be good candidates for desorption of analytes from the immuno-precolumn. When the solutions were used for desorption, however, serious problems arose during analyte preconcentration on the C_{18} precolumn and subsequent separation. If the analytes were preconcentrated on the C_{18} precolumn from micellar cetrimide solutions (containing concentrations five times greater than the c.m.c. of the surfactant) and subsequently separated, large interfering peaks occurring at the retention times of the analytes prevented quantification. If the experiments were performed with solutions containing SDS, the recovery of the analytes dropped to zero. Obviously the micellar solutions change the property of the analytical system such that efficient preconcentration and separation of the analytes is not possible.

Thermodesorption

Antibody–antigen interactions become weaker at higher temperatures. Therefore desorption from the immuno-precolumn at elevated temperature was investigated. The immunosorbent was packed into a 5.2 × 40 mm i.d. glass precolumn, which was placed in a microwave oven. Standard samples (50 ml) spiked with 5 μg l^{-1} each of EE, E1 and E2 were loaded onto the immuno-precolumn. The analyses were carried out according to the immunoselective procedure, except that no displacer was added to the desorbing solution. Instead, the microwave oven was programmed to raise the temperature at the start of the desorption and keep it constant during the desorption process.

Analyte recovery was found to improve with increasing temperature. The recoveries ($n = 2$) of EE, E1 and E2 with room temperature desorption were 53, 12 and 22%, respectively (*cf.* Fig. 5, column 1) and at 55 °C, the highest temperature tested, were 86, 43 and 69% (*cf.* Fig. 5, column 2). In both instances 60 ml of acetonitrile–water (5 + 95 v/v) were used for desorption. Some acetonitrile was added to prevent non-specific retention of the analytes on the immuno-precolumn. In an earlier study,[9] the use of 12 instead of 5% acetonitrile was found to enhance the desorption at room temperature. When using microwave desorption at 55 °C however, no significant difference in steroid recovery was found for desorbing solutions containing 5 or 12% acetonitrile (*cf.* Fig. 5, columns 3 and 4). Obviously the microwave action is the dominant desorbing effect. Reducing the volume of solution used during microwave desorption at 55 °C from 60 ml (Fig. 5, column 2) to 30 ml (Fig. 5, column 3) of acetonitrile–water (5 + 95 v/v) gave only a minor decrease in recovery. This indicates that most of the analytes are desorbed in the early part of the process. In order to determine whether the microwave action, or solely the heat generation as such, was responsible for desorption, a control experiment was set up in which the immuno-precolumn was inserted into a 55 °C water-bath during desorption. Under similar conditions no difference in recovery was found between microwave and water-bath heat generation (Fig. 5, columns 4 and 5).

After ten 'temperature runs', the decrease in the capacity of the immuno-precolumn was about 20%, indicating that, with this technique, repeated use of the immuno-precolumn is possible only for a limited number of analyses. The loss of capacity is probably not due to irreversible heat de-activation of the antibodies, but to decomposition of the agarose backbone: it is well known that agarose-based stationary phases decompose at elevated temperature. For this reason temperatures higher than 55 °C have not been tested. As this study was restricted to agarose-based immunosorbents, further use of thermodesorption, which will be more efficient with temperature-resistant phases, was not investigated here.

Non-selective Desorption With Aqueous Methanol

Another technique that can be employed for on-line desorption is non-selective elution with methanol–water (70 + 30 v/v), an alternative that is also being used in on-going work on anti-aflatoxin immuno-precolumns.[10] In this technique, after desorption the high methanol content of the eluate is reduced by on-line dilution with water, in order to allow concentration of the analytes on a reversed-phase column. A 16-fold dilution of the methanol–water (70 + 30 v/v) with water will result in a final methanol percentage of about 4%, a value sufficiently low for efficient trapping of the estrogens on the C_{18} precolumn. With a 10 × 4.0 mm i.d. immuno-precolumn, 600 μl of the methanol–water (70 + 30 v/v) were sufficient to

obtain a good, *viz.*, over 80%, recovery (n = 3) of all three analytes. The calibration graph, recorded by loading the steroids from a 5 ml standard sample, was linear up to individual amounts of steroid of 30 ng (total amount of steroid, 90 ng).

Initially, a rather persistent memory effect was observed for E1 and E2, although, surprisingly, not for EE. A partial solution for this problem was obtained by flushing the immuno-precolumn with methanol–water (70 + 30 v/v) containing various electrolytes or surfactants. Further work showed that the memory effect was completely eliminated upon desorption with 95% instead of 70% methanol. This procedure was used in all further work.

A volume of 3.7 ml of methanol–water (95 + 5 v/v) was chosen for desorption of the analytes from the 10 × 10 mm i.d. immuno-precolumn. The eluate was again diluted on-line with a 16-fold excess of water, before concentration on the C_{18} precolumn. Owing to the higher methanol concentration, flushing of the immuno-precolumn after desorption (step 6 of the final procedure) was performed with 5 instead of 20 ml of solution. The recoveries for EE, E1 and E2, if loaded from 30 ml of standard solutions, were 84, 84 and 90%, respectively. The recovery was constant [a relative standard deviation (RSD) of 2%; n = 4] for up to 100 ng of each steroid (total amount, 300 ng). For larger amounts the recovery slowly decreased, owing to the limited capacity of the immuno-precolumn. If the total amount of steroid did not exceed the immuno-precolumn capacity, good recoveries could also be achieved with larger sample volumes. For example, the recoveries for all three steroids were still over 80% if they were preconcentrated from 500 ml of standard solution containing 75 ng of each steroid.

Stability of the immuno-precolumn

The long-term stability of the 10 × 10 mm i.d. immuno-precolumn was assessed by measuring its capacity at regular intervals. The capacity had dropped by about 50% after 36 d of operation as can be seen in Fig. 6. During this time about 100 analyses were run; 20 of these were on urine samples. It is interesting that most of the capacity drop occurred during the days when only analyses of standards were performed (days 1–10). After that period of time, the capacity for EE, E1 and E2 reached plateau values of about 120, 300 and 180 ng, respectively. Obviously, it is not the urine analyses that are responsible for this loss of capacity.

The initial capacity decrease, which has also been observed in other work,[7–10,15] occurs because, during the early runs, any 'fragile' antibody molecules, *i.e.*, those improperly immobilized or easily subject to irreversible structural changes, will be lost. The extent of this capacity drop mainly depends on the immobilization chemistry and on the characteristics of the antibody used. With an anti-nortestosterone immuno-precolumn a capacity drop of 70%[7,8] was found before reaching plateau conditions. With a commercially available anti-aflatoxin immuno-precolumn the capacity drop was over 90%.[10]

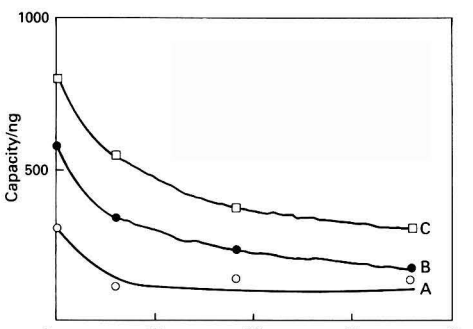

Fig. 6 Long-term stability of the 10 × 10 mm i.d. immuno-precolumn, expressed as its capacity for the estrogen: A, EE; B, E1; and C, E2. Day zero: first day of use

Analysis of Biological Samples Using Non-selective Desorption

Spiked urine samples

A chromatogram of a male volunteer's urine sample spiked with 5.1 μg l^{-1} of each of EE, E1 and E2, and of the corresponding blank urine are shown in Fig. 7(*a*). Fifteen millilitres of sample were diluted with 15 ml of water and loaded on to the 10 × 10 mm i.d. immuno-precolumn. The recoveries for EE, E1 and E2 were 70, 67 and 77% with RSDs of 4, 3 and 4 (n = 4). These values are somewhat worse than for standard samples, but better than for the plasma samples. Under these conditions the detection limit of the method is 0.2–0.5 μg l^{-1} (signal-to-noise ratio = 3 : 1). The detection can be improved by processing larger volumes of urine. It is worth noting that by analysing 75 ml instead of 15 ml of the same sample, as in Fig. 7(*a*), gave an identical blank chromatogram. That is, detection limits of 0.1 μg l^{-1} or below are easily attainable. Capacity measurements performed before and after 20 urine analyses showed that the immobilized antibodies were not affected by the urine samples.

Spiked plasma samples

A chromatogram of a plasma sample spiked with 12.5 μg l^{-1} of each of EE, E1 and E2, and of the corresponding blank plasma, is shown in Fig. 7(*b*). Six millilitres of sample were diluted with 24 ml of water and loaded onto the 10 × 10 mm i.d. immuno-precolumn. Unfortunately, a peak at the retention time of E2, corresponding to an amount of about 25 ng, was found in all of the blank plasma runs. As the sample was from a male volunteer, this peak cannot be due to E2, but it must be another unknown compound. The recoveries for EE, E1 and E2 were 50, 64 and 71% with RSDs of 7, 10 and 10 (n = 4) for peak area measurements. The immuno-precolumn showed a capacity decrease of about 30% after the analysis of ten plasma samples. Obviously, plasma components, *e.g.*, proteolytic enzymes, irreversibly de-activate the immuno-precolumn.

Conclusions

With the three estrogen steroids as test compounds, various immuno-precolumn desorption techniques to be used in on-line precolumn and LC systems have been evaluated.

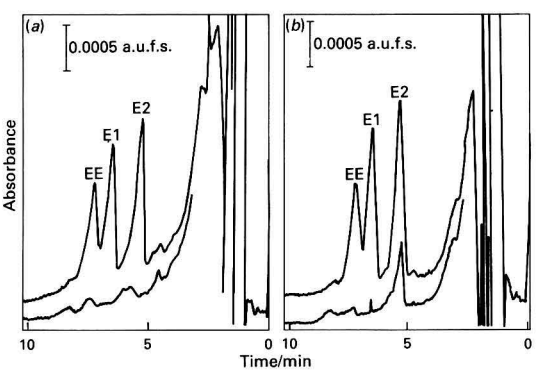

Fig. 7 Chromatograms of (*a*) a male urine sample spiked with 5.1 μg l^{-1} of each of the estrogens: EE, E1 and E2 and (*b*) a male plasma sample spiked with 12.5 μg l^{-1} of each of the three estrogens, and of the corresponding blank samples. Urine: 15 ml of sample were diluted with an equal volume of water and loaded onto the 10 × 10 mm i.d. immuno-precolumn. Plasma: 6 ml of sample were diluted with 24 ml of water and processed in the same way. The analyses were performed according to the non-selective desorption technique

Aqueous solutions of either high or low pH and solutions containing chaotropic compounds were ineffective. This finding, confirmed by studies with other types of immuno-precolumns, suggests that these conventional desorbing solutions can only be used, if the sorbed compounds (antigen or hapten) possess structural features that are prone to chaotropic or ionic changes. Cationic and anionic surfactant solutions were found to disrupt the antibody–antigen (or hapten) interaction if used in concentrations above their c.m.c. Concentrations of below the c.m.c. had no significant effect. Unfortunately, the practicability of micellar solutions is limited because it is difficult to concentrate and/or separate the desorbed species using a reversed-phase column.

On-line thermodesorption of the immuno-precolumn at 55 °C gave good recoveries, both with conventional water-bath heating and microwave heat generation. The stability of the immuno-precolumn was less than with the non-selective methanol desorption, probably due to the thermolability of the agarose material used. In further work, temperature-resistant stationary phases such as silica, glass or synthetic polymers should be evaluated. A significant advantage of the technique is that almost totally aqueous solutions are employed for desorption; consequently the degree of contamination will be low.

From among the methods tested, non-selective desorption from the immuno-precolumn with methanol–water (95 + 5 v/v) was found to be most practical. The eluate is diluted on-line with an excess of water and subsequently concentrated and separated in a reversed-phase LC system. While some problems remain to be solved with plasma samples, the results of urine analysis are excellent. The capacity of the immuno-precolumn remained constant during 20 runs each of 15 ml urine samples. The repeatability was satisfactory, and with 15–75 ml samples, detection limits (UV detection at 280 nm) of 0.05–0.5 $\mu g\ l^{-1}$ of steroid were obtained.

Compared with the previously published immunoselective technique,[7–9] where an excess of cross-reacting compounds is used as the displacer, non-selective methanol desorption shows several significant advantages and the chromatogram is cleaner because the broad displacer peaks are absent. Besides, a time-consuming search for and evaluation of the characteristics of proper displacers is superfluous. Generally speaking, if a suitable immuno-precolumn for a specific application is available, a non-selective desorption procedure can be developed within a relatively short time.

In principle, immunoselective desorption should show better selectivity than non-selective desorption, the additional selectivity is created during desorption. A cross-reacting compound will act as a displacer for selected antibodies only, non-specifically adsorbed compounds, or compounds captured by other types of antibodies, will not be desorbed. However, if the chromatograms recorded with both desorption techniques and performed with the same urine samples are compared (*cf.* reference 9 and this study), no essential difference in selectivity is found. Obviously, the immunoaffinity sorption process is so selective that further improvement is not easily achieved during desorption. Besides, any additional selectivity of the immunoselective desorption might be outweighed by the introduction of impurities into the system by the displacers. The main advantage of immunoselective desorption is that it can be performed with simpler instrumentation, as dilution of the eluate from the immuno-precolumn is not necessary.

This work was supported by the Dutch Foundation for Technical Science, grant No. VCH 46.0616. Organon (Oss, The Netherlands) is thanked for the gift of the anti-estrogen antiserum.

References

1 Janis, L. J., and Reigner, F. E., *J. Chromatogr.*, 1988, **444**, 1.
2 Nilsson, B., *J. Chromatogr.*, 1983, **276**, 413.
3 Reh, R., *J. Chromatogr.*, 1988, **433**, 119.
4 Rybacek, L., D'Andrea, M., and Tarnowski, J., *J. Chromatogr.*, 1987, **397**, 355.
5 Janis, L. J., Grott, A., Regnier, F. E., and Smith-Gill, S. J., *J. Chromatogr.*, 1989, **476**, 235.
6 Johansson, B., *J. Chromatogr.*, 1986, **381**, 107.
7 Farjam, A., de Jong, G. J., Frei, R. W., Brinkman, U. A. Th., Haasnoot, W., Hamers, A. R. M., Schilt, R., and Huf, F. A., *J. Chromatogr.*, 1988, **452**, 419.
8 Haasnoot, W., Schilt, R., Hamers, A. R. M., Huf, F. A., Farjam, A., Frei, R. W., and Brinkman, U. A. Th., *J. Chromatogr.*, 1989, **489**, 157.
9 Farjam, A., Brugman, A. E., Soldaat, A., Timmerman, P., Lingeman, H., de Jong, G. J., Frei, R. W., and Brinkman, U. A. Th., *Chromatographia*, 1991, **31**, 469.
10 Farjam, A., van de Merbel, N. C., Lingeman, H., Frei, R. W., and Brinkman, U. A. Th., *Int. J. Environ. Anal. Chem.*, in the press.
11 Phillips, T. M., *Recept. Biochem. Methodol.*, 1989, **14**, 129.
12 Davis, G. C., Hein, M. B., Chapman, D. A., Neely, B. C., Sharp, C. R., Durley, R. C., Biest, D. K., Heyde, B. R., and Carnes, M. G., *Plant Growth Substances*, Springer, Berlin, 1985, pp. 44–51.
13 Fuchs, Y., and Gertman, E., *Plant Cell. Physiol.*, 1974, **15**, 629.
14 Sundberg, B., Sandberg, G., and Crozier, A., *Phytochemistry*, 1986, **25**, 295.
15 Van de Water, C., Tebbal, D., and Haagsma, N., *J. Chromatogr.*, 1989, **478**, 205.

Paper 1/00874I
Received February 22nd, 1991
Accepted April 14th, 1991

Simultaneous Determination of Seven Divalent Metal Cations in Some Anaerobic Sealant Formulations Following Solid-phase Extraction and Separation on a Dynamically Coated C_{18} High-performance Liquid Chromatography Column

Marian Deacon and Malcolm R. Smyth*
School of Chemical Sciences, Dublin City University, Dublin 9, Ireland
Raymond G. Leonard
Loctite (Ireland) Ltd., Whitestown Industrial Estate, Tallaght, Co. Dublin, Ireland

A method has been developed for the simultaneous determination of eight divalent metal ions based on solid-phase extraction and separation on a dynamically coated C_{18} reversed-phase high-performance liquid chromatography column. The method has been applied to the determination of these metal ions in some anaerobic sealant formulations, with limits of detection as low as 30 ppb for certain metal ions. It has been shown that this approach is capable of distinguishing between free and complexed metal ions in such matrices.

Keywords: *anaerobic sealants; reversed-phase high-performance liquid chromatography; solid-phase extraction; trace metal analysis*

Anaerobic sealants are used predominantly in mechanical engineering applications. They are also used in a wide range of bonding, locking and retaining applications, and are designed to remain in the liquid form in air, but once confined between closely fitting active metal surfaces, to polymerize into tough, heat and solvent resistant solid materials. A typical formulation contains a monomer, free radical initiators, accelerators, metal chelating agents, plasticizers, thickeners and dyestuffs. The determination of trace metal ions in anaerobic sealant formulations is of vital importance, as these metal ions can initiate the polymerization process, resulting in premature setting of products in their packaging material. A metal ion can react with a peroxide initiator to form a free radical. Any oxygen present will quickly react with this radical to render it inactive. In the absence of oxygen, however, this free radical will react with the monomer to form a polymer as follows:

$$R\text{–}O\text{–}O\text{–}H + H^+ + M^{n+} \rightarrow RO^{\bullet} + M^{(n+1)+} + H_2O$$

$$R\text{–}O\text{–}O\text{–}H + M^{(n+1)+} \rightarrow R\text{–}O\text{–}O^{\bullet} + M^{n+} + H^+$$

$$RO^{\bullet} + \diagdown C{=}C \diagup \rightarrow RO\text{–}\overset{|}{C}\text{–}\overset{|}{C}^{\bullet} \quad \textit{etc.}$$

This requires, therefore, that free metal cations must be excluded from a typical product. This is achieved by monitoring the raw materials and the finished product for trace metal ion content, and by the addition of chelating agents to the product. To date, analysis of trace metal ion content has been carried out by atomic absorption spectroscopy or direct current plasma spectrometry.[1] Both of these techniques determine total metal ion concentrations and, as described, only allow for single element determination. There is therefore a need for a technique which allows for a multi-element determination approach, and one which can distinguish between free and complexed metal ions.

In previous papers, high-performance liquid chromatographic methods for the determination of Cu^{II} and Fe^{III} in anaerobic adhesive formulations using 8-hydroxyquinoline as a complexing agent,[2] and using a cation-exchange column have been described.[3] The first approach had the disadvantage that only a limited range of metal ions could be determined simultaneously, whereas the latter method suffered from incomplete resolution of the metal ions investigated. It was therefore decided to investigate the approach reported by Cassidy and Elchuk[4] and refined by Krol[5] using a C_{18} column dynamically coated with sodium octyl sulphonate for the particular industrial application described in this paper.

* To whom correspondence should be addressed.

Experimental

Reagents

All aqueous solutions were prepared with water obtained by passing distilled water through an ELGA-STAT (Elga, High Wycombe, UK) water purification apparatus. 4-(2-Pyridylazo)resorcinol (PAR) was obtained from Aldrich. Sodium octyl sulphonate was obtained from Rohm Chemicals. Tartaric and citric acids were obtained from Riedel-de Haen. Metal standards were prepared from atomic absorption standard metal ion solutions obtained from May and Baker, with the exception of Fe^{II} which was made from ammonium iron(II) sulphate hexahydrate. Isooctane and diethyl ether were obtained from Riedel-de Haen, whereas chloroform was obtained from Aldrich.

Apparatus

The high-performance liquid chromatography (HPLC) system consisted of a Waters 501 HPLC pump, a Waters RCSS Guard Pak Module, and a Waters μBondapak C_{18} cartridge (4.6 mm × 10 cm) contained within a Waters Z module. The eluted metal ions were detected after post-column derivatization with PAR reagent. The post-column reactant was delivered using a Waters reagent delivery module to a T-piece situated between the end of the column and the reaction coil. The complexed metal ions were detected using a Shimadzu 8PD-6AV ultraviolet detector. The detector output was monitored with a Drew Scientific data capture unit and the chromatograms were processed with a Roseate Chromatography data management package.

All sample preparation cartridges were obtained from Waters with the exception of the OnGuard H cartridge which was obtained from Dionex. Plastipak syringes from Becton Dickinson were used for the introduction of samples onto the sample preparation cartridges.

Methods

Solid-phase extraction was performed using a variety of sample preparation cartridges. The cartridges were first wetted with 2 ml of ethanol, then conditioned by washing with 5 ml of de-ionized water. Samples (30 ml) were then applied to the top of each cartridge and the metal ions eluted with 3 ml of the mobile phase. The first 1 ml (representing the dead volume of the cartridge) was discarded and the remaining 3 ml used for injection into the HPLC system. The spiking of metal ions into adhesive formulations was achieved using standards prepared in ethanol–water (90 + 10). The mobile phase consisted of 2 mmol dm^{-3} sodium octyl sulphonate, 20 mmol dm^{-3} citric acid and 30 mmol dm^{-3} tartaric acid, pH 3.4, as described by Krol.[5]

Results and Discussion

Optimization of Chromatographic Separation and Detection System

The choice of chromatographic conditions was made based on the work of Cassidy and Elchuk[4] and Krol.[5] Further optimization was then carried out with respect to the size of the sample loop, the length of the reaction coil and the temperature of the reaction coil.

The large capacity of the column and the large volume of eluents (3 ml), emanating from the solid-phase extraction cartridges used for sample preparation, required the use of a large sample loop. Sample loop sizes investigated were 200 μl, 500 μl, 1 ml and 2 ml. It was found that the peak height for each metal ion increased with increasing sample loop size up to 1 ml (Fig. 1). Further increase in the loop size to 2 ml resulted in the capacity of the column being exceeded. A 1 ml sample loop size was therefore used in all further investigations.

The length of the reaction coil from the mixing T-piece to the detector determines the reaction time of the PAR reagent with the metal ion. The length of the reaction coil was varied from 25 to 200 cm. For all metal ions investigated, the peak height increased with increasing length of the reaction coil (Fig. 2). However, a reaction coil length of greater than 135 cm produced a high back-pressure, which affected the mixing of the PAR reagent and column eluent in the mixing T-piece. Thus a reaction coil length of 135 cm was used in all further investigations.

The temperature of the reaction coil was then varied from room temperature to 60 °C (Fig. 3). For most metal ions the peak height remained relatively constant, but an increase was noted in the peak height of Fe^{III} above 40 °C, whereas a decrease was found for Zn^{II} between 10 and 40 °C. As the peak heights of most metal ions remained relatively constant, it was decided to maintain the reaction coil at room temperature.

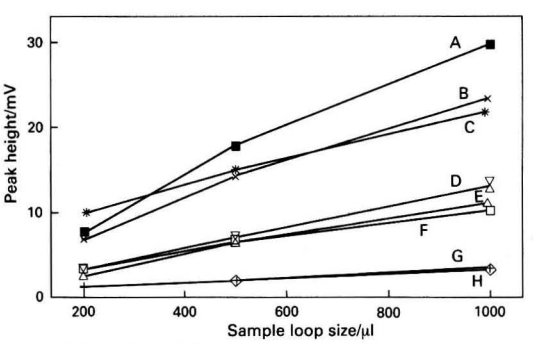

Fig. 1 Effect of sample loop size on peak height obtained following separation of eight divalent metal cations. A, Cu^{II}; B, Co^{II}; C, Zn^{II}; D, Mn^{II}; E, Fe^{II}; F, Ni^{II}; G, Pb^{II}; and H, Cd^{II}

The chromatographic separation of a 1 ppm mixture of eight divalent metal ions achieved using this system is shown in Fig. 4.

Optimization of Sample Preparation

Solid-phase extraction was preferred to liquid–liquid extraction because of the smaller amounts of sample, solvent and glassware needed, and considering also that liquid–liquid extraction is difficult to perform with samples which contain surfactants because of the formation of emulsions.

Six commercially available solid-phase extraction cartridges were investigated with regard to their adsorption properties for metal ions from aqueous solutions, and the subsequent release of the metal ions from the adsorption sites upon washing with the mobile phase. These included Silica, Florasil, Alumina, Diol and Accel Plus CM Sep-Paks, and the

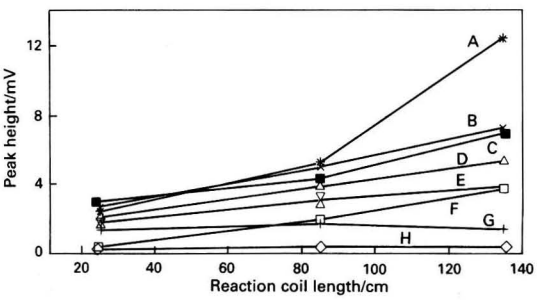

Fig. 2 Effect of length of reaction coil on peak height obtained following separation of eight divalent metal cations. A, Zn^{II}; B, Co^{II}; C, Cu^{II}; D, Fe^{II}; E, Mn^{II}; F, Ni^{II}; G, Pb^{II}; and H, Cd^{II}

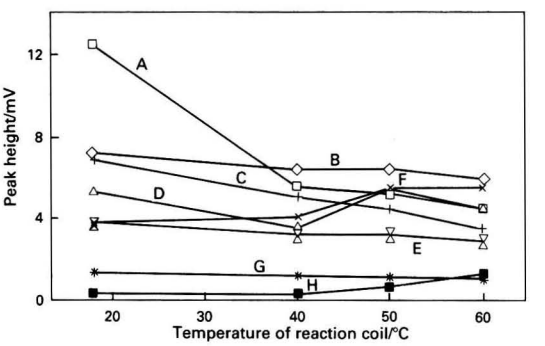

Fig. 3 Effect of temperature of reaction coil on peak height obtained following separation of eight divalent metal cations. A, Zn^{II}; B, Co^{II}; C, Cu^{II}; D, Ni^{II}; E, Mn^{II}; F, Fe^{II}; G, Pb^{II}; and H, Fe^{III}

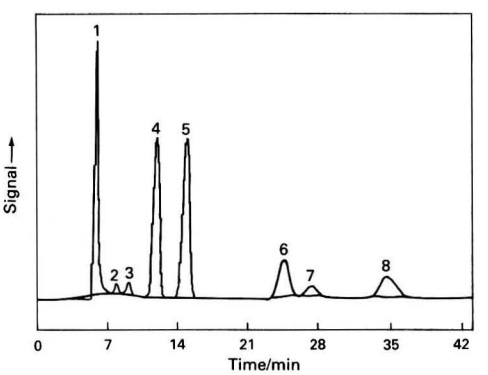

Fig. 4 Separation of a 1 ppm aqueous mixture of: 1, Cu^{II}; 2, Pb^{II}; 3, Ni^{II}; 4, Zn^{II}; 5, Co^{II}; 6, Fe^{II}; 7, Cd^{II}; and 8, Mn^{II}

OnGuard H sample preparation cartridge. The silica Sep-Pak proved the most promising in terms of recoveries of the majority of the metal ions studied. The recoveries of the eight divalent metal ions from 30 ml of de-ionized water spiked at the 100 ppb level following solid-phase extraction using the silica Sep-Pak ranged from 61% for Mn^{II} to 110% for Zn^{II}.

It was then decided to investigate the extraction of the metal ions from a typical plasticizer used in anaerobic adhesive formulations, *i.e.*, tetraethylene glycol di-(2-ethylhexanoate). The wetting–conditioning procedure was the same as that described above. A 30 ml sample of plasticizer solubilized in an equal volume of iso-octane was passed through the Sep-Pak with the aid of a 10 ml syringe at a rate of 2–3 ml min^{-1}. The Sep-Pak was then washed with 10 ml of iso-octane to remove any remaining plasticizer. The metal ions were eluted from the Sep-Pak with 3 ml of the mobile phase, the first 1 ml being discarded and the remaining 3 ml collected. This fraction was passed through a C_{18} Sep-Pak in order to remove any remaining organic components.

A typical chromatogram, obtained following this procedure, is shown in Fig. 5, where it can be seen that there was a good recovery for most of the metal ions except Fe^{II}. To investigate the loss of Fe^{II}, a liquid–liquid extraction technique was developed involving the extraction of 50 ml of plasticizer solubilized in 50 ml of iso-octane with 5 ml of the mobile phase. Again Fe^{II} was not extracted using this procedure. The loss of Fe^{II} can therefore be attributed either to complex formation with the plasticizer or interconversion of Fe^{II} to the Fe^{III} form. Unfortunately, although the analysis technique used is able to distinguish between Fe^{II} and Fe^{III}, the sensitivity for Fe^{III} is so low that it was not possible to use this technique to monitor such an interconversion process. Iso-octane was chosen as a solubilizer as it was the most non-polar solvent in which the plasticizer was soluble. This implied that any residual organic carryover in the elution of the metal ions with the mobile phase would be easily removed using the C_{18} Sep-Pak.

Procedures were then developed for raw materials, intermediate and finished products. For formulations which were not soluble in iso-octane, more polar solvents such as chloroform and dichloromethane were used. It was found, however, that when such solvents were employed, splitting of the Cu^{II} peak occurred. This was thought to be due to carryover of these solvents because of their miscibility with water and decreased retention on the C_{18} Sep-Pak. This problem was counteracted by employing a 10 ml wash with iso-octane following the 10 ml wash of the Sep-Pak with the solubilizing solvent (*i.e.*, chloroform–dichloromethane). As chloroform is miscible with iso-octane, the chloroform was removed, and the traces of the less polar iso-octane were trapped by passage through the C_{18} Sep-Pak. A typical chromatogram obtained for six of the metal ions following solid-phase extraction from a formulation containing triethylene glycol dimethacrylate, cumene hydroperoxide, saccharin, dodecyl methacrylate and a primary alcohol ethoxylate is shown in Fig. 6.

In samples containing aromatic amines such as *N*,*N*-dimethyl-*o*-toluidine and *N*,*N*-diethyl-*p*-toluidine, peak splitting again occurred. For the removal of these amines, solvents such as ethanol, acetone and diethyl ether were investigated. Diethyl ether proved to be the most suitable. Again, the order in which the washing of the Sep-Pak was carried out proved to be critical to prevent the carryover of washing solvents. Therefore, samples containing amines were solubilized in chloroform and passed through the Sep-Pak, which was then washed with 10 ml aliquots of the chloroform, followed by diethyl ether and iso-octane.

With samples containing a typical surfactant such as the linear primary alcohol-based ethoxylate (C_{12}–C_{15}) named dobanol 25–3, it was found that water was a better solubilizing agent than chloroform, and adjustment of the sample water mixture from the initial pH of 4.2 to a pH of 7.0 resulted in improved recoveries of the metal ions. The method involved solubilizing the sample in an equivalent volume of water and adjusting the pH to 7. This was applied to a pre-conditioned silica Sep-Pak. The Sep-Pak was then washed with water and 10 ml of iso-octane, and the metal ions were eluted with the mobile phase and passed through the C_{18} Sep-Pak.

The determination of six divalent metal ions, namely Cu^{II}, Ni^{II}, Zn^{II}, Co^{II}, Cd^{II} and Mn^{II} was then investigated in a typical anaerobic sealant. Linear calibration graphs were constructed for all the metal ions at concentration levels of between 60 and 500 ppb. Limits of detection from 40 to 70 ppb and recoveries of 61–110% were obtained for these metal ions using a sample size of 30 ml (Table 1).

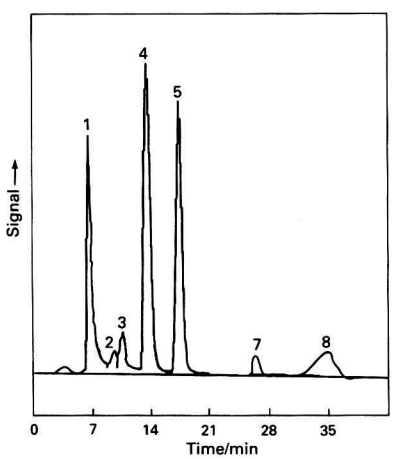

Fig. 5 Chromatogram obtained following solid-phase extraction of metal ions present at the 100 ppb level in a solution of tetraethylene glycol di-(2-ethylhexanoate). Peak numbers as in Fig. 4

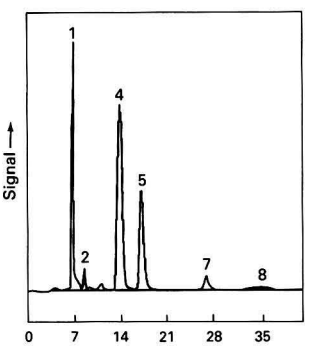

Fig. 6 Chromatogram obtained following solid-phase extraction of a sample of anaerobic sealant formulation containing 100 ppb of Cu^{II}, Pb^{II}, Zn^{II}, Co^{II}, Cd^{II} and Mn^{II}. Peak numbers as in Fig. 4

Table 1 Recoveries and limits of detection for metal ions using the proposed method

Metal ion	Recovery (%)	Limit of detection/ppb
Cu^{II}	80	60
Pb^{II}	93	70
Ni^{II}	89	70
Zn^{II}	110	40
Co^{II}	75	40
Fe^{II}	ND*	0
Cd^{II}	97	60
Mn^{II}	61	60

* ND = not determined.

In order to investigate the ability of the method to differentiate between free metal cations and their ethylenediaminetetracetic acid (EDTA) complexes, a sample of tetraethylene glycol di-(2-ethylhexanoate) was spiked at the 100 ppb level with the metal ions under investigation and an excess of EDTA was added. These samples were then extracted using the solid-phase extraction procedure described above. The chromatogram obtained showed no response for any of the metal ions investigated, indicating that the procedure could be used to detect free metal ions in the presence of complexed metal ions.

Conclusion

A method has been developed for the determination of eight transition metal ions in some anaerobic adhesive formulations following solid-phase extraction and separation on a dynamically coated C_{18} HPLC column. The method is easy to perform, offers good detection limits for most of the metal ions studied, provides a multi-element detection capability and permits the free and complexed metal ions to be distinguished in the sealant formulations studied.

References

1 Brennan, M., and Svehla, G., *Ir. Chem. News*, 1990 Autumn edition, 35.
2 Mooney, J. P., Meaney, M., Smyth, M. R., Leonard, R. G., and Wallace, G. G., *Analyst*, 1987, **112**, 1555.
3 O'Dea, P., Deacon, M., Smyth, M. R., and Leonard, R. G., *Anal. Proc.*, 1991, **28**, 82.
4 Cassidy, R. M., and Elchuk, S., *Anal. Chem.*, 1982, **54**, 1558.
5 Krol, J., *Waters Ion Chromatography Notes*, Waters Chromatography Division, Millipore, Milford, MA, 1988, vol. 2, p. 1.

Paper 1/00871D
Received February 22nd, 1991
Accepted April 8th, 1991

Thermal Degradation of Some Benzyltrialkylammonium Salts Using Pyrolysis–Gas Chromatography–Mass Spectrometry

Neville J. Haskins and Robert Mitchell*
SmithKline Beecham Pharmaceuticals, The Frythe, Welwyn, Hertfordshire AL6 9AR, UK

A number of benzyl quaternary ammonium salts have been examined by pyrolysis–gas chromatography–mass spectrometry using various temperatures for the pyrolysis. The products show that simple substitution reactions dominate at low temperatures with slight evidence for classical Hofmann degradation. Raising the temperature gave increasing concentrations of 1,2-diphenylethane and stilbene which must be produced by intermolecular reactions. There appeared to be a linear relationship between the amount of 1,2-diphenylethane produced and the temperature of the pyrolysis.

Keywords: *Benzyltrialkylammonium salts; pyrolysis–gas chromatography–mass spectrometry*

Quaternary ammonium salts such as choline (an endogenous component) are important in medical research, or as drugs (dequalinium bromide or propantheline bromide for example). However, the stability of such compounds at elevated temperatures is poor. The elimination of alkyl substituents from quaternary salts by either the Hofmann or Saytzeff reaction is well known. It was decided to examine the stability of benzyl quaternary ammonium salts at high temperature. This work describes the products formed by Curie-Point pyrolysis using support wires of various Curie-Point temperatures.

Experimental

All samples were obtained from Aldrich (Gillingham, Dorset, UK) and were used without further purification. Each of the salts was prepared for spectral analysis by dissolving it in methanol (100 mg per 10 ml) and adding 5 μl of the solution to a wire pre-washed in methanol. The wires were loaded into a glass carrier. The carriers were loaded into a Curie-Point pyrolyser (Horizon Instruments, Heathfield, Sussex, UK) and the radiofrequency field was applied for 4 s. Wires giving Curie-Points of 385, 510, 610 and 770 °C were used. Helium was passed over the wire at a flow rate of 1 ml min^{-1}.

The pyrolysate was trapped on a fused silica column (15 m × 0.25 mm i.d.) coated with BP-5 (SGE, Milton Keynes, Buckinghamshire, UK) at ambient temperature.

The column was heated from ambient temperature to 300 °C at a rate of 10 °C min^{-1}. The helium passing through the pyrolyser was used as the carrier gas at a flow rate of 1 ml min^{-1}. The column was passed directly into the electron ionization source of a VG Analytical 7070F double focusing mass spectrometer linked to a VG 2050 data system (VG Analytical, Wythenshawe, Manchester, UK). The mass spectrometer was continually scanned from 600 to 20 u at a rate of 1.5 s $decade^{-1}$ giving a total cycle time of about 3 s. Ionization was effected at 70 eV. After acquisition, spectra were transferred to a VG Analytical 11-250J data system for processing.

Results and Discussion

The benzyltrialkylammonium salts examined were benzyltrimethylammonium chloride (**I**), benzyltriethylammonium chloride (**II**), benzyldimethyldodecylammonium chloride (**III**), benzyldimethyltetradecylammonium chloride (**IV**), benzyldimethylhexadecylammonium chloride (**V**) and benzyldimethylstearylammonium chloride (**VI**).

Fig. 1 shows a typical reconstructed gas chromatogram obtained after the pyrolysis of benzyldimethylhexadecylammonium chloride (**V**). The major components are mainly those that might be expected from simple nucleophilic substitution reactions between the chloride anion and the quaternary cation (Scheme 1). This type of reaction in most instances should give rise to three pairs of compounds, consisting of the halide and the tertiary amine. This is observed in the pyrolysis of compound (**V**): the observed pairs are benzyl chloride and dimethylhexadecylamine; chloromethane and benzylhexadecylmethylamine; and 1-chlorohexadecane and benzyldimethylamine. The proportion of each pair varies, with the least abundant being benzyldimethylamine/chloroalkane. This order of abundance was observed for all the salts examined (Fig. 1).

The products from the substitution reactions are observed at all wire temperatures. The most studied reaction of quaternary ammonium salts is the Hofmann degradation[1] which should give rise to benzyldimethylamine, hydrogen chloride and the corresponding alkene (Scheme 2). Benzyldimethylamine can also arise from a substitution reaction, whereas hydrogen chloride is unlikely to be detected through a gas chromatograph. Accordingly, the evidence for Hofmann elimination depends on the detection of the alkene. Trace amounts of alkene were found but at a low concentration and only at the higher wire temperatures, implying that under the

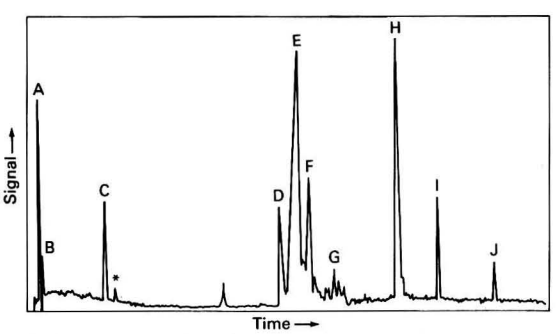

Fig. 1 Reconstructed gas chromatogram for the pyrolysate from the pyrolysis of benzyldimethylhexadecylammonium chloride at 385 °C. A, Benzyl chloride [relative molecular mass (M_r) = 126] and chloromethane (M_r = 50); B, dimethylbenzylamine (M_r = 135); C, 1,2-diphenylethane (M_r = 182); D, 1-chlorhexadecane (M_r = 260); E, dimethylhexadecylamine (M_r = 269); F, hexadecanoic acid (M_r = 256); G, dimethylheptadecylamine (M_r = 283); H, benzylhexadecylmethylamine (M_r = 345); I, unknown, but containing a C_{16} alkyl group?; J, unknown, but containing a C_{16} alkyl group?; and *, expected elution position of stilbene (observed with higher Curie-Point temperatures)

* Present address: The Sheffield Polytechnic, Sheffield S1 1WB, UK.

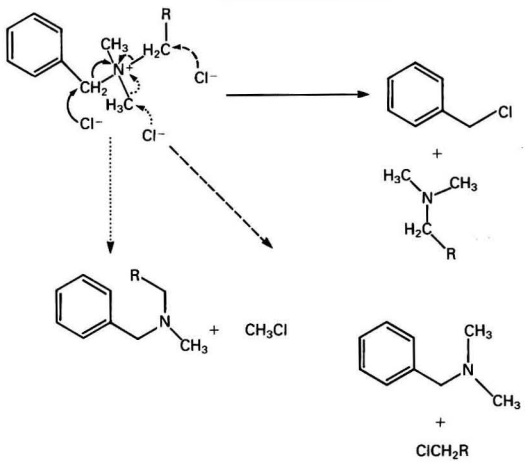

Scheme 1 Nucleophilic substitution reactions between the chloride anion and the quaternary cation

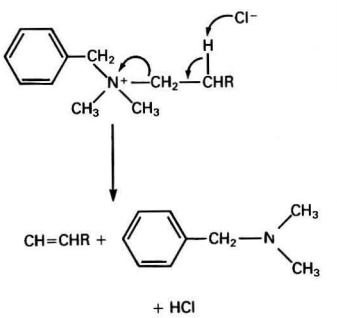

Scheme 2 Classical Hofmann degradation of a quaternary ammonium salt

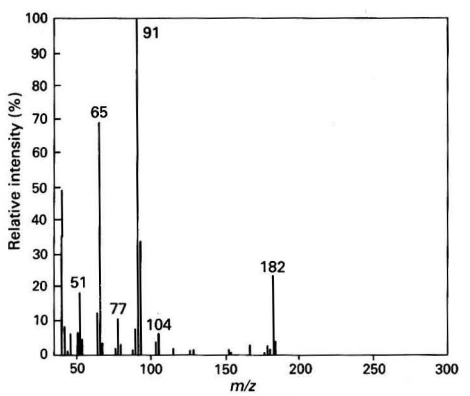

Fig. 2 Mass spectrum of 1,2-diphenylethane obtained after pyrolysis of benzyltrialkylammonium salts

conditions used for the pyrolysis, Hofmann elimination is not a major degradation pathway. One product observed (peak F, Fig. 1) was identified as hexadecanoic acid. This probably arises from oxidation of the hexadecyl moiety. Homologous acids were observed in the other long-chain alkyl quaternary salts. The amount was variable, suggesting that oxidation was caused by residual air after loading the pyrolyser.

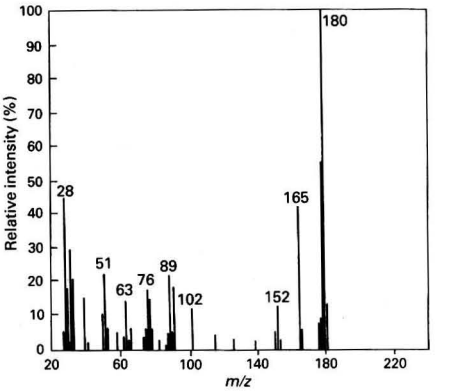

Fig. 3 Mass spectrum of stilbene obtained after pyrolysis of benzyltrialkylammonium salts

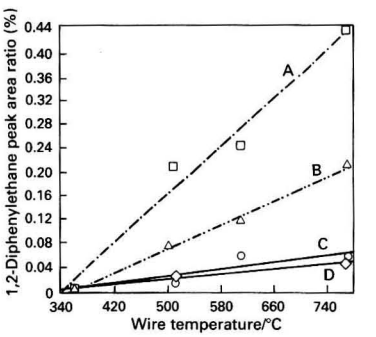

Fig. 4 Plot of p (%) *versus* T (°C), where p (%) = proportion of 1,2-diphenylethane formed on pyrolysis. A, Benzyltrimethylammonium chloride: $y = 0.00103x - 0.340$; B, benzyltriethylammonium chloride: $y = 0.00049x - 0.174$; C, benzyldimethyltetradecylammonium chloride: $y = 0.00014x - 0.043$; and D, benzyldimethylstearylammonium chloride: $y = 0.00010x - 0.028$

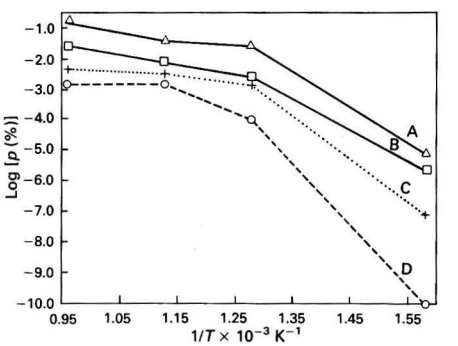

Fig. 5 Arrhenius plot of log [p (%)] *versus* $1/T$ (K), where p (%) = proportion of 1,2-diphenylethane formed on pyrolysis. A, Benzyltrimethylammonium chloride; B, benzyltriethylammonium chloride; C, benzyldimethyldodecylammonium chloride; and D, benzyldimethyltetradecylammonium chloride

At the highest wire temperatures additional products were observed. Examination of the spectra (Fig. 2) indicated that these were 1,2-diphenylethane and smaller amounts of stilbene (Fig. 3). Such products would require some type of reaction between two molecules of the quaternary cation or perhaps between benzyl chloride and the quaternary salt.

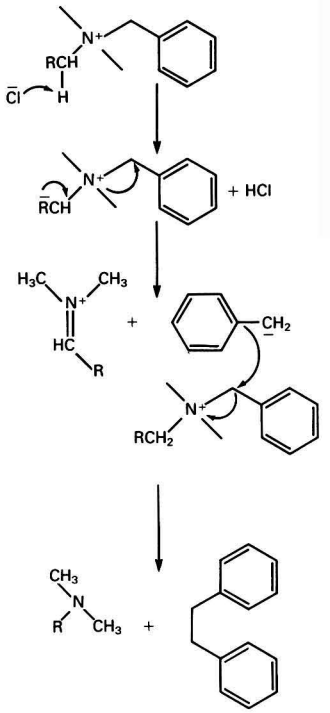

Scheme 3 Possible modification of the Stevens' rearrangement to explain the formation of 1,2-diphenylethane

Further examination of the proportion of 1,2-diphenylethane formed showed that it was linearly dependent on the wire temperature and appeared to be less abundant as the size of the alkyl substituents increased (Fig. 4). The classical Arrhenius plot showed a similar trend (Fig. 5).

The formation of 1,2-diphenylethane might arise from a combination of benzyl free radicals themselves, or generated from an ylide formed by abstraction of the α-proton (Scheme 3). Such reactions have been observed in the study of the Stevens' rearrangement carried out by Ollis *et al.*[1] However, the ylide in the Stevens' rearrangement is normally stabilized by the presence of a β-keto group. It must be stressed that in the present situation considerably higher temperatures are used and the concentrations are not equivalent. Hence the formation of 1,2-diphenylethane in the hot melt after pyrolysis is occurring under far more rigorous conditions than the normal Stevens' rearrangement.

The presence of stilbene could arise from a combination of carbenes formed by simple disproportionation of the intermediate ylide formed by elimination of a benzyl methylene proton (Scheme 4). The presence of such reactive species

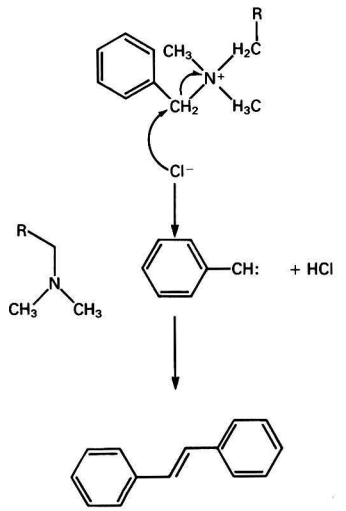

Scheme 4 Possible formation of stilbene *via* a carbene intermediate on pyrolysis

might account for trace amounts of higher relative molecular mass material seen after some reactions, but too weak to identify conclusively.

Conclusions

The analysis of quaternary salts has often generated problems owing to their non-volatility as intact species, and the formation of decomposition products if heat is used. This paper shows that the decomposition reactions are more complex than might be expected.

Pyrolysis of benzyl quaternary ammonium salts proceeds by several competing mechanisms. The products formed depend on the temperature of pyrolysis and the bulkiness of the alkyl substituents about the quaternary ammonium centre. At lower temperatures simple displacement reactions appear to predominate. At higher temperatures more complex multicentre reactions, probably involving free radicals, take place giving rise to 1,2-diphenylethane and trace amounts of stilbene.

Reference

1 Ollis, W. D., Rey, M., and Sutherland, I. O., *J. Chem. Soc., Perkin Trans. 1*, 1983, 1009.

Paper 1/01248G
Received March 15th, 1991
Accepted April 30th, 1991

High-performance Modular Spectrophotometric Flow Cell

João Carlos de Andrade and Kenneth E. Collins
Universidade Estadual de Campinas, Instituto de Química, C.P. 6154, 13081 Campinas, São Paulo, Brazil
Mônica Ferreira
Instituto Agronômico de Campinas, C.P. 28, 13001 Campinas, São Paulo, Brazil

A high-performance modular flow cell is described, which can be used in photometric or spectrophotometric detector systems for analytical and preparative scale low-pressure liquid chromatography, flow injection and related techniques. The basic design is that of an inner absorption cell unit sandwiched between two rugged supports. The novel aspects of this sandwiched cell are the wide range of interchangeable flow cell units of different dimensions that can be used, and the way in which the fluid flow occurs, essentially eliminating problems with gas bubbles and giving rapid cell clearance. The cell is compact and its versatility is enhanced by using optical fibre bundles to transmit the light beam to the optical path of the cell and then from there to the detector.

Keywords: *Modular flow cell; spectrophotometric detector; liquid chromatography; flow injection*

Flow cells are critical parts of the flow-through detectors used in chromatographic systems[1] and also in the detectors used in other types of systems, *e.g.*, for continuous-flow analysis, either segmented[2–4] or non-segmented.[5] It is the measurement of some property of the fluid as it passes through the flow cell that gives the necessary analytical signal.

Optical detector flow cells are usually purchased as an integral part of any commercially available detector system or constructed on-site by the user. Most flow cells are made in one of four basic configurations: 'Z',[6,7] 'U',[6,8–10] 'H',[6] or conical.[6,11,12]

These cells differ mainly in the way the fluid stream enters and leaves the illuminated absorption chamber. The details of the liquid flow path affect the laminar and turbulent aspects of fluid flow, which in turn determines the over-all dispersion and bubble retention characteristics of the flow cell. Many commercially available and laboratory-built flow cells have serious problems with gas bubbles and suffer from long peak clearance times.

We have designed a modular flow cell in which the components can be constructed in a typical machine shop at low cost. The basic unit consists of an inner absorption cell piece sandwiched between two rugged support pieces. A series of different flow cell volumes, pathlengths and fluid flow patterns can be obtained simply by replacing one inner piece with another, somewhat in the manner of changing the rotor of a high-performance liquid chromatography (HPLC) injection valve.

Incorporated into the inner cell design is the concept of introduction of the flowing fluid into, and its removal from, the inner light-path piece in a symmetrical way, by means of two or more entrance and exit channels, which avoids the non-symmetrical flow pattern inherent in conventional one-jet designs.

Experimental

Cell Design

The components of the proposed flow cell are shown in Fig. 1. Details of the light-source system (a 6 V, 10 W halogen lamp coupled to a compact collimating device[13] incorporating a 542 nm interference filter), the sensing system (a GaAsP Hamamatsu photodiode, Model G1126-02) and the corresponding electronic circuits are not included in Fig. 1 nor are they discussed below. However, all of the measurements were made under identical optical conditions, except for the tests with the commercial U-type cell.

The central piece of the flow cell (Fig. 1), which defines the fluid flow characteristics of the detection system, can be made of any hard material that is sufficiently inert to withstand the solvents and solutes to be used. Graphite-filled poly(tetrafluoroethylene) (PTFE) is a good choice as it is soft enough to cut the channels conveniently and it does not allow light scatter through the cell walls, as do translucent materials, such as white PTFE and Kel-F.

The flow path is of a modified Z-type, with coaxial entrance and exit tubes. This set-up permits the use of cells with a shorter light path, which may be of interest in micro-scale analytical work, such as HPLC. The inlet flow stream is directed into a circular channel around the centre hole, from which it is then directed through radial channels (three in the example shown) into the centre hole. Thus the flowing fluid essentially jets in a symmetrical way from the channels towards the centre of the light path, along the inner faces of the entrance and exit windows.

In the proposed cell the entrance and exit tubes consist of PTFE tubing ($\frac{1}{16}$ in o.d.) inserted into the appropriate holes in the cell body. The assembled cell easily supports a hydrostatic pressure of about 405 kPa without leakage. Conventional HPLC fittings could be used for applications of even higher pressure.

The three radial channel design shown in Fig. 1 can be ıced by that shown in Fig. 2.

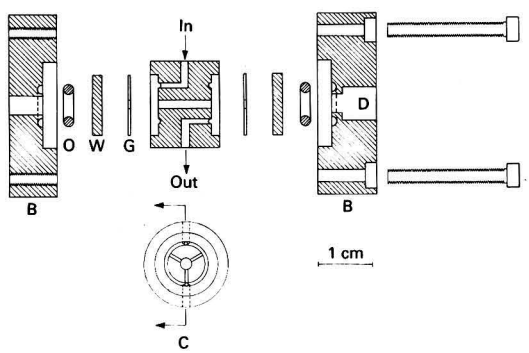

Fig. 1 Cross-section and front view of flow cell components: C, flow cell body; B, support pieces for cell and detection transducer; O, O-rings; W, windows of glass or fused silica; G, polytetrafluoroethylene sealing gasket; and D, well for detection transducer

The cell support pieces can be made of stainless steel, brass or hard organic polymer material and, if desired, can be made more compact than shown in Fig. 1.

Results and Discussion

Cell Performance

As the detector response should be a function of the amount of analyte present in the cell volume and independent of the existence of other components of the analytical system, such as a chromatographic column, the performance of the proposed flow cells was tested by using a single-line flow injection (FI) manifold.[5] Thus the dynamic tests were carried out by injecting, in triplicate, a desired volume (*e.g.*, 75 μl) of $KMnO_4$ solutions, having concentrations ranging from 4.0×10^{-5} to 6.0×10^{-4} mol dm^{-3}, into the carrier stream (water), prior to its entry into the detector cell. The transient peaks obtained in this manner give an FI-type calibration graph and simulate the chromatographic peaks, permitting the actual dynamic characteristics of the detector configuration being tested to be observed.

We have extensively tested cells having centre pieces of 1.5 mm i.d. and optical pathlengths of 5 mm (volume, 9 μl) and 10 mm (volume, 18 μl). The recorded peaks (Fig. 3) show a stable baseline and an excellent precision of response (see Table 1), comparable to those of high quality, but expensive, commercially available constant-volume flow cells. Results obtained with a Hellma U-type, 18 μl, 10 mm optical pathlength cell (with a Zeiss PM2A spectrophotometer operating at 542 nm) are also presented.

As the tests of the flow cells were carried out using a single-line FI manifold, comparisons of performance with respect to sensitivity (analytical response) were obtained through the dispersion coefficient[5] values, D, defined as the ratio of the absorbance for the transient FI peak (A) to that for the steady-state signal (A_0). As all of the variables such as carrier flow rate, reagent concentration, injection volume and

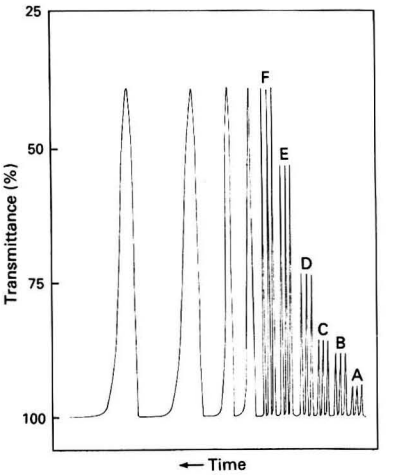

Fig. 3 Flow injection transient peaks obtained with a 9 μl flow cell. Sample, $KMnO_4$; injected volume, 75 μl; and carrier flow rate, 1.6 ml min^{-1}. Concentrations of the injected samples: A, 4.0×10^{-5}; B, 8.0×10^{-5}; C, 1.0×10^{-4}; D, 2.0×10^{-4}; E, 4.0×10^{-4}; and F, 6.0×10^{-4} mol dm^{-3}. The other peaks were obtained at increased recorder chart speeds

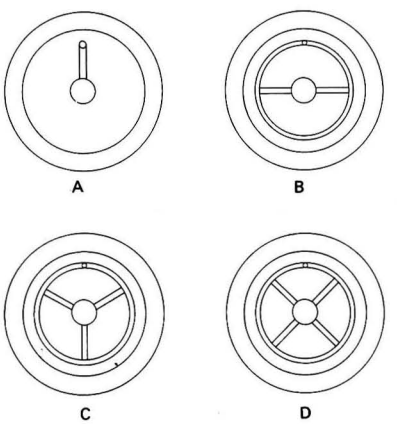

Fig. 2 Front view of channel configurations tested: A, Z-type flow cell; B, C and D, configurations with two, three and four channels, respectively. The inlet and outlet tube geometries and the flow cell dimensions are the same for all channel configurations (see Fig. 1)

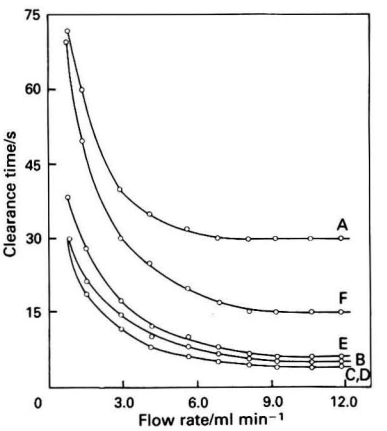

Fig. 4 Influence of the carrier flow rate on cell clearance times. Curves A, B, C and D correspond to the flow cells of Fig. 2. Curve E corresponds to a 10 mm optical pathlength flow cell (18 μl), with channel configuration C of Fig. 2. Curve F corresponds to a 10 mm optical pathlength U-type flow cell (18 μl). Sample, 6.0×10^{-4} mol dm^{-3} $KMnO_4$; injected volume, 75 μl

Table 1 Average relative standard deviation (RSD) and dispersion coefficient (D) values for various flow cells. The values were obtained using a carrier flow rate of 1.6 ml min^{-1} and a 6.0×10^{-4} mol dm^{-3} $KMnO_4$ solution. The RSD values were calculated for injection volumes of 10, 25, 50, 75 and 100 μl (n = 10). As the RSD values found were almost constant over this volume range, the values shown are the average

Flow cell	Volume/μl	Optical pathlength/mm	Average RSD (%)	D value*
U-type configuration (Hellma)	18	10	1.0	0.583
Three channel, Z type (Fig. 2, C)	18	10	1.2	0.847
Three channel, Z type (Fig. 2, C)	9	5	0.6	0.790
Z-type configuration (Fig. 2, A)	9	5	0.7	0.702

* Results from 75 μl injections.

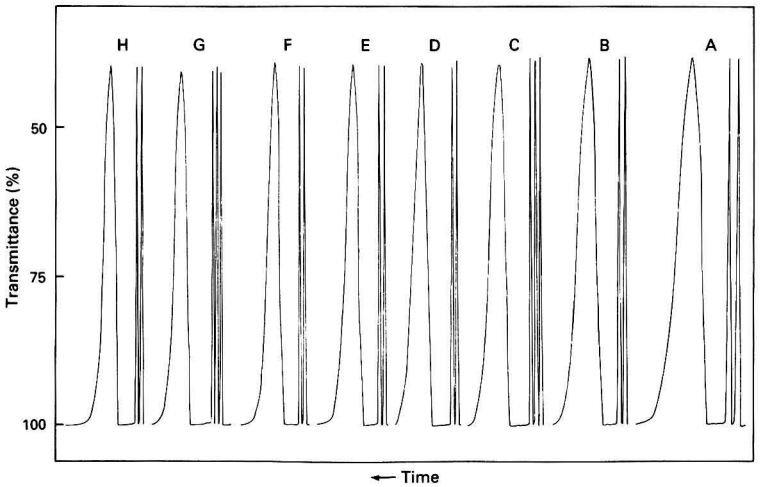

Fig. 5 Peak shape as a function of the carrier flow rate. Sample, 6.0×10^{-4} mol dm^{-3} $KMnO_4$; injected volume, 75 μl; and flow cell volume, 9 μl. Flow rates: A, 1.0; B, 1.6; C, 1.9; D, 2.2; E, 2.7; F, 3.0; G, 3.4; and H, 3.6 ml min^{-1}. The peaks were recorded at chart speeds of 6 and 63 mm min^{-1}

the FI manifold were kept constant for this set of data, it is inferred that values of D directly reflect the performance of the cells. These results are also shown in Table 1. It can be seen that the average relative standard deviation (RSD) for the commercial U-type cell is similar to that of the proposed three-channel cell, but the value of D is markedly lower.

The use of channels in both the entrance and exit sides of the proposed flow cell significantly improves the clearance time when compared with the Z-type cell having similar cell dimensions. Centre pieces with more than two radial channels all give similar results, as shown in Fig. 4; hence, there is little advantage in having more than three channels. The efficiency of solute clearance for the 9 μl three-channel flow cell is characterized by the peak profiles shown in Fig. 5.

The preliminary tests show that when radial channels are present only on the exit side of the cell, the results are similar to those obtained when radial channels are present on both the entrance and exit sides. If physical solute dispersion from the channel volume is not of concern, it is recommended that radial channels be placed on both sides of the cell, as a matter of convenience, when mounting the cell. In any configuration gas bubble problems are virtually non-existent.

Applications

The proposed cell can be incorporated into a dedicated detector or coupled with most conventional photometers and spectrophotometers by means of optical fibre bundles, without modification of the cell compartment. It functions particularly well in flow analysis systems where rapid cell clearance is desirable. This characteristic should be useful for determinations that involve frequent sampling in addition to on-line kinetic studies.

References

1 Stevenson, R. L., in *Liquid Chromatography Detectors*, ed. Vickrey, T. M., Marcel Dekker, New York, 1983, vol. 23, pp. 23–86.
2 Furman, W. B., and Walker, W. H. C., *Continuous Flow Analysis, Theory and Practice*, Marcel Dekker, New York, 1976.
3 Pasquini, C., and de Oliveira, W. A., *Anal. Chem.*, 1985, **57**, 2575.
4 de Andrade, J. C., Ferreira, M., Baccan, N., and Bataglia, O. C., *Analyst*, 1988, **113**, 289.
5 Růžička, J., and Hansen, E. H., *Flow-Injection Analysis*, Wiley, New York, 2nd edn., 1988.
6 White, P. C., *Analyst*, 1984, **109**, 677.
7 Kirkland, J. J., *Anal. Chem.*, 1968, **40**, 391.
8 Betteridge, D., Dagless, E. L., Fields, B., and Graves, N. F., *Analyst*, 1978, **103**, 897.
9 Weber, J. R., and Purdy, W. C., *Clin. Chem.*, 1980, **26**, 1010.
10 McClintock, S. A., Weber, J. R., and Purdy, W. C., *J. Chem. Educ.*, 1985, **62**, 65.
11 Stewart, J. E., *Appl. Opt.*, 1979, **18**, 5.
12 Stewart, J. E., *Appl. Opt.*, 1981, **20**, 654.
13 Moore, J. H., Davis, C. C., and Coplan, M. A., *Building Scientific Apparatus. A Practical Guide to Design and Construction*, Addison-Wesley, New York, 2nd edn., 1989, p. 145.

Paper 0/04932H
Received November 1st, 1990
Accepted May 16th, 1991

Generalized Treatment of a Stray Radiant Energy Test Method in Absorption Spectrometry

Paddy Fleming
Sligo Regional Technical College, Ballinode, Sligo, Ireland

The test method of Mielenz *et al.* used to determine the relative stray radiant energy (SRE) level in spectrophotometers is generalized for all sample cell to reference cell thickness ratios greater than unity. It is extended further to include situations where the required 'cut-off' solution is not transparent to the SRE. The experimental SRE value which ensued by applying the above method to a Shimadzu 260 ultraviolet/visible spectrophotometer is reconciled with the corresponding experimental values arising from two other SRE test methods.

Keywords: *Spectrophotometer; stray radiant energy; cell pathlength ratio*

In this paper a method for determining the relative stray radiant energy (SRE) in ultraviolet/visible (UV/VIS) spectrophotometers[1] is generalized to include all sample cell to reference cell thickness ratios greater than unity and instances where the transmittance of the 'cut-off' solution to SRE is not necessarily unity. The modified test method was used to determine the relative SRE level in a Shimadzu 260 spectrophotometer at a Mielenz peak[1] wavelength of 654 nm and with its spectral slit-width set at 1 nm. The exercise was repeated for the same instrumental conditions by using Fleming's transmittance ratio spectrometry method[2] and Fleming and O'Dea's direct transmittance method.[3]

Fleming's SRE test method[2] is based on transmittance ratio spectrometry and it may be regarded as the opposite side of the same coin as the test method of Mielenz *et al.*[1] Both test methods measure the differential absorbance of a solution placed in the sample beam relative to an identical solution placed in the reference beam while the sample cell is thicker than the reference cell. The Mielenz method gradually increases differential absorbance by wavelength scanning through the leading or trailing absorbance edge of a cut-off solution which has been placed in both the sample and reference beams, whereas the transmittance ratio method is carried out at a fixed wavelength while differential absorbance is gradually increased by advancing the concentration of the solution held in the sample and reference beams. The differential absorbance for both methods will not increase indefinitely but will peak at a value determined by the relative SRE level of the spectrophotometer, the cell pathlength ratio employed and the SRE transmittance of the test solution. The direct transmittance SRE test method involves determining the actual absorbances (A') of a series of concentrated solutions the monochromatic transmittances of which are at least a factor of 50 lower than the relative SRE level to be determined.

Although the Mielenz test method is presented here in a generalized form in order to accommodate the attenuation of the SRE by the sample, that attenuation must be determined independently. Fleming and O'Dea's direct transmittance SRE test method[3] yields accurate estimates of both the SRE and the attenuation of the SRE by the sample, and if the attenuation of the SRE by the sample is known then it may be used in the Mielenz method to give a further accurate estimate of the SRE, provided the same sample type is used under identical instrumental conditions in both the test methods.

The terms relative transmittance and differential absorbance are used synonymously in the text.

Formulation of Experimental Quantities

If the same cut-off solution is placed in the beams of a double beam, ratio recording spectrophotometer but the sample cell is α-times as thick as the reference cell ($\alpha = b_s/b_r$, where the subscripts s and r refer to the sample and reference beams, respectively, and b refers to the pathlength of the cells employed) then the transmittance of the sample beam solution relative to the reference beam solution, τ', in the presence of a relative SRE level of s is given by

$$\tau' = \frac{\tau_\lambda^\alpha + s\nu^\alpha}{\tau_\lambda + s\nu} \quad (1)$$

where τ_λ is the monochromatic transmittance of the reference beam solution and ν, which may be weakly dependent on λ, is its transmittance to SRE.

When scanning through the absorbance edge of the cut-off solution a relative transmittance minimum, *i.e.*, τ' (min) = τ'', will be encountered[1] at $\tau_\lambda = T$. If the derivative method is used, *i.e.*, setting $d\tau'/d\tau_\lambda$ equal to zero at $\tau_\lambda = T$, then eqn. (1) gives

$$T^\alpha + s\nu^\alpha = (T + s\nu)\alpha T^{\alpha-1} \quad (2)$$

Solving for s in eqn. (2) gives

$$s = \frac{(\alpha - 1)T^\alpha}{\nu^\alpha - \alpha\nu T^{\alpha-1}} \quad (3)$$

However, the spectrophotometric observable in this experiment is not T but τ''. If the expression for s given by eqn. (3) is substituted into eqn. (1), simplified and rearranged, then the following ensues:

$$T = (\tau''/\alpha)^{1/(\alpha-1)} \quad (4)$$

Eqn. (4) may now be substituted into eqn. (3) to give

$$s = \frac{(\alpha - 1)(\tau''/\alpha)^{\alpha/(\alpha-1)}}{\nu^\alpha - \nu\tau''} \quad (5)$$

Eqn. (5) is an exact general expression which relates the relative SRE level (s) to the Mielenz relative transmittance minimum (τ''), transmittance of the reference beam solution to SRE (ν), and sample cell to reference cell thickness ratio (α). The SRE transmittance was assumed to have remained constant over the spectral range covered by scanning through a Mielenz peak.

The transmittance ratio (r) at wavelength λ of a sample beam solution the cell pathlength of which is α-times greater than an identical reference beam solution is given by[2]

$$r = \frac{\tau_\lambda^\alpha + s\mu^{\alpha A_\lambda}}{\tau_\lambda + s\mu^{A_\lambda}} \quad (6)$$

where μ is the SRE transmittance of the reference sample the monochromatic transmittance (τ_λ) of which is 0.1 and $A_\lambda = -\log \tau_\lambda$. This transmittance ratio function has a minimum, r(min) = ρ, at a certain monochromatic reference

transmittance, $\tau_\lambda = t$, which is determined by s, μ and α. If μ is taken to be unity, then, by using the derivative method, an expression may be derived[2] which relates the relative SRE level to ρ and α

$$s = \frac{(\alpha - 1)\,(\rho/\alpha)^{\alpha/(\alpha-1)}}{1 - \rho} \qquad (7)$$

However, μ is less than unity and its experimental value must be determined independently before eqn. (6) may be numerically modelled for a selected value of α and trial relative SRE values. The trial relative SRE value which, when inserted into eqn. (6) for τ_λ values in the range $1 \leqslant \tau_\lambda \leqslant 0.1t$, gives the best match with experimental transmittance ratio measurements may be taken as the best estimate for the said relative SRE level.

The direct transmittance SRE test method[3] allows for the direct determination of μ and s through observing the actual transmittances (T') of an arithmetic series of concentrated solutions the monochromatic transmittances (τ_λ) of which are less than $0.02s$. The relationship between T', s, μ and τ_λ is then given by (where $A_\lambda = -\log_{10}\tau_\lambda$)

$$T' = s\mu^{A_\lambda} \qquad (8)$$

Taking the $\log_{10}$ of eqn. (8) gives

$$\log_{10}T' = \log_{10}s + A_\lambda \log_{10}\mu \qquad (9)$$

At these very high monochromatic absorbances eqn. (8) is a linear relationship between $\log_{10}T'$ and A_λ with a slope of $\log_{10}\mu$ and an ordinate intercept of $\log_{10}s$.

Experimental

All the spectrophotometric measurements reported here were made with a Shimadzu 260 double-beam spectrophotometer at a spectral slit-width setting of 1 nm. Matched pairs of 1, 2, 5, 10, 20, 50 and 100 mm quartz-glass cells were at hand. Therefore, various nominal sample to reference cell pathlength ratios were possible and the following nominal values were used: 2 (= 10/5 and 20/10), 2.5 (= 50/20), 4 (= 20/5) and 5 (= 50/10). The working solutions were obtained from a 50 g l^{-1} Orleans Blue food dye (E123) stock aqueous solution. The UV/VIS absorption spectrum of 10 g l^{-1} of the same solution in a 1 mm cell was given previously.[2] An arithmetic concentration series of the parent solution was prepared. The most dilute and concentrated members had monochromatic absorbances of 0.025 and 0.5, respectively, in a cell of pathlength 1 mm at 654 nm and the arithmetic series had an absorbance increment of 0.025. This yielded a set of 20 solutions the monochromatic absorbances of which, at 654 nm, ranged from A_{min} to A_{max} [incremented in steps (ΔA)] in various cell pathlengths (b) as follows:

$A_{min} + (\Delta A \times 19\ steps) = A_{max}$ in a b mm pathlength cell

$0.025 + (0.025 \times 19\ steps) = 0.5$ in a 1 mm pathlength cell

$0.050 + (0.050 \times 19\ steps) = 1.0$ in a 2 mm pathlength cell

$0.125 + (0.125 \times 19\ steps) = 2.5$ in a 5 mm pathlength cell

$0.250 + (0.250 \times 19\ steps) = 5.0$ in a 10 mm pathlength cell

$0.500 + (0.500 \times 19\ steps) = 10.0$ in a 20 mm pathlength cell

$1.250 + (1.250 \times 19\ steps) = 25.0$ in a 50 mm pathlength cell

The experimental cell pathlength ratios were determined by measuring the absorbance at 630 nm of a dilute Orleans Blue food dye (E123) solution in all the available cells and this yielded the following relative pathlengths: 1.00 ± 0.008; 2.00 ± 0.013; 5.00 ± 0.017; 10.00 ± 0.013; 20.01 ± 0.013; and 50.00 ± 0.039.

The Mielenz test method was applied repeatedly to the Shimadzu 260 spectrophotometer by scanning slowly in the range 750 ⩾ λ(nm) ⩾ 625, the spectral slit-width having been set at 1 nm. A food dye test solution had been placed in a pair of matched quartz cuvettes the nominal pathlength ratio of which was 2 (α = 10 mm : 5 mm). The ensuing differential absorbance spectra displayed the expected SRE Mielenz peaks at 654 nm. The monochromatic absorbance of the test solution at 654 nm in the 5 mm reference cuvette was 2.0 and the Mielenz peaks had an average absorbance of $A'' = 1.680 \pm 0.005$. Eqn. (4) predicts that if the absorbance of the reference sample in the Mielenz SRE test method ($-\log T$) is 2 and α is 2, then the absorbance of the Mielenz peak should be 1.699 ($-\log \tau''$). If a more concentrated member of the prepared Orleans Blue food dye test solutions had been used in the above experiment then the Mielenz peak would have occurred at a longer wavelength. The Mielenz analysis, $s \approx 0.25 \times 10^{-2A''}$, which is only applicable for α = 2, yields a relative SRE level of 0.000113 for the above experiment while eqn. (5), for ν = 1 and α = 2, yields s = 0.000116. If the Mielenz

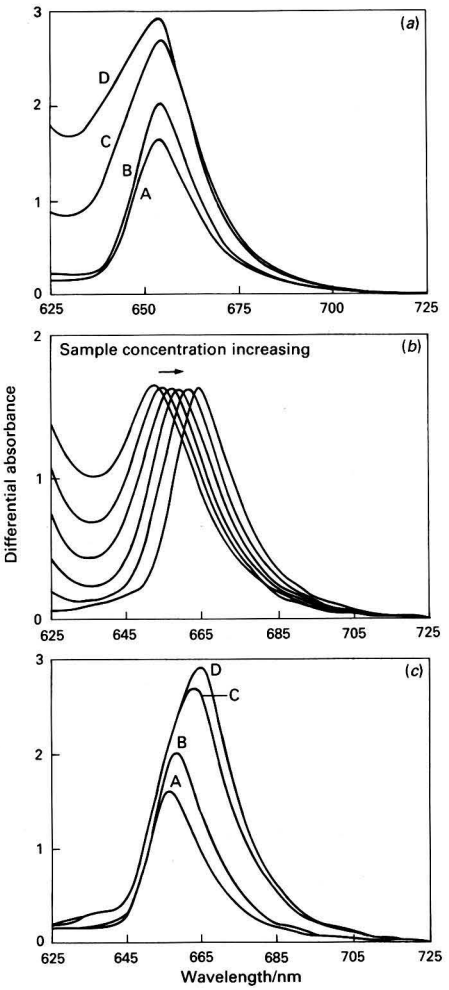

Fig. 1(*a*) Four Mielenz differential absorbance spectra in the wavelength range 725 ⩾ λ(nm) ⩾ 625 for nominal cell pathlength ratios (α_b) of A, 2; B, 2.5; C, 4; and D, 5. The Orleans Blue food dye concentration is gradually increased with decreasing α values so as to maintain the Mielenz peak at 654 nm. (*b*) Six Mielenz differential absorbance spectra in the range 725 ⩾ λ(nm) ⩾ 625 for a nominal cell pathlength ratio (α_b) of 2. (*c*) Four Mielenz differential absorbance spectra in the wavelength range 725 ⩾ λ(nm) ⩾ 625 for nominal cell pathlength ratios (α_b) of A, 2; B, 2.5; C, 4; and D, 5, and for a fixed concentration of Orleans Blue food dye

peak is to occur at 654 nm for all α values, then *a priori* knowledge of the absorbance of the test solution in the reference cell at 654 nm ($-\log T$) is necessary for each α value. A value for τ'' for a given α may be calculated using trial values for τ'' in eqn. (5) and assuming $s = 0.000116$ and $v = 1$. Eqn. (4) may then be employed to predict the appropriate approximate absorbance of the test solution which, when placed in the sample and reference cells, will give a Mielenz peak at 654 nm, *e.g.*, if $s = 0.000116$ and $\alpha = 2.5$, then $\tau'' = 0.0085$ satisfies eqn. (5) for $v = 1$, and eqn. (4) yields $T = 0.0226$ or $-\log T = 1.646$. This calculation procedure was executed in turn for $\alpha = 2.5$, 4 and 5 and was facilitated by having prior knowledge of the absorbance of the Mielenz peak (A'') at 654 nm which ensued from scanning the differential absorption of a selected food dye sample for $\alpha = 2$. The Mielenz test method was replicated for $\alpha = 2.5$, 4 and 5 by using the food dye sample of appropriate concentration for each α and then eqn. (5) (with $v = 1$) was used to calculate the relative SRE level. The resulting Mielenz differential absorbance spectra are given in Fig. 1(*a*). The Mielenz peaks occur at approximately the same wavelength (654 ± 0.5 nm) for all cell pathlength ratios used but increase in amplitude as α increases.

Fig. 1(*b*) displays six Mielenz differential absorbance spectra which were obtained for a constant nominal cell pathlength ratio of 2 (= 10/5) and by changing the sample concentration in the cuvettes for each scan. Note the red shift of the Mielenz peaks which occurs with increasing sample concentration.

Fig. 1(*c*) displays four Mielenz differential absorbance spectra which were scanned for constant sample concentration in the cuvettes and by changing the cell pathlength ratio between the following nominal values: 2 (= 10/5), 2.5 (= 50/20), 4 (= 20/5) and 5 (= 50/10). Note the red shift of the Mielenz peaks which occurs with increasing α values.

Fleming's transmittance ratio[2] and Fleming and O'Dea's direct transmittance[3] SRE test methods were also applied to the Shimadzu 260 spectrophotometer set at 654 nm and a spectral slit-width of 1 nm. The ensuing experimental determinations are plotted in Figs. 2 and 3. The above mentioned food-dye concentration series was appropriately employed in both tests.

Fig. 2 displays differential absorbance *versus* monochromatic reference absorbance plots for four cell pathlength ratios, $\alpha = b_s/b_r$. The experimental cell pathlength ratios are as follows: 20.01/10.00 = 2.001 ± 0.005; 50.00/20.01 = 2.499 ± 0.004; 20.01/5.00 = 4.00 ± 0.016; and 50.00/10.00 = 5.00 ± 0.01.

Fig. 3 is a plot on semi-log axes of the observed average transmittance (in 20 mm pathlength cells) of solutions (T') at 654 nm *versus* the respective monochromatic absorbance (A) in the range $0 \leqslant A \leqslant 10.0$. The exponential regression equation of fit to the linear part of the plot in the upper absorbance range is given by $T' = 0.000140 \times 10^{-0.029A}$.

Results

Eqns. (5) and (6) cannot be applied to the differential absorbance maxima in Fig. 1(*a*) and (*b*), respectively, without *a priori* knowledge of the transmittances of the samples to SRE at the wavelength of interest. The quantity 'v' in eqn. (5) is given by μ^A, where A ($= -\log_{10} T$) is the monochromatic

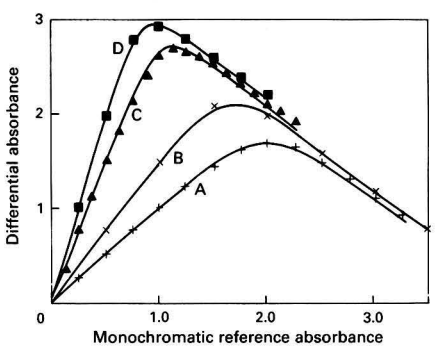

Fig. 2 Four plots of the differential absorbance *versus* the monochromatic reference absorbance of an arithmetic concentration series of Orleans Blue food dye (E123) solutions placed in pairs of cells the pathlength ratios (α_b) of which were: A, 2.001; B, 2.499; C, 4.00; and D, 5.00. The measurements were made at 654 nm and with a spectral slit-width of 1 nm

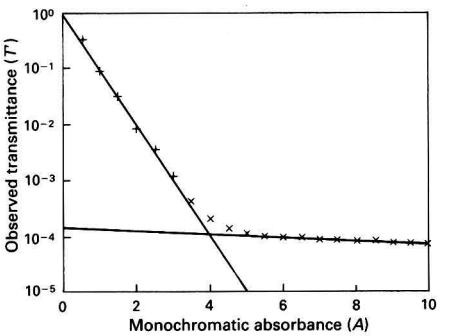

Fig. 3 Plot on semi-log axes of the observed transmittance (T') *versus* the monochromatic absorbance (A) at 654 nm and with a spectral slit-width of 1 nm. The measurements were made in a pair of matched 20 mm quartz cells with a Shimadzu 260 spectrophotometer. The analyte samples were dilutions of a 50 g l^{-1} Orleans Blue food dye in distilled water. The monochromatic absorbance range, $7 \leqslant A \leqslant 10$, yielded $s = 0.000140$ and $\mu = 0.935$

Table 1 Relative SRE level in a Shimadzu 260 spectrophotometer set at 654 nm and a spectral slit-width of 1 nm using a revised Mielenz *et al.*[1] and the transmittance ratio spectrometry[2] test methods

Cell pathlength ratio, $\alpha(= b_s/b_r)$	2.001 ± 0.005	2.499 ± 0.004	4.00 ± 0.016	5.00 ± 0.01
Mielenz's peak absorbance at 654 nm ($-\log_{10}\tau''$)	1.68	2.08	2.73	2.94
Monochromatic reference absorbance at 654 nm ($-\log_{10} T$) from eqn. (4)	2.00	1.65	1.10	0.90
Relative SRE level [$s(\times 10^{-4}) \pm 0.10$] from eqn. (5)				
(*a*) for $v = 1$	1.12	1.12	1.08	1.14
(*b*) for $v = 0.935^A$	1.53	1.51	1.46	1.55
Relative SRE level [$s(\times 10^{-4}) \pm 0.10$] from eqn. (7) and Fig. 2 maxima	1.04	1.01	1.14	1.13
Relative SRE level [$s(\times 10^{-4}) \pm 0.10$] from eqn. (6) for $\mu = 0.935$ in Fig. 2	1.35	1.25	1.45	1.40

absorbance at 654 nm of the reference beam sample used in the method of Mielenz *et al.* and μ has been defined in eqn. (6). However, eqn. (8), applied to the linear portion of the upper absorbance range of Fig. 3, yields the following experimental values for μ and s: $\mu = 0.935 \pm 0.015$ and $s = 0.000140 \pm 0.000015$. If the monochromatic absorbances at 654 nm of the reference beam samples are known, then eqn. (5) can be applied to the maxima in Fig. 1(*a*) to yield the relative SRE levels recorded in Table 1.

Eqn. (6) can then be used to generate four sets of data points, *i.e.*, a matching set of data points for each set of experimental differential absorbance points in Fig. 2, through using trial s values for the relative SRE level and a setting $\mu = 0.935$. The ensuing simulated curves are traced in Fig. 2 and the optimum trial relative SRE values are listed in the bottom row of Table 1.

Conclusion

The original purpose of this paper was to generalize the theoretical basis of the SRE test method developed by Mielenz *et al.*[1] so as to embrace all cell pathlength ratios greater than unity. The generalized theory was tested experimentally in this paper for four disparate cell pathlength ratios to yield relative SRE levels for a Shimadzu 260 spectrophotometer which agreed within the limits allowed by the experimental errors involved [see Table 1 for eqn. (5) and $v = 1$]. However, the test method, being sample based, would underestimate the relative SRE levels in spectrophotometers if the test solutions absorbed the SRE. This postulate was tested in this paper by comparing the relative SRE levels in a Shimadzu 260 spectrophotometer determined in three semi-independent ways under identical instrumental conditions. The SRE test methods of Mielenz *et al.*[1] and Fleming[2] yielded compatible SRE results if the SRE transmittance of the samples employed was assumed to be unity. The direct transmittance SRE test method of Fleming and O'Dea,[3] which allows for the non-transparency of the samples towards SRE, yielded an SRE value of 0.000140 ± 0.000015 for the Shimadzu 260 spectrophotometer at 654 nm and a spectral slit-width of 1 nm. This was significantly greater than the average SRE values of 0.000112 ± 0.000010 and 0.000108 ± 0.000010 which were obtained by the two other test methods mentioned, based on calculations using eqns. (5) and (7), respectively, for $v = \mu = 1$ and using four distinct cell pathlength ratios. These results may be reconciled with the direct transmittance SRE test method result if the SRE transmittance value yielded by the last test method, *i.e.*, $\mu = 0.935$, is employed in eqns. (5) and (6). Eqn. (5) with $\mu = 0.935$ gave $s = 0.000151 \pm 0.000010$ and eqn. (6) with $\mu = 0.935$ gave $s = 0.000136 \pm 0.000010$ from the curves of best fit to the experimental points in Fig. 2.

The three test methods gave relative SRE levels which agree within the experimental error, provided allowance is made for the absorption of the SRE by the test solution being used. However, only the direct transmittance SRE test method is self-contained in that it yields all the information required to specify the true relative SRE level in a spectrophotometer without having recourse to any other test method.

References

1 Mielenz, K. D., Weidner, V. R., and Burke, R. W., *Appl. Opt.*, 1982, **21**, 3354.
2 Fleming, P., *Analyst*, 1990, **115**, 375.
3 Fleming, P., and O'Dea, J., *Analyst*, 1991, **116**, 195.

Paper 1/00489A
Received February 4th, 1991
Accepted April 29th, 1991

Determination of Iron by Flow Injection Based on the Catalytic Effect of the Iron(III)–Ethylenediaminetetraacetic Acid Complex on the Oxidation of Hydroxylamine by Dissolved Oxygen

Andreu Cladera, Enrique Gómez, Jose Manuel Estela and Victor Cerdá*
Department of Chemistry, Faculty of Sciences, University of the Balearic Islands, E-07071 Palma de Mallorca, Spain

A flow injection (FI) spectrophotometric method for the determination of Fe based on the catalytic effect of the Fe^{III}–ethylenediaminetetraacetic acid–complex on the oxidation of hydroxylamine by dissolved oxygen in a basic medium is described. The FI manifold used was interfaced to a personal computer provided with appropriate software for automatic commanding of sample injection and data acquisition and processing. The absorbance response provided by the spectrophotometer was linear over the range 3.5–150 ng ml^{-1} of Fe, and the detection limit achieved was 2 ng ml^{-1}, with a relative standard deviation of 2.4% for 50 ng ml^{-1} of Fe^{III} ($n = 11$) and 6.7% for 5 ng ml^{-1} of Fe^{III} ($n = 11$). The only serious interferences with the determination were those of Co^{II}, Cr^{III} and Cu^{II}, but these could be reduced such that at 40, 40 and 10 times the Fe concentration they had no effect. The results provided by a normal and a reversed FI configuration were compared and the method was satisfactorily applied to the determination of Fe in natural waters and white wine at a sampling rate of 60 samples h^{-1}.

Keywords: *Flow injection; spectrophotometry; catalytic effect; iron(III)–ethylenediaminetetraacetic acid complex; iron determination*

Since flow injection (FI) was introduced by Růžička and Hansen in 1975,[1] continuous advances in this technique and its adaptation to different analytical methodologies, particularly spectrometric, electrochemical and separative, have testified to its enormous potential in various areas of interest such as environmental, pharmaceutical and clinical analysis. Throughout the intervening 15 years, FI has attracted a growing number of workers, who have found it to be a reproducible, rapid and inexpensive alternative to existing methodologies, in addition to a most flexible tool for adaptation to particular problems, as demonstrated by the increasing number of papers published on FI, most of which have been compiled in several books and reviews.[2–5]

The spectrophotometric determination of Fe in an FI system has been addressed by several workers. Mortatti *et al.*[6] used two different measurement wavelengths to avoid interferences and an automated system for the determination of 0.1–30 ppm of Fe at a high sampling frequency (180 h^{-1}). Other workers[7–9] accomplished the speciation of Fe^{II} and Fe^{III} by different procedures but over similar determination ranges. Ríos *et al.*[10] reported the individual and simultaneous determination of Fe, Cu and Al over the range 0.1–3.0 ppm (Fe) in synthetic waste water samples; however, the determination was subject to severe interferences from carbonate and phosphate ions. Finally, Leach *et al.*[11] succeeded in determining Fe at concentrations between 3.6 ppb and 0.71 ppm by using standard solutions in experiments mainly aimed at evaluating sample injection and differential detection. All of the above methods rely on the use of 1,10-phenanthroline or one of its derivatives as the complexing agent.

In previous work[12] a thermometric method was developed for the determination of Fe based on the catalytic effect of the Fe^{III}–ethylenediaminetetraacetic acid (EDTA) complex (FeY^-) on the oxidation of hydroxylamine by dissolved oxygen in a basic medium, which takes place according to the following reaction:

$$2NH_2O^- + 2O_2 \xrightleftharpoons{FeY^-} NO_2^- + NO^- + H_2O_2 + H_2O$$

As the reaction yields nitrite ions, it was envisaged that it could also be applied to the spectrophotometric determination of Fe by coupling it to the well-known Griess reaction.

In this work, and in a continuation of our research on the automation of analytical methods,[13–16] a semi-automated FI system was designed for the spectrophotometric determination of trace amounts of Fe on the basis of the above reaction, which, as predicted, provided increased reproducibility, sensitivity and sample throughput. The system was controlled by a personal computer and appropriate software which permitted: (*a*) commanding the automatic injection of samples; (*b*) acquisition of the spectra obtained by the diode array detector; (*c*) continuous recording of the spectra in addition to the FI recordings; and (*d*) processing of the FI peaks for obtaining the sample concentrations by automatic interpolation of their heights on the calibration graph.

The spectra used for the determination were obtained by subtracting the background signal due to the colour-forming, non-catalytic oxidation of hydroxylamine from the readouts recorded on passage of the sample through the flow cell. Likewise, the FI recordings reflected the changes with time in the differences between the signal at the absorption maximum (542 nm) and that at another wavelength at which readings were made on the baseline (700 nm).

Experimental

Reagents

All reagents were of analytical-reagent grade and all solutions were prepared in distilled water.

Phosphate buffer, 0.1 mol l^{-1}. Prepared from dipotassium hydrogen phosphate (Merck) and 1.75×10^{-3} mol l^{-1} EDTA solution obtained from the disodium salt (Probus); the pH was adjusted to 12.5 with NaOH solution.

Iron(III) standard solution containing 1000 μg ml^{-1} *of* Fe^{III} *in* 1% HNO_3. Prepared from iron(III) nitrate (Probus).

Hydroxylamine solution, 0.05 mol l^{-1}. Prepared from the hydrochloride (Probus) and neutralized with NaOH solution.

Sulphanilamide (SPA) (Merck) and N-(1-*naphthyl)ethylenediamine (NED) (Merck) solutions containing* 0.3% *of either substance in* 0.8 mol l^{-1} *HCl (Merck).*

The last three solutions were freshly prepared each day in order to avoid baseline noise as far as possible.

* To whom correspondence should be addressed.

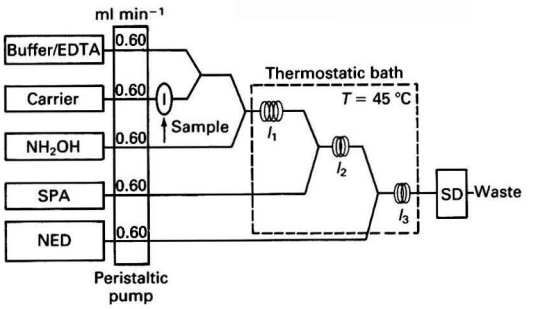

Fig. 1 Flow injection manifold used for the direct determination of Fe. I = Sample injector; SD = spectrophotometric detector; $l_1 = 5$ m; $l_2 = 1.5$ m; $l_3 = 2$ m; [EDTA] = 1.75×10^{-3} mol l^{-1}; [NH_2OH] = 0.05 mol l^{-1}; [SPA] = 0.3%; [NED] = 0.3%; and $T = 45$ °C

Apparatus

A customized semi-automated system equipped with an IBM-compatible computer for controlling injections and acquiring and processing the spectrophotometric data was used.

Fig. 1 shows a schematic diagram of the FI manifold, which consisted of an eight-way Gilson Minipuls 3 peristaltic pump, a Rheodyne 50 injection valve which was controlled by the computer *via* a mechanical actuator, a Techtron thermostatic bath and a Hewlett-Packard (HP) 8452A diode array spectrophotometer furnished with a flow cell with a pathlength of 10 mm and a void volume of 18 μl. All reactors and the injection loop were made from poly(tetrafluoroethylene) (PTFE) tubing of 0.5 mm i.d.

Data Acquisition and Processing

A special program was developed for instrumental control and data acquisition and processing that takes advantage of the full potential of the HP 8452A diode array detector for the rapid acquisition of spectra and optionally also allows complete spectra to be acquired at every point along the FI recording and absorbances measured at different wavelengths to be used. In order to take full advantage of these assets and reduce noise from the spectrophotometer lamp as far as possible, the FI recordings were obtained by assigning each point as the difference between the absorbance measured at the maximum absorption wavelength (542 nm) and that at a zero-absorption wavelength (700 nm). Such values were calculated by the computer and stored in a file for subsequent use. Optionally, all the acquired spectra can be stored in another file, which can be used for assaying different measurement wavelength combinations without the need to repeat the experiments.

The program also automatically processes the FI recordings obtained by detecting peaks, determining the baseline, calculating peak heights and areas, constructing calibration graphs and calculating the required concentrations.

Peaks were detected by using the first two derivatives of the experimental data, which were calculated by the Savitzky–Golay algorithm.[17] If the first and second derivatives were larger than pre-set values, the corresponding point was taken as the start of the peak; also, the point at which such a condition was met was taken as the end of the peak. Then, the peak baseline was determined from points in front of and behind the peak, and the peak height was calculated as the distance between the peak maximum, the point at which the first derivative changed sign, and the previously calculated baseline; if the height was lower than a pre-set value, the peak in question was rejected. Next, the areas of the peaks were determined by the trapezium method and the concentration corresponding to each peak was calculated by interpolation of the calibration graph, which was also constructed by using the program from one or several standard FI recordings on the basis of peak heights or areas according to the user's choice.

Procedure

The determination was started by circulating the different reagent streams through the FI system in order to allow the background colour due to the non-catalytic oxidation of hydroxylamine to develop. Once the absorbance was stable, the blank signal was obtained and assigned a zero value in the spectral recording. Then, the baseline of the FI recording was obtained and the program commanded injection of the sample (200 μl), the Fe concentration of which must be within the linear determination range. After the residence time had elapsed, a peak reflecting the colour increase resulting from the catalytic effect of the Fe^{III}–EDTA complex on the oxidation of hydroxylamine was obtained. The corresponding FI recording was stored in a pre-set file and processed in order to obtain the peak height over the baseline and the injected sample concentration by interpolation of the height on the calibration graph.

Results and Discussion

Optimization of Variables

As previously found for the thermometric method,[12] the maximum absorbance was obtained by using a 0.1 mol l^{-1} phosphate buffer of pH 12.5 as the medium for the catalysed reaction. Other buffers consisting of borax or NH_4^+–NH_3 yielded poorer results, while tris(hydroxymethyl)aminomethane provided approximately the same readings as those obtained with the phosphate buffer.

The spectrophotometric signal yielded by the azo dye was found to remain constant at HCl concentrations above 0.8 mol l^{-1}, which was therefore chosen as the working concentration.

The spectrophotometric signals provided by Fe^{III} standards were identical with those yielded by Fe^{II} solutions prepared from Mohr's salt; hence all the Fe present under the working conditions was in the Fe^{III} form.

The simplex method[18] was used to optimize simultaneously a set of eight parameters consisting of the three reactor coil lengths (l_1, l_2 and l_3) and five chemical variables, *viz.*, the concentrations of EDTA, hydroxylamine, SPA and NED, and the temperature of the thermostated bath in which the three reactors were immersed. The simplex programme was run by using one-directional simple advancement, contraction and no quadratic interpolation.

The simplex optimization was performed by measuring the height of the peak obtained on injection of 100 μl of a 50 ng ml^{-1} standard of Fe^{III} and plotting the difference between the absorbance of the catalysed and uncatalysed (baseline) reaction. A maximum working temperature of 45 °C was used in order to avoid an excessively noisy baseline. The optimum conditions thus determined are shown in Table 1 and correspond to step 11 in Fig. 2, which shows the variation of the signal as a function of the simplex evolution.

Finally, the variation of the signal as a function of the injected sample volume was studied. It was found that while the signal increased by 40% when 150 rather than 100 μl was used as the injected volume, an increase in the injected volume, from 150 to 200 μl increased the signal by only 25%. In order to avoid potential diffusion problems and an inordinate decrease in the sample throughput, it was decided not to use larger injected volumes.

After the optimum working conditions had been established, the linear determination range was evaluated, and was found to be between 3.5 and 150 ng ml^{-1} of Fe, the detection limit being 2.0 ng ml^{-1}. The equation obtained was: $A = 0.019$

Table 1 Optimum working conditions as established by the simplex method

	[EDTA]/ mol l^{-1}	[NH_2OH]/ mol l^{-1}	[SPA] (%)	[NED] (%)	T/ °C	l_1/ m	l_2/ m	l_3/ m
Normal FI	1.75×10^{-3}	0.05	0.3	0.3	45	5.0	1.5	2.0
Reversed FI	1.85×10^{-3}	0.01	0.5	0.5	20*	4	0	0

* Room temperature.

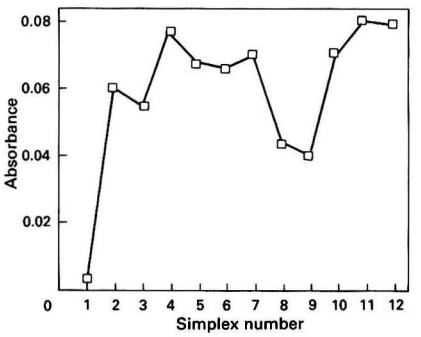

Fig. 2 Variation of peak height as a function of the simplex evolution. [Fe^{III}] = 50 ng ml^{-1}; and injected sample volume = 100 µl

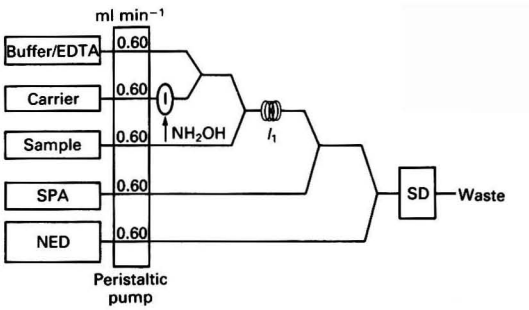

Fig. 4 Reversed FI manifold used for the determination of Fe. l_1 = 4 m; [EDTA] = 1.85×10^{-3} mol l^{-1}; [NH_2OH] = 0.01 mol l^{-1}; [SPA] = 0.5%; and [NED] = 0.5%

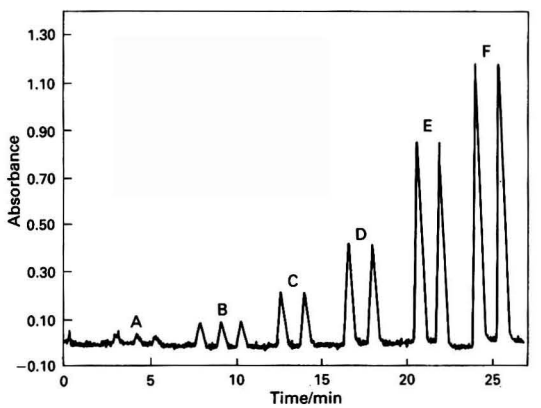

Fig. 3 Flow injection recording obtained by using the normal FI manifold for the construction of the calibration graph from triplicate injections (V_i = 200 µl) of A, 5; and B, 10 ng ml^{-1} of Fe^{III} and duplicate injections of C, 25; D, 50; E, 100; and F, 150 ng ml^{-1} of Fe^{III}. The working conditions used are given in Table 1

$+ 7.52 \times 10^{-3}c$; ($r = 0.9992$), where c is the Fe^{III} concentration in ng ml^{-1} (r = correlation coefficient).

The detection limit was taken as five times the standard deviation of the base line noise ($\sigma = 2.5 \times 10^{-3}$), and the quantification limit as ten times the same parameter. Fig. 3 shows six points of the corresponding FI recording. The repeatability of the proposed method was found to be 6.7 and 2.4% for 5 and 50 ng ml^{-1} of Fe^{III} (n = 11), respectively.

In order to compare the working conditions established by the procedure described above with those of a reversed FI system, the manifold shown in Fig. 4 was used, the representative variables of which were also optimized by the simplex method, but using the ratio of the signals yielded by the catalysed and uncatalysed reaction (*i.e.*, the peaks obtained by injection of an Fe standard and distilled water, respectively, through the sample channel) instead; this ensured that the highest sensitivity in the lowest height of the peak blank was obtained. The conditions thus established are also summarized in Table 1. As the increased sensitivity obtained also provided a more convenient operational procedure resulting from the possibility of using the baseline as the blank, it was decided to use the manifold depicted in Fig. 1 for all subsequent experiments.

Effect of Foreign Ions

The potential interfering effect of various ions that were added to solutions containing 50 ng ml^{-1} of Fe^{III} in different proportions in relation to the analyte concentration was studied.

Table 2 lists the results obtained. A given ion was considered to interfere with the determination if it resulted in a signal variation greater than $\pm 2\sigma$. As can be seen, few ions were found to interfere with the proposed method. The most serious interferences were from Co^{II}, Cr^{III} and Cu^{II}, which increased the height of the peak yielded by the analyte alone. The interference from the divalent ions at concentrations up to 40 times higher than that of the analyte was readily overcome by injecting 1% ammonia solution (Merck) into the stream containing EDTA and the buffer; direct incorporation in the sample caused the analyte to precipitate. On the other hand, the interference from Cr^{III} was eliminated at interferent-to-analyte ratios below 10 if ammonia solution was added to the EDTA channel and 2 ml of 0.05 mol l^{-1} tartrate solution were added to the sample.

The weak interference from Ca and Mg was investigated in detail because of their significance in the analysis of very hard waters. This interference was found to arise from the complexation of the two alkaline earth metal ions by EDTA; hence, relatively large concentrations of these two ions will lead to an insufficient concentration of EDTA for complete formation of the Fe^{III}–EDTA complex, thereby preventing catalysis of the oxidation of hydroxylamine. The interfering effect of Ca and Mg can be halved by doubling the EDTA concentration used or, provided the analyte concentration allows, by diluting the sample; even if the interferent-to-analyte ratios remain constant, the amount of EDTA removed from the medium will obviously be reduced by 50%. Fig. 5 shows the interfering effect of Ca and Mg on the determina-

Table 2 Tolerated foreign ion-to-analyte ratios in the determination of 50 ng ml^{-1} of Fe^{III}

Foreign ion	[Ion] : [Fe^{III}]
Cl^-, NO_3^-, SO_4^{2-}, CO_3^{2-}, Ca^{II}, Ba^{II}, Pb^{II}	1000*
Mg^{II}, Cd^{II}, Zn^{II}, Ni^{II}, Al^{III}	400
Mn^{II}	5
Cu^{II}	1 (40)†
Co^{II}	0.5 (40)†
Cr^{III}	0.5 (10)‡

* Maximum concentration tested.
† In the presence of 1% ammonia solution.
‡ In the presence of 1% ammonia solution and 2×10^{-3} mol l^{-1} tartrate.

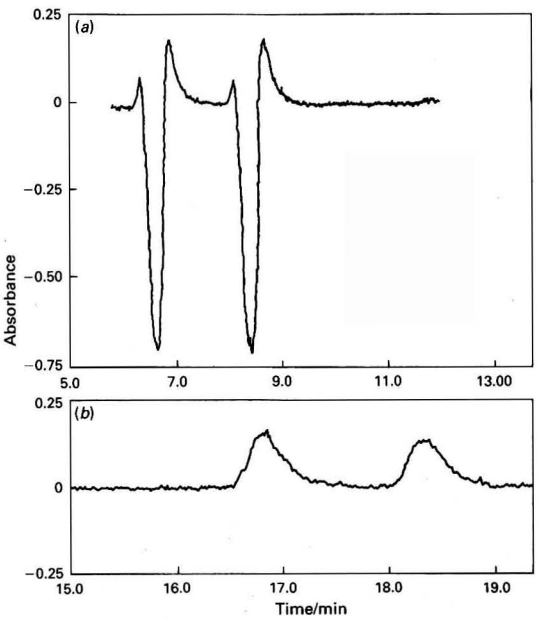

Fig. 5 Determination of Fe in tap water. (*a*) Interference from Ca and Mg. (*b*) Elimination of the two interferents by a 1 + 5 dilution of the sample

tion of Fe in hard tap water and the elimination of such an effect by diluting the original sample five-fold.

Applications

The proposed method was applied to the determination of Fe in waters from various sources and in white wines.

For drinking waters, international legislation classifies Fe as an undesirable component. Hence, the proposed method is interesting because it allows the determination of this metal in a simple and fast way within legally permitted ranges.

Table 3 lists the dilutions used and the results obtained by using both the proposed method and a standard atomic absorption procedure, with standard additions, as reference.[19] When a graphite furnace was used the ashing and atomizing temperatures were optimized (1200 and 2100 °C, respectively) and magnesium nitrate was added as a chemical modifier. As can be seen, the results obtained were consistent. In all the water samples analysed, the Fe concentrations found were below the maximum level allowed by the legislation (up to 200 ng ml^{-1}).

Table 3 Results obtained for the determination of Fe in real samples

		[Fe^{III}]/μg ml^{-1}	
Sample	Dilution	Proposed method	Atomic absorption method*
Mineral water	—	0.0043	0.0044†
Well water	—	0.017	0.018†
Tap water (Palma de Mallorca)			
Zone 1	1 + 4	0.10	0.11†
Zone 2	1 + 4	0.072	0.079†
Zone 3	1 + 4	0.047	0.045†
Zone 4	1 + 4	0.059	0.065†
White wine	1 + 99	2.8	2.4

* Reference 19.
† Using a graphite furnace.

However, application of the proposed method to rosé and red wines provided different results from those yielded by the reference method, probably because of the presence of an additive, the interference from which could not be overcome by masking or mineralization.

Conclusions

The working conditions used in the proposed method for the spectrophotometric determination of Fe in an FI system are very similar to those employed in the previously reported thermometric procedure[12] as far as the development of the catalytic reaction involved is concerned.

Operationally, the spectrophotometric method is more sensitive, reproducible and rapid than its thermometric counterpart, although the latter is subject to less serious interferences and hence is more selective. This is consistent with the features of the two techniques used. In addition, the thermometric method does not require the use of a coupled reaction; hence it is subject to fewer background perturbations.

The normal FI configuration used was found to provide better results than the reversed FI manifold tested, partly because of the colour arising from the non-catalytic reaction taking place in the latter instance.

The proposed method has a linear determination range with a lower limit similar to the lowest reported in the literature,[11] but with the added advantage of being applicable to real samples.

The authors thank the DGICyT (Spanish Council for Research in Science and Technology) for financial support granted for the realization of this work as part of Project PA 86-0033.

References

1 Růžička, J., and Hansen, E. H., *Anal. Chim. Acta*, 1975, **78**, 145.
2 Růžička, J., and Hansen, E. H., *Flow Injection Analysis*, Wiley, New York, 1981.
3 Růžička, J., and Hansen, E. H., *Anal. Chim. Acta*, 1986, **179**, 1.
4 Valcárcel, M., and Luque de Castro, M. D., *Flow Injection Analysis: Principles and Applications*, Ellis Horwood, Chichester, 1987.
5 *Quím. Anal.*, 1989, **8**(2), Special Issue.
6 Mortatti, J., Krug, F. J., Pessenda, L. C. R., Zagatto, E. A. G., and Jorgensen, S. S., *Analyst*, 1982, **107**, 659.
7 Bubnis, B. P., Straka, M. R., and Pacey, G. E., *Talanta*, 1983, **30**, 841.
8 Lynch, T. P., Kernoghan, N. J., and Wilson, J. N., *Analyst*, 1984, **109**, 843.

9 Faizullah, A. T., and Townshend, A., *Anal. Chim. Acta*, 1985, **167**, 225.
10 Ríos, A., Luque de Castro, M. D., and Valcárcel, M., *Analyst*, 1985, **110**, 277.
11 Leach, R. A., Růžička, J., and Harris, J. M., *Anal. Chem.*, 1983, **55**, 1669.
12 Gómez, E., Estela, J. M., and Cerdá, V., *Thermochim. Acta*, 1991, **176**, 121.
13 Cerdá, V., and Ramis, G., *An Introduction to Laboratory Automation*, Wiley, New York, 1990.
14 Maimó, J., Cladera, A., Más, F., Forteza, R., Estela, J. M., and Cerdá, V., *Int. J. Environ. Anal. Chem.*, 1989, **35**, 161.
15 Cladera, A., Caro, A., Estela, J. M., and Cerdá, V., *Int. J. Environ. Anal. Chem.*, 1990, **43**, 11.
16 Cladera, A., Estela, J. M., and Cerdá, V., *J. Autom. Chem.*, 1990, **12**, 108.
17 Savitzky, A., and Golay, M. J. E., *Anal. Chem.*, 1964, **36**, 1627.
18 Morgan, L., and Deming, S. N., *Anal. Chem.*, 1974, **46**, 1170.
19 Perkin-Elmer Handbooks: *Analytical Methods for Atomic Absorption Spectrophotometry* and *HGA-400 Graphite Furnace. Operator's Manual*, Perkin-Elmer, Norwalk, CT, 1984.

Paper 1/00703C
Received February 14th, 1991
Accepted April 25th, 1991

Simultaneous Determination of Toxic Metabolites by Linear Combination Derivative Spectrophotometry

Lin Liming
Weifang Drug Control Institute, Shandong, People's Republic of China
Zhao Naixin*
Weifang Medical College, Shandong, People's Republic of China

A linear combination derivative spectrophotometric method is described. The method overcomes the problem of overlapping in derivative spectrophotometry and allows the maximum use of quantitative information. In addition, the method can be used to increase the selectivity, sensitivity and accuracy of the simultaneous analysis of multicomponent mixtures. The application of the method to the simultaneous determination of bongkrekic acid and toxoflavin, the toxic metabolites produced by *Pseudomonas farinofermentans*, is described.

Keywords: *Linear combination derivative spectrophotometry;* pseudomonas farinofermentans; *bongkrekic acid; toxoflavin*

Derivative spectrophotometry is zero-order spectrophotometry transformed by differential calculus. It has the ability to separate the signal of the constituent to be determined from the signals of interfering constituents by mathematical processes and to enhance the sensitivity of the determination;[1] however, derivative spectrophotometry has some limitations for the determination of a constituent, the spectrum of which severely overlaps those of interfering constituents. In order to obtain better selectivity, sensitivity and accuracy, a linear combination derivative spectrophotometric method has been developed. The method overcomes the problem of overlapping in derivative spectrophotometry and permits the maximum use of quantitative information.

Bongkrekic acid and toxoflavin, the toxic metabolites produced by *Pseudomonas farinofermentans*, play an important role in food poisoning caused by fermented corn meal and white fungus (*Tremella fuciformis*) contaminated with bacteria.[2,3] It has also been found that an unknown yellowish substance is present in the metabolites. To date, there have been no reports on the simultaneous determination of these two toxins. After a simple extraction procedure, the two toxins can be determined satisfactorily by the method described here without the need for separation.

Theory

In measurements using a derivative spectrum, suppose that there is no linear relationship between two constituents each of which accords with Beer's law.

If the measured wavelength combination is taken as λ_i and the reference wavelength combination as λ_j, and if the derivative spectra of the two constituents, the unknown component a and the interfering component b, in solution, overlap, the linear combination derivative values will be $\sum_{i=1}^{m} Di_a$, $\sum_{i=1}^{m} Di_b$, $\sum_{j=1}^{n} Dj_a$ and $\sum_{j=1}^{n} Dj_b$, respectively.

Considering the different wavelengths, the measured linear combination derivative values of a mixture are the sum of the linear combination derivative values of all the constituents, *i.e.*,

$$Dc_i = \sum_{i=1}^{m} Di_a + \sum_{i=1}^{m} Di_b \quad (1)$$

$$Dc_j = \sum_{j=1}^{n} Dj_a + \sum_{j=1}^{n} Dj_b \quad (2)$$

where D denotes the derivative value of the absorbance, the subscript i denotes the ith measurement wavelength, the subscript j denotes the jth reference wavelength (j can be 1 or 2 points) and c is the concentration of the mixture.

On the same derivative curve, the ratio of the linear combination derivative at λ_i and λ_j is equal to K, and can be written as:

$$\sum_{i=1}^{m} Di_b - K \sum_{j=1}^{n} Dj_b = 0 \quad (3)$$

$$i.e., \; K = \sum_{i=1}^{m} Di_b / \sum_{j=1}^{n} Dj_b \quad (4)$$

Let

$$\Delta Dc = Dc_i - KDc_j \quad (5)$$

from eqns. (1) and (2) we obtain

$$\Delta Dc = \left(\sum_{i=1}^{m} Di_a + \sum_{i=1}^{m} Di_b\right) - K\left(\sum_{j=1}^{n} Dj_a \quad \sum_{j=1}^{n} Dj_b\right) \quad (6)$$

from eqns. (3) and (6) we obtain

$$\Delta Dc_i = \sum_{i=1}^{m} Di_a - K \sum_{j=1}^{n} Dj_a \quad (7)$$

If

$$Di_a = \frac{d\varepsilon_{i_a}}{d\lambda_i} c_a \quad (8)$$

$$Dj_a = \frac{d\varepsilon_{j_a}}{d\lambda_j} c_a \quad (9)$$

then

$$\Delta Dc = \left(\sum_{i=1}^{m} \frac{d\varepsilon_{i_a}}{d\lambda_i} - K \cdot \sum_{i=1}^{n} \frac{d\varepsilon_{j_a}}{d\lambda_j}\right) c_a \quad (10)$$

where $d\varepsilon/d\lambda$ is the derivative value of the absorption coefficient. Hence ΔDc depends only on the concentration of component a; however, it accords with Beer's law as before, *i.e.*, the interference from component b is eliminated.

Suppose that the derivative spectra of two components are as shown in Fig. 1, in which curves a and b overlap and that the selected wavelengths are λ_1, λ_2, λ_3. If b is taken as the interfering component, then:

$$K = \frac{Db_{\lambda_1} + Db_{\lambda_3}}{Db_{\lambda_2}} \; i.e., \; \Delta Db = Db_{\lambda_1} + Db_{\lambda_3} - KDb_{\lambda_2} = 0$$

where the linear combination value of the component to be determined (a) is

$$\Delta Da = (Da_{\lambda_1} + Da_{\lambda_3}) - KDa_{\lambda_2} = |Da_{\lambda_1}| + |Da_{\lambda_3}| + |KDa_{\lambda_2}|$$

* To whom correspondence should be addressed.

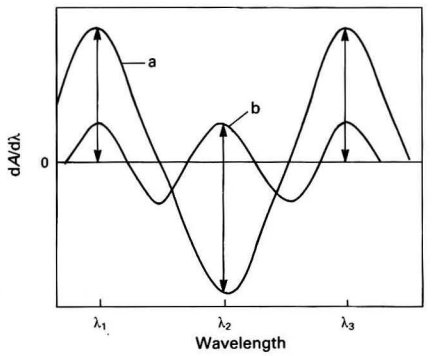

Fig. 1 Ideal model of derivative spectra (see text for details of a and b)

Similar results are obtained by using a as the interfering component and b as the component to be determined (all the derivative values were substituted by experimentally determined positive or negative values).

Hence, by selecting an appropriate wavelength combination, the value of K can be found and then by linear combination the interference from one component can be eliminated such that the absolute value of the derivative of the other component can be determined. This will allow the simultaneous determination of the two components.

If the measured wavelength combinations are chosen at the zero-crossing point of the derivative spectrum of the interfering component, the calculation of K can be avoided and the component of interest can be determined directly based on the linear combination derivative values.

If a number of wavelength points (say 2–5 points), at which the value of Di_a/Di_b is large, are found for the measured wavelength combination λ_i and a number of wavelength points (say 1–2 points), at which the value of Dj_a/Dj_b is small, are found for the reference wavelength combination λ_j, and the wavelength points are chosen at points on the spectral curves where the slopes are as flat as possible, *i.e.*, at peaks and valleys, it is known from eqn. (10) that the total derivative absorption coefficient is many times greater than that of a single wavelength; hence the sensitivity will be increased.

From error transmission, the accuracy of ΔDc is indicated by the relative standard deviation (RSD)

$$\mathrm{RSD} = \left(\sum_{i=1}^{m} \delta i^2 - K . \sum_{j=1}^{n} \delta j^2 \right)^{1/2} / \Delta Dc \qquad (11)$$

where δi and δj denote the measurement error of each measured point expressed as the standard deviation. From eqn. (11) it can be seen that the total standard deviation, *i.e.*, the numerator in eqn. (11), is less than the sum of the linear standard deviations, and that the value of ΔDc, *i.e.*, the denominator in eqn. (11), is a single linear combination. When the number of measurement points is increased, the increase in the denominator will exceed that of the numerator; hence the accuracy will be improved.

Experimental

Instrumentation and Reagents

A Shimadzu UV-210A spectrophotometer with a DES-2 derivative attachment was used. Standard toxoflavin was prepared according to the procedure of van Damme *et al.*[4] The product was recrystallized from propan-1-ol, filtered and dried *in vacuo* below 40 °C to constant mass. The identity and purity of the product were confirmed by its melting-point, by chromatography, and from ultraviolet and infrared absorption spectra. Bongkrekic acid was kindly provided by the Bagian Medisch Chenmie Fakultas Kedokteran Vrije Universitas (V.U.), Amsterdam, The Netherlands. All other reagents were of analytical-reagent grade.

Table 1 Conditions for the determination of bongkrekic acid in toxoflavin

Sample	Order of derivative	Scan speed/ nm min^{-1}	Scan range/ nm	Slit-width/ nm
Bongkrekic acid	First derivative	100	360–270	1
Toxoflavin	First derivative	100	330–240	1

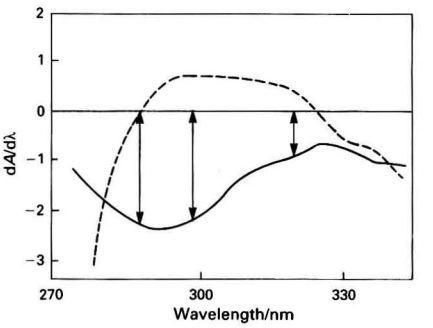

Fig. 2 First-derivative spectra of bongkrekic acid (solid line) and toxoflavin (broken line)

Preliminary Extraction of the Culture of *Pseudomonas farinofermentans*

A 50 ml volume of the culture, which had been incubated for 48 h, was taken and sufficient solid ammonium sulphate was added in order to obtain a saturated solution. The solution was filtered and 5 g of sodium chloride were added to the filtrate. Exactly 20 ml of the filtrate were taken and the pH was adjusted to 7–8 with sodium hydroxide (1 mol dm^{-3}).[5] The filtrate was extracted twice with half its volume of light petroleum (b.p. range, 40–60 °C) after which the pH of the aqueous phase was adjusted to 2–3 with hydrochloric acid (1 mol l^{-1}). The aqueous phase was then extracted with three 20 ml portions of chloroform. The chloroform extracts were combined and the volume was made up to exactly 100 ml with chloroform.

Selection of Experimental Conditions

Solvent

At pH 2, bongkrekic acid and toxoflavin can be extracted simultaneously into chloroform. The extract was analysed by derivative spectrophotometry. The experimental stability and linearity range can meet the requirement of the determination. The conditions used for the determination of bongkrekic acid and toxoflavin are given in Table 1.

Determination of bongkrekic acid

The first-derivative spectra of bongkrekic acid and toxoflavin are shown in Fig. 2. Based on the derivative spectrum of bongkrekic acid, two wavelengths, the measured wavelength combination λ_i and the reference wavelength combination λ_j, were chosen at the peak and valley, respectively, of the derivative spectrum of the interfering constituent, toxoflavin. Different concentrations of toxoflavin were scanned in order to obtain its first-derivative spectrum. The measured wavelength combination λ_i, 290 and 300 nm, and the reference

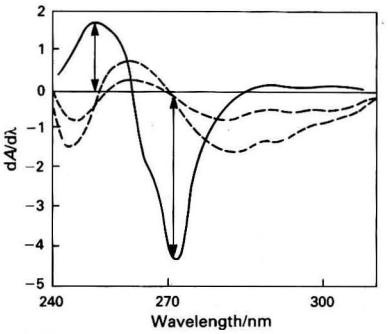

Fig. 3 First-derivative spectra of toxoflavin (solid line) and bongkrekic acid (broken lines)

Table 2 Linearity ranges and minimum measuring concentrations of bongkrekic acid and toxoflavin

Bongkrekic acid*		Toxoflavin	
Concentration/ μg ml^{-1}	ΔDc	Concentration/ μg ml^{-1}	ΔDc
2.65	1.66	2.24	2.50
3.98	2.73	4.48	5.38
4.77	3.37	6.72	8.27
5.30	3.82	7.84	9.73
6.63	4.85	8.96	11.2
7.95	5.92	11.2	14.1
9.28	6.99	13.4	16.9
Linearity range (μg ml^{-1}):			
2.65–9.28		2.24–13.4	
Minimum measuring concentration (μg ml^{-1}):			
2.65		2.24	
Regression equation:			
c(μg ml^{-1}) = 1.245 × ΔDc + 0.574 (r = 0.9999)		c(μg ml^{-1}) = 0.7735 × ΔDc + 0.311 (r = 0.9999)	

* K = 1.65.

wavelength combination λ_j, 320 nm, were chosen at the zero-crossing point and at the flat region of the derivative curves where the derivative curve of bongkrekic acid exhibits a maximum. Based on the derivative values for different concentrations of toxoflavin at the wavelengths stated above, the value of K was calculated according to eqn. (4); $K = D^{TOX}_{290,300}/(D^{TOX}_{320})$, the average value being K = 1.65 (n = 5) (RSD = 0.32%). The linear combination derivative value of bongkrekic acid, $\Delta Dc^{BON} = D^{BON}_{290,300} - 1.65D^{BON}_{320}$, was utilized to determine bongkrekic acid.

Determination of toxoflavin

As shown in Fig. 3, the measured wavelength λ_i and the reference wavelength λ_j were chosen at the zero-crossing points, 252 and 272 nm, respectively, of the derivative curve of bongkrekic acid, the interfering constituent. Calculation could be carried out directly according to the linear combination derivative values of the two wavelengths of toxoflavin. The eqn. $\Delta Dc = D^{TOX}_{252} - D^{TOX}_{272}$ was utilized to determine toxoflavin. [Note: the value of D^{TOX}_{272} was negative.]

Linearity ranges and minimum measuring concentrations are shown in Table 2.

Recovery Study and Sample Analysis

A synthetic mixture of bongkrekic acid and toxoflavin was prepared. The ratio of bongkrekic acid to toxoflavin was fixed so that it corresponded to the ratio found in the metabolites produced by *Pseudomonas farinofermentans*. After treating the solution as described under Preliminary Extraction of the Culture of *Pseudomonas farinofermentans*, an appropriate amount of the chloroform solution was taken and made up to exactly 100 ml with chloroform. Recoveries were calculated according to the regression equation. The results are presented in Table 3.

Table 3 Recovery of bongkrekic acid and toxoflavin

	Bongkrekic acid			Toxoflavin		
No.	Added/ μg ml^{-1}	Found/ μg ml^{-1}	Recovery (%)	Added/ μg ml^{-1}	Found/ μg ml^{-1}	Recovery (%)
1	3.56	3.55	99.58	4.48	4.52	100.9
2	3.56	3.53	99.21	4.48	4.43	98.87
3	3.56	3.57	100.3	5.60	5.66	101.1
4	4.87	4.87	100.0	5.60	5.59	99.87
5	4.87	4.91	100.9	7.91	7.80	98.56
6	4.87	4.81	98.7	7.91	7.89	99.75
7	5.20	5.21	100.2	7.91	8.01	101.3
8	5.20	5.26	101.1	10.32	10.28	99.58
9	6.43	6.36	98.97	10.32	10.49	101.6
10	6.43	6.49	100.9	10.32	10.34	100.2
Mean	99.99 ± 0.85% (RSD)			100.17 ± 1.03% (RSD)		

Table 4 Simulated data for the linear combination derivative spectrophotometric method

Di	$D\lambda_1$	$D\lambda_2$	$D\lambda_3$
Di_a	2.5	−2.5	2.5
Di_b	1.0	1.0	1.0

Sample analysis

A 20 ml volume of *Pseudomonas farinofermentans* culture was taken and treated as described under Preliminary Extraction of the Culture of *Pseudomonas farinofermentans*. The remainder of the procedure was the same as that described under Recovery Study. As the concentration of toxoflavin was relatively low, the standard additions method was adopted. The content of bongkrekic acid was 60–80 μg ml^{-1} and that of toxoflavin 16–18 μg ml^{-1}. Six different culture samples were analysed.

Discussion

Based on previous work,[6,7] an analytical calculation method for analysing the quantitative information on a mixed system by utilizing the combination of derivative spectrophotometry and mathematical treatment has been developed here. By using this method, binary mixtures in which the spectra of the constituents interfere with each other to such an extent that the direct use of derivative spectrophotometry is not possible, can be analysed. In addition, the resolution and the adaptability of the spectra are enhanced.

In comparison with an ultraviolet spectrum, a derivative spectrum has advantages such as the distinct increase of specific absorption peaks, the presence of positive and negative values above and below the baseline, the formation of a zero-crossing point where the derivative curve crosses the baseline at a certain wavelength, the formation of a straight line by the elimination of sample turbidity or of the flat region of the spectral curve, *etc.* If all these advantages are used and combined with mathematical analysis, it is possible not only to retain the advantages of a derivative spectrum, but also to maximize the use of quantitative information and to increase the selectivity and the measurement accuracy.

By inspection of an ideal model utilizing eqn. (11), the relationship between the improvement of the accuracy and the number of determination points can be studied.

Suppose that: (*i*) the accuracy of the determination of Di, $\delta i = 0.01$ ($i = 1, 2, 3$); and (*ii*) the derivative spectra of two components a and b are as shown in Fig. 1; their derivative values and data for various determination points are presented in Table 4.

Single-point method. Component a is determined alone [*i.e.*, component b is absent or the contribution of component b is zero (zero-crossing point)]. Take an arbitrary point in the range $D\lambda_1$–$D\lambda_3$:

$$\text{RSD} = \frac{0.01}{2.5} \times 100\% = 0.40\%$$

Two-point combination method. Take an arbitrary point in $D\lambda_1$ and $D\lambda_3$ with $D\lambda_2$, and proceed according to the combination method described above:

$$K = 1.0/1.0 = 1.0$$

$$\Delta Di_a = 2.5 - (-2.5) = 5$$

$$\text{RSD} = \frac{(0.01^2 + 0.01^2)^{\frac{1}{2}}}{5} \times 100\% = 0.28\%$$

Three-point combination method. Take $D\lambda_1$, $D\lambda_3$ and $D\lambda_2$:

$$K = (1.0 + 1.0)/1.0 = 2.0$$

$$\Delta Di_a = 2.5 + 2.5 - 2.0 \times (-2.5) = 10$$

$$\text{RSD} = \frac{(0.01^2 + 0.01^2 + 2.0^2 \times 0.01^2)^{\frac{1}{2}}}{10} \times 100\% = 0.24\%$$

Hence from an inspection of the ideal model it can be seen that the accuracy determined by the three-point combination method is greater than that obtained by either the two-point combination or the single-point method; however, as the number of points used is increased, the extent to which the accuracy can be improved further gradually diminishes. The situation described above exists only under ideal conditions; under normal conditions, provided the wavelength combination was suitable, relatively ideal conditions could also be obtained.

The critical factor in the successful application of the proposed method is the choice of the wavelength combination. As a derivative value can have a positive or negative sign, then, by choosing the appropriate wavelength at which to combine the plus or minus values, it is possible not only to eliminate the interference but also to increase the sensitivity.

It has been shown that the proposed method can be applied successfully to the determination of bongkrekic acid and toxoflavin in the culture of *Pseudomonas farinofermentans*. The method might also be used to determine these two toxins in body fluids or in contaminated foodstuffs such as fermented corn meal and white fungus contaminated with bacteria.

References

1 Chen, G., Huang, X., Liu, W. Z., and Wang, Z., *Ultra-violet and Visible Spectroscopy*, Atomic Energy Press, Beijing, 1980, pp. 207–216 (in Chinese).
2 Research Group for Pathogenesis of Fermented Corn Flour Poisoning, *Zhongguo Yixue Kexueyuan Xuebao*, 1980, **2**, 77.
3 Zhao, N., Wang, C., Li, Z., Wang, F., Lin, L., and Yu, X., *Zhongguo Gonggong Weishong Zazki*, 1987, **6**, 65 (in Chinese).
4 van Damme, P. A., Jahannes, A. G., Cox, H. C., and Berends, W., *Recl. Trav. Chim. Pays-Bas Belg.*, 1960, **79**, 255.
5 Hu, W., Chen, X., Wang, P., Tian, C., Du, C., Meng, H., and Meng, Z., *Weishong Yanjiu*, 1984, **13**, 34 (in Chinese).
6 Lin, L., *Yaoxue Xuebao*, 1988, **23**, 53.
7 Lin, L., *Fenxi Huaxue*, 1990, **18**, 773.

Paper 0/02654I
Received June 13th, 1990
Accepted April 22nd, 1991

Polymer-based Cation-selective Electrodes Modified With Naphthalenesulphonates

Tatsuhiro Okada, Hidenori Hayashi,* Kazuhisa Hiratani, Hideki Sugihara and Naoto Koshizaki
Industrial Products Research Institute, M.I.T.I., Yatabe, Tsukuba, Ibaraki 305, Japan

Polymer-based cation-selective electrodes based on cation exchangers incorporated in electrochemically polymerized pyrrole films deposited on solid electrodes are described. Pyrrole was polymerized anodically on Pt or pyrolytic graphite electrodes from CH_3CN–H_2O mixtures of various proportions together with naphthalenesulphonate compounds as dopants in the polymerized film. The pH was adjusted to 1–2 with $HClO_4$ and polymerization was accomplished by galvanostatic methods. Hence electrodes selective to monovalent cations were prepared. The composition of the CH_3CN–H_2O solvent was found to be an important factor governing the e.m.f. response of the electrodes. X-ray photoelectron spectroscopic analysis revealed that the amount of naphthalenesulphonate relative to polypyrrole varied with the composition of the CH_3CN–H_2O solvent used for the electrochemical polymerization. A sulphur to nitrogen ratio >0.20 was required for a Nernstian response to cationic activities. The monovalent/divalent selectivity was between −2.8 and −3.4, and was most pronounced for the naphthalenetrisulphonate compound. Although there were small differences in the selectivities of the electrodes towards monovalent cations, it might be possible to obtain specific ion selectivities by modification of the polymer films. The possibility of constructing miniaturized cation-selective electrodes by means of an electrochemical procedure was also demonstrated.

Keywords: *Poly(pyrrole) film; cation-selective electrode; electrochemical polymerization; naphthalenesulphonate*

There have been numerous applications of liquid membrane type ion-selective electrodes based on neutral carriers in the analytical and clinical fields, because of the ease of achieving high ion selectivity and sensitivity by the use of specially synthesized ion-ligating compounds.[1,2] In this instance ion-selective membranes, composed of, for example, a poly(vinyl chloride) matrix containing a solvent mediator (plasticizer), ion-selective agents and lipophilic additives, are utilized for detecting specific ions in solution. An electromotive force (e.m.f.) arises across the membrane which separates two solutions with different ionic activities; from this e.m.f. value the activities of the primary ion can be measured even in the presence of other interfering ions in the solution.

However, there are limitations with this type of electrode because of the number of components required for its construction. For example, the electrode assembly typically has the following composition: inner reference electrode (*e.g.*, Ag–AgCl) | inner solution of constant ionic activity ‖ ion-selective membrane ‖ test solution | outer reference electrode (*e.g.*, KCl solution–AgCl–Ag). If the first part of this assembly could be replaced by a solid material so that the composition was: solid electrode | ion-selective layer | test solution | outer reference electrode, then this would be a novel type of construction. In fact, such electrodes were constructed by using solid-state ion conductors for the sensing materials, prior to the development of the neutral carrier based ion-selective electrodes.[1]

Owing to the increasing demands for the application of ion-selective electrodes in the fields of clinical and micro-analytical measurements of ions, the miniaturization of electrodes is attracting considerable interest.[3] In order to accomplish this, coated wire electrodes and ion-selective field effect transistor electrodes are being developed.[4] Another possibility is to form an ion sensing layer on a small tip of material (electron conductor) by chemical methods. This type of electrode has been fabricated for pH sensing electrodes,[5] chloride and perchlorate electrodes,[6,7] glucose sensors, *etc.*,[8] but very few electrodes of this type have been reported for sensing cations of common interest. In this work, electrodes modified with poly(pyrrole) films containing ion-selective compounds were investigated in order to establish a method for preparing polymer-based cation-selective electrodes.

* Present address: Mitsubishi Denki Builtechno Service Company, Arakawa 7-19-1, Tokyo 116, Japan.

Experimental

Solutions for Electrochemical Polymerization of Pyrrole

Solutions of pyrrole (0.06–0.15 mol dm^{-3}) and $(C_2H_5)_4NBF_4$ (0.01 mol dm^{-3}) in CH_3CN as solvent were used for the determination of the optimum conditions for the electrochemical polymerization of the pyrrole film on Pt sheets. The temperature was 25 °C and the pH was adjusted to 1, 3 or 5 with the use of H_2SO_4, CF_3CO_2H or $HClO_4$, respectively.

Solutions (0.01 mol dm^{-3}) of sodium naphthalene-1-sulphonate (1-NSNa), sodium naphthalene-2-sulphonate (2-NSNa), disodium naphthalene-1,5-disulphonate (1,5-NDSNa), disodium naphthalene-2,6-disulphonate (2,6-NDSNa), disodium naphthalene-2,7-disulphonate (2,7-NDSNa) and trisodium naphthalene-1,3,6-trisulphonate (1,3,6-NTSNa) were used instead of $(C_2H_5)_4NBF_4$ as dopants in the poly(pyrrole) film. The solvent was a mixture of CH_3CN and H_2O in various proportions. The pH was adjusted to 1–2 with $HClO_4$.

All the solutions were de-aerated by bubbling nitrogen through them, and were stirred with a magnetic stirrer both before and during the electrolysis, except when the cyclic voltammograms were being recorded.

Electrodes and Electrochemical Polymerization

The electrodes used were Pt, Au (sheets), pyrolytic graphite (basal plane), Ta, Mo, W, Ir, Ni, Sn, Ag and In (bars or wires). The area of the electrodes exposed to the electrolytes was less than 0.5 cm^2. The electrodes were polarized by a potentiostat (Nikko Keisoku DPGS-1), together with a voltage scanner (Hokuto Denko HB-103) and a coulometer (Hokuto Denko HF-201). Cyclic voltammograms were obtained at a scan rate of 0.1 V s^{-1}. For the anodic polymerization of the pyrrole film, the current was applied galvanostatically for a fixed number of coulombs to the electrodes. The potentials of the electrodes were measured against an Ag–AgCl reference electrode in the same solution.

Characteristics of the Polymer Modified Electrodes

Electrodes coated with poly(pyrrole) films (amount of charge: 2.88 C cm^{-2} at 8×10^{-4} A cm^{-2}) were conditioned for 2 h in 1×10^{-2} mol dm^{-3} LiCl solution. The response of the electrodes to solutions of alkali and alkaline earth metal chlorides was measured using an automated testing apparatus.[9] The electrochemical system used for the e.m.f. measurements was assembled as follows: Pt | poly(pyrrole) film | test solution | 0.1 mol dm^{-3} NH_4NO_3 | saturated KCl–AgCl–Ag.

The composition of the poly(pyrrole) films deposited on Pt sheets by passing a charge of 2.88 C cm^{-2} at 8×10^{-4} A cm^{-2} was analysed with an X-ray photoelectron spectroscopic analyser [Physical Electronics; target, Mg(Kα); acceleration voltage, 10 kV; current, 40 mA]. Also, for the determination of the bulk composition of the films, the surfaces were sputtered with Ar^+ ions and then analysed by *X*-ray photoelectron spectroscopy (XPS). In experiment 1, Ar^+ sputtering was conducted at a current density of 1×10^{-7} A cm^{-2} for 10 min (total dose 4×10^{14} ions cm^{-2}) and in experiment 2, at a current density of 1×10^{-6} A cm^{-2} for 10 min (total dose 4×10^{15} ions cm^{-2}), following the sputtering in experiment 1.

Results

Cyclic Voltammograms of Pyrrole Polymerization

The cyclic voltammograms of Pt in pyrrole–CH_3CN solutions with the anionic dopant $(C_2H_5)_4NBF_4$ are shown in Figs. 1 and 2 over potential ranges of 0.0–0.6, 0.0–0.8 and 0.0–1.0 V *versus* Ag–AgCl; The poly(pyrrole) film started to be deposited at potentials greater than 0.8 V *versus* Ag–AgCl, with a marked increase in the current in the voltammograms.

The pH of the solution had a marked effect on the characteristics of the film; the adherence of the film and the extent of deposition were more pronounced at lower pH values. The concentration of pyrrole monomer in the solution was also an important factor in the extent of polymerization as indicated by an increase in the current; however, above 0.1 mol dm^{-3} the effect was not significant in the tested range 0.06–0.15 mol dm^{-3} pyrrole. Of the acids (H_2SO_4, CF_3CO_2H and $HClO_4$) used for pH adjustment, $HClO_4$ proved to be the most suitable for deposition of a thick film and for good e.m.f. response of the electrodes. Hence, a 0.1 mol dm^{-3} pyrrole solution adjusted to pH 1–2 with $HClO_4$ was used as the standard solution for electrochemical polymerization.

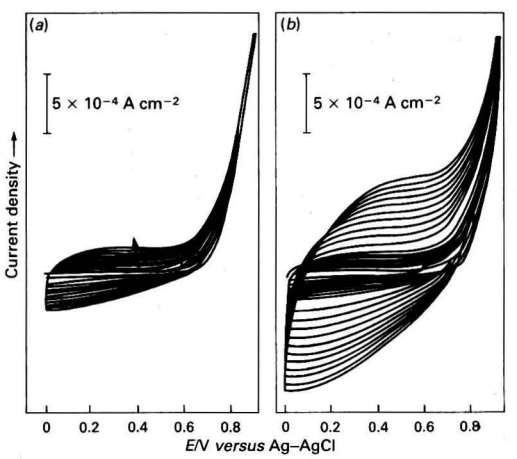

Fig. 1 Cyclic voltammograms of Pt in pyrrole–CH_3CN solutions. The 0.0–0.6, 0.0–0.8 and 0.0–1.0 V scans are superimposed. Composition of the solution: $(C_2H_5)_4NBF_4$, 0.01 mol dm^{-3}; pyrrole: (*a*) 0.06 and (*b*) 0.10 mol dm^{-3}, pH adjusted to 1 with $HClO_4$. The arrow shows the increase in the current during the potential sweep

The electrode material also affected the characteristics of the deposited film. Of the materials tested, Pt, pyrolytic graphite and Ta were found to be the most suitable for deposition of the poly(pyrrole) film and also the e.m.f. response, as shown below. The other materials, except for Au, did not exhibit good adherence to the film, and corrosion of the substrates was observed in acidic pyrrole solutions. It appears that the substrate needs to be chemically stable and also adhesive to the deposited films.

Cyclic voltammograms of Pt over the potential range 0.0–0.8 V *versus* Ag–AgCl in 0.01 mol dm^{-3} 1-NSNa and 0.1 mol dm^{-3} pyrrole solutions at pH 1 are shown in Fig. 3 for

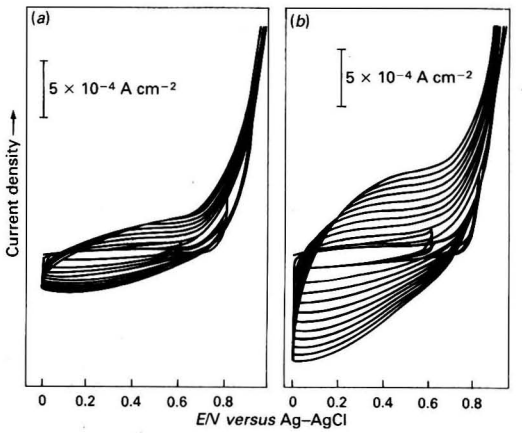

Fig. 2 Cyclic voltammograms of Pt in pyrrole–CH_3CN solutions. The 0.0–0.6, 0.0–0.8 and 0.0–1.0 V scans are superimposed. Composition of the solution: $(C_2H_5)_4NBF_4$, 0.01 mol dm^{-3}; pyrrole, 0.15 mol dm^{-3}, pH adjusted to (*a*) 3 and (*b*) 1 with $HClO_4$

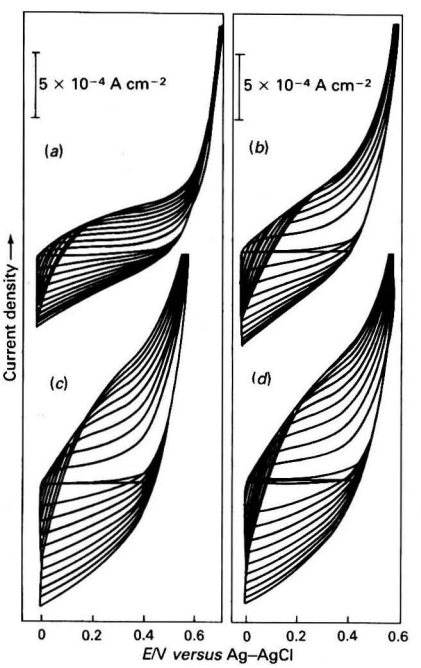

Fig. 3 Cyclic voltammograms of Pt at 0–0.8 V *versus* Ag–AgCl in 0.01 mol dm^{-3} 1-NSNa and 0.10 mol dm^{-3} pyrrole solutions with CH_3CN–H_2O as the solvent. CH_3CN–H_2O: (*a*) 100 + 0; (*b*) 90 + 10; (*c*) 70 + 30; and (*d*) 50 + 50. The pH was adjusted to 1 with $HClO_4$

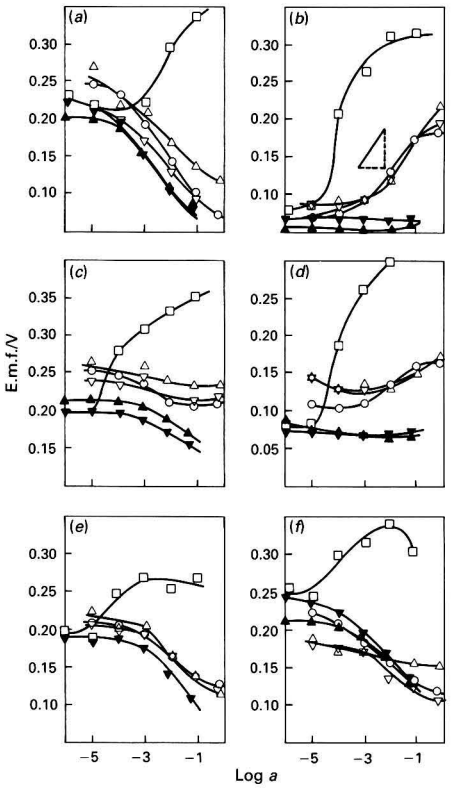

Fig. 4 E.m.f. response of electrodes composed of poly(pyrrole) films deposited on Pt from 0.01 mol dm^{-3} 1-NSNa and 0.10 mol dm^{-3} pyrrole solutions with various proportions of CH_3CN–H_2O as the solvent. CH_3CN–H_2O: (*a*) 100 + 0; (*b*) 90 + 10; (*c*) 70 + 30; (*d*) 50 + 50; (*e*) 30 + 70; and (*f*) 0 + 100. The triangle [in (*b*)] shows the slope of Nernstian response for monovalent cations. Log *a* is the log of the activity of metal ions. □, H^+; △, Li^+; ▽ Na^+; ○, K^+; ▲, Mg^{2+}; and ▼, Ca^{2+}

CH_3CN–H_2O solvent mixtures of various proportions. It appears that 1-NSNa also acts as a dopant in the poly(pyrrole) film. Deposition of the film started to occur at potentials greater than 0.8 V for all the solutions tested, and the current increased slightly as the proportion of H_2O in the CH_3CN–H_2O solvent mixture increased. However, the e.m.f. characteristics of the electrodes are not merely determined by the amount of film deposited, as will be shown below.

E.m.f. Characteristics of the Electrodes

Pyrrole was polymerized by a galvanostatic method on Pt sheets from various types of solutions containing pyrrole and a naphthalenesulphonate. In most instances the current density was 8.0×10^{-4} A cm^{-2} and the amount of charge passed was 2.88 C cm^{-2}. The current density was fixed to give an electrode potential more positive than 0.8 V, as described above. The pH was adjusted to 1–2 with $HClO_4$. Smooth, black films were deposited on the surface of Pt electrodes. The thickness of the films under these conditions was greater than 30 μm. The e.m.f. response of cells containing Pt electrodes coated with poly(pyrrole) films deposited from 0.01 mole dm^{-3} 1-NSNa and 0.1 mol dm^{-3} pyrrole solutions with various proportions of CH_3CN–H_2O as the solvent is shown in Fig. 4.

A Nernstian response to the activities of cations was obtained only over a very limited range of CH_3CN–H_2O solvent compositions, the optimum being CH_3CN–H_2O (90 + 10). In this instance the monovalent/divalent cation selectivity (log $k^{pot}_{Na/Mg}$) was −2.8. For other proportions of CH_3CN–H_2O, the responses were sub-Nernstian, except for the H^+ ion. In some instances, the electrodes showed responses to chloride ions with negative slopes in the e.m.f. *versus* log *a* curves (see also reference 6). The response time of the electrodes to the change in ionic concentration was 10–20 s; the e.m.f. values attained were stable for more than 10 min. The electrodes showed good reproducibility for repeated e.m.f. measurements. The drift in the electrode potentials was about 5 mV d^{-1}. The current density and the total charge for electrochemical polymerization had very little influence on the e.m.f. characteristics of the electrodes, as far as the black film was concerned. A similar result was found when pyrolytic graphite was used as the substrate for the polymerization of pyrrole, as shown in Fig. 5. A bare Pt sheet, bare pyrolytic graphite and a poly(pyrrole) film deposited on these materials using $(C_2H_5)_4NBF_4$ as a dopant did not exhibit a Nernstian reponse. The compound 2-NSNa also showed the same e.m.f. characteristics as 1-NSNa.

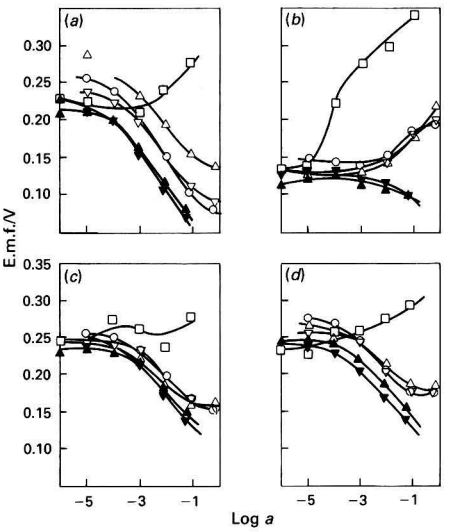

Fig. 5 E.m.f. response of electrodes composed of poly(pyrrole) films deposited on a basal plane of pyrolytic graphite from 0.01 mol dm^{-3} 1-NSNa and 0.10 mol dm^{-3} pyrrole solutions with various proportions of CH_3CN–H_2O as the solvent. CH_3CN–H_2O: (*a*) 100 + 0; (*b*) 90 + 10; (*c*) 80 + 20; and (*d*) 70 + 30. Log *a* is the log of the activity of metal ions. Symbols as identified in Fig. 4

When a disodium naphthalenedisulphonate was used instead of 1-NSNa, the range of CH_3CN–H_2O solvent compositions over which a Nernstian response was obtained was wider than that for 1-NSNa. This is shown for 2,7-NDSNa in Fig. 6. The monovalent/divalent cation selectivity (log $k^{pot}_{Na/Mg}$) was −2.8 for the electrodes prepared using CH_3CN–H_2O (90 + 10). The e.m.f. response characteristics of 1,5-NDSNa and 2,6-NDSNa were similar to those of 2,7-NDSNa.

The naphthalenetrisulphonate derivative, 1,3,6-NTSNa, showed the best e.m.f. response compared with the mono- and disulphonate derivatives. This is shown in Fig. 7. The monovalent/divalent cation selectivity (log $k^{pot}_{Na/Mg}$) was −3.4 for the electrodes prepared using CH_3CN–H_2O (90 + 10). The Nernstian response increased in the order monosulphonate < disulphonate < trisulphonate derivatives of naphthalene.

Composition of the Polypyrrole Film

The poly(pyrrole) films deposited on Pt sheets from a 0.01 mol dm^{-3} 1-NSNa and 0.1 mol dm^{-3} pyrrole solution and a

1,3,6-NTSNa and 0.1 mol dm^{-3} pyrrole solution in three CH_3CN–H_2O solvent mixtures of different composition were analysed by XPS. A typical spectrum is shown in Fig. 8. From a window analysis of the X-ray photoelectron spectroscopic peaks, the atomic concentration of C, O, N, S in the pyrrole films was calculated. The results are shown in Table 1. Also, the atomic concentration in the bulk of the two different films containing 1-NSNa or 1,3,6-NTSNa is shown in Fig. 9. Compared with the composition at the outermost surface of the poly(pyrrole) films, the atomic concentration of C was higher in the bulk of the films, whereas that of the other elements was lower. However, the sulphur to nitrogen (S : N) ratio was almost constant or somewhat higher in the bulk of the films compared with that at the surface.

Discussion

By comparing the results in Table 1 and Fig. 9 with the e.m.f. response of the electrodes, the following conclusions can be drawn. (1) The amount of S in the poly(pyrrole) film is greater

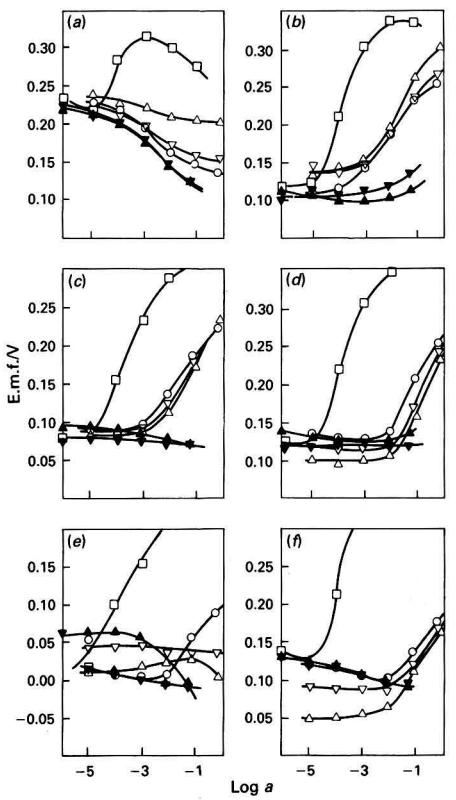

Fig. 6 E.m.f. response of electrodes composed of poly(pyrrole) films deposited on Pt from 0.01 mol dm^{-3} 2,7-NDSNa and 0.10 mol dm^{-3} pyrrole solutions with various proportions of CH_3CN–H_2O as the solvent. CH_3CN–H_2O: (*a*) 100 + 0; (*b*) 90 + 10; (*c*) 70 + 30; (*d*) 50 + 50; (*e*) 30 + 70; and (*f*) 0 + 100. Log *a* is the log of the activity of the metal ions. Symbols as identified in Fig. 4

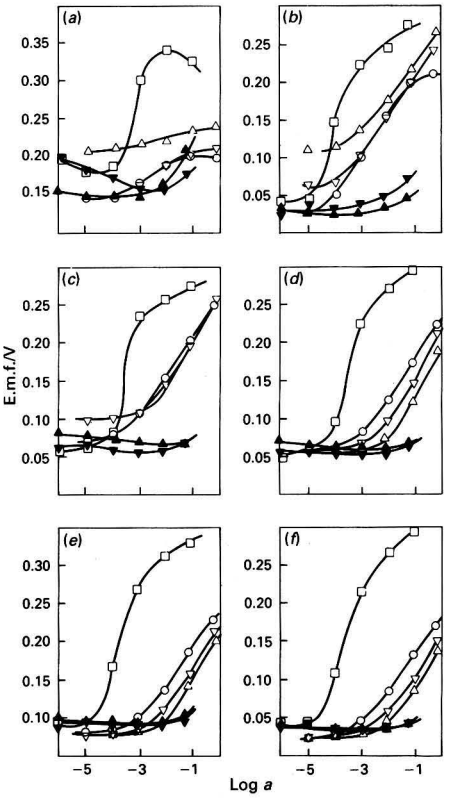

Fig. 7 E.m.f. response of electrodes composed of poly(pyrrole films) deposited on Pt from 0.01 mol dm^{-3} 1,3,6-NTSNa and 0.10 mol dm^{-3} pyrrole solutions with various proportions of CH_3CN–H_2O as the solvent. CH_3CN–H_2O: (*a*) 100 + 0; (*b*) 90 + 10; (*c*) 70 + 30; (*d*) 50 + 50; (*e*) 30 + 70; and (*f*) 0 + 100. Log *a* is the log of the activity of the metal ions. Symbols as identified in Fig. 4

Table 1 Atomic concentrations of C, O, N and S in poly(pyrrole) films deposited on Pt. Analysed by XPS peak height sensitivities. Values in parentheses were determined by peak area sensitivities obtained using XPS

		Atomic concentration (%)				Atomic ratio,
Dopant	CH_3CN–H_2O	C	O	N	S	S : N
1-NSNa	90 + 10	75.1	15.1	7.7	2.1	0.27
		(75.3)	(18.0)	(5.4)	(1.3)	(0.24)
	50 + 50	79.4	13.8	5.9	0.8	0.14
		(77.9)	(16.7)	(4.6)	(0.8)	(0.17)
	0 + 100	78.4	11.2	8.8	1.6	0.18
		(78.2)	(14.5)	(5.9)	(1.4)	(0.24)
1,3,6-NTSNa	90 + 10	76.5	13.0	8.5	2.0	0.24
		(76.8)	(15.8)	(6.0)	(1.3)	(0.22)
	50 + 50	72.7	14.3	10.7	2.3	0.21
		(74.9)	(16.5)	(6.9)	(1.7)	(0.25)
	0 + 100	68.7	18.1	10.1	3.1	0.31
		(71.1)	(18.3)	(8.1)	(2.5)	(0.31)

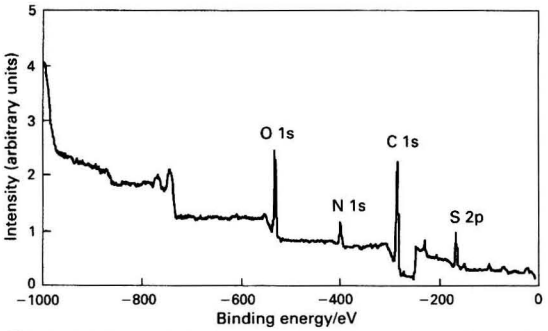

Fig. 8 X-ray photoelectron spectroscopic spectrum of a poly(pyrrole) film deposited from 0.01 mol dm^{-3} 1,3,6-NTSNa and 0.10 mol dm^{-3} aqueous pyrrole solutions. pH, 1–2 ($HClO_4$); CH_3CN–H_2O, 0 + 100; electrode, Pt; and charge passed, 2.88 C cm^{-2}

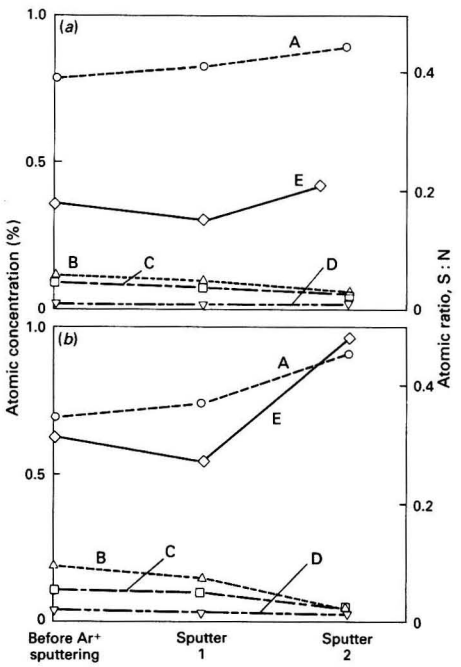

Fig. 9 Atomic concentrations and S : N ratios for poly(pyrrole) films before and after sputtering with Ar^+ (see under Experimental). A, C; B, O; C, N; D, S; and E, S/N. (*a*) Poly(pyrrole) film deposited on Pt from 0.01 mol dm^{-3} 1-NSNa and 0.10 mol dm^{-3} pyrrole aqueous solutions. (*b*) Poly(pyrrole) film deposited on Pt from 0.01 mol dm^{-3} 1,3,6-NTSNa and 0.10 mol dm^{-3} pyrrole aqueous solutions

for the 1,3,6-NTSNa doped film than for the 1-NSNa doped film. (2) For the 1-NSNa doped film, the highest S : N ratio is obtained when CH_3CN–H_2O (90 + 10) is used as the solvent, whereas for the 1,3,6-NTSNa doped film the highest S : N ratio is obtained for films deposited from H_2O. (3) In all instances, the electrodes show a Nernstian response when the S : N ratio on the surface of the poly(pyrrole) film is >0.20.

It appears that the density of the sulphonic acid groups in the film plays an important role with respect to the e.m.f. characteristics of the electrodes. The sulphonic acid groups in the naphthalene compounds could act as anionic counter ions and compensate for the positively charged imino groups in the poly(pyrrole) network. Also, the remaining sulphonic acid groups could form cation-exchange sites for positive ions in the solution. Hence the charge density of the sulphonic acid groups would be a major factor governing the Nernstian response of the electrodes. The compositon of the solvent plays a significant role in determining the inclusion of the naphthalene derivatives in the poly(pyrrole) film during the electrochemical polymerization from electrolyte solutions.

In this work it has been demonstrated that polymer-based cation-selective electrodes can be constructed by electrochemical polymerization methods using solid materials such as Pt and pyrolytic graphite as substrates. Although poly(pyrrole)-based anion-selective electrodes have been prepared successfully by doping chloride or perchlorate ions during electrochemical polymerization,[6,7] very few electrodes of this type selective to cations have been reported. The proposed method offers the possibility of preparing a novel type of polymer-based cation-selective electrode. The method could also be applied to other types of polymers, such as poly(thiophene), poly(aniline), and their derivatives. The salient features of the proposed method for constructing cation-selective electrodes are as follows. (1) Adhesive, flawless films of uniform thickness can be deposited on the surface of solid substrates by electrochemical polymerization. (2) The amount of the ion-selective layer deposited can easily be controlled by controlling the conditions of the electrolysis. (3) The response times of the electrodes are very short in comparison with those of coated wire electrodes, which are typically more than 30 s. (4) Miniaturized electrodes could easily be constructed by using tips or fibres as substrate materials.

Specific cation selectivities could be studied further by modifying the polymer films with dopants which have specific ligating abilities towards such cations. Further investigations in this area are currently in progress.

The authors thank the Tomoe Kogyo Co. Ltd., Tokyo, for supplying the pyrolytic graphite discs.

References

1 *Ion-Selective Electrodes in Analytical Chemistry*, ed. Freiser, H., Plenum Press, New York, 1978, vol. 1.
2 Ammann, D., Morf, W. E., Anker, P., Meier, P.C., Pretsch, E., and Simon, W., *Ion-Sel. Electrode Rev.*, 1983, **5**, 3.
3 *Ion Measurements in Physiology and Medicine*, eds. Kessler, M., Harrison, D. K., and Hoper, J., Springer-Verlag, Berlin, 1985.
4 *Physical Methods of Chemistry. Volume II: Electrochemical Methods*, eds. Rossiter, B. W., and Hamilton, J. F., Wiley, New York, 1986, ch. 2.
5 Ohnuki, Y., Matsuda, H., Ohsaka, T., and Oyama, N., *J. Electroanal. Chem. Interfacial Electrochem.*, 1983, **158**, 55.
6 Dong, S., Sun, Z., and Lu, Z., *Analyst*, 1988, **113**, 1525.
7 Lu, Z., Sun, Z., and Dong, S., *Electroanalysis*, 1989, **1**, 271.
8 Couves, L. D., and Porter, S. J., *Synth. Met.*, 1989, **28**, C761.
9 Okada, T., Hiratani, K., and Sugihara, H., *Analyst*, 1987, **112**, 587.

Paper 1/00873K
Received February 22nd, 1991
Accepted May 3rd, 1991

Determination of Glutathione at Enzyme-modified and Unmodified Glassy Carbon Electrodes

Chi Hua and Malcolm R. Smyth*
School of Chemical Sciences, Dublin City University, Dublin 9, Ireland
Ciaran O'Fagain
School of Biological Sciences, Dublin City University, Dublin 9, Ireland

The oxidation of the reduced form of glutathione (GSH) was found to occur at a decreased overpotential at a glassy carbon electrode when 1.2 mol dm^{-3} of dipotassium hydrogen phosphate were used as the supporting electrolyte. The resulting current for the oxidation peak of GSH varied linearly over the concentration range 0.16–2.4 mmol dm^{-3} GSH. The reaction between GSH and hydrogen peroxide catalysed by the enzyme GSH-peroxidase (GSH-PX) could be monitored using a glassy carbon electrode with GSH-PX immobilized under a layer of Nafion film.

Keywords: *Reduced glutathione; amperometric biosensor; glutathione peroxidase*

Glutathione exists in the human body in both the reduced (GSH) and oxidized (GSSG) forms and is essential for many metabolic processes.[1] In particular it affords protection against metabolic stresses. Firstly, it can reduce membrane substances such as peroxides and free radicals non-enzymically. Secondly, through the action of glutathione-*S*-transferases, it can be conjugated to xenobiotic or electrophilic compounds thus aiding in their detoxification.[2] Defects in glutathione synthesis and metabolism are associated with disease states in humans, and levels of glutathione and its metabolizing enzymes may be significant in cancer.[3] Glutathione peroxidase (GSH-PX) (glutathione: hydrogen peroxide oxidoreductase, E.C. 1.11.1.9) is found in many animal tissues and is regarded as a major protective system against endogenously and exogenously induced hydrogen and lipid peroxides.[4] The enzymic activity of GSH-PX is the major pathway for the elimination of hydrogen peroxide in red blood cells,[5] which are extremely sensitive to the accumulation of peroxide.[2] It catalyses the reaction between reduced glutathione and hydrogen peroxide (or organic peroxides) resulting in the reduction of the peroxide as follows:

$$2GSH + H_2O_2 \rightarrow GSSG + 2H_2O$$

The enzyme, GSH-PX, possesses an unusual feature, an essential selenocysteine residue. It is an analogue of the amino acid cysteine but contains selenium in place of sulphur.[3,6] The enzyme obtained from beef red blood cells has a relative molecular mass of 85 000 and appears to consist of four identical sub-units, with one atom of selenium in each.[7]

It is important to have suitable analytical methods to follow the reaction process of GSH with hydrogen and lipid peroxides. A variety of electroanalytical methods have been developed for the detection of GSH.[4,8–11] Methods based on mercury electrodes[11] may be undesirable because of their possible toxicity. Reduced glutathione can also be oxidized at bare carbon electrodes; however, inconveniently large working potentials are needed.[8] Modified carbon paste electrodes have therefore been studied in order to reduce the overpotential for the determination of GSH and have shown promise.[8,12] Recently, Wring *et al.*[9] have developed a carbon electrode chemically modified with cobalt phthalocyanine. The modified electrode was found to reduce greatly the overpotential necessary for the oxidation of GSH at the carbon electrode surface.

The overpotential required for the oxidation of GSH can also be reduced by the use of high concentrations of potassium phosphate as the supporting electrolyte, as described in this paper. The reaction of GSH with hydrogen peroxide on a glassy carbon electrode surface immobilized with GSH-PX is also reported.

Experimental

Chemicals and Reagents

All chemicals were of analytical-reagent grade unless stated otherwise. The GSH and GSH-PX were purchased from Sigma, while Nafion (in aliphatic alcohols + 10% water) was purchased from Aldrich. The supporting electrolytes used were prepared with de-ionized water obtained by passing distilled water through a Millipore Milli-Q water purification system.

Apparatus

Differential potential voltammetry (DPV) was performed using an EG&G Princeton Applied Research Model 174A polarographic analyser. A three-electrode cell was employed incorporating either a glassy carbon or a modified glassy carbon electrode plus a saturated calomel (SCE) reference electrode and a platinum wire counter electrode.

Construction of the Electrode

The enzyme-modified electrode was prepared by placing 2 μl of enzyme solution containing GSH-PX at a concentration of 5 mg ml^{-1} onto the surface (3 mm in diameter) of a glassy carbon electrode. After the solution had dried on the surface, 2 μl of a solution containing a suitable concentration of Nafion were applied to the electrode. After the Nafion solution had evaporated to dryness, the electrode was washed with de-ionized water before use.

Voltammetric Procedure

Differential potential voltammetry was first performed on suitable blank solutions, then on solutions containing GSH. The voltammetric conditions were in most instances as follows: initial potential, +0.20 V; scan rate, 10 mV s^{-1}; pulse height, 10 mV; and final potential, 0.95 V.

* To whom correspondence should be addressed.

Results and Discussion

Effect of the Composition of the Electrolyte

The effect of the concentration of phosphate buffers was first investigated in order to optimize the response for GSH at a glassy carbon electrode. It was found that GSH yielded an oxidation peak at +0.51 V when 1.2 mol dm^{-3} dipotassium hydrogen phosphate was used as the electrolyte. A similar response was obtained with saturated disodium hydrogen phosphate as the electrolyte. The response of GSH decreased by 70% when the concentration of dipotassium hydrogen phosphate was decreased to 0.12 mol dm^{-3} and no response was observed when 0.012 mol dm^{-3} disodium hydrogen phosphate was used as the electrolyte. This result indicated that it was essential to have a high concentration of phosphate in the electrolyte in order to obtain the oxidation peak for GSH. Reduced glutathione has been reported previously to be oxidized at glassy carbon electrodes at high working electrode potentials in a medium consisting of 0.1 mol dm^{-3} monochloroacetate (pH 3) and methanol in the proportion of 95 + 5 (% v/v), but the oxidation current was concealed by the background current.[11] The oxidation of GSH at glassy carbon electrodes in concentrated phosphate buffer has not been reported. This system provided a convenient method for the detection of GSH with glassy carbon electrodes. However, a high concentration of phosphate is not desirable for detection following high-performance liquid chromatography because it would be likely to cause high pressure in the column.

Effect of pH on the Response of GSH at the Bare Glassy Carbon Electrode

The effect of pH on the response of GSH at the bare glassy carbon electrode was studied by varying the pH of solutions containing 1.2 mol dm^{-3} dipotassium hydrogen phosphate and 1.6 mmol dm^{-3} GSH. As shown in Fig. 1, the peak current increased when the pH was increased from 6 to 10. Reduced glutathione has been reported to be unstable in alkaline solution as it is easily oxidized.[8] Similarly, the electrochemical oxidation of GSH was also facilitated in high pH medium at glassy carbon electrodes. This is consistent with the results obtained using a carbon electrode modified with cobalt phthalocyanine, as reported by Wring *et al.*[8]

Linearity of Response

The linearity of the response for GSH at the glassy carbon electrode was studied by varying the concentration of GSH in a buffer solution containing 1.2 mol dm^{-3} dipotassium hydrogen phosphate adjusted to pH 9.0. The resulting voltammograms are shown in Fig. 2. A linear response was obtained over the GSH concentration range 0.16–2.4 mmol dm^{-3} with a correlation coefficient of 0.9986, a slope of 33.6 μA mol^{-1} and an intercept on the current axis of −0.00321 μA.

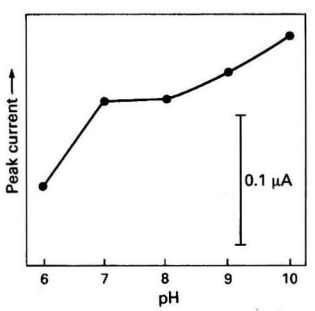

Fig. 1 Effect of pH on the response of GSH at a glassy carbon electrode obtained by analysing solutions containing 1.2 mol dm^{-3} dipotassium hydrogen phosphate and 1.6 mmol dm^{-3} GSH, adjusted to different pH values

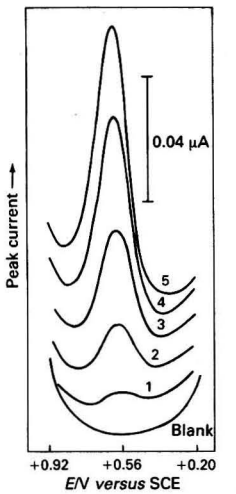

Fig. 2 Voltammograms of GSH obtained by analysing different concentrations of GSH in 1.2 mol dm^{-3} dipotassium hydrogen phosphate adjusted to pH 9.0. 1, 0.158; 2, 0.474; 3, 1.106; 4, 1.738; and 5, 2.370 mmol dm^{-3} GSH in the electrolyte

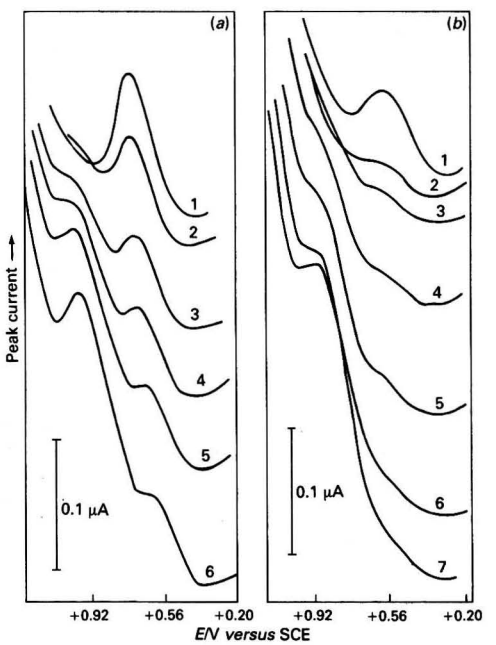

Fig. 3 Reaction of GSH with hydrogen peroxide monitored with a glassy carbon electrode modified with either (*a*) a Nafion film or (*b*) GSH-PX and Nafion. Curve 1, obtained by analysing a sample solution containing 1.2 mol dm^{-3} dipotassium hydrogen phosphate and 2.6 mmol dm^{-3} GSH adjusted to pH 7.0; curves 2–7, successive additions of 4.4 mol dm^{-3} hydrogen peroxide to the sample solution

Modification of a Glassy Carbon Electrode With Glutathione Peroxidase

Different methods of immobilizing GSH-PX onto a glassy carbon electrode were investigated. The GSH-PX solution was first placed on the glassy carbon electrode surface and left to dry. This method was not successful as the GSH-PX on the electrode surface quickly dissolved in the electrolyte solution. A dialysis film was then placed over the enzyme layer on the electrode surface. In this instance, however, no response could be seen for GSH, because GSH could not penetrate through the dialysis film to reach the electrode surface. A film of Nafion was then used to cover the enzyme on the electrode by placing 2 μl of Nafion solution over the enzyme on the electrode surface. After the Nafion solution had dried, the electrode was tested for the determination of GSH. It was found that if the concentrated Nafion solution (as obtained from the supplier) was placed on the electrode surface, no response for GSH appeared. Diluting the Nafion solution 10-fold with water before modification also did not result in a response to GSH. If the Nafion solution was diluted 100-fold with water before being used in the modification process, the oxidation peak for GSH appeared. A thin and even film could be seen on the electrode surface. The Nafion solution was also diluted 300-fold with water before being applied to the electrode surface. In that instance, however, the resulting film was poorly distributed on the electrode surface and contained many large pores. It was found that the Nafion solution diluted 100-fold was the best for the modification. This result indicated that the size of the pores in the Nafion film could be conveniently controlled by suitable dilution of the Nafion solution with water before making the film, so that desired compounds could penetrate the film to reach the electrode surface. This method of modification provides a general way of immobilizing enzymes or some other modifying materials onto an electrode surface, thus providing the system with both size- and charge-selective properties.

Monitoring of Reaction of GSH With Hydrogen Peroxide at Unmodified and Enzyme-modified Electrodes

The reaction of GSH with hydrogen peroxide was investigated by analysing solutions containing 1.2 mol dm^{-3} dipotassium hydrogen phosphate and 2.6 mmol dm^{-3} GSH, to which various concentrations of hydrogen peroxide were added at specified pH values. Modified and unmodified electrodes were both used to monitor changes in the concentration of GSH. At pH 8 and 9, a bare glassy carbon electrode was used to follow the reaction. It was found that on addition of hydrogen peroxide to the solution containing GSH, the peak height of GSH decreased and finally disappeared when more hydrogen peroxide was added, indicating that hydrogen peroxide oxidized GSH chemically at these pH values. At pH 7, when a bare glassy carbon electrode or a glassy carbon electrode covered solely with Nafion film was used, the peak due to GSH remained in spite of the addition of hydrogen peroxide to the GSH solution. When more hydrogen peroxide was added, a peak corresponding to hydrogen peroxide appeared at +0.88 V, while the GSH peak remained constant. If a GSH-PX modified electrode was used at this pH value, the GSH peak rapidly decreased in size on addition of hydrogen peroxide to the GSH solution. After further addition of hydrogen peroxide, the GSH peak disappeared and the peak for hydrogen peroxide appeared (Fig. 3). This result showed that the reaction between GSH and hydrogen peroxide, catalysed by the immobilized GSH-PX at the electrode surface, could be followed with this system.

Conclusion

A much lower overpotential for the oxidation of GSH at a glassy carbon electrode was obtained using a high concentration of dipotassium hydrogen phosphate as the supporting electrolyte. The modification of a glassy carbon electrode with GSH-PX provided a means of monitoring the enzymic reaction of GSH with hydrogen peroxide in aqueous solution.

This work was funded through a grant (SC/90/118) from EOLAS (The Irish Science and Technology Agency) under the Scientific Research Programme.

References

1 Meister, A., *J. Biol. Chem.*, 1988, **263**, 17205.
2 Matthews, C. K., and Van Holde, K. E., *Biochemistry*, Benjamin-Cummings, California, 1990, p. 711.
3 Meister, A., and Anderson, M. E., *Ann. Rev. Biochem.*, 1983, **62**, 711.
4 Wendel, A., *Methods Enzymol.*, 1981, **77**, 325.
5 Cohen, G., and Hochstein, P., *Biochemistry*, 1963, **2**, 1420.
6 Forstrom, J. W., Zakowski, J. J., and Tappel, A. L., *Biochemistry*, 1978, **17**, 2639.
7 Flohe, L., *Ciba Found. Symp.*, 1979, **65**, 95.
8 Wring, S. A., Hart, J. P., and Birch, B. J., *Analyst*, 1989, **114**, 1563.
9 Wring, S. A., Hart, J. P., and Birch, B. J., *Analyst*, 1989, **114**, 1571.
10 Halbert, M. K., and Baldwin, R. P., *Anal. Chem.*, 1985, **57**, 591.
11 Allison, L. A., and Shoup, R. D., *Anal. Chem.*, 1983, **55**, 8.
12 Halbert, K. H., and Baldwin, R. P., *J. Chromatogr.*, 1985, **345**, 43.

Paper 1/01049B
Received March 16th, 1991
Accepted May 10th, 1991

Amperometric Monitoring of Bacteria-induced Milk Acidity Using a Platinum Disc Microelectrode

M. Antonietta Baldo, Salvatore Daniele* and Gian A. Mazzocchin
Department of Physical Chemistry, University of Venice, Calle Larga S. Marta, 2137, 30123 Venice, Italy
Marco Donati
Direzione Scientifica, Parmalat SpA, Parma, Italy

The acidity induced by the action of bacteria in milk samples was monitored amperometrically by using a platinum microelectrode. The measurements were performed directly on commercial packs of milk, stored at 32 °C, and were continued for 9–10 d after inoculation. The data were compared with those obtained by measuring the pH of the samples and the results are discussed on the basis of the metabolism of each bacterial species. The effects of the following bacteria were examined: *Staphylococcus aureus, Bacillus cereus, Streptococcus faecalis, Bacillus subtilis, Aeromonas, and Corynebacterium.*

Keywords: *Microelectrode; milk; acidity; bacteria; amperometry*

Numerous micro-organisms, predominantly bacteria, can proliferate in milk, thus changing its properties.[1] In particular, bacterial fermentation can cause the production of some acids, such as lactic and acetic acids.

Bacterial growth and action in milk can be either deliberately induced under controlled conditions, as in the manufacture of fermented products, or undesired, and the production of acids can cause sourness.

The acidity induced by the microbic contamination of milk supplies coming from farms is normally determined by measuring the pH of the milk, and a parallel microbiological test is also performed in order to determine the bacterial population.

The buffering action of the numerous acidic and basic groups present in milk often leads to a negligible pH change, when, for instance, the amount of acids produced is low. Hence the determination of the amount of acids formed, instead of the pH, should, in principle, be a more sensitive method for measuring the change in the acidity of the medium. A useful parameter for this purpose is the titrable acidity of milk.[2]

It has recently been shown[3] that it is possible to measure the acidity of milk samples amperometrically by using a platinum microelectrode. In the present paper this method was used to monitor the change in the titrable acidity of milk caused by the presence of bacteria in the milk samples; the data obtained were compared with those obtained by pH measurements.

The effect of the following bacterial species on the change in acidity was examined: *Staphylococcus aureus, Bacillus cereus, Streptococcus faecalis, Bacillus subtilis, Aeromonas* and *Corynebacterium*.[4]

Experimental

Electrodes and Instrumentation

In order to prepare the microelectrode, a platinum wire of diameter 25 μm was sealed directly in glass as reported previously.[5] Prior to each measurement, the electrode was polished with graded alumina powder (down to 0.05 μm) on a polishing microcloth. The reference electrode used was a saturated calomel electrode.

The experiments with the platinum microelectrode were carried out in a two-electrode cell configuration maintained in a Faraday cage made of sheets of aluminium to avoid external noise. Linear sweep and cyclic voltammetric waves were generated by a Princeton Applied Research 175 function generator; a Keithley Model 485 picoammeter served as a current-measuring device, and data were plotted with a Hewlett-Packard 7045 B *x–y* recorder.

A Metrohm 605 pH-meter was employed for pH measurements.

The samples were kept at 32 °C in a Memmert thermostatic oven until required for measurement.

Samples and Procedure

Bovine milk samples were kindly provided by Parmalat (Parma, Italy). The analyses were performed directly on the pack containing the milk; the electrodes were inserted into the pack through an appropriate hole made immediately before the analysis.

Contaminated samples were prepared by inoculation, under aseptic conditions, of a number of different mesophyll facultatively anaerobic bacterial species (*Staphylococcus aureus, Bacillus cereus, Streptococcus faecalis, Bacillus subtilis, Aeromonas* and *Corynebacterium*) which can contaminate milk supplies.[6] Cell concentrations for each micro-organism were adjusted to a target range of 10–100 colony-forming units (cfu) per 0.5 l of milk. The inoculated milk samples were then stored for 9–10 d at 32 °C, which are typical favourable conditions for bacterial growth.

For each experimental datum at least three replicates both for current and pH measurements were performed on two samples of the same stock of milk.

Results and Discussion

Principle of the Amperometric Method

The amperometric method is based on the determination of the current of peak (1) in Fig. 1, which can be recorded in milk samples with a platinum disc microelectrode at scan rates lower than 10 mV s^{-1}. The reduction mechanism occurring at this peak has been studied in detail elsewhere;[3] it involves a sequence in which both the preceding and following chemical reactions are associated with the transfer of electrons. The mechanism proposed is as follows:

$$H_nA\text{–}M \rightleftharpoons H^+ + H_{(n-1)}A\text{–}M$$

$$H_2PO_4^- \rightleftharpoons H^+ + HPO_4^{2-}$$

$$H^+ + e^- \rightleftharpoons \tfrac{1}{2}H_2$$

$$H_2PO_4^- + Ca^{2+} \rightleftharpoons CaHPO_4(s)$$

$$2HPO_4^{2-} + 3Ca^{2+} \rightleftharpoons Ca_3(PO_4)_2(s) + 2H^+$$

* To whom correspondence should be addressed.

where H_nA is the generic acid interacting with the micellar aggregate M present in the milk. The sparingly soluble $CaHPO_4$ and $Ca_3(PO_4)_2$, formed in competitive equilibria, precipitate onto the electrode surface, thus causing inhibition of the electrode process and giving rise to the peak-shaped wave instead of the expected steady-state limiting current plateau.[7] Moreover, the addition of bases or acids leads to a decrease or increase in peak (1), respectively,[3] as a consequence of acid–base equilibria which take place in the bulk solution, leading ultimately to the formation or dissociation of $H_2PO_4^-$.[3] Consequently, by monitoring the peak (1) height, the variation of the acid concentration in the medium can be measured.

Applications to Contaminated Samples

The acidity induced by bacterial fermentation of ultra-high temperature treated (UHT) sterilized milk samples contaminated deliberately was followed amperometrically for 220 h; the corresponding behaviour of uncontaminated milk samples was taken as a reference.

The results obtained at different times for the peak (1) height and the corresponding pH value, from a series of measurements on reference samples and the contaminated samples, are presented in Table 1. For ease of interpretation of the data, Figs. 2 and 3 show the variation (in %) of the current height of peak (1) and pH with respect to the blanks under the same experimental conditions.

From these data, it can be seen that the sensitivity of the amperometric method is greater than that of the potentiometric method. For instance, data concerning the reference samples[1] reported in Table 1 indicate that after storage for 220 h at 32 °C a moderate increase in the peak height of about 10% is observed, whereas the variation in pH is small. The increment in the acidity of the uncontaminated samples is probably due to changes in composition during storage of the milk at 32 °C, caused by, for instance, the liberation of phosphoric acids from their esters by enzymic action, or the production of free fatty acids by lipolysis, which is known to occur on increasing the temperature of milk.[1]

Inoculated samples produced an increase in acidity in all instances, but to an extent that depended on the products formed from the metabolism of each bacterial species.

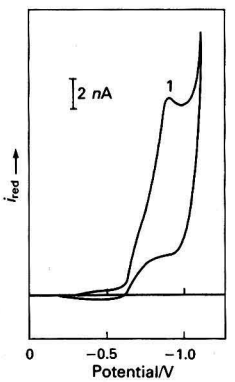

Fig. 1 Cyclic voltammogram recorded at a 25 μm platinum microelectrode on an untreated fresh whole bovine milk sample. Scan rate, 5 mV s^{-1}. For an explanation of peak 1, see text

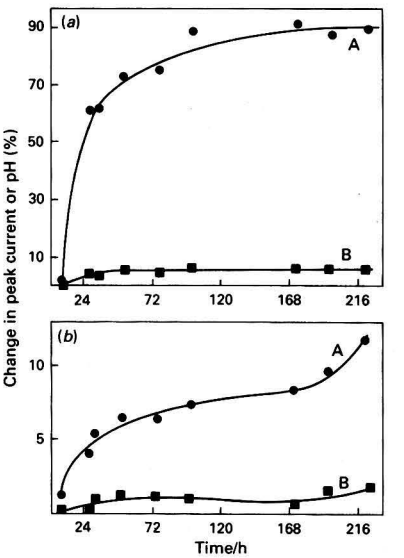

Fig. 2 Variation of A, peak current and B, pH with time for bovine milk samples inoculated with (*a*) *Bacillus cereus* and (*b*) *Staphylococcus aureus* at 32 °C

Table 1 Peak currents ($i \pm 0.1$ nA)* and pH values (±0.01) obtained for bovine milk samples contaminated with different bacterial species under aseptic conditions

	Samples (1) contaminated with:						Samples (2) contaminated with:									
	Reference samples (1)		*Bacillus cereus*		*Staphylococcus aureus*		Reference samples (2)		*Streptococcus faecalis*		*Bacillus subtilis*		*Aeromonas*		*Coryne-bacterium*	
Time/h	*i*/nA	pH	*i*/nA	pH	*i*/nA	pH	*i*/nA	pH	*i*/nA	pH	*i*/nA	pH	*i*/nA	pH	*i*/nA	pH
8	16.1	6.67	16.3	6.67	16.3	6.66	15.1	6.72	15.0	6.72	15.4	6.69	15.2	6.72	15.0	6.72
26	17.0	6.67	27.3	6.41	17.7	6.66	—	—	—	—	—	—	—	—	—	—
31	17.1	6.65	27.7	6.39	18.0	6.60	16.1	6.66	17.0	6.62	16.8	6.63	26.3	6.20	16.2	6.64
50	17.2	6.65	29.5	6.32	18.3	6.58	—	—	—	—	—	—	—	—	—	—
74	17.5	6.64	30.5	6.31	18.6	6.57	16.7	6.65	19.0	6.00	17.6	6.63	28.0	6.16	—	—
98	17.5	6.65	32.8	6.29	18.8	6.58	—	—	—	—	—	—	—	—	—	—
147	—	—	—	—	—	—	17.7	6.64	22.5	5.60	20.3	6.59	30.3	6.14	17.8	6.62
170	17.6	6.63	34.0	6.27	19.3	6.58	—	—	—	—	—	—	—	—	—	—
194	17.6	6.62	33.0	6.28	19.5	6.53	17.8	6.63	28.1	5.48	21.5	6.55	37.0	5.97	19.7	6.62
220	17.5	6.64	33.0	6.27	19.6	6.53	—	—	—	—	—	—	—	—	—	—

* Average values obtained from five replicates (relative standard deviation <1.5%).

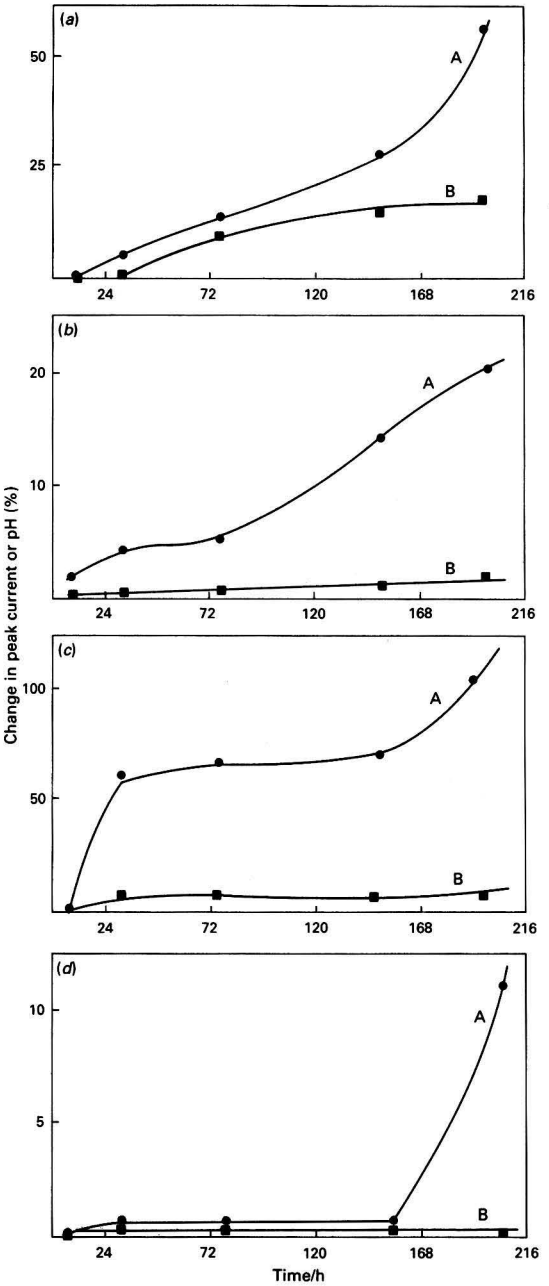

Fig. 3 Variation of A, peak current and B, pH with time for bovine milk samples inoculated with (*a*) *Streptococcus faecalis*; (*b*) *Bacillus subtilis*; (*c*) *Aeromonas*; and (*d*) *Corynebacterium* at 32 °C

Bacillus cereus is known to produce, among other species, phospholipase C, which hydrolyses phosphoglycerides leading to the formation of phosphoric acids.[8,9] *Streptococcus faecalis* degrades carbohydrates, particularly D-gluclose, through homolactic fermentation, yielding lactic acid as the sole end product.[8,9] These characteristics explain the large increase in the peak current (1) and the corresponding decrease in pH observed in the presence of these two types of micro-organism, as shown in Table 1 and Figs. 2(*a*) and 3(*a*). Data obtained for *Bacillus cereus* indicate a higher activity with respect to *Streptococcus faecalis* in relation to the amount of acids produced, whereas the decrease in the pH does not correspond to the rate at which the acids are formed. A possible explanation for this behaviour is that the mixture of phosphoric acids, such as, for instance, $H_2PO_4^-$ and HPO_4^{2-}, produced by *Bacillus cereus*, might act as a buffer system. This would lead to a smaller pH change in these milk samples compared with those contaminated with *Streptococcus faecalis* which yields lactic acid as the sole product. On the other hand, as shown previously,[3] the increment of the peak current (1) is dependent on the amount of $H_2PO_4^-$ or lactic acid formed regardless of their strength, and is related only to the number of hydrogen ions released in their dissociation, which is one for both species at the pH of milk.

Table 2 Analysis of UHT bovine milk samples 216 h after inoculation with different bacterial species, kept at 4 °C and equilibrated at 32 °C immediately before the measurements

Sample	*i* (±0.1)/ nA	pH (±0.01)
Reference	15.4	6.74
Streptococcus faecalis	15.1	6.72
Bacillus subtilis	15.0	6.72
Aeromonas	14.9	6.70
Corynebacterium	15.0	6.72

More interesting results were obtained when the samples were contaminated with *Staphylococcus aureus* and *Bacillus subtilis*, both of which are proteolytic bacteria and are able to ferment carbohydrates.[10] These characteristics can lead either to the formation of amino acids, nitrogen bases and ammonia, or to the formation of acids such as lactic and butyric acids. These products have different effects on the pH, and the expected result is a small variation in this parameter with respect to the blank. As the production of acids is the predominant process,[8] in agreement with the experimental data obtained here, the peak current (1) increases progressively with time [see Table 1 and Figs. 2(*b*) and 3(*b*)]; however, a significant variation in the current response (about 10–15%) is evident only some 144–192 h after the inoculation.

Similarly, *Aeromonas* are also able to ferment carbohydrates yielding acids,[11] but the simultaneous production of indole from their metabolism attenuates their effect on the pH. This verifies the experimental findings reported here, in that a large increase in the peak current corresponds to a moderate decrease in the pH [see Table 1 and Fig. 3(*c*)].

Corynebacterium is a lipolytic micro-organism[10] exhibiting clearly defined nutritional needs and characterized, under normal conditions, by a very slow growth rate.[8] From the data obtained in the presence of this species [see Table 1 and Fig. 3(*d*)], it can be stated that only the amperometric method provided evidence for the alteration of the sample during the period of analysis (220 h), with an increase in the current of about 11% with respect to the blank, whereas the pH response remained virtually unchanged, with a variation of only 0.1–0.2% (which is within the experimental error). The possibility of having some type of warning sign in this instance is very important from a sanitary point of view, as *Corynebacterium* is recognized as an agent of some of the diseases transmitted by milk, for instance, diphteritis.[8,10]

Influence of the Temperature and the Interaction With the Atmosphere

The growth rate of the bacterial population is governed by various factors, such as the temperature and the oxygen level. Moreover, if the samples come into contact with the environment, other bacteria, apart from those studied here, might contaminate the milk.

Table 3 Peak currents ($i \pm 0.1$ nA),* pH values (±0.01) and their variation (in %) obtained for bovine milk samples contaminated with different bacterial species, kept at 32 °C, under aerobic conditions

					Samples contaminated with:															
	Reference samples				*Streptococcus faecalis*				*Bacillus subtilis*				*Aeromonas*				*Corynebacterium*			
Time/h	*i*/nA	Δ*i* (%)†	pH	ΔpH (%)‡	*i*/nA	Δ*i* (%)†	pH	ΔpH (%)‡	*i*/nA	Δ*i* (%)†	pH	ΔpH (%)‡	*i*/nA	Δ*i* (%)†	pH	ΔpH (%)‡	*i*/nA	Δ*i* (%)†	pH	ΔpH (%)‡
8	15.1	0.00	6.72	0.00	15.0	0.00	6.71	0.00	15.4	0.00	6.69	0.00	14.8	0.00	6.72	0.00	15.0	0.00	6.71	0.00
26	16.6	9.94	6.62	1.50	17.0	13.3	6.52	2.81	16.6	7.80	6.62	1.10	26.0	75.7	6.28	6.46	16.4	9.30	6.64	1.10
56	18.3	21.2	6.56	2.44	25.0	66.7	5.55	17.3	70.0	354	4.44	33.6	39.3	165	5.57	17.1	23.8	58.7	6.28	6.38
75	32.3	114	5.56	17.3	44.0	193	4.91	26.9	89.5	481	4.32	35.4	86.5	484	4.48	33.2	26.2	74.7	6.17	8.00
146	102	579	4.41	34.3	70.0	367	4.54	32.4	91.0	491	4.39	34.4	85.0	474	4.51	33.0	82.5	450	4.53	32.5
194	102	579	4.42	34.2	72.0	380	4.49	33.1	91.5	494	4.38	34.5	—	—	—	—	83.5	457	4.52	32.6

* Average values obtained from three replicates (relative standard deviation <1.5%).
† Variation of the peak current with respect to the initial value.
‡ Variation of the pH value with respect to the initial value.

The current (*i*) and pH values obtained for a number of milk samples treated with some of the micro-organisms listed in Table 1, but stored at 4 °C for 216 h, are given in Table 2. At this temperature the inoculated bacteria do not grow to any significant extent and their activity is negligible,[1] in agreement with the experimental results obtained here, the responses found being very close to the initial responses. At this temperature the methods studied are unable to provide evidence for bacterial contamination.

Data for a series of measurements performed on samples inoculated with several different bacteria, kept at 32 °C, are presented in Table 3. A hole was made in the packs in order to allow interaction between the milk and the atmosphere. A large enhancement of the peak current and a corresponding large decrease in the pH was observed for both the reference and the contaminated samples. These values greatly exceed those obtained under aseptic conditions and the variations are not easily predictable. These findings demonstrate that the data reported in Table 1 are not affected by external influences.

In conclusion, an amperometric method based on the use of a microelectrode has been shown to be useful for monitoring the variations in the acidity of milk, caused by microbic contamination; the method appears to be more sensitive than the potentiometric method usually applied for this purpose. Moreover, as the use of microelectrodes generally leads to a simplification of the instrumentation and requires small volumes for the analysis,[7] miniaturization of the apparatus should be possible.

The authors thank D. Rudello for skilful experimental assistance. Financial aid from the Italian National Research Council (CNR) is also gratefully acknowledged.

References

1 Walstra, P., and Jenness, R., *Dairy Chemistry Physics*, Wiley, New York, 1984.
2 Egan, H., Kirk, R. S., and Sawyer, R., *Pearson's Chemical Analysis of Foods*, Churchill Livingstone, New York, 1981.
3 Daniele, S., Baldo, M. A., Ugo, P., and Mazzocchin, G. A., *Anal. Chim. Acta*, 1990, **238**, 357.
4 Banwart, G. J., *Basic Food Microbiology*, Van Nostrand Reinhold, New York, 1981.
5 Fleischmann, M., Lasserre, F., Robinson, J., and Swan, D., *J. Electroanal. Chem. Interfacial Electrochem.*, 1984, **177**, 97.
6 Silliker, J. H., Elliott, R. P., Baird-Parker, A. C., Bryan, F. L., Christian, J. H. B., Clark, D. S., Olson, J. C., and Roberts, T. A., *Microbial Ecology of Foods*, Academic Press, New York, 1980.
7 Fleischmann, M., Pons, S., Rolison, D. R., and Schmidt, P. P., *Ultramicroelectrodes*, Datatech, Morganton, 1987.
8 Tiecco, G., *Microbiologia Degli Alimenti di Origine Animale*, Edagricole, Bologna, 1984.
9 Lehninger, A. L., *Biochemistry*, Worth, New York, 1975, p. 291.
10 Vitagliano, M., *Industrie Agrarie*, UTET, Torino, 1976, p. 413.
11 Alais, C., *Scienza del Latte*, Tecniche Nuove, Milan, 1988.

Paper 1/00368B
Received January 25th, 1991
Accepted May 3rd, 1991

Study of Complexation Equilibria Using Polarized Metallic Electrodes

V. F. Vetere and R. Romagnoli*
CIDEPINT, Research and Development Center for Paint Technology, CIC–CONICET, Calle 52 Entre 121 y 122, (1900) La Plata, Argentina

The response of a metallic electrode depends on its chemical nature and on the characteristics of the environment. The response time and the repeatability of the measurements depend on the previous history of the electrode and are determined by its superficial structure. In a very general sense, it can be stated that a metallic electrode seldom acquires the potential predicted by the Nernst equation, because the equilibrium $M^0 \rightleftharpoons M^{z+} + ze^-$ is not easily established at the electrode surface. Here, the response of an anodically polarized electrode was studied in relation to the response time and the repeatability of the measurements; the electrode was then employed to determine stability constants by a procedure described in the literature. In order to be suitable for analytical purposes, an electrode must give fast and reproducible measurements. By polarizing a metallic electrode with low anodic current intensities a fast response time and good repeatability were achieved. The response time was less than 10 s. This procedure enables base metal electrodes to be employed in situations where platinum, mercury or gold electrodes are preferred. In order to determine stability constants, a metallic electrode was chosen (according to the cation of which the complexes were to be studied) and was polarized anodically with different current intensities. The potential of the electrode was recorded for increasing ligand concentrations. This particular technique has some advantages with respect to the most common methodologies currently known. The problem of the dependence of the shape and the position of the polarization curves on the stability constants of the complex ions and the influence of the electrode surface in voltammetric techniques is solved by working at low anodic current intensities and by taking measurements when the electrochemical equilibrium has been reached. The equilibrium $M^0 \rightleftharpoons M^{z+} + ze^-$ is readily achieved at the electrode surface when the electrode is polarized; this represents a considerable advance with respect to potentiometric techniques in general. The total cation concentration does not change during the determination, and depends on the magnitude of the polarizing current. The free ligand concentration virtually coincides with the total ligand concentration because the concentration of cation generated at the electrode/solution interface is about 1×10^{-5} mol dm^{-3}.

Keywords: *Complexation equilibria; polarized metallic electrode; stability constant; potentiometry*

The purpose of the work described here was to develop a potentiometric method employing polarized electrodes which could be applied in the field of electroanalysis. In this particular instance it was used to determine the stability constants of complex ions. Firstly, the response of a metallic electrode polarized with low anodic current densities was studied. In the second stage, the polarized metallic electrode was employed in the above-mentioned potentiometric technique, which, in turn, was applied to the determination of the stability constants of complex ions. The use of polarized metallic electrodes enables the calculation of the formation constants to be simplified. The response of a metallic electrode depends on its chemical nature and on the nature of its environment. The response time and the repeatability of the measurements depend on the previous history of the electrode and are determined by its superficial structure. For this reason, a platinum electrode is preferred to other indicator electrodes in potentiometry. A platinum electrode is inert and does not take part in most chemical reactions. Silver, copper, zinc, cadmium and mercury electrodes can be used in this way but with some limitations. Most metals are not suitable for use as indicator electrodes in potentiometry because the equilibrium $M^0 \rightleftharpoons M^{z+} + ze^-$ is not easily established at the electrode surface.[1] These electrodes, in almost all instances, under practical conditions do not acquire the electrode potential predicted by the Nernst equation.[2] These factors seriously affect the measurements, particularly the potentiometric measurements; however, these electrodes are used for this type of determination because only potential changes related to concentration changes are of interest.[1,2] The difficulties increase as the complexes become weaker and the metal used for the electrode becomes less noble.

Several different treatments can be used to overcome the difficulties mentioned above. Each treatment attempts to generate a definite and reproducible superficial configuration.[3–5] Some are not sufficiently effective whereas others are too complex and laborious to be employed in the field of analytical chemistry.

Voltammetric techniques are often used to study metal–ligand equilibria in solution. The electrode processes must be reversible and the chemical equilibrium fast. The ligand concentration, the stability constants and the nature and state of the electrode surface all affect the shape and position of the peaks in the voltammograms.[4,6–10] The displacement of the waves depends on the ligand concentration in the bulk solution and on the stability constants of the complexes. The ligand concentration must be higher than the metal ion concentration.[11–14] Gampp[15] has developed a technique to calculate stability constants for complex ions at low metal to ligand ratios. This procedure involves application of the least-squares and simulation methods to data obtained from cyclic or linear-sweep voltammetry. Most workers employ a mercury or platinum electrode as these offer advantages with respect to other metallic electrodes.[4,16]

In the work described here, the response of an anodically polarized base metal electrode was studied in relation to the response time and the repeatability of the measurements. Low anodic current densities were employed. In order to be suitable for analytical purposes an electrode must give fast and repeatable measurements. The treatment applied was compared with other treatments, which are reported to yield reproducible surfaces.

Hence, the metallic electrode was polarized in solutions containing different ligand concentrations and the electrode potential recorded for each concentration. The total metal concentration was constant for each polarization current. This procedure is advantageous for ions which are susceptible to

* To whom correspondence should be addressed.

atmospheric oxidation, because the manipulation of such ions is avoided by generating them at the electrode–solution interface.

The equilibrium constants were calculated by taking into account conventional calculation procedures.[17–19] The values obtained using this technique were compared with those reported in the literature.[20]

Experimental

Four copper disc and four lead disc electrodes, made from the corresponding metallic rods of spectrochemical purity, were used. The electrodes were 0.5 cm in diameter and were supported in Teflon bars, polymeric acrylic matrices or Araldite resin bodies. For potentiometric measurements, with no polarization of the electrode, the exposed area was increased to approximately 4 cm^2. Each electrode was abraded with No. 600 emery paper and de-greased with alkaline substances such as sodium carbonate or calcium hydroxide. The working electrode is shown in Fig. 1.

The reference electrode was an Orion Model 90-01 saturated calomel electrode (SCE). The electrolytic cell is illustrated in Fig. 2. The potential measurements were made with an Orion Model 701 A voltmeter.

The electrodes were dipped into copper(II) or lead perchlorate solutions, of varying concentration from 1×10^{-4} to 1×10^{-1} mol dm^{-3}, including solutions in which the cation concentration was equal to zero. The ionic strength was adjusted with a sodium perchlorate solution of higher concentration to match the value of a 1 mol dm^{-3} sodium perchlorate solution.

In the first stage, the electrodes were polarized anodically with different currents *viz.*, 100, 50 and 25 μA, in order to study their behaviour. In all instances, the response time and the final value attained by the electrode potential were recorded. The current was then switched off and the time required for the potential to reach a final stable value was recorded again. This procedure was repeated four times. The polarization circuit is shown in Fig. 3. The results obtained are presented in Tables 1 and 2.

The electrodes were subjected to other surface treatments (as described in the literature[3,4]) such as: mechanical polishing, chemical etching and electroplating. In this instance, the stabilization of the electrode potential took 2–4 h and differences in the measured values ranged from 20 to 50 mV. When the electrodes were subjected to anodic polarization the response time was less than 10 s and an insignificant scatter in the measurements was observed.

In the second stage, in order to determine the stability constants of complex ions, a metallic electrode was chosen (according to the cation of which the complexes were to be studied) and was polarized anodically with different current intensities. The potential of the electrode was recorded for increasing ligand concentrations. The electrode potential in the absence of polarization was also recorded.

The systems copper acetate, lead acetate and lead oxalate were studied. Hence, it was necessary to prepare a set of acetate solutions with concentrations ranging from 1×10^{-4} to 2 mol dm^{-3} and a set of oxalate solutions with concentrations varying from 1×10^{-4} to 0.25 mol dm^{-3}. The ionic strength was kept constant at the above-mentioned level. The results obtained are shown in Fig. 4.

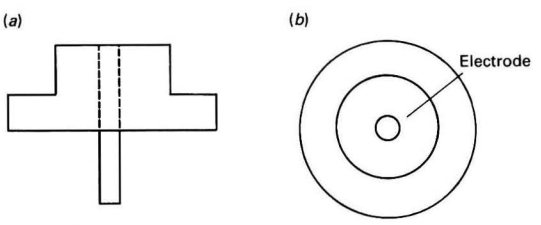

Fig. 1 Working electrode: (*a*) side view; and (*b*) top view

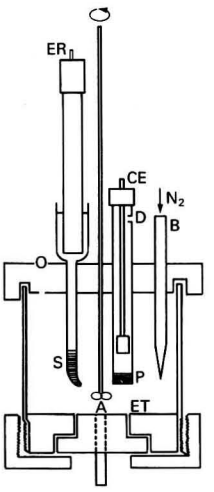

Fig. 2 Electrolytic cell: ET, working electrode; CE, counter electrode; ER, reference electrode; P, sintered glass; S, agar bridge; A, stirrer; B, nitrogen bubbler tube; and O and D, holes

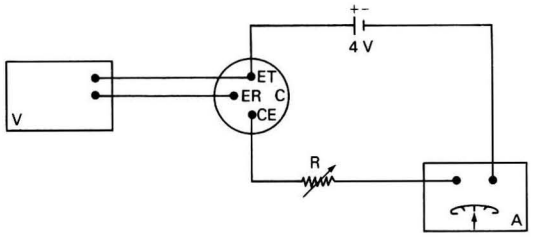

Fig. 3 Polarizing circuit: ET, working electrode; CE, counter electrode; ER, reference electrode; C, electrolytic cell; V, voltmeter; A, ammeter; and R, variable resistance

Table 1 Copper electrode potential E (mV) *versus* SCE for several molar concentrations of added cation and for different anodic polarizations

[Cation]/ mol dm^{-3}	i/μA			
	100	50	25	0
0	−27.5	−41.0	−53.9	−87.0
1.0×10^{-4}	−10.8	−13.3	−14.4	−14.9
1.0×10^{-3}	+15.5	+15.2	+15.1	+15.0
1.0×10^{-2}	+45.1	+45.0	+44.8	+45.2
1.0×10^{-1}	+75.0	+75.2	+74.9	+75.1

Table 2 Lead electrode potential E(mV) *versus* SCE for several molar concentrations of added cation and for different anodic polarizations

[Cation]/ mol dm^{-3}	i/μA			
	100	50	25	0
0	−515.6	−524.6	−531.0	−575.0
1.0×10^{-4}	−495.6	−497.1	−497.8	−499.0
1.0×10^{-3}	−467.6	−467.8	−467.9	−468.1
1.0×10^{-2}	−437.0	−437.0	−436.8	−437.1
1.0×10^{-1}	−406.0	−406.1	−406.2	−406.0

In all instances, the solutions were previously de-gassed with purified nitrogen and stirred at 1800 rev min^{-1}. The working temperature was 20 ± 0.2 °C.

Results and Discussion

Study of the Electrode Response

This study will be restricted to the anodically polarized electrodes because the other treatments applied to the electrodes did not yield reproducible responses within a relatively short time.

A simplified model was developed in order to understand the response of an anodically polarized electrode. When the electrochemical equilibrium is reached, the electrode potential is related to the concentration by a relationship described by the Nernst equation. Two cases must be considered.

(1) No complexing agent is added to the system under study:

$$E_0 = K + a \log(c_{M_0} + c_{M_a}) \quad (1)$$

(with no current flowing through the cell)

$$E = K + a \log(c_{M_0} + c_{M_a} + k_i) + \eta(e) \quad (2)$$

(current flowing through the cell)

(2) A complexing agent is added to the system:

$$E'_0 = K + a \log(c_{M_0} + c_{M_a}) f \quad (3)$$

(with no current flowing through the cell)

$$E' = K + a + \log (c_{M_0} + c_{M_a} + k_i) f + \eta'(e) \quad (4)$$

(current flowing through the cell)

where E = electrode potential *versus* SCE, E_0 = electrode potential when no current is flowing in the cell, E' = electrode potential in the presence of a complexing agent, K = electrode constant (this resembles the parameter E in the Nernst equation), a = Nernstian slope [$a = 2.3RT/zF$ (R = gas constant, T = temperature, z = charge and F = Faraday constant)], c_{M_0} = cation activity generated spontaneously at the electrode–solution interface, c_{M_a} = added cation activity, k_i = cation activity generated because of the current flow at the electrode–solution interface, f = fraction of uncomplexed cation (= free cation activity/total cation concentration), and $\eta(e)$ and $\eta'(e)$ = polarizations at the electrode–solution interface, different from concentration polarization.

It has been shown that the slope of the plot of E *versus* log c_{M_a} is $a/2.3$.[11] From the data in Tables 1 and 2, the values of a and K were calculated to be 30 mV $decade^{-1}$ and +105 mV *versus* SCE, respectively, for the copper electrode, and 31 mV $decade^{-1}$ and −375 mV *versus* SCE, respectively, for the lead electrode.

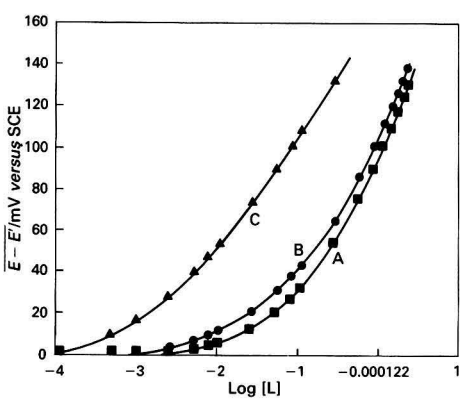

Fig. 4 Average electrode potential difference ($\overline{E - E'}$) as a function of log [L] for A, copper acetate; B, lead acetate; and C, lead oxalate

From eqn. (1) c_{M_0} was calculated to be 4.0×10^{-7} mol dm^{-3} for the copper electrode and 3.5×10^{-7} mol dm^{-3} for the lead electrode.

From eqn. (2), the cation concentration at the electrode–solution interface for a given anodic current intensity can be calculated in the usual way.[11] It ranges from 4.0×10^{-7} to 3.8×10^{-5} mol dm^{-3} for the copper electrode and from 3.5×10^{-7} to 2.9×10^{-5} mol dm^{-3} for the lead electrode when the current intensity is varied from 0 to 100 μA.

As the value of $E' - E$ is similar to $E_0' - E_0$ (see Tables 1 and 2 and Fig. 4), it can be concluded that the difference $\eta'(e) - \eta(e)$ approaches zero; hence the calculation of f is unaffected by the polarizations occurring at the electrode surface.

Calculation of the Stability Constants

The material balance equations for a multi-stage equilibrium involving complex ions are:

$$c_M = [M] + [ML] + [ML_2] + [ML_3] + \ldots \quad (5)$$

$$c_L = [L] + [ML] + 2[ML_2] + 3[ML_3] + \ldots \quad (6)$$

where M = metal and L = ligand. In order to solve these equations it is necessary to know c_M and c_L and to determine [M] or [L] experimentally. Several calculation procedures have been described in the literature.[17–19] When employing polarized electrodes, the cation concentration generated at the interface by polarization is about 1×10^{-5} mol dm^{-3}; hence it can be stated that $[L] = c_L$. The value of the quotient $c_M/[M]$, which is the inverse of f, must be known instead of [M]. This value can be obtained from the plot of $\overline{E - E'}$ *versus* log [L] (Fig. 4). Once this value has been obtained, the successive formation constants (k) can easily be obtained by regression analysis using eqn. (7):

$$\frac{1}{f} = c_M/[M] = 1 + k_1[L] + k_1k_2[L] + k_1k_2k_3[L]^3 + \ldots \quad (7)$$

In this instance a regression analysis computer program was employed[21] based on the procedure described by Marquardt.[22] The results are presented in Table 3 and compared with those reported in the literature.[20] Good agreement was found.

Conclusions

By polarizing a metallic electrode with low anodic current intensities, a fast response time and good repeatability were achieved. The response time is less than 10 s. This procedure proved to be superior to coating the electrode with the corresponding metal at constant current intensities. The other surface treatments applied did not yield repeatable responses and good response times unless the electrodes were subsequently polarized with low anodic current intensities.

When working at low anodic current intensities, the electrode slopes appeared to be Nernstian. The cation concentration generated at the electrode/solution interface does not compete with the concentration of the metal because the current intensities are low.

When low anodic current intensities are employed, the polarizations occurring at the electrode/solution interface cancel each other out; hence the calculations carried out from the potential measurements are not subject to any serious error from the polarizations.

The electrode polarized in this way could be used to determine free metal concentrations in the same way as a primary electrode, provided that $[M^{2+}] >> c_{M_0}$, but with two advantages: better repeatability and a faster response time.

When determining equilibrium constants, the problem of the dependence of the shape and position of the polarization curves on the stability constants of the complex ions is avoided

Table 3 Comparison of the experimental values of the stability constants (k) with those obtained from the literature for media of ionic strength 1 mol dm^{-3}

			Literature values*		Experimental values	
Ligand	Metal	Equilibrium	Temperature/ °C	k	Temperature/ °C	k
Acetate	Cu	$[ML] \rightleftharpoons [L][M]$	25	51.3	20	49.2
		$[ML_2] \rightleftharpoons [ML][L]$		10.0		10.6
		$[ML_3] \rightleftharpoons [ML_2][L]$		2.45		2.35
		$[ML_4] \rightleftharpoons [ML_3][L]$		0.63		0.66
	Pb	$[ML] \rightleftharpoons [L][M]$	25	126	20	123
		$[ML_2] \rightleftharpoons [ML][L]$		7.58		8.33
		$[ML_3] \rightleftharpoons [ML_2][L]$		2.63		2.30
		$[ML_4] \rightleftharpoons [ML]_3[L]$		0.20†		0.30
Oxalate	Pb	$[ML] \rightleftharpoons [M][L]$	25	2089	20	2100
		$[ML_2] \rightleftharpoons [ML][L]$		151		150

* Reference 20.
† This value corresponds to an ionic strength of zero.

by polarizing the electrode with low anodic current intensities and taking measurements when the electrochemical equilibrium has been reached. The equilibrium $M^0 \rightleftharpoons M^{z+} + ze^-$ is readily achieved at the electrode surface when the electrode is polarized. This represents a considerable advance with respect to potentiometric techniques in general.

The total cation concentration does not change during the determination, and depends on the magnitude of the polarizing current. It is not necessary to know the true value of the cation concentration at the electrode/solution interface; instead, the fraction of uncomplexed cation (f) is calculated from potential measurements. The free ligand concentration virtually coincides with the total ligand concentration over the whole range of concentrations because the concentration of cation generated at the electrode/solution interface is about 1×10^{-5} mol dm^{-3}.

This methodology is not restricted to mercury or noble metal electrodes; base metal electrodes can be employed provided they are polarized with low anodic current intensities and provided the metal does not become passive in the chosen medium. Unstable cations can be studied by using this procedure because it is not necessary to handle solutions of the cation, which is generated electrolytically at the electrode/solution interface.

We thank CIC (Comisión de Investigaciones Científicas) and CONICET (Consejo Nacional de Investigaciones Científicas y Técnicas) for their sponsorship of this research.

References

1 Harris, D. C., *Quantitative Chemical Analysis*, Freeman, New York, 1987.
2 Delahay, P., *New Instrumental Methods in Electrochemistry*, Interscience, New York, 1954.
3 *Encyclopedia of Electrochemistry of the Elements*, ed. Bard, A. J., Marcel Dekker, New York, 1978.
4 Charlot, G., Badoz-Lambling, J., and Trémillon, B., *Electrochemical Reactions*, Elsevier, Amsterdam, 1962.
5 Cerviño, R. M., Triacca, W. E., and Arvía, A. J., *J. Electroanal. Chem.*, 1985, **182**, 51.
6 Killa, H. M., Mercer, E. E., and Philp, R. H., *Anal. Chem.*, 1984, **56**, 2401.
7 Killa, H. M., and Philp, R. H., *J. Electroanal. Chem.*, 1984, **175**, 223.
8 Savéant, J. M., and Xu, F., *J. Electroanal. Chem.*, 1986, **208**, 197.
9 Spell, J. E., and Philp, R. H., *J. Electroanal. Chem.*, 1980, **112**, 281.
10 Castleberry, A. A., Mercer, E. E., and Philp, R. H., *J. Electroanal. Chem.*, 1987, **216**, 1.
11 Bard, A. J., and Faulkner, L. R., *Electrochemical Methods*, Wiley, New York, 1980.
12 Lingane, J. J., *Chem. Rev.*, 1941, **29**, 1.
13 De Ford, D. D., and Hume, D. N., *J. Am. Chem. Soc.*, 1951, **73**, 5321.
14 Schaap, W. B., and MacMasters, D. L., *J. Am. Chem. Soc.*, 1961, **83**, 4699.
15 Gampp, H., *Anal. Chem.*, 1987, **59**, 2456.
16 Kolthoff, I. M., and Lingane, J. J., *Polarography*, Interscience, New York, 1952, vol. 1.
17 Yatsimirskii, K. B., and Vasil'ev, V. P., *Instability Constants of Complex Compounds*, Consultant Bureau Enterprises, New York, 1960.
18 Sullivan, J. C., and Hindman, J. C., *J. Am. Chem. Soc.*, 1952, **74**, 6091.
19 Rossotti, F. J. C., and Rossotti, K. S., *Acta Chem. Scand.*, 1955, **9**, 1166.
20 Martell, A. E., and Smith, R. M., *Critical Stability Constants. Volume 3. Other Organic Ligands*, Plenum Press, New York, 1979.
21 Marquardt, D. W., Share Program No. 3094, 1963.
22 Marquardt, D. W., *SIAM J. Appl. Math.*, 1963, **11**, 431.

Paper 0/01529F
Received April 4th, 1990
Accepted April 22nd, 1991

Differential-pulse Polarographic Behaviour of Selenium in the Presence of Copper, Cadmium and Lead

Hasan Aydin
Gazi Universitesi, Fen-Edebiyat Fakultesi, Kimya Bolumu, Ankara, Turkey
G. H. Tan*
Department of Chemistry, University of Malaya, 59100 Kuala Lumpur, Malaysia

A differential-pulse polarographic method for the determination of Se is described. The effect of Cu, Pb and Cd on the Se peaks was studied. In order to find a suitable medium, $HClO_4$ (pH 1), 0.1 mol dm^{-3} KNO_3 (pH 4), a buffer solution of pH 4 (CH_3COOH–H_3BO_3–H_3PO_4), a buffer solution of pH 9 (NH_3–NH_4Cl) and 10% Na_2SO_3 (pH 9.5) were studied. In NH_3–NH_4Cl and 10% Na_2SO_3 media the expected peak for SeO_3^{2-} was not observed; however, the $SeSO_3^{2-}$ ion gave a peak at −800 and −600 mV, respectively. In addition, in the CH_3COOH–H_3BO_3–H_3PO_4 buffer solution of pH 4, SeO_3^{2-} gave two peaks at −610 and −1310 mV. The detection limit for Se in a buffer solution (pH = 4) of CH_3COOH–H_3BO_3–H_3PO_4 was 1×10^{-8} mol dm^{-3}. The method was applied to some environmental samples.

Keywords: *Selenium; lead; cadmium; differential-pulse polarography; environmental samples*

The importance of Se as an essential trace element together with Cu, Cd and Pb in animal nutrition, natural waters and waste waters has stimulated the development of many sensitive analytical methods for its determination. In order to measure the amount of Se in different media, atomic absorption spectrometry,[1,2] neutron-activation analysis,[3] chromatography,[4] polarography,[5–9] differential-pulse stripping voltammetry,[10] cathodic stripping voltammetry,[11] anodic stripping voltammetry[12–14] and titrimetry[15] have been used. However, some of these methods require elaborate instrumentation and precisely controlled experimental conditions. The determination of Se by pulse polarographic methods is well-known, having been studied by many workers. The main difficulty encountered in the past has been the influence of heavy metal ions on the determination of Se by electrochemical or other methods. However, in order to eliminate these interferences, many workers have used Chelex-100 resin,[8] ion-exchange separation[16] and other methods.

This paper describes a simple pulse polarographic method for the determination of Se, Cu, Cd and Pb in various environmental samples. The proposed method permits the determination of Se in the presence of heavy metal ions. In addition, the effect of the metal ion concentrations on the Se peak, the effect of the medium on the peak potentials of Se and the application of the method to some environmental samples are also described.

Experimental

Apparatus

Polarograms were obtained with a Princeton Applied Research PAR 174 A polarographic analyser and a Hewlett-Packard *x–y* type recorder. A two-electrode system was used, with a dropping mercury electrode (DME) as the working electrode and a saturated calomel electrode (SCE) as the reference electrode.

Reagents

All reagents used were of analytical-reagent grade. Distilled, de-ionized water was used for preparing all the solutions and at all stages of analysis.

* To whom correspondence should be addressed.

Buffer solution (pH 4). Prepared by mixing equal parts of 0.04 mol dm^{-3} CH_3COOH, 0.04 mol dm^{-3} H_3Po_4 and 0.04 mol dm^{-3} H_3BO_3. The pH of the resulting solution was adjusted to 4.0 by the addition of about 25 ml of 0.2 mol dm^{-3} NaOH solution to 100 ml of this stock solution.

Ammonia–ammonium chloride buffer solution. Prepared by dissolving 100 g of NH_4Cl in 380 ml of NH_3 solution and diluting to 500 ml with de-ionized water.

Stock standard Se solution, 1×10^{-2} mol dm^{-3}. Prepared by dissolving 0.1729 g of Na_2SeO_3 in 100 ml of de-ionized water.

Working standard Se solutions, 1×10^{-4} *and* 1×10^{-5} mol dm^{-3}. Prepared fresh each day by diluting the 1×10^{-2} mol dm^{-3} stock standard solution.

Working standard Cu^{II} *solutions,* 1×10^{-4} *and* 1×10^{-5} mol dm^{-3}. Prepared by diluting a 1×10^{-2} mol dm^{-3} stock solution of $Cu(NO_3)_2$.

Working standard Pb^{II} *solutions,* 1×10^{-4} *and* 1×10^{-5} mol dm^{-3}. Prepared by diluting a 1×10^{-2} mol dm^{-3} stock solution of $Pb(NO_3)_2$.

Working standard Cd^{II} *solutions,* 1×10^{-4} *and* 1×10^{-5} mol dm^{-3}. Prepared by diluting a 1×10^{-2} mol dm^{-3} stock solution of $Cd(NO_3)_2$.

Procedure

Synthetic samples for analysis were prepared by adding aliquots of a concentrated supporting electrolyte solution to the analyte solution and the pH was measured with a pH meter. Thorough de-aeration of the solution to be analysed was required to avoid interference from reduction of dissolved oxygen. Pre-purified nitrogen was used for de-aeration after pre-saturating the gas with water by bubbling it through freshly prepared de-ionized water. Nitrogen was passed through the solutions for about 30 min before each experiment. In order to study the interference of heavy metal ions on the Se peak and to determine the peak potentials of the heavy metal ions and Se, various experiments were carried out by adding the interferents to the supporting electrolyte both before and after the addition of Se.

The influence of the potential scan rate, mercury drop time and supporting electrolyte solutions on the peak height was studied. In each experiment, one of the parameters was varied while the others were kept constant.

Water samples from the Klang River (see Fig. 1 for map) were used for application of the method. A 5 ml volume of HNO_3, $HClO_4$–HNO_3–H_2SO_4 (24 + 24 + 2), $HClO_4$–HNO_3 (1 + 1) or HCl–HNO_3 (3 + 1) was added to 100 ml of the water

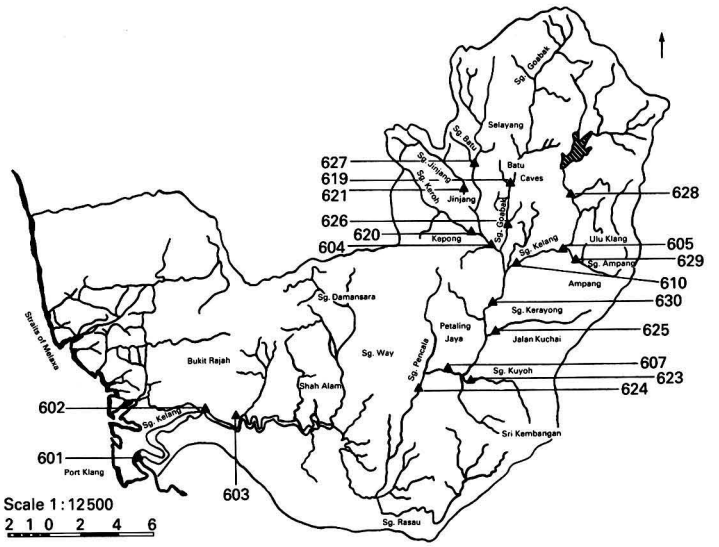

Fig. 1 Klang River basin: sampling station (▲ = sampling station)

Table 1 Peak potential of Cu, Pb, Cd and Se in various media

Supporting electrolyte	pH	Peak potential/mV *versus* SCE				
		Cu	Pb	Cd	Se	$SeSO_3^{2-}$
$HClO_4$	1.0	0.00	−415	−615	−510	—
0.1 mol dm^{-3} KNO_3	4.0	−60	−370	−480	−650	—
Buffer solution*	4.0	−0.00	−390	−680	−610 −1310	—
Buffer solution†	9.5	−270	−490	−780	—	−800
10% Na_2SO_3	9.3	—	—	−610	—	−600

* CH_3COOH–H_3BO_3–H_3PO_4.
† NH_3–NH_4Cl.

sample and the volume was then reduced to 10 ml by evaporation. After this procedure, the volume was adjusted to 100 ml with distilled water. The samples that had been acidified only with HNO_3 were not heated. The pH of the samples was adjusted to 4 with NaOH solution. After pH adjustment, 5 ml of 0.1 mol dm^{-3} KNO_3 (pH 4) or buffer solution of pH 4 were added to 20 ml of the sample solution. In order to obtain the $SeSO_3^{2-}$ ion, 1.0 g of Na_2SO_3 was added to the acidified sample solution. The pH of the solutions was adjusted to 7–8 by using NaOH solution and 10 ml of 10% Na_2SO_3 solution were then added to each sample. In order to accelerate the formation of $SeSO_3^{2-}$, the solutions were heated. A 5 ml volume of 10% Na_2SO_3 or NH_3–NH_4Cl buffer solution was added to 20 ml of these solutions before analysis.

Results and Discussion

In differential-pulse polarography the peak potential of metal ions depends on the supporting electrolyte and on the pH of the electrolyte solution. The electrolytes mentioned above were used for the determination of the peak potential of Cu, Pb, Cd and Se. The results of these experiments are given in Table 1.

It was found that the use of a buffer solution containing CH_3COOH, H_3BO_3 and H_3PO_4 to determine the amounts of Cu, Pb, Cd, and Se gave two peaks for Se at −610 and −1310 mV (see Fig. 2). The influence of Cu, Pb and Cd ions on these peaks was studied and it was found that the second peak for Se

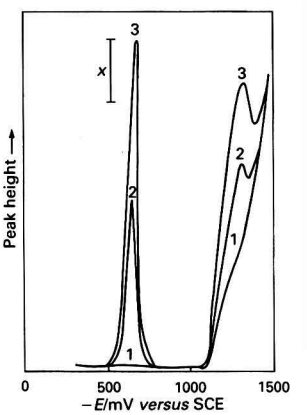

Fig. 2 Differential-pulse polarographic behaviour of Se^{IV}. 1, Blank solution; 2, 63.9 μg l^{-1} of Se^{IV}; and 3, 127.8 μg l^{-1} of Se^{IV}. Measurement of the peak height is indicated by *x*

at −1310 mV could be used for the determination of Se in the presence of Cu, Pb and Cd. The peak at −1310 mV was still observed when the Se concentration was 1×10^{-7} mol dm^{-3}. When Cu, Pb and Cd solutions were added to the Se solution,

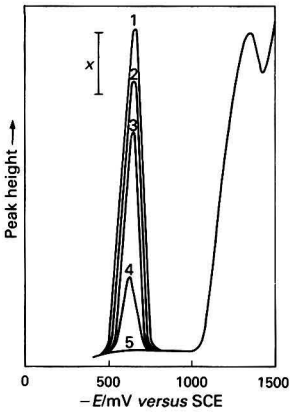

Fig. 3 Effect of Pb^{II} and Cd^{II} on the determination of Se^{IV}. 1, 127.8 μg l^{-1} of Se^{IV}; 2, 38.3 μg l^{-1} of Pb^{II} + 127.8 μg l^{-1} of Se^{IV}; 3, 78.6 μg l^{-1} of Pb^{II} + 127.8 μg l^{-1} of Se^{IV}; 4, 24.4 μg l^{-1} of Cd^{II} +78.6 μg l^{-1} of Pb^{II} + 127.8 μg l^{-1} of Se^{IV}; and 5, 48.8 μg l^{-1} of Cd^{II} + 78.6 μg l^{-1} of Pb^{II} +127.6 μg l^{-1} of Se^{IV}. Measurement of the peak height is indicated by *x*

Table 2 Effect of Pb and Cd on the determination of Se in buffer solution (pH 4)

Concentration/10^{-6} mol dm^{-3}			Peak height (arbitrary units)			
SeO_3^{2-}	Pb^{2+}	Cd^{2+}	Se	Se*	Pb	Cd
1.0	—	—	25†	7	—	—
2.0	—	—	50†	14	—	—
2.0	0.26	—	42†	14	12	—
2.0	0.52	—	34†	14	24	—
2.0	0.52	0.22	11†	14	24	—
2.0	0.52	0.44	—	14	24	—
2.0	0.52	1.10	15‡	14	24	—
2.0	0.52	2.50	71§	14	24	5
2.7	0.52	2.50	54§	21	24	5
3.4	0.52	2.50	37§	28	24	5

* At −1300 mV.
† At −610 mV.
‡ At −560 mV.
§ At −580 mV.

Table 3 Effect of Se on the determination of Cu, Pb and Cd in buffer solution (pH 4)

Concentration/10^{-6} mol dm^{-3}				Peak height (arbitrary units)				
Se	Cu	Pb	Cd	Se	Se*	Cu	Pb	Cd
—	0.72	—	—	—	—	5	—	—
—	0.72	—	0.78	—	—	5	—	3
—	2.10	—	1.60	—	—	16	—	7
—	2.10	0.87	1.60	—	—	16	4	7
—	2.10	1.70	3.20	—	—	16	8	14
0.76	2.10	1.70	3.20	—	2	16	8	10
2.30	2.10	1.70	3.20	—	6	14	8	6
3.80	2.10	1.70	3.20	—	10	11	8	2
5.30	2.10	1.70	3.20	—	14	10	8	0.5
9.10	2.10	1.70	3.20	—	24	7	8	—

* At −1300 mV.

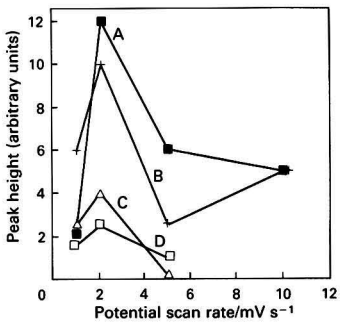

Fig. 4 Effect of sweep rate on the peak height of Se^{IV} at different mercury drop times in buffer solution (pH = 4). Drop time: A, 0.5; B, 1.0; C, 2.0; and D, 5.0 s

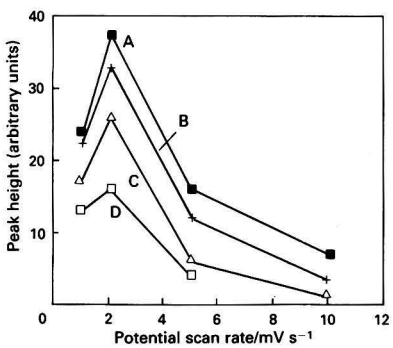

Fig. 5 Effect of sweep rate on the peak height of Se^{IV} at different mercury drop times in 10% Na_2SO_3 solution. Drop time: A, 0.5; B, 1.0; C, 2.0; and D, 5.0 s

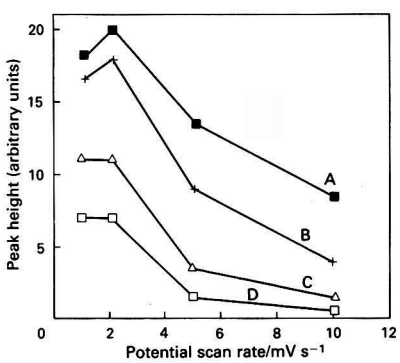

Fig. 6 Effect of sweep rate on the peak height of Se^{IV} at different mercury drop times in NH_3–NH_4Cl buffer solution. Drop time: A, 0.5; B, 1.0; C, 2.0; and D, 5.0 s

these ions were found to affect the Se peak at −610 mV (Table 2). However, these ions did not interfere with the other Se peak at −1310 mV (see Fig. 3). Hence it was possible to determine 1 × 10^{-7} mol dm^{-3} Se in a solution containing Cu, Pb and Cd ions with a relative standard deviation of 1.5%. In addition, it was found that the influence of Cd was greater than that of Cu and Pb. For instance, when Se was added to a buffer solution (pH 4) containing Cu, Pb and Cd ions, the Cd peak began to decrease and eventually became a small peak, after which the Cu peak also began to decrease. In another experiment with a buffer solution (pH 4) containing SeO_3^{2-}, Pb and Cd ions were added respectively. In this experiment, after observing the influence of Pb on the Se peak, Cd ion was added. The effect of Pb and Cd ions on the Se peak is shown in Tables 2 and 3. In this experiment the peak potential of Se changed from −610 to −560 mV after the addition of Cd. When Se was added to the same solution, the same peak was shifted to −580 mV. In addition, the unknown peak at −420

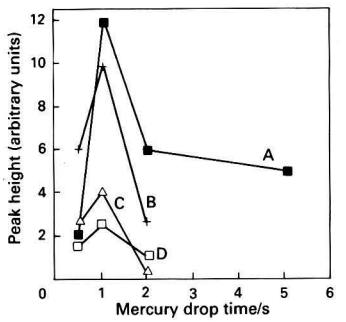

Fig. 7 Effect of mercury drop time on the peak height of Se^{IV} at different scan rates in the buffer solution (pH = 4; peak potential = −540 mV). Scan rate: A, 1; B, 2; C, 5; and D, 10 mV s^{-1}

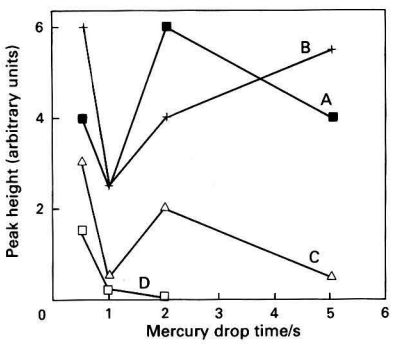

Fig. 8 Effect of mercury drop time on the peak height of Se^{IV} at different scan rates in the buffer solution (pH = 4; peak potential = −1310 mV). Scan rate: A, 1; B, 2; C, 5; and D, 10 mV s^{-1}

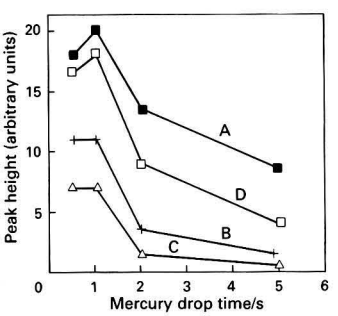

Fig. 9 Effect of mercury drop time on the peak height of Se^{IV} at different scan rates in NH_3–NH_4Cl buffer. Scan rate: A, 1; B, 2; C, 5; and D, 10 mV s^{-1}

mV *versus* SCE was not observed until the addition of Cd after which the height of this peak increased with the addition of Cd^{2+} and SeO_3^{2-} solutions, respectively. The height of the unknown peak was proportional to the concentration of Cd and Se added to the buffer solution, *i.e.*, the addition of Cu, Pb and Cd did not affect the Se peak at −1310 mV.

In 10% Na_2SO_3 or NH_3–NH_4Cl buffer solution, the Se peak was not observed between 0.00 and −1600 mV. However, when $SeSO_3^{2-}$ was added to the 10% Na_2SO_3 or NH_3–NH_4Cl buffer solution the Se peak was observed at −600 and −800 mV, respectively. Dunhu *et al.*[7] observed the Se peak at −570 mV in the $HClO_4$–Na_2SO_3–NH_3–NH_4Cl–NH_2OH–HCl–KIO_3 system (pH 10). They attributed this peak to the $SeSO_3^{2-}$ ion.

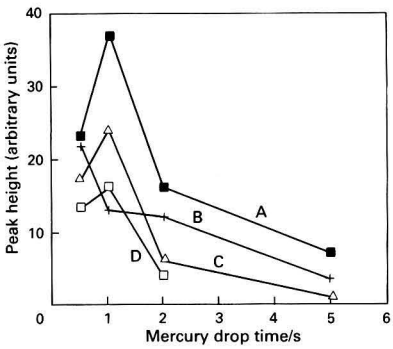

Fig. 10 Effect of mercury drop time on the peak height of Se^{IV} at different scan rates in 10% Na_2SO_3 solution. Scan rate: A, 1; B, 2; C, 5; and D, 10 mV s^{-1}

Table 4 Determination of Cu, Pb, Cd and Se in water samples from the Klang River in Malaysia

Sample No.	Monitoring station No.*	Concentration of elements in sample (ppb)				Se added to sample (ppb)	Se found (ppb)
		Cu	Pb	Cd	Se		
1	624	—	62	22	—	35	33
2	610	—	37	8	—	16	16
3	629	—	33	—	—	16	15
4	628	—	32	5	—	25	26
5	605	—	39	3	—	25	23
6	626	—	42	3	—	25	23
7	627	—	41	12	—	35	33
8	621	—	50	5	—	16	14
9	604	—	43	—	—	16	15

* See Fig. 1 for map showing location of each station No.

In order to obtain the $SeSO_3^{2-}$ ion, Na_2SO_3 solution was added to an acidic SeO_3^{2-} solution. The amorphous Se formed was filtered off and then dissolved in 10% Na_2SO_3 solution. In order to accelerate the formation of $SeSO_3^{2-}$ the solution was heated. This species undergoes electrochemical reduction on the DME and forms a distinct pulse polarographic wave. The mechanism of this reaction is:

$$SeSO_3^{2-} + 2e^- \rightarrow Se^{2-} + SO_3^{2-}$$

The $SeSO_3^{2-}$ ion is initially decomposed into Se and SO_3^{2-}. Selenium is adsorbed on the electrode surface and reduced to Se^{2-} at a potential of −600 mV in 10% Na_2SO_3 and −800 mV in NH_3–NH_4Cl buffer solution.

In order to obtain the maximum peak height, the effect of sweep rate and drop time of the DME on the peak height was studied at different scan rates in buffer (pH 4), 10% Na_2SO_3 and NH_3–NH_4Cl solutions. The results are shown in Figs. 4–10. In each experiment, one parameter was varied while the others were kept constant. The results showed that a higher scan speed resulted in a decrease in resolution and peak height. In addition, the effect of the potential scan rate on the peak height and mercury drop time varied according to the pH, peak potential and electrolyte solutions. For instance, the effect of the mercury drop time on the peak height of Se^{IV} at different scan rates in a buffer solution of pH 4 varied according to the peak potential of Se^{IV}. In order to obtain better resolution, scan rates of 1 and 2 mV s^{-1} were used. From the results presented in Figs. 7–10, the appropriate mercury drop time was selected.

The wet digestion methods described above were applied to the river water samples. However, no significant differences

between the methods were found. Therefore, the digestion method involving the use of HNO_3 without heating was employed for the determination of Cu, Pb, Cd and Se. In addition, when a buffer solution of pH 4 was added to the samples, no detectable amounts of Cu and Se were found (Table 4). However, when Se was added to the samples before wet digestion, Se peaks were observed at −610 and −1310 mV. The results of these experiments obtained by using the peak at −1310 mV are shown in Table 4.

References

1 Sturgeon, R. E., Willie, S. N., and Berman, S. S., *Anal. Chem.*, 1985, **57**, 6.
2 Vijan, P. N., and Wood, G. R., *Talanta*, 1976, **23**, 1.
3 Kronborg, O. J., and Steinnes, E., *Analyst*, 1975, **100**, 835.
4 Shimoishi, Y., *Analyst*, 1976, **101**, 298.
5 Christian, G. D., and Knoblock, E. C., *Anal. Chem.*, 1963, **35**, 1128.
6 Hasdemir, E., and Somer. G., *Analyst*, 1990, **115**, 297.
7 Dunhu, W., Diyang, Z., and Xiaoming, L., *Analyst*, 1989, **114**, 793.
8 Batley, G. E., *Anal. Chim. Acta*, 1986, **187**, 109.
9 Bound, G. P., and Forbes, S., *Analyst*, 1978, **103**, 176.
10 Vos, L., Komy, Z., Reggers, G., Roekens, E., and van Grieken, R., *Anal. Chim. Acta*, 1986, **184**, 271.
11 Dennis, B. L., Moyers, J. L., and Wilson, G. S., *Anal. Chem.*, 1976, **48**, 1611.
12 Posey, R. S., and Andrews, R. W., *Anal. Chim. Acta,* 1981, **124**, 107.
13 Aydin, H., and Somer, G., *Anal. Sci.*, 1989, **5**, 89.,
14 Aydin, H., unpublished results.
15 Aydin, H., and Somer, G., *Talanta*, 1989, **36**, 723.
16 Adeloju, S. B., Bond, A. M., Briggs, M. H., and Hughes, H. C., *Anal. Chem.*, 1983, **55**, 2076.

Paper 1/00167A
Received January 14th, 1991
Accepted May 7th, 1991

Thermodynamic and Kinetic Implications Involved in the Titration of Polyfunctional Acids by Catalytic Thermometric Titrimetry

Oswaldo E. S. Godinho, Helena S. Nakatani, Ivo M. Raimundo Jr., Luiz M. Aleixo and Graciliano de Oliveira Neto
Instituto de Química, Universidade Estadual de Campinas, C.P. 6154, 13081 Campinas, São Paulo, Brazil

The influence of the concentration of reactants on the results of titrations of salicylic acid in acetone with potassium and tetramethylammonium hydroxides in propan-2-ol were investigated. The titrations were performed by catalytic thermometric titrimetry using acetone as the end-point indicator and by potentiometric titrimetry. These and other results are discussed in terms of the equilibrium and kinetic aspects involved in the titrations of polyfunctional acids capable of forming intramolecular hydrogen bonds.

Keywords: *Catalytic titrimetry, thermometric titrimetry, hydrogen bond, salicylic acid*

Vaughan and Swithenbank[1] introduced acetone as a thermometric end-point indicator in the titration of a variety of acidic substances with strong bases. In their method, the rise in temperature, caused by the exothermic reaction of dimerization of acetone catalysed by the excess of strong bases, is employed to locate the end-point of the titration.

Greenhow and co-workers[2–6] performed an extensive and systematic study of the titration of polyfunctional acids by catalytic thermometric titrimetry. They have shown the possibility of obtaining selectivity by appropriate control of the stoichiometry at the end-point of the titration. According to these workers, the variation of stoichiometry can be attained by choosing the appropriate end-point indicator, sample solvent, titrant or in some instances the concentration of titrant.

They have investigated more specifically the influence of titrant and sample solvent on the stoichiometry attained in the titration of some hydrogen bonded polyfunctional acids.[5] The influence of the sample solvent is related to the extent of dissociation of the titrant ion-pair with potassium hydroxide as titrant whereas tetrabutylammonium hydroxide is considered to be completely dissociated. A mechanism, which considered the formation of a four-centre intermediary between the half-neutralized difunctional acid and the potassium hydroxide ion-pair, was presented to explain the results. The neutralization and indicative reactions are considered to be competitive processes.

In this paper, a study of the influence of the sample and titrant concentrations on the titration of salicylic acid (in acetone) with potassium hydroxide (in propan-2-ol) is presented. The results are compared with those obtained by using tetramethylammonium hydroxide as the titrant.

These and other results, in the literature, are explained by considering the thermodynamic and kinetic aspects involved in the titrations of polyfunctional acids capable of forming intramolecular hydrogen bonds. In this context, the influence of the nature of the titrant and concentrations of both titrant and sample on the extension and rate of neutralization reactions are discussed. The mechanism employed to relate the rate of neutralization reaction of polyfunctional acids, capable of forming intramolecular hydrogen bonds, with the concentration of sample and titrant is based on recent investigations by Hibbert and Spiers.[7] These workers investigated the kinetics of the removal of protons from substituted salicylates, by hydroxyl ions and buffers. Finally, the comparison of the rates of neutralization and catalysed reactions is employed to discuss the stoichiometries obtained at the end-point.

Experimental

Reagents

Salicylic acid and potassium hydroxide were of analytical-reagent grade. Acetone and propan-2-ol, of laboratory-reagent grade, were dried with 3 Å molecular sieves before use.

Solutions of 0.5 and 1.0 mol dm^{-3} potassium and tetramethylammonium hydroxide in propan-2-ol were prepared and standardized with benzoic acid in ethanol using phenolphthalein as indicator. Other solutions were prepared by appropriate dilution of the 0.5 and 1.0 mol dm^{-3} solutions in propan-2-ol.

Apparatus

A motor driven micrometer syringe, as described by Greenhow and Spencer,[8] was employed to introduce the titrant at a constant delivery rate in both the potentiometric and thermometric titrations. In the thermometric titrations the temperature changes were detected by means of a thermistor placed in one arm of a Wheatstone bridge, and were recorded on a strip-chart recorder as described elsewhere.[9] A Micronal B 375 pH meter, a platinum electrode and a nichrome wire inserted into the titrant solution were employed in the potentiometric titrations.

Procedure

In the thermometric titrations, the desired volume of salicylic acid solution was pipetted into a 25 ml unsilvered Dewar flask and diluted with acetone to 10 ml. In both the potentiometric and thermometric titrations the titrant was added at a constant delivery rate of 0.13 ml min^{-1}. During the titrations the solutions were stirred with a magnetic stirrer. The amount of salicylic acid was adjusted in order that the volume of titrant delivered at the end-point of titration was between 0.25 and 0.5 ml. The concentration of propan-2-ol was kept between 2.5 and 5.0%.

Results and Discussion

The results of the titrations of salicylic acid in acetone with potassium and tetramethylammonium hydroxides in propan-2-ol by catalytic thermometric titrimetry are presented in Fig. 1. For potassium hydroxide, it was observed that the stoichiometry attained at the end-point increases from ≈1 to

≈2 when the concentration of the titrant is increased from 0.01 to 0.5 mol dm^{-3}. It was also observed that when the titrant is tetramethylammonium hydroxide, only one group is titrated and the stoichiometry is independent of the concentration of the reactants.

The results obtained by thermometric titrimetry with tetramethylammonium hydroxide as titrant are explained by considering the small second dissociation constant of salicylic acid. Consequently, the concentration of hydroxyl ions necessary to start the catalysed reaction is attained before the second equivalence point. In fact, as can be seen in Fig. 2, the dissociation constant is not sufficiently large to produce the second inflection in the potentiometric titration curve of salicylic acid with 0.1 and 0.8 mol dm^{-3} tetramethylammonium hydroxide solutions. However, the inflection corresponding to the titration of the phenolic group (absent when 0.1 mol dm^{-3} potassium hydroxide is used) is observed when 1.0 mol dm^{-3} potassium hydroxide is used as the titrant.

Another point to be considered is that when potassium hydroxide is used as the titrant at concentrations above 0.1 mol dm^{-3}, the formation of a white precipitate of potassium salicylate is observed. Therefore it is necessary to consider, in addition to the neutralization reaction, the precipitation of potassium salicylate.

$$HSal^- + OH^- \rightleftharpoons Sal^{2-} + H_2O \quad (1)$$

$$Sal^{2-} + 2K^+ \rightleftharpoons K_2Sal(s) \quad (2)$$

The precipitation of potassium salicylate causes a displacement to the right of the equilibrium represented in eqn. (1).

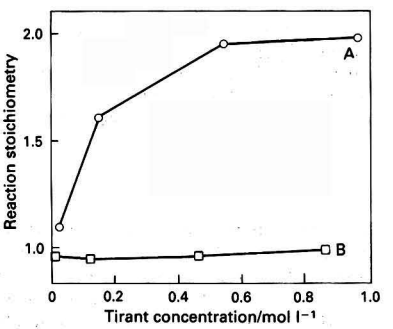

Fig. 1 Effect of concentration on the titration of salicylic acid in acetone by catalytic thermometric titrimetry. Titrant: A, KOH in propan-2-ol; and B, Me_4NOH in propan-2-ol. Volume of acetone, 10 ml. Concentration of salicylic acid = 1/40 of the concentration of the titrant

Therefore, if potassium hydroxide is used in place of tetramethylammonium hydroxide, the reaction in eqn. (1) will occur, to a large extent, before the concentration of hydroxyl ions reaches the value necessary to start the catalysed reaction.

Furthermore, in catalytic titrimetry it is necessary to consider the competition between the determinative and the indicative reactions.[5,6] These implications are particularly important in the titration of hydrogen bonded acids, as with the second acidic group of salicylic acid, where the rates of the neutralization reaction are not diffusion controlled as for normal acids.[10]

According to Hibbert and Spiers,[7] the removal of the second proton from substituted salicylates involves two steps; breaking of the hydrogen bond and proton transfer. For salicylic acid, these two steps are represented by the following equations:

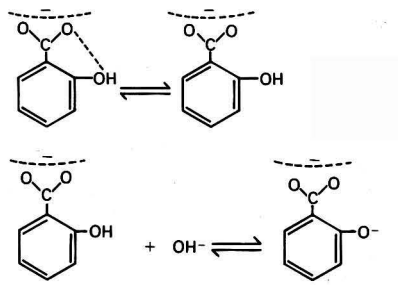

These workers have shown in their studies using dimethyl sulphoxide–water mixtures that, for concentrations of hydroxyl ions above 0.02 mol dm^{-3}, the breaking of the hydrogen bond is the rate-limiting step and that below this value the proton transfer is the rate-limiting step. In the range of concentration of hydroxyl ions below 0.02 mol dm^{-3}, the rate of the reaction increases linearly with the increase of concentration of hydroxyl ions. Above this value the rate of reaction varies little and tends to be independent of the concentration of hydroxyl ions.

In the application of this mechanism to these results, it is assumed that when using potassium hydroxide as the titrant the concentration of hydroxyl ions is in the concentration range where proton transfer is the rate-limiting step. This assumption is reasonable as, in this medium, potassium hydroxide is present mainly as ion pairs.[5,6] Consequently, the rate of the neutralization reaction increases to a larger extent than that of the catalysed reaction with the increase of

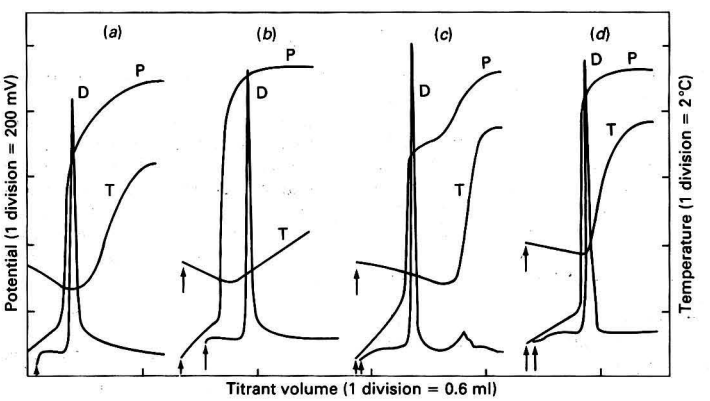

Fig. 2 Potentiometric and thermometric titration curves of salicylic acid in acetone. Concentration of salicylic acid = 1/40 of the concentration of the titrant. Volume of acetone, 10 ml. (*a*) KOH 0.1 mol dm^{-3} in propan-2-ol; (*b*) Me_4NOH 0.1 mol dm^{-3} in propan-2-ol; (*c*) KOH 1.0 mol dm^{-3} in propan-2-ol; and (*d*) Me_4NOH 0.8 mol dm^{-3} in propan-2-ol. P, Potentiometric titration curve; D, first derivative of potentiometric titration curve; and T, thermometric titration curve. The arrows indicate the start of the titrations

concentration of potassium hydroxide. This mechanism is consistent with the fact that the stoichiometry at the end-point increases with an increase in the concentration of potassium hydroxide and salicylic acid. The fact that the phenolic group of salicylic acid is not titrated at the end-point with tetramethylammonium hydroxide has already been explained by considering the value of the dissociation constant of the acid.

However, Greenhow and Shafi[5] have compared the titration of a variety of polyfunctional acids with tetrabutylammonium and potassium hydroxide by employing acrylonitrile as the end-point indicator. Among the acids investigated, the benzenecarboxylic acids are of particular interest to the kinetic considerations studied in this paper. They have shown that, while all of the acidic groups are titrated with 0.5 mol dm^{-3} potassium hydroxide as the titrant, only some of these groups are titrated with 0.1 mol dm^{-3} tetrabutylammonium hydroxide. This behaviour is observed in benzenecarboxylic acids, with the exception of terephthalic acid, capable of forming intramolecular hydrogen bonds. These differences in stoichiometry obtained with the two different titrants are not observed when using benzenecarboxylic acids, which do not form intramolecular hydrogen bonds.

It is not possible to explain the low stoichiometry obtained with tetrabutylammonium hydroxide on the basis of equilibrium considerations. In fact, the pK_a values for these acids in water vary from 1.40 to 6.96. As tetrabutylammonium hydroxide is completely dissociated,[5,6] it is supposed that the concentration of hydroxyl ions is in the concentration range where the breaking of the hydrogen bond is the rate-limiting step. Therefore, when the rate of production of the 'opened' form of the acid [eqn. (3)], capable of reacting with hydroxyl ions, is not sufficiently high, an excess of hydroxyl ions sufficient to start the catalysed reaction is available. When potassium hydroxide is used as the titrant, ion pairs are mainly present and the concentration of hydroxyl ions is low. Therefore, it is reasonable to suppose that the system is in the concentration range where proton transfer is the rate-limiting step. Consequently, the rate of consumption of hydroxyl ions is sufficient to prevent the start of the catalysed reaction.

Finally, in order to acertain if a given acidic group of a polyfunctional acid capable of forming hydrogen bonds can be titrated at the end-point, it is necessary to consider both the thermodynamic and the kinetic implications involved in the titration. Firstly, it is necessary to consider the value of the dissociation constant of the acidic groups and also the possibility of displacement of the equilibrium by virtue of the precipitation of the anion formed. Next it is necessary to take into account that the removal of protons from such acidic groups by hydroxyl ions is not diffusion controlled as for normal acids. Either the breaking of the hydrogen bond or proton transfer is the rate-limiting step, depending on the conditions under which the titration is performed. By the appropriate choice of the conditions and by considering the competition between the neutralization and catalysed reactions, it is possible to obtain selectivity in the titrations.

The authors thank the Fundação de Amparo à Pesquisa do Estado de São Paulo for financial support and Dr. F. Y. Fujiwara for reviewing the English text.

References

1 Vaughan, G. A., and Swithenbank, J. J., *Analyst*, 1965, **90**, 594.
2 Greenhow, E. J., and Spencer, L. E., *Analyst*, 1973, **98**, 90.
3 Greenhow, E. J., and Hargitt, R., *Proc. Soc. Anal. Chem.*, 1973, **10**, 276.
4 Greenhow, E. J., and Shafi, A. A., *Proc. Anal. Div. Chem. Soc.*, 1975, **12**, 286.
5 Greenhow, E. J., and Shafi, A. A., *Analyst*, 1976, **101**, 421.
6 Greenhow, E. J., *Chem. Rev.*, 1977, **77**, 835.
7 Hibbert, F., and Spiers, K. J., *J. Chem. Soc., Perkin Trans. 2*, 1989, **2**, 67.
8 Greenhow, E. J., and Spencer, L. E., *Analyst*, 1973, **98**, 98.
9 Chagas, A. P., Godinho, O. E. S., and Costa, J. L. M., *Talanta*, 1977, 24, **593.**
10 Eigen, M., *Angew. Chem., Int. Ed. Engl.*, 1964, **3**, 1.

Paper 1/00038A
Received January 3rd, 1991
Accepted March 19th, 1991

Iodimetric Method for the Determination of Mono- and Disaccharides With Vanadium(v) in Perchloric Acid

Amalendu Banerjee, Banasri Hazra, Anuva Putatunda, Dinabandhu Mandal, Gopal Chandra Banerjee and Sachchidananda Dutt
Department of Chemistry, Jadavpur University, Calcutta-700 032, India

Sodium (or ammonium) metavanadate in dilute perchloric acid was found to be a suitable reagent for the determination of fructose, mannose, galactose, arabinose, ribose, xylose, sucrose and maltose. A mixture containing the saccharide and an excess of the reagent was refluxed over a small flame for 40 min. The residual metavanadate was determined iodimetrically. The amount of saccharide was then determined by standardizing the metavanadate solution against either sodium thiosulphate solution or the respective saccharide solution of known strength; the latter procedure gave consistently better results.

Keywords: *Mono- and disaccharide determination; metavanadate–dilute perchloric acid; iodimetric method*

The development of a simple and precise method[1] for the determination of glucose led us to investigate its application to the determination of mono- and disaccharides. In addition to the methods cited previously,[1] both spectrophotometric[2–4] and spectrofluorimetric[5] methods for the determination of various sugars have been reported. The determination of glucose and other sugars by different colorimetric methods has been discussed by several workers.[6–10] Chromatographic[11–13] and polarographic[14,15] methods for the determination of sugars have also been reported. Bark *et al.*[16] developed a thermometric method for this purpose. An automated assay for the direct determination of D-fructose in a mixture with D-glucose has been developed.[17] The simple and rapid determination of ketoses by circular dichroism measurements has recently been reported.[18]

Experimental

The saccharides (Merck) were stored over concentrated sulphuric acid in a desiccator for at least 1 week before use. It is known that fructose is hygroscopic and becomes moist on prolonged exposure to the atmosphere. Hence it was dried at 50 °C under vacuum for 16 h and then analysed. (Found: C, 40.37; H, 6.70. Calc. for $C_6H_{12}O_6$: C, 40.00; H, 6.67%). Sodium (or ammonium) metavanadate, perchloric acid (70%), potassium iodide, potassium dichromate (all of guaranteed-reagent grade, Merck), sodium thiosulphate (Merck) and hydrochloric acid (analytical-reagent grade, Biosol) were used. A freshly prepared starch solution was used as the indicator. Doubly distilled water (prepared by refluxing over $KMnO_4$) was used throughout.

Preparation and Standardization of Sodium Thiosulphate Solution

Sodium thiosulphate pentahydrate (25 g) was dissolved in water (400 ml) and allowed to stand at room temperature for 48 h with occasional stirring, during which time a small amount of a colourless precipitate was formed. The solution was filtered through cotton wool and the clear filtrate diluted to 1000 ml. The sodium thiosulphate solution thus obtained was standardized iodimetrically using standard potassium dichromate solution.[19] This solution can be diluted further whenever required.

Preparation and Iodimetric Standardization of the Vanadium(v) Solution

The clear yellow solution obtained by dissolving sodium (or ammonium) metavanadate (0.05 mol) in hot water (200 ml) was allowed to cool to room temperature. It was poured slowly into a cold solution of perchloric acid (70%; 170 ml) in water (200 ml) with stirring, whereupon a transparent yellow solution of the metavanadate (approximately 0.1 mol l^{-1}, caused by the reduction of V^V to V^{IV}) was obtained. This solution was standardized iodimetrically by the method described previously.[1]

Standardization of the Metavanadate Solution With Standard Fructose Solution: Determination of Fructose in Solutions of Unknown Strength

A solution of fructose (0.9244 g dl^{-1}) was prepared. A mixture of this fructose solution (2 ml) and the standardized metavanadate solution (30 ml, added from a burette) was placed in a standard-jointed round-bottomed flask (100 ml) fitted with a condenser (8 in) and was heated under reflux over a small flame for 40 min. The resulting green–blue solution was cooled to room temperature. The condenser was washed with water (10 ml) and the washings were added to the reaction mixture. The residual metavanadate was determined iodimetrically.[1] The end-point was indicated by a sharp and stable colour change from purple to deep blue. Blank experiments were carried out in the above procedure, which was adopted for the determination of fructose in solutions of unknown strength (Table 1).

The titre values remained unchanged on refluxing the reaction mixture for different periods of time ranging from 30

Table 1 Determination of fructose in solutions of unknown strength with a vanadium(v) solution, which was standardized against a fructose solution of known strength

Solution No.	Fructose concentration/g dl^{-1}	
	Actual	Found*
1	0.1084	0.1072 ± 0.0015
2	0.3299	0.3321 ± 0.0002
3	0.4561	0.4575 ± 0.0026
4	0.6867	0.6822 ± 0.0025
5	0.7709	0.7743 ± 0.0020
6	0.9048	0.9051 ± 0.0065
7	0.9770	0.9765 ± 0.0016
8	1.3976	1.3913 ± 0.0015
9	2.8956	2.9148 ± 0.0028
10	5.5740	5.5037 ± 0.0035
11	6.9672	7.0453 ± 0.0030
12	10.9192	10.6147 ± 0.0053

* Mean of six determinations ± standard deviation.

to 120 min. This was found to be true for all of the sugars studied. Therefore, refluxing for 40 min is recommended.

Determination of Fructose in a Solution With Vanadium(v) Standardized Against a Glucose Solution of Known Strength

The solutions of glucose (1.0564 g dl^{-1}) and fructose (1.2668 g dl^{-1}) were taken as the known and the unknown solutions, respectively. The metavanadate solution was standardized against the glucose solution (2 ml for each experiment) and then fructose (2 ml for each experiment) was determined using the standardized metavanadate solution as described above (Table 2).

Determination of Fructose Taken in the Solid State

Accurately weighed samples of fructose (30–150 mg) were placed in a standard-jointed round-bottomed flask (100–250 ml) and treated with a known excess of the metavanadate solution (40–160 ml depending on the amount of fructose taken). Each reaction mixture was then refluxed for 40 min and the excess of metavanadate was determined in the usual way (Table 3).

Calculations

Equal volumes of known and unknown sugar solutions were taken for each determination. If W is the concentration of sugar (g dl^{-1}) present in a solution of known strength, z is the titre value (ml) of thiosulphate solution required for a blank titration of the vanadium(v) solution taken, and x and y are the titre values (ml) of the same thiosulphate solution required for the determination of the residual vanadium(v) after the oxidation of sugar solutions of known and unknown strengths, respectively, then the concentration of sugar S (g dl^{-1}) present in the solution of unknown strength is given by:

$$S = \frac{W(z - y)}{(z - x)}$$

Determination of Other Monosaccharides

A number of other monosaccharides, *viz.*, mannose, galactose, arabinose, ribose and xylose, were determined using the procedure described above for the determination of fructose. In each instance the respective monosaccharide solution was standardized against the same monosaccharide solution of known strength, and also against a standard glucose solution. The results are presented in Tables 4–14.

Determination of Disaccharides

Sucrose and maltose were also determined by the procedure described above. In this instance the respective disaccharides were standardized against the same sugar and also against each other. The results are presented in Tables 15–18.

Table 2 Determination of fructose in solutions of unknown strength with a vanadium(v) solution, which was standardized against a glucose solution of known strength

Solution No.	Fructose concentration/g dl^{-1}	
	Actual	Found*
1	1.2668	1.2748
2	0.9048	0.9054
3	0.7709	0.7742

* Mean of six determinations.

Table 3 Determination of fructose, by directly weighing solid fructose into the reaction flask, with a vanadium(v) solution, which was standardized against either a fructose or glucose solution

Experiment No.	Amount of fructose/g	
	Actual	Found
1	0.0365	0.0361
2	0.0510	0.0506
3	0.0680	0.0677
4	0.0877	0.0874
5	0.0911	0.0917
6	0.1218	0.1222

Table 4 Determination of mannose in solutions of unknown strength with a vanadium(v) solution, which was standardized against a mannose solution of known strength

Solution No.	Mannose concentration/g dl^{-1}	
	Actual	Found*
1	1.0310	1.0260
2	0.3093	0.3110
3	0.5155	0.5124
4	0.7217	0.7158

* Mean of six determinations.

Table 5 Determination of mannose in solutions of unknown strength with a vanadium(v) solution, which was standardized against a glucose solution of known strength

Solution No.	Glucose concentration/g dl^{-1}	Mannose concentration/g dl^{-1}	
		Actual	Found*
1	1.0962	1.0310	1.0257
2	1.0962	0.7418	0.7437
3	1.0962	0.3093	0.3115

* Mean of six determinations.

Table 6 Determination of galactose in solutions of unknown strength with a vanadium(v) solution, which was standardized against a galactose solution of known strength

Solution No.	Galactose concentration/g dl^{-1}	
	Actual	Found*
1	0.1600	0.1614
2	0.3440	0.3431
3	0.6032	0.6022

* Mean of six determinations.

Table 7 Determination of galactose in solutions of unknown strength with a vanadium(v) solution, which was standardized against a glucose solution of known strength

Solution No.	Glucose concentration/g dl^{-1}	Galactose concentration/g dl^{-1}	
		Actual	Found*
1	0.2587	0.8051	0.8030
2	0.2587	0.6032	0.6050
3	0.2587	0.1600	0.1620

*Mean of six determinations.

Table 8 Determination of arabinose in solutions of unknown strength with a vanadium(v) solution, which was standardized against an arabinose solution of known strength

Solution No.	Arabinose concentration/g dl^{-1}	
	Actual	Found*
1	0.2724	0.2787
2	0.4086	0.4086
3	0.5448	0.5404

* Mean of six determinations.

Table 9 Determination of arabinose in solutions of unknown strength with a vanadium(v) solution, which was standardized against a glucose solution of known strength

Solution No.	Glucose concentration/ g dl^{-1}	Arabinose concentration/g dl^{-1}	
		Actual	Found*
1	1.0962	0.6811	0.6813
2	1.0962	0.9572	0.9580
3	1.0962	1.0852	1.0876

*Mean of six determinations.

Table 10 Determination of ribose in solutions of unknown strength with a vanadium(v) solution, which was standardized against a ribose solution of known strength

Solution No.	Ribose concentration/g dl^{-1}	
	Actual	Found*
1	0.9335	0.9325
2	0.8090	0.8069
3	0.5601	0.5617
4	0.3734	0.3790

* Mean of six determinations.

Table 11 Determination of ribose in solutions of unknown strength with a vanadium(v) solution, which was standardized against a glucose solution of known strength

Solution No.	Glucose concentration/ g dl^{-1}	Ribose concentration/g dl^{-1}	
		Actual	Found*
1	0.9587	0.9335	0.9276
2	0.9587	0.8090	0.8122
3	0.9587	0.6265	0.6295

* Mean of six determinations.

Table 12 Determination of ribose, by directly weighing solid ribose into the reaction flask, with a vanadium(v) solution, which was standardized against either a ribose or glucose solution

Experiment No.	Amount of ribose/g	
	Actual	Found
1	0.0672	0.0667
2	0.0759	0.0751
3	0.0882	0.0887
4	1.2628	1.2648

Table 13 Determination of xylose in solutions of unknown strength with a vanadium(v) solution, which was standardized against a xylose solution of known strength

Solution No.	Xylose concentration/g dl^{-1}	
	Actual	Found*
1	0.9950	0.9934
2	0.8182	0.8192
3	0.7620	0.7649
4	0.3640	0.3627

* Mean of six determinations.

Table 14 Determination of xylose in solutions of unknown strength with a vanadium(v) solution, which was standardized against a glucose solution of known strength

Solution No.	Glucose concentration/ g dl^{-1}	Xylose concentration/g dl^{-1}	
		Actual	Found*
1	0.2587	0.8182	0.8195
2	0.2587	0.4142	0.4152
3	0.2587	0.3640	0.3680

*Mean of six determinations.

Table 15 Determination of sucrose in solutions of unknown strength with a vanadium(v) solution, which was standardized against a sucrose solution of known strength

Solution No.	Sucrose concentration/g dl^{-1}	
	Actual	Found*
1	0.1212	0.1218 ± 0.0004
2	0.3049	0.3059 ± 0.0038
3	0.4279	0.4258 ± 0.0047
4	0.5000	0.5013 ± 0.0067
5	0.7660	0.7704 ± 0.0086
6	0.9080	0.9057 ± 0.0054
7	1.5820	1.5714 ± 0.0045
8	3.2418	3.2615 ± 0.0091
9	5.4720	5.5134 ± 0.0048

* Mean of six determinations ± standard deviation.

Table 16 Determination of sucrose, by directly weighing solid sucrose into the reaction flask, with a vanadium(v) solution, which was standardized against a sucrose solution of known strength

Experiment No.	Amount of sucrose/g	
	Actual	Found
1	0.0520	0.0524
2	0.0616	0.0615
3	0.0671	0.0671
4	0.0941	0.0930
5	0.0996	0.1004
6	0.1035	0.1020
7	0.1409	0.1402
8	0.1577	0.1594
9	0.1680	0.1690

Table 17 Determination of maltose in solutions of unknown strength with a vanadium(v) solution, which was standardized against a maltose solution of known strength

Solution No.	Maltose concentration/g dl^{-1}	
	Actual	Found*
1	4.6468	4.6906
2	0.9777	0.9635
3	0.7708	0.7771
4	0.5950	0.5979
5	0.3854	0.3891

* Mean of six determinations.

Interference Studies

It was observed[1] that toluene, acenaphthene, styrene, phenol, 2-naphthol, benzaldehyde, cyclohexanol, nitrobenzene, aniline, mandelic acid, salicylic acid, formic acid, *N*,*N*-dimethylformamide and chloroform were serious interferents, whereas benzene, naphthalene, ethanol, *tert*-butanol, benzophenone, glycine and dimethyl sulphoxide interfered to a lesser extent. Acetone and acetic acid did not interfere. Depending on the properties of the interferents, some of them can be removed by appropriate techniques such as evaporation, steam distillation and solvent extraction.

Discussion

As reported previously,[1] doubly distilled water must be used throughout in order to avoid inconsistent results. The approximately 0.1 mol l^{-1} metavanadate solution has to be prepared very carefully. Solutions of sodium (or ammonium) metavanadate (0.05 mol) in hot water (200 ml) and perchloric acid (70%; 170 ml) in water (200 ml) must be cooled separately to room temperature and the solutions mixed very slowly with constant stirring. Rapid addition of the metavanadate solution to the perchloric acid leads to a rise in temperature, and the formation of a red precipitate, which renders the solution

Table 18 Determination of maltose in solutions of unknown strength with a vanadium(v) solution, which was standardized against a sucrose solution of known strength

Solution No.	Sucrose concentration/ g dl^{-1}	Maltose concentration/g dl^{-1}	
		Actual	Found*
1	1.2960	1.2765	1.2700
2	1.2960	0.9635	0.9530
3	1.2960	0.3854	0.3882

* Mean of six determinations.

unsuitable for use. It should be noted that the strength of the reagent is critical, as a more concentrated metavanadate solution invariably caused the red precipitate to appear during refluxing, whereas with very dilute metavanadate solutions the consumption of the reagent by the sugar was incomplete even on prolonged refluxing. The recommended procedure is to reflux a known volume of a saccharide solution for 40 min with a known volume of the oxidant solution composed of metavanadate (1 g) and a mixture of perchloric acid (70%; 30 ml) and water (72 ml). Refluxing for less than 30 min resulted in the incomplete oxidation of all the mono- and disaccharides; beyond 30 min no change of titre values was noted on prolonging the time of reflux up to 120 min. Perchloric acid having this specified dilution does not liberate iodine from potassium iodide under the experimental conditions.

The vanadium(v) solution was standardized[1] by titration against a thiosulphate solution of known strength.[19] Hence, a known volume of the metavanadate solution (taken from a burette) was heated under reflux for 40 min, cooled and then determined iodimetrically. Identical results were obtained when this titration was conducted at room temperature, thereby confirming that the metavanadate solution is not affected by refluxing; it also remained unchanged on storage, even after 6 months at room temperature. The volume of water required for the washings in each titration was restricted to 10 ml in order to ensure that a stable end-point was obtained. Moreover, in order to ensure that the reaction conditions are identical in each instance, the standardization of vanadium(v) through refluxing is recommended.

The lower and upper limits of the accurate determination of fructose were established by using the metavanadate solution standardized against a fructose solution of known strength (approximately 1%). The results are given in Table 1, which shows that accurate results were obtained when the concentration of the fructose solution ranged from 0.3 to 3.0 g dl^{-1}; however, with either very dilute or very concentrated solutions the results were inaccurate. Similarly, the metavanadate solution standardized against a sucrose solution of known strength (approximately 1%) was used to ascertain the upper and lower limits of the accuracy of the determination of sucrose in solution (Table 15). The results show that the accuracy of the method is good; however, the precision is moderate for the determination of sucrose. It should be noted that accurately weighed samples of mono- and disaccharides, placed directly in the reaction flask, also afforded good results (Tables 3, 12 and 16). Moreover, it was observed that metavanadate solutions standardized against a monosaccharide did not afford good results for the determination of the disaccharides, and *vice versa*. Further studies in this area, particularly on the determination of sugar alcohols, saccharic acids and other classes of sugars, and also on product analysis, are currently in progress.

Conclusion

A method for the determination of mono- and disaccharides has been developed, which is less hazardous and tedious than Fehling's method (see Table 19), although the latter is suitable for the determination of mixtures of reducing monosaccharides (*e.g.*, glucose) and non-reducing disaccharides (*e.g.*, sucrose). Glucose or sucrose solutions of known strengths can be employed for the standardization of the metavanadate solution for the determination of mono- and disaccharides, respectively. Better results are obtained if a metavanadate solution standardized against a saccharide solution of known strength is employed for the determination of the same saccharide. The advantages of the proposed method are: (*i*) inexpensive and non-toxic chemicals are used; (*ii*) simultaneous determinations can be carried out in any laboratory; and (*iii*) the end-point is stable and sharp.

Table 19 Comparison of the standard Fehling's method with the proposed metavanadate method

	Fehling's method	Metavanadate method
1	Sugar determined in solution	Sugar determined in solution and also in the solid state
2	Titration carried out under boiling conditions; hence, difficult and hazardous	Iodimetric titration carried out at room temperature; hence the method is much easier
3	The end-point is unstable and difficult to ascertain even with Methylene Blue as indicator, particularly under conditions of insufficient illumination	The end-point is stable, sensitive and very sharp (purple to deep blue) and can be ascertained without any difficulty
4	Comparatively large amounts (decigrams) of sugars are required	Relatively small amounts (milligrams) of sugar can be determined
5	Not very accurate; error is occasionally within ±5%	Very accurate; error is generally within ±1%
6	Time required for each titration is 10–15 min	Refluxing followed by titrimetric analysis requires 40 min
7	Only one experiment can be carried out at a time	Simultaneous determinations can be carried out
8	Applicable to reducing sugars only; hence, mixtures containing mono- and disaccharides can be determined	Applicable to all types of sugars, including sugar alcohols, saccharic acids and related compounds. Mixtures containing mono- and disaccharides cannot be determined
9	Less susceptible to interference from different classes of organic compounds	Various organic and inorganic materials interfere

The authors thank S. P. Bag, Head of the Department of Chemistry, Jadavpur University, and G. Raymahasay, M/S. Life Pharmaceuticals, Calcutta, for generous support of this work. A. P. thanks B. Bose, Head of the Department of Chemistry, Lady Brabourne College, for helpful suggestions and B. H. thanks the University Grants Commission, New Delhi, for a Research sponsorship.

References

1 Banerjee, A., Hazra, B., Chatterjee, H., Banerjee, S., and Dutt, S., *Analyst*, 1989, **114**, 1151.
2 Zipf, R. E., and Waldo, A. L., *J. Lab. Clin. Med.*, 1952, **39**, 497.
3 Ando, M., and Kiuchi, R., *Nippon Nogei Kagaku Kaishi*, 1964, **38**, 428; *Chem. Abstr.*, 1965, **63**, 4501b.
4 Rogers, C. J., Chambers, C. W., and Clarke, N. A., *Anal. Chem.*, 1966, **38**, 1851.
5 Lokar, L. C., *Univ. Studi Trieste, Fac. Econ. Commer., Ist. Merceol.*, (*Pubbl.*), 1965, **25**, 24; *Chem. Abstr.*, 1967, **66**, 34 656w.

6 Nanba, A., and Matsuo, Y., *Hakko Kyokaishi*, 1963, **21**, 105; *Chem. Abstr.*, 1965, **62**, 15 432c.
7 Avigad, G., *Carbohydr. Res.*, 1968, **7**, 94.
8 Kachalova, M. F., Kulikov, Yu. M., Kozlov, V. V., and Khrustaleva, V. N., *Izv. Vyssh. Uchebn. Zaved., Pishch. Tekhnol.*, 1971, **6**, 154; *Chem. Abstr.*, 1972, **76**, 142 114x.
9 Namigohar, F., Makhani, M., and Kamal, F., *Q. J. Crude Drug Res.*, 1981, **19**, 169; *Chem. Abstr.*, 1982, **96**, 129 873y.
10 Tsutsui, K., Tanaka, T., and Oda, T., *Anal. Biochem.*, 1977, **79**, 349.
11 Barbiroli, G., *Rass. Chim.*, 1965, **17**, 62; *Chem. Abstr.*, 1965, **63**, 11 843d.
12 Bracher, C., and Bauly, L. E., *Food Manuf.*, 1965, **40**, 38; *Chem. Abstr.*, 1965, **63**, 13 549f.
13 Sweely, C. C., Wells, W. W., and Bentley, R., *Methods Enzymol.*, 1966, **8**, 95; *Chem. Abstr.*, 1968, **69**, 16 709y.
14 Nanba, A., and Matsuo, Y., *Hakko Kogaku Zasshi*, 1964, **42**, 216; *Chem. Abstr.*, 1966, **65**, 36e.
15 Corlett, R. D., Breck, W. C., and Hay, G. W., *Can. J. Chem.*, 1970, **48**, 2474.
16 Bark, L. S., Edwards, D., and Prachuabpaibul, P., *Proc. Soc. Anal. Chem.*, 1974, **11**, 170.
17 Kennedy, J. F., and Chaplin, M. F., *Carbohydr. Res.*, 1975, **40**, 227.
18 Kimura, A., Chiba, S., and Yoneyama, M., *Carbohydr. Res.*, 1988, **175**, 17.
19 Vogel, A. I., *A Text-Book of Quantitative Inorganic Analysis*, Longman, London, 4th edn., 1978, p. 376.

Paper 0/05627H
Received December 14th, 1990
Accepted May 9th, 1991

Application of a Microwave Oven for Drying and Nitric Acid Extraction of Mercury and Selenium From Fish Tissue

Suei Y. LamLeung, Vincent K. W. Cheng and Yuet W. Lam
Department of Chemistry, Hong Kong Baptist College, 224 Waterloo Road, Kowloon, Hong Kong

The drying and nitric acid digestion of fish tissue using a microwave oven for the determination of Hg and Se were studied. For the drying process, the method was compared with the freeze-drying method. The water content found in the muscle of tilapia, *Oreochromis mossanicus*, by using a freeze dryer at −40 °C and a pressure of ≤10 μmHg for 24 h, and a microwave oven (convection mode) at 70 °C for 3 h was 78.16 and 78.09% m/m, respectively. The Hg and Se levels found in fish tissues dried by the two methods were consistent with a 95% confidence level. The efficiency of dissolution of Hg and Se from dried muscle of tilapia, using concentrated HNO_3 in the closed vessel microwave digestion method was found to be much greater than that of traditional open vessel digestion. The microwave heating digestion method was tested satisfactorily using two certified reference materials. The recovery of added standards of Hg and Se was found to be 84.8 and 96.6%, respectively.

Keywords: *Microwave heating and drying; fish tissue; nitric acid ashing; selenium determination; mercury determination*

The process of drying and dissolution of biological materials is a lengthy task. The application of a microwave oven for wet ashing in a closed vessel containing geological and biological materials has been found to be an efficient method for the preparation of sample solutions for metal determination.[1–3] A study of the application of a commercial microwave oven in drying and wet ashing of fish tissue for the determination of Hg and Se is reported here. Only HNO_3 was used in this ashing process, as it is a strong oxidizing agent and also the nitrates of most metals are soluble in water. Low microwave power was used for safety reasons.

A sample of muscles of small individuals of tilapia of length <19 cm was used for the investigation of the microwave and freeze-drying processes. The muscles of large individuals of tilapia of length 26–31 cm were used for the study of the wet ashing processes in a closed vessel by microwave heating and in an open vessel by thermal heating.

Recovery of added standards using the microwave method of digestion in a closed vessel was also studied. The microwave digestion method was tested by its application to two certified reference materials.

Experimental

Apparatus

A commercial microwave oven (Sharp, Model R-9H10) with a frequency of 2450 MHz (power output of 750 W for microwave mode and 1500 W for convection heating) and a turntable was used for digestion and drying without modification. Sample digestion was carried out in capped 60 ml polytetrafluoroethylene (PTFE) vessels (Savillex, Model 561R2). A block digestor (Techne, Model DG-1) with a temperature controller (Techne, Model TC-D1A) was used for open vessel digestion of samples. For the wet ashing process, a wide-mouthed earthenware vessel with a lid was used as it protects the microwave oven from the corrosive vapour released or from any explosion of the digestion vessel. All containers were treated successively with detergent (washing), tap water (rinsings), 70% m/m HNO_3 for glassware (rinsing) or 0.5% m/v HNO_3 for plastics (soaked for at least 24 h).

An atomic absorption spectrometer (Varian, Model SpectrAA-10) equipped with a hydride vapour generation accessory (Perkin-Elmer, Model MHS-10) was used for the determination of Hg and Se.

A freeze dryer (Labconco 75034) was used for drying the fresh muscle of tilapia collected from a local river.

Reagents

All chemicals used were of analytical-reagent grade. A stock solution of 1000 μg ml^{-1} of Hg was prepared by dissolving 1.080 g of HgO in the minimum volume of HCl (1 + 1), and diluting to 1 l with 1.5% m/v HCl. A stock solution of 1000 μg ml^{-1} of Se was prepared by dissolving 1.000 g of Se in approximately 5 ml of 70% m/m HNO_3, and diluting to 1 l with 5% m/v H_2SO_4.

Working standard solutions were prepared immediately before use by serial dilution of the stock solutions. The working ranges were as follows: Hg, 2–16 ppb for sample analysis and 50–200 ppb for recovery investigation; and Se, 2–12 ppb for sample analysis and 50–120 ppb for recovery investigation.

The reducing solution was prepared fresh daily by dissolving 6 g of $NaBH_4$ and 2 g of NaOH in 200 ml of distilled water.

Samples

The axial muscle of tilapia, *Oreochromis mossanicus* (Peters), collected from a local river, and National Research Council Canada (NRCC) certified reference materials (DORM-1, Dogfish Muscle and DOLT-1, Dogfish Liver) were studied.

Analytical Procedure

During wet digestion in a closed vessel by microwave heating the following precautions must be considered: the mass of sample used for digestion should not be greater than 0.2 g; the total volume of reactants should not exceed one tenth of the volume of the container;[4] the heating times at high power should not be longer than 5 min; the digestion vessel must be cooled before opening; and a digestion vessel with a pressure releasing cap should be used.

Drying of sample

A collection of axial muscles of small individuals (<19 cm in length) of tilapia caught from a local river was homogenized in a stainless-steel blender. About half of the sample, 50 g, was spread thinly on several clean watch-glasses and placed in a microwave oven. The samples were dried (convection mode) at 70 °C for 2–3 h until constant mass was obtained. The

samples were removed from the oven and turned over every 20 min to ensure thorough drying. The remaining portion of the sample was dried in a freeze dryer at −40 °C and <10 μmHg for 24 h. The axial muscles of large individuals (26–31 cm) of tilapia were treated in the same manner using a microwave oven.

Dissolution of sample

The microwave digestion of tilapia tissues or certified reference material was carried out using four replicates of about 0.2 g of the dried muscle weighed into a dried, cleaned PTFE digestion vessel. A 4 ml aliquot of 70% m/m HNO_3 was added to each digestion vessel. Four tightly capped digestion vessels and one small beaker filled with 30 ml of water were placed in a wide-mouthed earthenware vessel. The lidded vessel was placed in the microwave oven. The samples were treated using three heating stages: low power (10%) for 8 min, medium–low power (30%) for 8 min and medium power (50%) for 4 min.[5] The earthenware vessel was removed from the microwave oven and then uncovered and cooled to room temperature. The cap of the digestion vessel was opened slightly to release any pressure before being removed. The digest was quantitatively transferred into a 100 ml beaker and evaporated to <1 ml by heating to decompose any unused HNO_3. The solution was filtered through Whatman No. 42 filter-paper and quantitatively transferred into a 25 ml calibrated flask. It was diluted to volume with 0.1% m/v HNO_3. The solution was then stored in a polyethylene bottle.

For open vessel thermal digestion, four replicates of a sample (about 2 g) of dried muscle of tilapia were weighed into four 50 ml boiling tubes. The sample was pre-digested at 20 °C for 24 h with 10 ml of 70% m/m HNO_3. The sample was then heated at 100 °C for 3 h. Three additional portions of 5 ml of 70% m/m HNO_3 were introduced into the boiling tube successively at intervals of 30 min. When a clear solution was obtained, the temperature was raised to 130 °C to decompose all the unused HNO_3. After cooling, the digest was filtered through Whatman No. 42 filter-paper then quantitatively transferred into a 25 ml calibrated flask and diluted to volume with 0.1% m/v HNO_3. The sample was stored in a polyethylene bottle for elemental determination.

Recovery of added standard

A known mass of the analyte, 100, 200, 300 and 400 ng of Hg and 100, 140, 200 and 240 ng of Se, together with 4 ml of 70% m/m HNO_3 were introduced into the Teflon digestion vessel. The digestion process in the microwave oven was the same as for the fish sample.

Mercury and selenium determination

In each trial, 10 ml of the sample solution or working standard solution were used. A 1 ml volume of 30% HCl and 2 ml of reducing agent (a mixture of 3% m/v $NaBH_4$ and 1% m/v NaOH) were added to the vapour generator. The solution was continuously purged with a stream of N_2 at a pressure of 250 Pa. The absorbance at 253.7 nm was measured for the determination of Hg and at 196.0 nm for Se.[6]

An acid blank solution was used in the determination of the analytes.

Results and Discussion

The data given in Table 1 indicate that the quality of the microwave-dried tissue was satisfactory. The colour of the microwave-dried tissue was similar to that of sun-dried tissue. The water content found in the species studied was 78.09% m/m (by microwave drying) and 78.16% (by freeze-drying). There was no significant difference ($P > 0.05$) in the values of Hg and Se found in specimens dried by the two methods. These results were consistent with results reported by Koh.[7]

The recovery of the added Hg and Se standards digested by microwave heating in a closed vessel was also found to be satisfactory (Table 2). The recovery of added standard was

Table 1 Water content and concentration of Hg and Se in muscle of small species of tilapia dried by a freeze dryer and microwave oven

Analyte	Microwave oven	Freeze dryer
Water content (% m/m)	78.09	78.16
Hg/μg g^{-1} dry mass	3.777 ± 0.198*	3.846 ± 0.127*
Se/μg g^{-1} dry mass	2.224 ± 0.021*	2.176 ± 0.022*

* Mean values with standard deviations for four replicate determinations.

Table 2 Recovery of added standard after microwave heating under pressure in the presence of 70% m/m HNO_3

Element	Added/ng	Found*/ng	Recovery (%)	Mean (%)
Hg	100	84.5 ± 0.0	84.5 ± 0.0	
	200	177.9 ± 0.9	89.0 ± 0.5	
	300	252.8 ± 1.4	84.3 ± 0.5	
	400	325.0 ± 2.4	81.3 ± 0.6	84.8 ± 3.2
Se	100	98.1 ± 0.0	98.1 ± 0.0	
	140	139.5 ± 4.4	99.6 ± 3.1	
	200	197.4 ± 3.4	98.7 ± 1.7	
	240	215.6 ± 2.7	89.8 ± 1.1	96.6 ± 4.5

* Mean values with standard deviations for triplicate determinations.

Table 3 Comparison of the dissolution of dried muscle of large species of tilapia by using closed vessel microwave digestion and open vessel digestion in the presence of 70% m/m HNO_3, shown by recovery of added analytes

	Recovery/μg g^{-1}	
Element	Microwave digestion* (closed vessel)	Open vessel digestion
Hg	3.91 ± 0.29	1.24 ± 0.02
Se	1.71 ± 0.08	1.25 ± 0.00

* Mean values with standard deviations for four replicate determinations.

Table 4 Comparison of the found and certified values of Hg and Se in the NRCC certified reference materials DORM-1 and DOLT-1 (reference 9)

		Hg		Se	
Sample		Found*/ μg g^{-1}	Certified value/μg g^{-1}	Found†/ μg g^{-1}	Certified value/μg g^{-1}
DORM-1	Trial 1	0.759 ± 0.030		1.44 ± 0.03	
	Trial 2	0.754 ± 0.019		1.43 ± 0.01	
	Mean	0.757 ± 0.025	0.798 ± 0.074	1.44 ± 0.02	1.62 ± 0.12
DOLT-1	Trial 1	0.185 ± 0.026		6.64 ± 0.16	
	Trial 2	0.194 ± 0.012		6.60 ± 0.15	
	Mean	0.190 ± 0.019	0.225 ± 0.037	6.62 ± 0.16	7.34 ± 0.42

* Mean value with standard deviation for four replicate determinations using cold vapour atomic absorption spectrometry.
† Mean value with standard deviation for four replicate determinations using hydride generation atomic absorption spectrometry.

found to be 84.8 ± 3.2 and 96.6 ± 4.5% for Hg (100–400 ng) and Se (100–240 ng), respectively.

The dissolution of the more volatile Hg and Se from fish tissue was superior to the traditional open vessel digestion (Table 3). The recovery of Hg and Se from samples of the large tilapia by open vessel digestion was only 35 and 68%, respectively, of the recovery by microwave heating under pressure. The results show that the closed digestion vessel can contain the samples tightly and the sample tissue is digested more completely at an elevated temperature and under pressure by microwave heating.[8]

The microwave method was tested by studying two NRCC certified reference materials. A comparison of the values of Hg and Se found in DORM-1 (Dogfish Muscle) and DOLT-1 (Dogfish Liver) with the certified values is given in Table 4.[9] The mean concentration of Hg found was within one standard deviation of the certified value in both the Dogfish Muscle and Dogfish Liver. For Se, the mean concentration was within two standard deviations of the certified value. The recovery of Hg from Dogfish Muscle and Dogfish Liver was 94.9 and 84.4%, respectively. For Se, the recovery was 88.9 and 90.2%, respectively.

In conclusion, a method of microwave heating has been applied for the effective determination of the more volatile elements (Hg and Se) in biological samples. Microwave heating can be used for drying and wet ashing of fish tissue more efficiently than thermal heating in an open vessel in terms of a shorter time and smaller amounts of chemicals consumed.

References

1 Fischer, L. B., *Anal. Chem.*, 1986, **58**, 261.
2 Bettinelli, M., Baroni, U., and Pastorelli, N., *Anal. Chim. Acta*, 1989, **225**, 159.
3 Aysola, P., Anderson, P., and Langford, C. H., *Anal. Chem.*, 1987, **59**, 1582.
4 Gedye, R., Smith, F., and Westaway, K., *Educ. Chem.*, 1988, **25**, 55.
5 Vermeir, G., Vandecasteele, C., and Dams, R., *Anal. Chim. Acta*, 1989, **220**, 257.
6 Tsalex, D. L., *Atomic Absorption Spectrometry in Occupational and Environmental Health Practice*, CRC Press, Boca Raton, FL, 1986, vol. 2, pp. 127–145 and 167–178.
7 Koh, T. S., *Anal. Chem.*, 1980, **52**, 1978.
8 Kingston, H. M., and Jassie, L. B., *Anal. Chem.*, 1986, **58**, 2534.
9 Marine Analytical Chemistry Standards Program, Dogfish Muscle and Liver Reference Materials for Trace Metals, National Research Council Canada, Ottawa, 1986.

Paper 1/01249E
Received March 15th, 1991
Accepted May 20th, 1991

Separation of Niobium From Chloride Media by Solvent Extraction With Dicyclohexyl-18-crown-6

N. V. Deorkar and S. M. Khopkar*
Department of Chemistry, Indian Institute of Technology, Powai, Bombay-400 076, India

Niobium was quantitatively extracted from 7–10 mol dm^{-3} hydrochloric acid with 2.0×10^{-2} mol dm^{-3} dicyclohexyl-18-crown-6 in dichloromethane. The metal was stripped from the organic phase with 0.1 mol dm^{-3} sulphuric acid and determined spectrophotometrically at 540 nm as its complex with 4-(2-thiazolylazo)resorcinol. This method permits the sequential separation of niobium from vanadium, tantalum, zirconium, hafnium and iron.

Keywords: *Niobium; solvent extraction; crown ether; separation; spectrophotometry*

Solvent extraction is a useful method for the separation of niobium and tantalum. Diethyl ether,[1] 8-hydroxyquinoline[2] and *N*-benzoyl-*N*-phenylhydroxylamine[3] have been used for the separation of these two elements as they do not extract tantalum. Isobutyl methyl ketone[4] and tributyl phosphate (TBP)[5] have been applied as extractants for tantalum. The separation of niobium from tantalum has been carried out with Amberlite LA-2 from malonate media;[6] tantalum was not extracted and was therefore separated from niobium. In extraction–chromatography, bis-(2-ethylhexyl)phosphoric acid has also been used to separate niobium from tantalum.[7] Dibenzo-18-crown-6 has been used for the extractive spectrophotometric determination of niobium.[8,9] However, no systematic investigations into solvent extraction separation with crown ethers have been carried out so far; such studies are described in this paper.

Experimental

Apparatus and Reagents

An Orion Model 901 ion analyser with a combined glass and calomel electrode, an Electronic Corporation of India (ECIL) Model GC866C spectrophotometer with 10 mm matched Corex glass cuvettes, and a wrist-action flask shaker were used.

A stock solution of niobium (1 mg ml^{-1}) was prepared by first fusing 0.370 g of niobium pentoxide with potassium hydrogen sulphate. The fused mass was then dissolved in 20 ml of 20% tartaric acid solution and made up to 250 ml with de-ionized water. The solution was standardized gravimetrically.[10] A solution containing 25 μg ml^{-1} of niobium was prepared by appropriate dilution of the stock solution.

15-Crown-5 (15C5), 18-crown-6 (18C6), dibenzo-18-crown-6 (DB18C6), dicyclohexyl-18-crown-6 (DC18C6) and dicyclohexyl-24-crown-8 (DC24C8) (Merck) were used without further purification.

General Procedure

To an aliquot of a solution containing 25 μg of niobium, hydrochloric acid was added in order to adjust the concentration of the latter to 7 mol dm^{-3} in a total volume of 10 ml. The solution was transferred into a separating funnel. Then, 10 ml of a 2.0×10^{-2} mol dm^{-3} solution of the appropriate crown ether in dichloromethane were added. The solution was shaken on the wrist-action flask shaker for 10 min. The two phases were allowed to settle and separate. Niobium was stripped from the organic phase with 10 ml of 0.1 mol dm^{-3} sulphuric acid and determined spectrophotometrically at 540 nm as its complex with 4-(2-thiazolylazo)resorcinol (TAR).[11]

* To whom correspondence should be addressed.

Results and Discussion

Effect of Hydrochloric Acid Concentration

Of all the acids examined in the extraction, *viz.*, nitric, sulphuric, perchloric and hydrochloric, only the last named was found to be effective, the ideal concentration for a phase ratio of 1 : 1 for the quantitative extraction of niobium with 2.0×10^{-2} mol dm^{-3} DC18C6 being 7.0–10.0 mol dm^{-3} hydro-

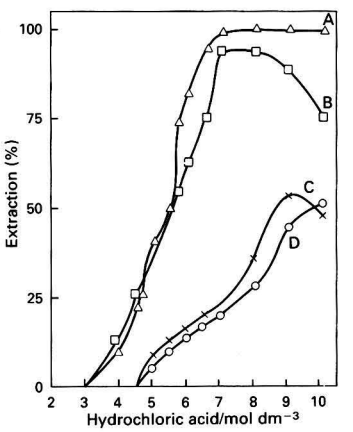

Fig. 1 Extraction of niobium as a function of the hydrochloric acid concentration. A, DC18C6; B, DC24C8; C, 18C6; and D, DB18C6

Table 1 Effect of the DC18C6 concentration on the extraction of niobium

[DC18C6]/ 10^{-3} mol dm^{-3}	Extraction (%)	*D*
0.5	22.2	0.285
1.0	35.5	0.550
1.5	44.4	0.80
1.7–2.0	47.3	0.90
2.5	48.8	0.953
2.7	54.5	1.2
3.0	58.3	1.4
3.5	62.9	1.7
3.7–4.0	66.6	2.0
4.5	68.7	2.2
5.0	70.6	2.4
5.5	71.4	2.5
6.0	72.9	2.6
10.0	81.5	4.4
15.0	93.6	14.4
20–50	100.0	∞

Table 2 Effect of stripping agents

Stripping agent	Niobium stripped (%)							
	0.01 mol dm^{-3}	0.05 mol dm^{-3}	0.1 mol dm^{-3}	0.5 mol dm^{-3}	1.0 mol dm^{-3}	2.0–4.0 mol dm^{-3}	5.0 mol dm^{-3}	6.0 mol dm^{-3}
HCl	45.0	62.5	100	100	100	100	61.7	20.0
HNO_3	31.0	56.9	78.0	100	100	100	100	96.1
H_2SO_4	52.1	87.0	100	100	100	100	100	100
$HClO_4$	38.6	61.0	73.1	100	100	100	100	100
CH_3COOH	13.3	33.3	46.6	68.3	87.6	100	100	100

Table 3 Separation of niobium from binary mixtures. Amount of Nb taken, 25 μg

Foreign ion	Added as	Ratio	Tolerance limit/mg
Li^{I}	LiCl	1:200	5.0
Na^{I}	NaCl	1:120	3.0
K^{I}	KCl	1:100	2.5
Be^{II}	$BeCl_2$	1:100	2.5
Ca^{II}	$CaCl_2·6H_2O$	1:100	2.5
Mg^{II}	$MgSO_4·7H_2O$	1:110	2.75
Sr^{II}	$Sr(NO_3)_2·2H_2O$	1:80	2.0
Ba^{II}	$Ba(NO_3)_2·4H_2O$	1:80	2.0
Al^{III}	$Al(NO_3)_3·3H_2O$	1:50	1.25
Bi^{III}	$Bi(NO_3)_3·5H_2O$	1:40	1.0
Sb^{III}	$SbCl_3$	1:4	0.10
Sc^{III}	$Sc(NO_3)_3$	1:120	3.0
Y^{III}	$Y(NO_3)_3$	1:100	2.5
Ti^{IV}	$Ti(SO_4)_2$	1:30	0.75
Zr^{IV}	$Zr(NO_3)_4·4H_2O$	1:20	0.50
Hf^{IV}	$Hf(SO_4)_2·4H_2O$	1:30	0.75
V^{IV}	$VOSO_4·H_2O$	1:40	1.0
Ta^{V}	Ta_2O_5	1:40	1.0
Cr^{III}	$Cr(NO_3)_3$	1:50	1.25
Mn^{II}	$MnSO_4·4H_2O$	1:40	1.0
Fe^{III}	$FeCl_3$	1:4	0.10
Ni^{II}	$NiSO_4·6H_2O$	1:40	1.0
Zn^{II}	$ZnSO_4·7H_2O$	1:80	2.0
Cd^{II}	$3CdSO_4·8H_2O$	1:80	2.0
U^{VI}	$UO_2(NO_3)_2·6H_2O$	1:2	0.05
Th^{IV}	$Th(NO_3)_4·4H_2O$	1:80	2.0
La^{III}	$La(NO_3)_3·6H_2O$	1:50	1.25
Ce^{III}	$Ce(NO_3)_3·6H_2O$	1:80	2.0
Nd^{III}	$Nd(NO_3)_3·6H_2O$	1:40	1.0
NO_3^-	HNO_3	1:200	5.0
SO_4^{2-}	H_2SO_4	1:200	5.0
ClO_4^-	$HClO_4$	1:200	5.0
Citrate	Citric acid	1:120	3.0
Acetate	Acetic acid	1:200	5.0
Tartrate	Tartaric acid	1:40	1.0

chloric acid (Fig. 1). The extraction with the other crown ethers was incomplete but 95% extraction was obtained over a narrow acidity range.

Effect of Crown Ether Concentration

The optimum concentration of crown ether for the quantitative extraction of niobium was ascertained by extracting the latter with various concentrations of crown ether (in the range from 0.5×10^{-3} to 5.0×10^{-2} mol dm^{-3}) (Table 1). The extraction was 71% with 5×10^{-3} mol dm^{-3} DC18C6 and quantitative with 2.0×10^{-2} mol dm^{-3} DC18C6.

Effect of Counter Ions

A study of the extraction of niobium in the presence of various counter ions and from mineral acids showed that quantitative extraction was obtained only from hydrochloric acid.

Effect of Diluent

Of the solvents examined, *viz.*, benzene, toluene, xylene, carbon tetrachloride, chloroform, dichloromethane, 1,2-dichloroethane and nitrobenzene, the last three gave 100% extraction. Dichloromethane was preferred as the diluent because it gave better phase separation.

Effect of Stripping Agents

Niobium was stripped after extraction with various concentrations of acids (0.01–6 mol dm^{-3}). Hydrochloric (0.1–4 mol dm^{-3}), nitric (0.5–5 mol dm^{-3}), sulphuric (0.1–6 mol dm^{-3}), perchloric (0.5–6 mol dm^{-3}) and acetic (2–6 mol dm^{-3}) acids were effective in stripping the niobium completely. Sulphuric acid was preferred as the stripping agent (Table 2) as it could be used over a wide range of concentrations and facilitated spectrophotometric determination.

Effect of Period of Shaking

A study of the extraction as a function of time indicated that equilibration for 10 min was adequate for the quantitative extraction of niobium.

Nature of Extracted Species

The nature of the extracted species was ascertained by plotting log D (D = distribution ratio) *versus* log [DC18C6] at 7 mol dm^{-3} hydrochloric acid and log D *versus* log [hydrochloric acid] at 2.0×10^{-2} mol dm^{-3} DC18C6. The corresponding slopes were 0.81 and 6.2, respectively. The probable composition of the extracted species is $[(NbCl_6)^- (H_3O·DC18C6)^+]$. These findings are in agreement with those reported previously by other workers.[9,12,13]

Separation of Niobium From Binary Mixtures

Niobium was extracted in the presence of a number of foreign ions (Table 3). The tolerance limit was defined as the amount of foreign ion causing an error of ±2.0% in the recovery of niobium. Alkali metals, alkaline earth metals, scandium and yttrium were tolerated at a ratio of 100:1, while bismuth, titanium, vanadium, tantalum, chromium, manganese, nickel and neodymium were tolerated at a ratio of 40:1. Antimony, iron(III) and uranium(VI) were tolerated at a lower ratio of 4:1. The anions studied were tolerated at a ratio of 200:1.

Separation of Niobium and Tantalum

Niobium and tantalum were separated by first extracting niobium from 7 mol dm^{-3} hydrochloric acid with 2.0×10^{-2} mol dm^{-3} DC18C6, when tantalum was not extracted.

Separation of Niobium From Multicomponent Mixtures

Niobium was separated from several multicomponent mixtures. In those separations involving 3 or 4 metals, tantalum, vanadium and chromium were not extracted, while zirconium,

Table 4 Separation of niobium from multicomponent mixtures

Mixture No.	Components	Extractant	Counter ion	Stripping agent	Reagent for determination
1	Nb	DC18C6, 0.02 mol dm^{-3}	7 mol dm^{-3} HCl	0.1 mol dm^{-3} H_2SO_4	TAR (540)*
	Hf	DC18C6, 0.07 mol dm^{-3}	9 mol dm^{-3} HCl	0.1 mol dm^{-3} $HClO_4$	Xylenol Orange (540)
	Ta	Not extracted	—	Aqueous phase	Brilliant Green (650)
2	Zr	TBP, 0.75 mol dm^{-3}	8 mol dm^{-3} HNO_3	1 mol dm^{-3} H_2SO_4	Arsenazo III (655)
	Nb	DC18C6, 0.02 mol dm^{-3}	7 mol dm^{-3} HCl	0.1 mol dm^{-3} H_2SO_4	TAR (540)
	Ta	Not extracted	—	Aqueous phase	Brilliant Green (650)
3	Th	18C6, 0.065 mol dm^{-3}	0.04 mol dm^{-3} picric acid (pH 2.0)	0.5 mol dm^{-3} HNO_3	Arsenazo III (650)
	Nb	DC18C6, 0.02 mol dm^{-3}	7 mol dm HCl	0.1 mol dm^{-3} H_2SO_4	TAR (540)
	Ta	Not extracted	—	Aqueous phase	Brilliant Green (650)
4	Fe^{III}	DB18C6, 0.01 mol dm^{-3}	7 mol dm^{-3} HCl	0.05 mol dm^{-3} H_2SO_4	1,10-Phenanthroline (510)
	Nb	DC18C6, 0.02 mol dm^{-3}	7 mol dm^{-3} HCl	0.1 mol dm^{-3} H_2SO_4	TAR (540)
	Cr^{III}/Ta	Not extracted	—	Aqueous phase	AAS† (319)/Brilliant Green (650)
5	Pb^{II}	DB18C6, 0.02 mol dm^{-3}	0.01 mol dm^{-3} picric acid (pH 3.0)	1 mol dm^{-3} $HClO_4$	AAS† (217.0)
	Nb	DC18C6, 0.02 mol dm^{-3}	7 mol dm^{-3} HCl	0.1 mol dm^{-3} H_2SO_4	TAR (540)
	V^{IV}	Not extracted	—	Aqueous phase	AAS† (318.4)
6	Nb	DC18C6, 0.02 mol dm^{-3}	7 mol dm^{-3} HCl	0.1 mol dm^{-3} H_2SO_4	TAR (540)
	Ta	DC18C6, 0.05 mol dm^{-3}	3.5 mol dm^{-3} HCl + 0.2 mol dm^{-3} KF	0.1 mol dm^{-3} $HClO_4$	Brilliant Green (650)
	V^{IV}	Not extracted	—	Aqueous phase	AAS† (318.4)
7	Mo^{VI}	DB18C6, 0.01 mol dm^{-3}	6 mol dm^{-3} HCl	0.1 mol dm^{-3} NaOH	Tiron (390)
	Nb	DC18C6, 0.02 mol dm^{-3}	7 mol dm^{-3} HCl	0.1 mol dm^{-3} H_2SO_4	TAR (540)
	Mn^{II}	Not extracted	—	Aqueous phase	Brilliant Green (650)

* Values in parentheses are the wavelengths at which the determinations were carried out.
† Determination carried out by atomic absorption spectrometry.

thorium, iron and molybdenum were invariably extracted before the extraction of niobium; hafnium was extracted after the extraction of niobium. The results of these separations are given in Table 4.

The proposed method is simple, rapid and selective. The separation of niobium from vanadium, tantalum, zirconium, hafnium and iron is significant as these elements are associated with each other in ores and minerals.

The authors thank the Council of Scientific and Industrial Research (India) for sponsoring this project and for awarding a Senior Research Fellowship to one of them (N. V. D.).

References

1 Lauw-Zecha, A. B. H., Lord, S. S., Jr., and Hume, D. N., *Anal. Chem.*, 1952, **24**, 1169.
2 Luke, C. L., *Anal. Chim. Acta*, 1966, **34**, 165.
3 Lyle, S. J., and Shendrikar, A. D., *Talanta*, 1965, **12**, 573.
4 Theodore, M. L., *Anal. Chem.*, 1958, **30**, 465.
5 Morris, D. F. C., Scargil, D., and Olya, A., *Talanta*, 1960, **4**, 194.
6 Rao, R. R., and Khopkar, S. M., *Anal. Lett.*, 1984, **17**, 523.
7 Vin, Y. Y., and Khopkar, S. M., *Talanta*, 1991, **38**, in the press.
8 Hubert-Pfalzgraf, L. G., and Tsunoda, M., *Inorg. Chim. Acta*, 1980, **38**, 43.
9 Blanco-Gomis, D., Arribas Jimeno, S., and Sanz-Medel, A., *Talanta*, 1982, **29**, 761.
10 Mjumdar, A. K., and Mukherjee, A. K., *Anal. Chim. Acta*, 1958, **19**, 23.
11 Patrovsky, V., *Talanta*, 1965, **12**, 971.
12 Caletka, R., Hausbeck, R., and Krivan, V., *Talanta*, 1986, **33**, 219.
13 Davey, D. E., Catral, R. W., Cardwell, T. J., and Magee, R. J., *J. Inorg. Nucl. Chem.*, 1978, **40**, 1135.

Paper 1/00453K
Received January 31st, 1991
Accepted April 29th, 1991

Synthesis of a Phosphoramidate Chelating Fibre and Its Adsorption of Trace Amounts of Gallium and Indium

Xingyin Luo,* Zhixing Su, Xijun Chang, Guangyao Zhan and Xihuan Chao
Department of Chemistry, Lanzhou University, Lanzhou 730000, People's Republic of China

The phosphoramidate chelating fibre was synthesized in the laboratory, using poly(vinyl chloride) fibre as a starting material, and for optimizing the conditions for synthesis. The structure of the chelating fibre was determined by infrared spectrometry. The parameters studied, in order to concentrate trace amounts of Ga and In using the chelating fibre, included acidity, flow rate, saturating capacity of adsorption, effect of re-use, interfering ions and desorption. Real samples enriched in Ga and In were analysed by using inductively coupled plasma optical emission spectrometry. When the concentrations of both Ga and In were 0.04 mg l^{-1}, the relative standard deviation was 3.4% for Ga and 3.6% for In.

Keywords: *Phosphoramidate chelating fibre; synthesis; adsorption; gallium and indium; inductively coupled plasma optical emission spectrometry*

The spectrophotometric determination of Ga and In by a solvent extraction method using a phosphonium organic reagent or diethyl ether–benzene have been reported previously,[1,2] however, the procedures were tedious and involved the use of toxic reagents. The adsorption of Ga and In by polystyrene–phosphoric acid resins has also been studied,[3,4] but the conditions for the synthesis of the resin are extreme, and the reaction process is exothermic.[5] The synthesis of a polyacrylamide oxime–carboxylic acid chelating fibre from polyacrylonitrile fibre and its application to the concentration and determination of many elements has been reported.[6] However, the selectivity of the phosphoramidate chelating fibre for the adsorbtion of Ga and In is superior to that of the polyacrylamide oxime–carboxylic acid chelating fibre.

In the present paper, the synthesis of the phosphoramidate chelating fibre and its structure as determined by infrared (IR) spectrometry, are reported. The performances of the chelating fibre in adsorbing trace amounts of Ga^{III} and In^{III} ions are studied in detail. The proposed method has the advantages of a fast adsorption rate, few interferences, convenient operation and good accuracy.

Experimental

Apparatus

An inductively coupled plasma optical emission spectrometer (ICP/6500, Perkin-Elmer), a Fourier transform IR spectrometer (5-Dx Nicolet), Model 1106 elemental analyser (Carlo Erba) and a Tiantsin Model pH s-73 pH meter were used in this study. A three-necked flask with a stirrer, a thermometer and a spherical condenser pipe were used in the synthesis of the chelating fibre.

The adsorbing column, 0.2 g of chelating fibre, was loaded in a glass tube (12 cm in length, 0.6 cm i.d., 0.15 cm i.d. at the lower end).

Materials and Reagents

The poly(vinyl chloride) (PVC) fibre was washed, prior to use, with distilled water and ethanol and dried under IR radiation. All reagents used were of analytical-reagent grade unless specified otherwise. Specpure Ga_2O_3 and In_2O_3 were purchased from the Shanghai Chemical factory. Stock solutions of Ga and In, at a concentration of 1 g l^{-1}, were prepared by dissolving 0.3361 g of Ga_2O_3 and 0.6045 g of In_2O_3 in 250 ml of dilute HCl 4 mol dm^{-3}. Mixed standard solutions of Ga and In, each at a concentration of 20 mg l^{-1}, were prepared by diluting the stock solution with distilled water and adding concentrated HCl so that the final solutions were 1 mol dm^{-3} in HCl. Distilled water was used throughout the procedure.

Synthesis of the Chelating Fibre

Dried PVC fibre (30 g), 30 ml of distilled water and 300 ml of ethylenediamine were placed in a three-necked flask. After the mixture had been refluxed for 3 h at 110–115 °C with slow stirring, it was filtered, washed with distilled water until the pH of the washings was neutral and dried by IR radiation. The nitrogen content of the fibre containing amino groups (aminated fibre) obtained under the optimized reaction condition was 13.46%. Following Mannich's reaction,[7] the aminated fibre, CH_2O and $(CH_3O)_3PO$ (1 + 4 + 8) were placed in a three-necked flask and 1–2 ml of glacial acetic acid was added. After refluxing for 3 h at 80–90 °C, the phosphoramidate fibre was obtained through filtration, washing and drying. The phosphonium content of the phosphoramidate fibre obtained under the optimized reaction conditions was 10.78%.

Analytical Procedures

Portions of the mixed standard solution containing Ga and In were pipetted into beakers and diluted with distilled water to 100–500 ml. They were adjusted to a pH of 2.5 and passed through columns packed with the chelating fibre at a flow rate of 4–5 ml min^{-1}. The adsorbed Ga or In was desorbed quantitatively by passing 8 ml of 4 mol dm^{-3} HCl and 2–3 ml of distilled water through the columns in sequence and the effluents were collected. Each of the effluents was evaporated to about 3 ml on a hot-plate, then transferred into a 5 ml calibrated flask and diluted to the mark with distilled water. Gallium and In were determined by an ICP/6500 spectrometer (forward power 1100 W, viewing height 15 mm, Ar plasma gas flow 14 l min^{-1}, Ar auxiliary gas flow 0.4 l min^{-1}, Ar nebulizer gas flow 1.0 l min^{-1} and wavelengths, Ga 294.364 nm and In 303.936 nm).

Results and Discussion

Selection of Conditions for Synthesis

The effects of conditions used for synthesis on the phosphoric content of the chelating fibre were examined. The results shown in Table 1 indicate that a higher content of P can be obtained. However, if the proportion of materials used is

* To whom correspondence should be addressed.

Table 1 Effect of synthesis conditions on the P content of the fibre

Material*	P content† (%)	Time/ h	P content‡ (%)	Solvent	P content§ (%)
1 + 3 + 6	8.43	1.0	6.11	HCl + AcOH	5.46
1 + 4 + 8	10.97	3.0	10.54	AcOH	10.78
1 + 6 + 12	11.83	5.0	11.62	C_2H_5OH	11.00

* Aminated fibre in g + CH_2O in ml + $(CH_3O)_3PO$ in ml.
† Time, 3 h, solvent AcOH.
‡ Material 1 + 4 + 8, Solvent, AcOH.
§ Material 1 + 4 + 8, time, 3 h.

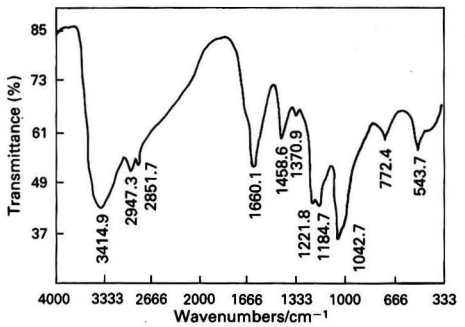

Fig. 1 Infrared spectrum of the phosphoramidate chelating fibre

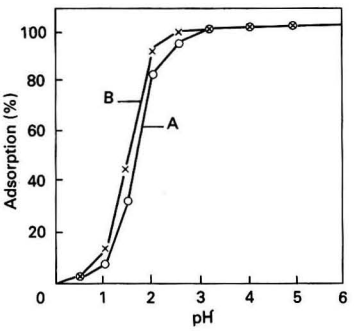

Fig. 2 Adsorption efficiency of A, Ga; and B, In as a function of pH

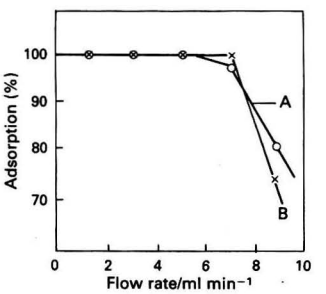

Fig. 3 Adsorption efficiency of A, Ga; and B, In as a function of flow rate

inadequate and the reaction time is too long, the mechanical strength of the chelating fibre obtained is affected, moreover, the catalytic effect of acid in Mannich's reaction must be taken into consideration.[7] Therefore, the following conditions were selected for the synthesis: aminated fibre–CH_2O–$(CH_3O)_3PO$ (1 + 4 + 8); AcOH, 1–2 ml; refluxing time, 3 h; and refluxing temperature, 80–90 °C.

Structure of the Chelating Fibre

The IR spectrum of the phosphoramidate chelating fibre is shown in Fig. 1. According to the reference spectra,[8] the peaks in Fig. 1 can be assigned as follows: ν_{max}/cm^{-1} 3414.9 (νN-H), 2947.3 and 2852.7 (δ CH_2 and ν CH), 1660.1 (δ N-H), 1184.7 (ν C-NH and $\delta_p CH_3$ of P-O-CH_3), 1221.8 (ν P = O), 1042.7 (ν P-O-C and δ C-N), 772.4 (ν P-O-C) and 1458.6 (δ_s CH_2) (ν, stretching vibration; δ, bending vibration; δ_s, scissor vibration; and δ_p, rocking vibration). Evidently, there is an N-$[CH_2PO(OCH_3)_2]_2$ group present in the chelating fibre. The peak identities indicate that the expected product, *i.e.*, the phosphoramidate chelating fibre was obtained. Therefore, based on the work described in previous publications,[7,9] the synthesis reaction for the chelating fibre can be written as shown in Scheme 1.

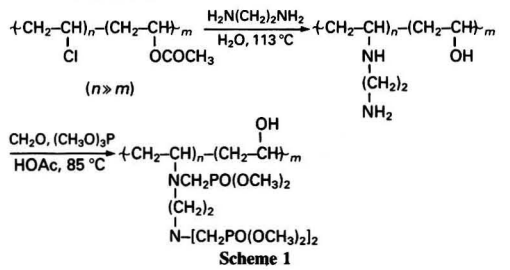

Scheme 1

Acidity of Quantitative Enrichment

Portions of the mixed standard solution containing equal concentrations of Ga and In were pipetted into beakers and diluted to equal volumes with distilled water. The solutions were adjusted to the desired pH in the range 1–6, and Ga and In ions were concentrated in the adsorption columns as described above. The results of the determination, indicated in Fig. 2, show that the recoveries of Ga and In are in the range 97–103% at pH 2.5. In addition, As^{3+}, Ge^{4+}, Tl^{+}, Tl^{3+}, Zn^{2+}, Cd^{2+}, Co^{2+}, Ni^{2+}, Ca^{2+}, Mg^{2+}, K^{+} and Na^{+} ions are not adsorbed by the chelating fibre at pH 2.5, and Bi^{3+}, Sb^{3+}, Sn^{4+} and Pb^{2+} are barely adsorbed (5–20%). Therefore, the adsorption of Ga and In at pH 2.5 is not interfered with by these ions.

Adsorption Rate

Using the proposed procedure, the flow rates for the adsorption of Ga and In on the chelating fibre column were varied between 1 and 9 ml min^{-1}. The results, given in Fig. 3, show that Ga and In can be adsorbed quantitatively at flow rates below 7 ml min^{-1}. However, considering the complexity of the samples analysed (real samples containing interfering ions), the flow rates for the adsorption of Ga and In were selected to be 4–5 ml min^{-1}.

Adsorbing Capacity and Rate Constant

Two portions of 0.1 g of the chelating fibre were placed in two conical flasks and Ga or In stock solution at a concentration of

1 mg ml^{-1} was added. The solutions were diluted to equal volume (the concentration of Ga or In was then 0.2 mg ml^{-1}) and the acidity of the solutions was adjusted to pH 2.5 while shaking them on a vibrator. Subsamples analysed at regular intervals of 10 min for Ga and 1 h for In until equilibrium was reached (about 60 min for Ga and 6 h for In), *i.e.*, the concentrations of Ga and In determined in the conical flasks did not vary. The static saturation adsorption capacity (Q_e) of the chelating fibre is calculated to be 36 mg g^{-1} for Ga and 79 mg g^{-1} for In. According to Brykina *et al.*,[10] the isothermal adsorption equation for a low concentration of ions can be expressed as $-\ln(1-F) = kt$, where $F = Q_t/Q_e$ (Q_t represents the adsorption capacity at reaction time t). The values of k, obtained from the slope of a linear calibration graph, are 1.0×10^{-3} s^{-1} for Ga and 2.4×10^{-4} s^{-1} for In.

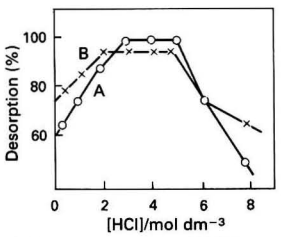

Fig. 4 Effect of the concentration of HCl on the desorption efficiency for A, Ga; and B, In (volume of HCl, 8 ml)

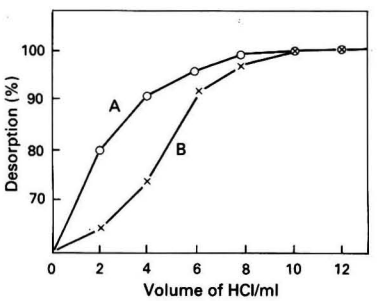

Fig. 5 Desorption efficiency for A, Ga; and B, In as a function of the volume of HCl. Concentration of HCl, 4 mol dm^{-3}

Table 2 Interference of concomitant ions on Ga and In at a concentration of 0.040 mg l^{-1}

Interfering ion	Concentration/mg l^{-1}	Recovery (%) Ga	In
Ca^{2+}	20	103	94
Mg^{2+}	20	100	95
Ni^{2+}	20	101	100
Cd^{2+}	20	102	102
Zn^{2+}	20	92	96
Al^{3+}	20	90	100
Cu^{2+}	15	91	95
$Cr_2O_7^{2-}$	15	92	94
Fe^{3+}	15	95	97

Desorption Conditions

Gallium and In adsorbed by the chelating fibre were desorbed with 0.5–8 mol dm^{-3} HCl. The results show that Ga and In can be desorbed quantitatively with 8 ml of 2–5 mol dm^{-3} HCl (Fig. 4) and (6–12 ml of 4 mol dm^{-3} HCl Fig. 5). The recoveries of Ga and In are in the range 93–100%. Therefore, 8 ml of 4 mol dm^{-3} HCl was selected as appropriate for desorption. In addition, from Fig. 4, it can be seen that the desorption efficiency for Ga and In is decreased when the concentration of HCl is >5 mol dm^{-3}. This is because the N–H and P=O groups in the chelating fibre are changed into NH_2^+ and P=OH$^+$, respectively with increasing concentrations of H$^+$. Under such conditions, some $GaCl_4^-$ or $InCl_4^-$ is attracted by the fibre and desorbtion becomes difficult.

Stability and Re-use of the Chelating Fibre

When the chelating fibre, stored for 2 years, was used for adsorbing trace amounts of Ga and In, the results obtained were similar to the original recoveries, *i.e.*, recoveries of Ga and In were still in the range of 92–100%. By following the proposed procedure of analysis, the chelating fibre could be re-used more than eight times, and the recoveries of Ga and In remained in the range 95–105%.

Interfering Ions

The different interfering ions were added to the diluted standard solution containing Ga and In, prepared as described under Analytical Procedures, the results for the determination of Ga and In are given in Table 2. The results show that a 500-fold excess of Ca^{2+}, Mg^{2+}, Cd^{2+}, Zn^{2+} and Al^{3+}; a 300-fold excess of Cu^{2+} and $Cr_2O_7^{2-}$; and a 100-fold excess of Fe^{3+} ions causes little interference.

Precision and Analysis of Real Samples

Portions of a standard solution containing equal concentrations of Ga and In were pipetted into beakers accurately and diluted with distilled water to give a concentration of 0.040 mg l^{-1}. According to the described procedure, the diluted solutions were concentrated and determined. The average results for seven determinations were 0.039 mg l^{-1} for Ga and 0.040 mg l^{-1} for In and the relative standard deviations were 3.4% for Ga and 3.6% for In. The concentrations of Ga and In in real samples were determined by the standard additions method. The results are given in Table 3. It can be seen that the recoveries after the addition of Ga and In standards are satisfactory and the concentrations of Ga and In determined in waste liquid by the proposed method are in agreement with the analytical results obtained by a factory laboratory.

Conclusion

The proposed method of using a phosphoramidate chelating fibre to selectively adsorb and separate trace amounts of Ga and In from sample solutions is feasible. The proposed method also proved to be efficient for the determination of

Table 3 Results for real samples

Sample*	Concentration/mg l^{-1} Found			Average	Added/ mg l^{-1}	Total concentration/mg l^{-1} Found			Average	Recovery (%)
1 Ga	—	—	—	—	0.040	0.040	0.039	0.039	0.039	97.5
In	0.042	0.043	0.043	0.043	0.040	0.083	0.084	0.084	0.084	101
2† Ga	0.031	0.032	0.031	0.031	0.040	0.070	0.071	0.070	0.070	98.6
In	0.024	0.023	0.024	0.024	0.040	0.065	0.064	0.065	0.065	102

* Sample 1 is waste water from a non-ferrous metal smelting plant, sample 2 is waste liquid from a factory laboratory.
† The results obtained from the factory laboratory for sample 2 are 0.032 mg l^{-1} for Ga and 0.024 mg l^{-1} for In.

trace amounts of Ga and In in real samples. The method is rapid, accurate and convenient. The chelating fibre is stable and its synthesis is also simple and economical.

References

1 Levin, I. S., Azareiko, T. G., and Balakireva, N. A., *Zh. Anal. Khim.*, 1968, **23**, 1013.
2 Hu, Z. D., and Zhao, Z. F., *Spectrophotometric Methods*, The Peoples' Publishing House, Ningxia, China, 1987, p. 318.
3 Wang, N. D., Wang, Y. J., Ma, J. Z., and Xu, X. H., *J. Hangzhou Univ.*, 1986, **13**, 456.
4 Wang, N. D., Xiong, C. H., Ji, F. G., and Zhu, G. H., *Chem. Chin. Univ.*, 1986, **7**, 765.
5 Huo, B. L., Zhang, Q. X., Qian, T. B., Chen, W. Z., and Hou, W. T., *Pet. Chem. Ind.*, 1978, **4**, 344.
6 Chang, X. J., Zhan, G. Y., Su, Z. X., and Luo, X. Y., *Fenxi Huaxue*, 1986, **14**, 1.
7 Wan, D. Z., *Mannich Reaction and Mannich Base Chemistry*, Science Publishing House, Beijing, 1986, pp. 82 and 340.
8 Dong, Q. N., *IR Spectrum Methods*, Publishing House of the Chemical Industry, Beijing, 1979, pp. 104, 168, 200.
9 Birum, G. H., *J. Org. Chem.*, 1974, **39**, 209.
10 Brykina, G. D., Marchak, T. V., Krysina, L. S., and Velyavskaya, T. A., *Zh. Anal. Khim.*, 1980, **35**, 2294.

Paper 1/00371B
Received January 25th, 1991
Accepted April 18th, 1991

BOOK REVIEWS

Computer Applications in Chemistry. An Introduction for PC Users

K. Ebert, H. Ederer and T. L. Isenhour. Pp. xii + 714. VCH. 1989. Price DM98.00; £35.45 (Hardback). ISBN 3 527 27807 9 (VCH Verlagsgesellschaft); 0 89573 864 3 (VCH Publishers).

For anyone concerned with the design of undergraduate chemistry courses and related programmes of study, there are constant problems associated with incorporating new material at the expense of more traditional topics. One such area, which always produces as many different opinions as participants in the discussion, is computing and how much time should be devoted to its teaching. That the modern graduate should be aware of the use and impact of computers in chemistry, and be confident to use these machines, is beyond doubt. The nature and content, however, of any computer course are more debatable. With the wide range of software tools now available for data manipulation and analysis, the question must be asked as to whether programming in its traditional style is a suitable subject for the majority of students or a distraction from the problem to be solved. This book is for those, teachers and students, who are keen to learn programming as an integrated component of the chemistry studies. It is a programming tutorial text and is not, as the title may imply, a review of the use and applications of microcomputers in the laboratory.

The book is extremely well written and produced. In its 750 pages it contains a wealth of material relevant to undergraduate and postgraduate chemistry courses and the authors are to be congratulated on the selection and treatment of the broad spectrum of topics employed to illustrate the features of programming style and syntax. The book provides a comprehensive introductory programming manual for chemists using PC microcomputers. From a brief introduction of the fundamental elements of programming, including the use of flow-charts, the reader is led through the solving of simple equations, the use of loops, arrays, non-numerical data processing and computer graphics. The main body of the text uses the design and application of BASIC programme, in particular the BASICA dialect of the language from IBM, but conversion to other BASICS languages is trivial. The algorithm for every program used, and there are more than 80 provided, is discussed fully and the code is provided on a 5¼ in disk accompanying the text. Simple programs include the calculation of molecular formulae from elemental analysis, the emitted energy distribution according to Planck's law and the diffusion potentials of electrolyte solutions. More complex calculations involve the simulation of a copolymer sequence, the determination of Bragg's scattering angle for XR(D) studies and the calculation of the number of structural isomers of a compound using graph theory. Matrix operations, including the calculation of eigervalues, are covered in some depth. Methods for solving differential equations receive their own chapter, which is fairly substantial. Separate chapters are also devoted to the topics of computer graphics and data acquisition.

The final chapter of the book, about 200 pages, provides the programs in PASCAL and the source code is available, as text files, on a second disk provided with the book.

This book is excellent value for money, and for any undergraduate chemistry course employing programming as a tool for students the material provided is to be recommended. With access to a PC and this text, a student can reinforce the more formal lectures and learn of and appreciate the potential of modern microcomputers. In the readable style adopted throughout, the book will appeal to students and will provide a most valuable guide for independent, student centred studies.

M. J. Adams

Element Concentration Cadasters in Ecosystems. Methods of Assessment and Evaluation

Edited by H. Lieth and B. Markert. Pp. x + 448. VCH. 1990. Price DM164.00. ISBN 3-527-28054-5 (VCH, Weinheim); 0-89573-962-3 (VCH, New York).

This book reports the proceedings of a Workshop held in March 1989 at Osnabrück, which brought together analysts and ecologists to consider problems in environmental analytical chemistry and interpretation of data. The multi-author volume consists of seven sections contributed by authors predominantly from Europe but also Japan and USA.

The editors propose the adoption of an holistic approach to environmental studies and use of element concentration cadasters in ecosystems. A cadaster lists groups of elements, in a sample, in increasing order of concentration in ranges covering one order of magnitude. These lists form a rather untidy table of thirteen columns covering the over-all concentration range from 10^{-6} to 10^{6} mg kg^{-1}. This table, together with a heading containing other relevant information, constitutes a cadaster. The authors suggest that this arrangement of data will facilitate intercomparisons of samples from different compartments of ecosystems. It is an interesting and useful concept that merits further development and evaluation.

Modern multi-element analysis techniques produce masses of data, which are often difficult to rationalize and interpret. In many environmental disorders problems arise from imbalance between elements, as much as from excess or deficiency of one particular element. The advantage of multi-element analysis techniques in these situations is therefore enormous.

The book contains sections on sampling, sample preparation, instrumental measurement, quality control and data evaluation, use and interpretation of multi-element data and political aspects. Problems of sampling and sample variability, particularly in biological investigations, where a large number of variables may be involved, is amply emphasized in six papers on this topic. Living plants are dynamic systems and great care is necessary in sampling if meaningful results are to be obtained. This is well illustrated in relation to the sampling of tree leaves. The sampling of soils is well documented and computer-aided sampling for multi-element analysis discussed. Sampling errors in environmental studies are often considerably greater than the analytical errors.

The sample preparation stages of drying, sieving, milling, grinding *etc.* are often essential and can pose problems of contamination as can the use of chemicals and equipment during fluxing, dissolution, precipitation or extraction in the laboratory treatment of samples prior to instrumental analysis. Analytes can also be lost during sample preparation by such processes as volatilization. These problems are fully illustrated and discussed by a number of authors.

The section on instrumental measurement contains four papers dealing with AAS, ICP-AES, ICP-MS and INAA. Although conventional AAS is still widely used as a technique for the determination of a single element, it is evident that the multi-element capability of ICP-AES is being increasingly applied to environmental analysis.

Quality assurance and testing of accuracy of results by the use of certified reference materials becomes increasingly necessary as environmental data are compared across international frontiers. The reproducibility of methodologies can be easily tested but good accuracy is also essential if such data are to be used, for example, for modelling purposes. These aspects are strikingly emphasized in a contribution from the BCR Organization in Brussels.

The section on use and interpretation of multi-element data is made up of thirteen papers covering such widely-ranging topics as mining pollution, food chemistry, soils, plants, peats, forest ecosystems, invertebrates, radionuclides, air pollution and forest decline. The final paper addresses the problem of risk assessment in environmental studies in the Netherlands.

The constructive interaction between analysts and data-users reported in this compilation is both timely and progressive. The book is well presented and indexed, and will provide much of value to both analysts and environmentalists.

M. L. Berrow

Analytical Profile of the Resin Spot Test

Vladimir Grdinić, Svjetlana Luterotti and Laila Stefanini-Orešić. Pp. 385. CRC Press. 1990. Price £156.00. ISBN 0 8493 4708 4.

The resin spot test is a generic term applied to a collection of simple, inexpensive and easy to use analytical methodologies, based on the detection of analytes by colour development, facilitated by means of reaction with or adsorption by functionalized resins.

This book contains a wealth of detailed information on the application of resin spot tests to inorganic and organic microchemical analysis. An extensive set of primary literature references accompany each chapter. Many of these are 20–30 years old, and the most up-to-date reference I found, quoted during a cursory inspection, was 1987. Much of the literature cited is of Japanese or East European origin, perhaps reflecting something of the historical development of the technique.

The book is split into seven chapters. The first gives an overview of the resin spot test from a historical perspective, highlighting the role of ion exchanger functionality in determining its field of application. The second, and largest chapter, provides a detailed examination of the chemistry of sorbents and the different modes of analyte interaction and detection. The effects of other parameters, such as the nature of the solvent, pH, analyte concentration, time dependence of colour development and temperature are also described using examples. More specific methodology is described in Chapter 3, which deals with the practical issues around the use of equipment, generic method types, and criteria for the selection of a particular approach. Examples of particular determinations are used to illustrate the appropriate methodology, in sufficient detail to allow replication in the reader's own laboratory. The literature available on qualitative inorganic analysis and organic analysis is summarized in the form of extended tables in Chapters 4 and 5, respectively. This form of presentation allows rapid access to the relevant source material together with an indication of the language of the original paper. Obviously this approach does not lend itself to a critical review, but the authors do state that the references have been consulted directly, which is presumably some guarantee of accuracy. One of the major limitations of spot tests is that the methodology is perceived to be qualitative in nature. In Chapter 6, the case is put for semi-quantitative and quantitative application of resin spot tests, in conjunction with colorimetric detection. Most of the tests cited relate to elemental determinations and indicate the potential for selective measurement of analyte species in terms of oxidation state. In the final chapter, a survey is made of the use of resin spot tests in particular fields, including biomedical and forensic analysis, pharmaceutical, nuclear, food, and environmental applications. Once again, the examples quoted are detailed enough to be carried out in practise. An extensive bibliography of some 148 references is associated with this chapter.

The book is extremely well produced, and the contents are well packed into its pages, while retaining excellent typeface clarity. Diagrams and reaction schemes are also of a high standard. There is an extensive list of contents, and a glossary of symbols and abbreviations in addition to a useful summary of terms and definitions used in connection with resin spot tests. The book contains a 15 page subject index and a 7 page author index. There are a number of appendices included, which provide reference information on sensitivity, comparison of ion exchangers and sources of supply, and calculation of test limits.

The book will undoubtedly be of use to those interested in the use of functionalized columns for preconcentration and extraction or derivatization of analytes, *e.g.*, for use with flow injection protocols, as it contains a large collection of useful chemistries. The book is well written, and it is relatively easy to access the appropriate information. It will be equally valuable to the specialist as a concise source of information, and to the more general reader as an introduction to the field. Unfortunately, the rather high price will tend to limit its appeal to those without budgetary constraints. As a summary of the field, however, the book is undoubtedly a comprehensive reference work, and can be commended to libraries of institutions with interests in microchemical analysis.

J. Marshall

Handbook of Furnace Atomic Absorption Spectroscopy

Ashma Varma. Pp. 428. CRC Press. 1990. Price £156.00. ISBN 0-8493-3243-5.

This book addresses everyone using graphite furnace atomic absorption spectrometry as a tool for trace analysis. It is divided into three sections. The first gives a rather concise introduction to GFAAS. Principles of the method, instrumentation and parameters of analysis are briefly explained. About 800 references (up to 1987) are given for this topic. The second section takes about three quarters of the book and lists the elements that can be determined by GFAAS in alphabetical order. On one page, instrumental parameters and standard operating conditions are collected, together with a general note, *e.g.*, on the composition of the solutions used for the analysis of the element, purge gas or analytical precision. A literature list in temporal order is added for every element without any further explanations and comments. In the last section the reader finds a list of books on AAS, manufacturers of spectrometers and accessories together with a glossary of terms and definitions useful for GFAAS.

The information on the operating conditions has to be used with some care. Relatively high char temperatures are recommended for some elements, *e.g.*, Tl or Sb, which leads, in my experience, to considerable losses of the analyte. Pyrolytic-graphite coated graphite tubes are proposed for all elements, although many elements can be successfully determined by using the cheaper normal graphite furnaces. Furthermore, information on chemical interferences, which are so harmful in the determination of an element in a difficult matrix, was missing and also any way of overcoming them, *e.g.*, by addition of a chemical modifier. This information must be drawn from the original papers, which are, however, given in the reference list, for every element.

The handbook might be of interest to those beginning in graphite furnace analysis. The instrumental parameters and operating conditions can also be found in normal laboratory manuals however, but the complete literature list for every element will surely help to solve analytical problems: although this help, at £156, has a fairly high price.

W. Wendl

Modern Aspects of Electrochemistry. No. 21
Edited by Ralph E. White, J. O'M. Bockris and B. E. Conway. Pp. xiii + 321. Plenum Press. 1990. Price $69.50 (USA). ISBN 0 306 43313 3.

Like its forbears in the series this book is dedicated to the pure electrochemist interested in the intricacies of events at electrodes for their own sake, rather than for what they can be made to do. Nevertheless, there is much that is interesting here in the wider pursuit of knowledge, even if one looks at the conventional type of electrochemical article on the nickel oxide electrode.

The book is a six chapter work and, with one exception, each is by American-based authors, despite the crop of European sounding names. The exception is the chapter on reaction kinetics and mechanisms on metal single-crystal electrode surfaces by Radoslav Adžić of the University of Belgrade, who makes acknowledgement to British electrochemists. By its nature this would seem to be far from analytical science, but then an understanding of the events at electrodes can be of direct benefit to the advance of analytical science; this will be in electrochemical sensing, *e.g.*, in the detection of carbon monoxide for which there is a need for good sensors. Here the oxidation of carbon monoxide is addressed, and although the analytical implications are not mentioned, they cannot be far removed.

It is in the first chapter, devoted to scanning tunnelling microscopy, that there is analytical science, in this instance directed to exploring events at electrodes. The technique, for which the developers Gerd Binnig and Heini Rohrer were awarded the 1986 Nobel Prize in physics, has already attracted the attention of many in the analytical community. The basic principles are here, and the specific application mentioned is of special interest in view of the ability of the technique to give atomic resolution images of surfaces immersed in aqueous media. There are other virtues of the technique, such as permitting local surface modification. The recognition of this development can be viewed as being akin to the development of nuclear magnetic resonance in the 1950s, and which is now so widespread in its use.

Surface electrochemistry is facilitated by various approaches. One of these is the use of radioactive tracers for measuring absolute concentrations directed to molecular and atomic exchanges between the surface and electrolyte phases and another for investigating interfacial kinetics of adsorption and desorption processes. This is skilfully described against the background of the nature of surfaces and of the techniques and instruments employed.

The chapter on the electrochemistry of metallic glasses is by implication specialized. Apart from describing the characteristics, it emphasizes the differences between glassy metallic layers and polycrystalline alloys of similar composition. The final chapter is devoted to d.c. relaxation techniques for investigating fast electrode reactions. It emphasizes the gains to be obtained by also using digital instrumentation and curve-fitting data evaluation methods.

Although the contributions are from six groups of authors, the quality of the production of the book is very high, which can be attributed to the careful editing. There are copious references, some very clear and well-produced diagrams, a cumulative author index and a subject index to Volumes 1–21, and a very adequate subject index to the contents of this volume. It is clearly a book for dedicated electrochemists, but it can also be a source of good ideas and wider knowledge made available to many others.

J. D. R. Thomas

CUMULATIVE AUTHOR INDEX

JANUARY–SEPTEMBER 1991

Alan Date Memorial Award 1991

In recognition of the considerable contribution made by Dr Alan Date to the field of inductively coupled plasma source mass spectrometry, an annual commemorative award has been created to encourage talented young scientists to broaden their overseas scientific experience.

Candidates should be working in the field of atmospheric pressure plasma source mass spectrometry (inorganic) and will be required to submit a written resume of their work in this field. It is intended that this may form the basis of a publication.

An amount of up to £1000 will be available to the successful candidate(s)

Closing date for submissions will be October 26th 1991.

Further details of the award may be obtained from:

Dr Robert Hutton, VG Elemental, Ion Path, Road Three, Winsford, Cheshire, CW7 3BX, UK.

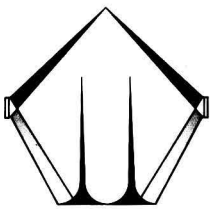

Sixth Biennial National Atomic Spectroscopy Symposium

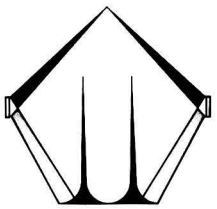

will be held at

Polytechnic South West, Plymouth, UK

22–24 July 1992

The symposium will provide a forum where interesting and useful applications of atomic spectroscopy can be reported and discussed. In addition to plenary, invited and submitted lectures, a particular feature of the meeting will be the presentation of posters. There will also be an exhibition and a social programme for delegates and their guests.

Scientific programme will include:

Plenary Lecturers—

M.W. Blades (*Vancouver, BC, Canada*)
B.V. L'vov (*Leningrad, USSR*)
J.W. McLaren (*Ottawa, Ontario, Canada*)
K. Niemax (*Dortmund, Germany*)
B.L. Sharp (*Loughborough, UK*)

Invited Lecturers—

J. S. Crighton (*Sunbury-on-Thames, UK*)
H. Falk (*Kleve, Germany*)
S.J. Hill (*Plymouth, UK*)
D. Littlejohn (*Glasgow, UK*)
C. McLeod (*Sheffield, UK*)
G. Schlemmer (*Überlingen, Germany*)
P. Stockwell (*Sevenoaks, UK*)
J.F. Tyson (*Amherst, MA, USA*)
J.G. Williams (*Egham, UK*)
A.M. Ure (*Glasgow, UK*)

This meeting is organized by the Atomic Spectroscopy Group, Analytical Division of The Royal Society of Chemistry.

Further information can be obtained from the Chairman of the organizing committee:

Dr S.J. Hill, Department of Environmental Sciences, Polytechnic South West, Drake Circus, Plymouth, Devon PL4 8AA, UK.

FIRST FOLD HERE

THE ANALYST READER ENQUIRY SERVICE
For further information about any of the products featured in the advertisements in this issue, write the appropriate number on the postcard, detach and post.

FOLD HERE

THE ANALYST READER ENQUIRY SERVICE

SEP'91

For further information about any of the products featured in the advertisements in this issue, please write the appropriate number in one of the boxes below.
Postage paid if posted in the British Isles but overseas readers must affix a stamp.

PLEASE USE BLOCK CAPITALS LEAVING A SPACE BETWEEN WORDS *Valid 12 months*

1 NAME

2 COMPANY

PLEASE GIVE YOUR BUSINESS ADDRESS IF POSSIBLE. IF NOT, PLEASE TICK HERE ☐

3 STREET

4 TOWN

5 COUNTY
POST CODE

6 COUNTRY

7 DEPARTMENT/
DIVISION

8 YOUR JOB TITLE/
POSITION

9 TELEPHONE NO

OFFICE USE ONLY REC'D PROC'D

FOLD HERE

Postage will be paid by Licensee

Do not affix Postage Stamps if posted in Gt. Britain, Channel Islands, N. Ireland or the Isle of Man

BUSINESS REPLY SERVICE
Licence No. WD 106

Reader Enquiry Service
The Analyst
The Royal Society of Chemistry
Burlington House, Piccadilly
LONDON
W1E 6WF
England

ANALAO 116(9) 881–974 (1991) September 1991

The Analyst

The Analytical Journal of The Royal Society of Chemistry

CONTENTS

Typeset and printed by Black Bear Press Limited, Cambridge, England